



June 7, 2018

10 CFR 50.90
Docket No. 50-443
SBK-L-18074

U. S. Nuclear Regulatory Commission
Attn: Document Control Desk
Washington, DC 20555-0001

Seabrook Station
Response to Request for Additional Information Regarding
License Amendment Request 16-03

References:

1. NextEra Energy Seabrook, LLC letter SBK-L-16071, "License Amendment Request 16-03, Revise Current Licensing Basis to Adopt a Methodology for the Analysis of Seismic Category I Structures with Concrete Affected by Alkali-Silica Reaction," August 1, 2016 (ML16216A240).
2. NRC, "Request for Additional Information Regarding License Amendment Request Related to Alkali-Silica Reaction (CAC No. MF8260)," August 4, 2017 (Accession Number ML17214A085).
3. NextEra Energy Seabrook, LLC letter SBK-L-17156, "Response to Request for Additional Information Regarding License Amendment Request 16-03 Related to Alkali-Silica Reaction (CAC No. MF8260)," October 03, 2017 (Accession Number ML17277A337).
4. NRC, "Seabrook Station, Unit No. 1 - Request for Additional Information Regarding License Amendment Request Related to Alkali-Silica Reaction (CAC No. MF8260; EPID L-2016-LLA-0007)," October 11, 2017 (Accession Number ML17261B217).
5. NextEra Energy Seabrook, LLC letter SBK-L-17204, "Response to Request for Additional Information Regarding License Amendment Request Related to Alkali-Silica Reaction (CAC No. MF8260); EPID L-2016-0007)," December 11, 2017 (Accession Number ML17345A641).

6. NRC, "Seabrook Station, Unit No. 1 - Request for Additional Information Regarding ASR Amendment Request, May 1, 2018 (Accession Number ML18121A399).

In Reference 1, NextEra Energy Seabrook, LLC (NextEra Energy Seabrook) submitted License Amendment Request 16-03, requesting an amendment to the license for NextEra Energy Seabrook. Specifically, the proposed change revises the NextEra Energy Seabrook Updated Final Safety Analysis Report (UFSAR) to include methods for analyzing Seismic Category I structures with Alkali-Silica Reaction (ASR) affected concrete.

In Reference 2, the NRC requested additional information to complete the review of the NextEra Energy Seabrook License Amendment Request 16-03.

In Reference 3, NextEra Energy Seabrook submitted letter SBK-L-17156 and provided additional information requested in Reference 2.

In Reference 4, the NRC requested additional information to complete the review of the NextEra Energy Seabrook License Amendment Request 16-03, following the submittal in Reference 3.

In Reference 5, NextEra Energy Seabrook submitted letter SBK-L-17204 and provided additional information requested in Reference 4.

In Reference 6, the NRC requested additional information to complete the review of the NextEra Energy Seabrook License Amendment Request 16-03, following the submittal in Reference 5.

Enclosure 1 provides NextEra Energy Seabrook's response to the NRC's Request for Additional Information (RAI) provided in Reference 6, concerning the License Amendment Request 16-03 related to Alkali-Silica Reaction.

Enclosure 2 provides the revised NextEra Energy Seabrook Updated Final Safety Analysis Report (UFSAR) Section 1.8 and 3.8 markups as referenced in the RAI responses within Enclosure 1.

Enclosure 3 provides the updated methodology document for the analysis of Seismic Category I structures with concrete affected by Alkali-Silica Reaction for Seabrook Station.

Enclosure 4 provides the final Simpson Gumpertz & Heger Document No. 170444-L-003 Rev. 1, "Response to RAI-D8-Attachment 1 Example Calculation of Rebar Stress For a Section Subjected to Combined Effect of External Axial Moment and Internal ASR," which had been previously submitted via SBK-L-17204 (Reference 5) as part of Enclosure 2. The conclusion and results of the revised version remain unchanged and serve to finalize previous statements of preliminary information.

Enclosure 5 provides Simpson Gumpertz & Heger calculations supporting the response provided to RAI D10 regarding cracked section properties used for the evaluation of the RHR vault and Spent Fuel pool walls.

This document does not alter the conclusion in Reference 1 that the change does not involve a significant hazards consideration pursuant to 10 CFR 50.92, and there are no significant environmental impacts associated with this change.

No new or revised commitments are included in this letter.

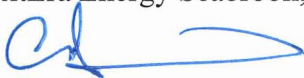
If you have any questions regarding this correspondence, please contact Mr. Kenneth Browne, Licensing Manager, at (603) 773-7932.

I declare under penalty of perjury that the foregoing is true and correct.

Executed on June 7, 2018.

Sincerely,

NextEra Energy Seabrook, LLC



Christopher Domingos
Site Director

Enclosures:

- Enclosure 1 – Response to Request for Additional Information Regarding License Amendment Request 16-03 Related to Alkali-Silica Reaction
- Enclosure 2 – NextEra Energy Seabrook Updated Final Safety Analyses Report Markup of Sections 1.8 and 3.8 – Design of Structures, Components, Equipment and Systems – Design of Category I Structures
- Enclosure 3 – Simpson Gumpertz & Heger Document No. 170444-MD-01, Rev. 1, “Methodology for the Analysis of Seismic Category I Structures with Concrete Affected by Alkali-Silica Reaction,” for Seabrook Station.
- Enclosure 4 – Simpson Gumpertz & Heger Document No. 170444-L-003 Rev. 1, “Response to RAI-D8-Attachment 1 Example Calculation of Rebar Stress For a Section Subjected to Combined Effect of External Axial Moment and Internal ASR.”
- Enclosure 5 - Simpson Gumpertz & Heger calculations supporting the response provided to RAI D10 regarding cracked section properties used for the evaluation of the RHR vault and Spent Fuel pool walls.

cc: D. H. Dorman NRC Region I Administrator
J. C. Poole NRC Project Manager
P. C. Cataldo NRC Senior Resident Inspector
E. H. Gettys NRC Project Manager, License Renewal

Mr. Perry Plummer
Director Homeland Security and Emergency Management
New Hampshire Department of Safety
Division of Homeland Security and Emergency Management
Bureau of Emergency Management
33 Hazen Drive
Concord, NH 03305
perry.plummer@dos.nh.gov

Mr. John Giarrusso, Jr., Nuclear Preparedness Manager
The Commonwealth of Massachusetts
Emergency Management Agency
400 Worcester Road
Framingham, MA 01702-5399
John.Giarrusso@massmail.state.ma.us

Enclosure 1 to SBK-L-18074

Response to Request for Additional Information Regarding License Amendment
Request 16-03 Related to Alkali-Silica Reaction

REQUEST FOR ADDITIONAL INFORMATION (RAI)
REGARDING LICENSE AMENDMENT REQUEST (LAR) 16-03 TO REVISE
CURRENT LICENSING BASIS TO ADOPT A METHODOLOGY FOR THE ANALYSIS
OF SEISMIC CATEGORY I STRUCTURES WITH CONCRETE AFFECTED BY
ALKALI-SILICA REACTION,
NEXTERA ENERGY SEABROOK,
LLC, SEABROOK STATION
DOCKET NO. 50-443

References:

1. Letter SBK-L-16071, dated August 1, 2016, from Ralph A. Dodds III, NextEra Energy Seabrook to USNRC regarding the Request to Adopt a Methodology for Analysis of Seismic Category I Structures with Concrete Affected by Alkali-Silica Reaction (ADAMS Accession No. ML16216A240).
2. Letter SBK-L-17156, dated October 3, 2017, from Eric McCartney, NextEra Energy Seabrook to USNRC regarding the Response to Request for Additional Information Regarding License Amendment Request 16-03 Related to Alkali-Silica Reaction (CACMF8260) (ADAMS Accession No. ML17277A337).
3. Letter SBK-L-17204, dated December 11, 2017, from Eric McCartney, NextEra Energy Seabrook to USNRC regarding the Response to Request for Additional Information Regarding License Amendment Request Related to Alkali-Silica Reaction (CAC MF8260; EPID L-2016-LLA-0007) (ADAMS Accession No. ML17345A641).

Regulatory Requirement

The regulatory requirements below apply generically to all RAIs. Additional regulatory requirements specific to an RAI are stated in the Background Section of the RAI.

Section 3.1 of the Seabrook Station UFSAR discusses how the principal design features for plant structures, systems and components important to safety meet the NRC General Design Criteria (GDC) for Nuclear Power Plants, specified in Appendix A to 10 CFR Part 50 and identifies any exceptions that are taken. This section indicates, in part, that the principal design features for Seabrook structures did include, among others, meeting the requirements of General Design Criteria (GDC) 1, 2 and 4 of 10 CFR 50, Appendix A.

10 CFR Part 50, Appendix A, GDC 1, Quality Standards and Records, requires, in part, structures be designed and tested to quality standards commensurate with the importance of the safety functions to be performed. Where generally recognized codes and standards are used, they shall be evaluated to determine their applicability, adequacy, and sufficiency and shall be supplemented or modified as necessary to assure a quality product in keeping with the required safety function. Based on the LAR and UFSAR Section 3.8, the Seabrook seismic Category I concrete structures, other than containment, were designed in accordance with ACI 318-71, while the containment was designed in accordance with ASME Section III, Division 2, 1975 Edition.

10 CFR Part 50, Appendix B, Criterion III “Design Control” requires, in part, that the design control measures shall assure that applicable regulatory requirements and the design basis, as defined in 10 CFR 50.2 and as specified in the license application, for applicable structures are correctly translated into specifications, drawings, procedures and instructions. These measures shall include provisions to assure that appropriate quality standards are specified and included in design documents and that deviations from such standards are controlled. Design changes, including field changes, shall be subject to design control measures commensurate with those applied to the original design.

RAI-D10 (Follow-up to RAI-D2)

Background

Supplement 4 in the response to RAI-D2 (Reference 3), and Section 5.6 of the Methodology Document, states, “the ratio of cracked over uncracked moment of inertia for flexural behavior can be calculated using ACI 318-71 equation 9-4 or it is acceptable to define the cracked moment of inertia as 50% of the gross moment of inertia.” In the basis for Supplement 4, the licensee states that the ratio of cracked to uncracked (gross) moment of inertia of 0.5 is consistent with the provisions of ACI 318-14 Section 6.6.3.1.2, ASCE 43-05 Table 3-1, and ASCE 4-16 Table 3-2. The staff notes that these cited document sources did not consider ASR-affected concrete. Supplement 5 states, “axial and shear cracking reduces the corresponding stiffness of a structural member. The effect of cracking on reducing the axial and shear stiffness of structural components may be considered in analysis.”

Section 4.4.5 and Appendix A of the Methodology Document describe equations for calculating reduced flexural rigidity, axial rigidity and shear rigidity, respectively, based on (1) effective moment of inertia (I_e) using ACI 318-71 equation 9-4 and the cracking moment (M_{cr}) using the ACI 318-71 code equations 9-4 and 9-5 with modulus of rupture $f_r = 7.5\sqrt{f'_c}$; (2) the cracking strain $\epsilon_{cr} = f_i/E_c$, where $f_i = 5\sqrt{f'_c}$, and (3) shear strain using Reference A6 therein; all of which are from sources that do not consider ASR-affected concrete.

Issue

Reports MPR-4288 and MPR-4273 (Enclosures 5 and 6 of the August 2016 LAR submittal) describe the plant-specific MPR/FSEL Large Scale Test Program (LSTP). The Reinforcement Anchorage Test Program and the Shear Test Program of the LSTP described in Reports MPR-4273 (Section 5.2 and 5.3) and MPR-4288 generated experimental data that provides insights on stiffness (flexural and shear) of ASR-affected test specimens. The results of the LSTP appear to indicate that the stiffness of ASR-affected test specimens is higher than the control specimen and show an increasing trend in stiffness and a delay in the onset of flexural cracking, with an increasing level of ASR-expansion. This behavior is attributed to the ASR-induced prestress effect in the test specimens.

Section 6.3.5 “ASR Effects on Flexural Stiffness” of Report MPR-4288 states, in part: “Results from the tests of ASR-affected specimens demonstrated that the flexural rigidity increases with the severity of ASR. The increased rigidity could be viewed as an improvement for the seismic response.” Section 5.3.4 of Report MPR-4273 states, in part: “Figure 5-10 shows that the stiffness in ASR-affected test specimens is clearly greater than the control

specimen and there is an increasing trend with respect to through-thickness expansion.” Figures 5-5 and 5-7 of the report also provide insights on shear stiffness and flexural stiffness in ASR-affected test specimens.

It appears that results and data from the LSTP was not considered in the proposed procedure for developing cracked section properties in the method of evaluation of Seabrook ASR-affected structures. No technical justification is provided for the applicability and validity of supplements 4 and 5 for ASR-affected concrete. The ‘internal prestressing’ effect noted in the LSTP would result in the observed increase in stiffness (flexural, shear) and delay in the onset of flexural cracking. This is considered in the procedure when developing the ASR load (demand), S_a , in the proposed method of evaluation for ASR-affected concrete; however, it appears that there has been no consideration of the ASR prestressing effect in the proposed procedure for determining reduction in axial, shear and/or flexural rigidity (stiffness) for implementing cracked section properties.

Request:

With regard to ASR effects on stiffness and the implementation of cracked section properties, explain how the relevant experimental data obtained on LSTP specimens are considered in the procedure in the Methodology Document (Section 4.4.5 and Appendix A, and supplements 4 and 5 in Section 5.6) for determining reduced stiffness (flexural, shear, and axial) in implementing cracked section properties. Explain whether and how the ASR prestressing effect is applied to the calculation of cracking moment, cracking strain, and shear strain for ASR-affected members, and provide supporting technical basis.

NextEra Energy Seabrook’s Response to RAI-D10

NextEra Seabrook has revised the “Methodology Document” (Enclosure 3) to modify the cracking moment equation and to clarify the strain definitions for crack initiation for structural members subjected to ASR expansions. The Methodology Document, with revised Sections 4.4.5, 5.6 and Appendix A, provides cracked section properties consistent with stiffnesses observed in the MPR/FSEL Large Scale Test Programs (LSTPs). The revised equation for cracking moment simulates the observed flexural stiffness increases, which are caused by delayed onset of flexural cracking. The Methodology Document revision further clarifies that the tensile and shear crack initiations are based on concrete strain after overcoming the concrete prestressing effects due to ASR expansion.

The completed calculations are not impacted by the changes made in Revision 1 of the Methodology Document because of one or more of the following reasons:

- No structural cracking was used to reduce member stiffness,
- Stiffness reduction due to cracking (tensile, shear, or flexure) is computed based on concrete strain after overcoming compressional pre-straining due to ASR induced prestressing, or based on field measurements using structural crack widths,
- Flexural stiffness reduction in members is not impacted by ASR expansion because:
 - Members have zero or negligible ASR expansions, or
 - Members are under net tension at flexural cracking locations
 - Member stiffness reductions used are confirmed per Revision 1 of the Methodology Document

The Reinforcement Anchorage and the Shear Test Programs described in Report MPR-4273 (Sections 5.3 and 5.2) provide insights on stiffness (flexural and shear) of ASR-affected test specimens. The results of the LSTP indicate that the stiffness of ASR-affected test specimens is higher than the control specimen due to a delay in the onset of flexural cracking with an increasing level of ASR-expansion. This behavior is attributed to the ASR-induced prestressing effect in the test specimens.

1. FLEXURAL STIFFNESS

1.1. MPR/FSEL REINFORCEMENT ANCHORAGE TEST PROGRAM

The Reinforcement Anchorage Test Program, consisting of specimens with different ASR expansion levels, shows the impact of ASR expansion on the flexural stiffness of the specimens:

- MPR-4273, Section 5.3 summarizes the Reinforcement Anchorage Test Program. Figure 5.7 of MPR-4273 provides load-displacement plots for the control test and the test specimen that exhibited the highest level of ASR expansion. This figure shows the control specimen started cracking at very low load relative to that required for flexural yielding. Following crack initiation, the stiffness of the member decreased due to flexural cracking. The stiffness of the ASR-affected specimen was higher than the stiffness of the control specimen above the low applied load at which flexural cracking occurred in the control specimen. At higher loads (following the initiation of flexural cracking), the reduced stiffness of the cracked ASR-affected specimens was approximately 30-35% relative to the uncracked section (MPR-4262, Section 7.4.1), which is consistent with the behavior expected from cracked sections.
- MPR-4262, Section 7.4.2 presents the effects of ASR-induced prestressing on moment-curvature response of a member with no ASR expansion and members with increasing level of ASR expansions. This study concludes with Figure 7-18 showing analytical results that are consistent with the Reinforcement Anchorage Test Program that the onset of flexural cracking is delayed with increasing level of ASR expansions.

In summary, the increased flexural stiffness with the progression of ASR is attributable to the ASR-induced prestressing effect in the test specimens resulting in delayed flexural crack initiation.

1.2. PARAMETRIC STUDY FOR ONSET OF FLEXURAL CRACKING

A parametric study was performed to evaluate the impact of ASR expansion on the onset of flexural cracking for a typical 2 ft thick wall/slab with two different levels of reinforcement ratios as follows:

- a) Member with #8@12in., representing a section with a relatively low reinforcement ratio
- b) Member with #11@6in., representing a section with a relatively high reinforcement ratio

The member is first pre-loaded with ASR expansion values corresponding to Cracking Index (CI) values of 0.0, 0.5, 1.0, 1.5, and 2.0 mm/m. The applied moment on each member is then increased to simulate the section moment-curvature behavior for a member with different level of CI value. The member is analyzed using fiber modeling where concrete fibers are modeled by nonlinear concrete behavior in compression and tension, and reinforcement is also assigned a bilinear elastic-plastic behavior. Figures 1(a) and 1(b) show the increased moment for onset of flexural cracking with increasing ASR expansion (increased CI values). This is consistent with the results of the MPR/FSEL LSTP that attributes the increased stiffness to a delay of flexural cracking onset due to ASR-induced prestressing.

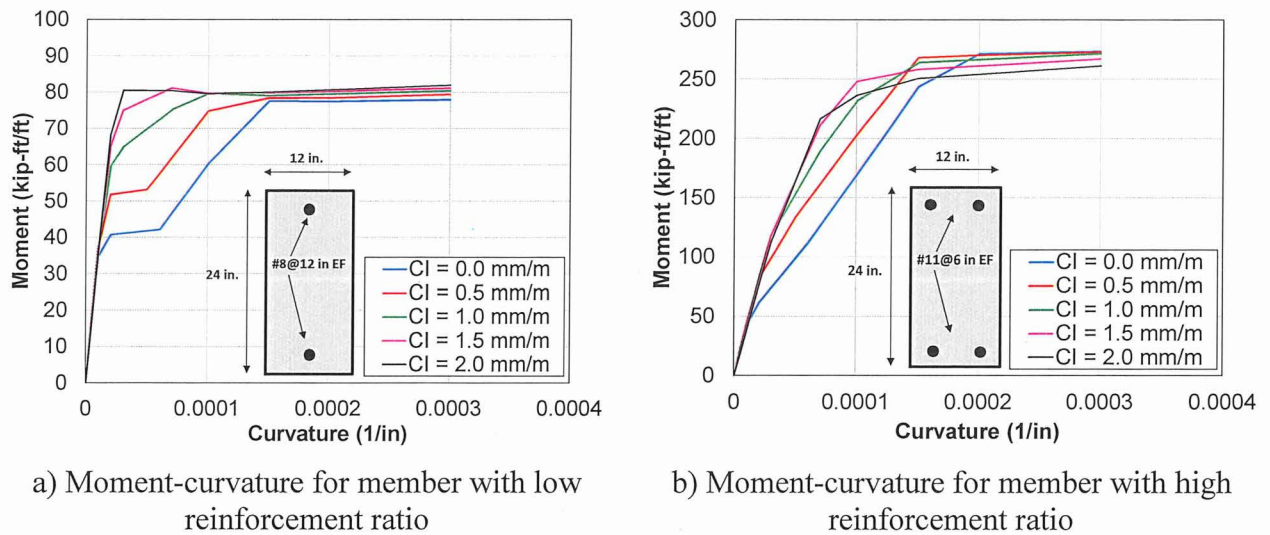


Figure 1: The effect of ASR prestressing on onset of flexural cracking

1.3. REVISION TO METHODOLOGY DOCUMENT FOR FLEXURAL CRACKING

Revision 1 of the Methodology Document requires checking for onset of flexural cracking based on the strain or moment. The finite element modeling procedure described in the Methodology Document consists of modeling the concrete section thickness with a single element and modeling reinforcement with two orthotropic elements. Section 4.4.5 of the Methodology Document is revised to clarify that to initiate cracking from tension, the strain in the concrete element must first overcome the compressive prestressing strain. Similarly, if the cracking moment is to be used for checking the onset of flexural cracking, the prestressing effects of ASR must be overcome. Therefore, equation 9.5 of ACI 318-71, which is also presented in Section 4.4.5 of the Methodology Document, is modified to account for the ASR prestressing behavior as follows:

$$M_{cr} = \frac{(f_r + f_p)I_g}{y_t}$$

where f_r is the concrete modulus of rupture, f_p is the compressive stress in concrete section, I_g is the gross moment of inertia, and y_t is the distance between the extreme tensile fiber and the centerline of the cross-section. The additional term " f_p " delays the formation of flexural cracks based on the presence of any compressive stress, due to prestressing effect of ASR or any other load effects, in the section. The value of f_r is calculated using Equation 9-5 of ACI 318-71 as:

$$f_r = 7.5\sqrt{f'_c}$$

where f'_c is the specified compressive strength of the concrete. Table 1 presents the flexural cracking calculated using the modified equation for M_{cr} defined above for the same two members with relatively high and low reinforcement ratios.

Table 1: Cracking Moment Accounting for ASR Prestressing

Member with Low Reinforcement Ratio			Member with High Reinforcement Ratio		
CI (mm/m)	Initial stress in concrete (psi)	Mcr (kip-ft/ft)	CI (mm/m)	Initial stress in concrete (psi)	Mcr (kip-ft/ft)
0	0	39.4	0	0	39.4
0.5	75.7	46.7	0.5	246	63.1
1	151.4	54.0	1	482	85.7
1.5	227.1	61.2	1.5	707	107.3
2	302.7	68.5	2	921	127.9

Table 1 shows that the cracking moment increases with increasing ASR expansion level, which is consistent with the results of parametric studies presented in Figure 1 and with the conclusions of the Reinforcement Anchorage Test Program.

In conclusion, the revised Methodology Document provides sufficient detail and equations to simulate the onset of flexural cracking accounting for concrete compression due to ASR expansion and is consistent with observations from the Reinforcement Anchorage Test Program of delayed onset of cracking due to increasing ASR expansion.

2. SHEAR CRACKING

2.1. MPR/FSEL LARGE SCALE SHEAR TEST PROGRAM

The Shear Test Program, consisting of specimens with different ASR expansion levels, shows the impact of ASR expansion on the shear stiffness of the specimens:

- MPR-4273 Section 5.2 presents the shear test program. Figure 5.5 of the report provides normalized shear stress-deflection plots for the shear test specimens. This figure shows that the formation of diagonal cracking that represents shear capacity as defined by ACI 318 increases with increasing ASR expansion. The apparent increase in shear capacity caused by ASR is attributed to the prestressing effects due to ASR expansion.
- MPR-4262, Volume II, Appendix J, contains the laboratory reports on the Shear Test Program, which includes a quantitative evaluation of the change in shear capacity with increasing ASR. It concludes that the shear strength of the samples increased with the increased ASR expansion level due to ASR-induced prestressing in the specimens.

In summary, the shear cracks form at higher loading values as the level of ASR expansion increases. The delay in the formation of shear cracks is due to overcoming the compressive strain in concrete due to ASR-induced prestressing behavior.

2.2. ANALYTICAL STUDY FOR ONSET OF SHEAR CRACKING

An analytical study was performed to evaluate the impact of ASR expansion on the onset of shear cracking for a simply supported beam as depicted in Figure 2. The study considered a simplistic problem by using average stresses (compared to expected stress profiles) to demonstrate the effect pre-compression has on shear crack initiation. Two cases are considered:

- a) A member with no internal ASR expansion
- b) A member with internal ASR that induces pre-compression in the section

The applied load V induces an average shear stress in the concrete section of τ_{xy} (different values for Case a and Case b), and ASR expansion causes an average pre-compressive axial stress in concrete section of $\sigma_x = -f_p$ due to the restraining effect of rebars as schematically shown in Figure 2. Note that for the purpose of this study, flexure stresses need not be considered because only the average axial stress is needed; therefore flexural stresses are not computed and not depicted in Figure 2.

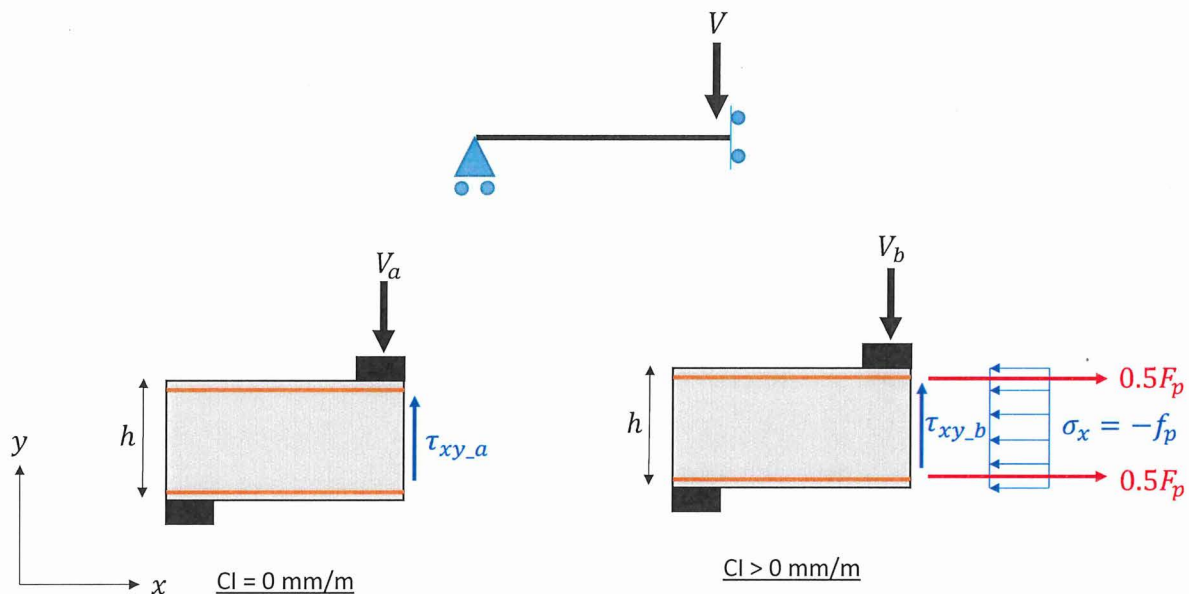


Figure 2: Induced stress due to shear and ASR expansion

The average axial and shear stresses in the concrete section can be found by satisfying the equilibrium conditions (per unit width) in x and y as follows.

<u>Case a (CI = 0 mm/m)</u>	<u>Case b (CI > 0 mm/m)</u>
$\sigma_x = 0, \sigma_y = 0, \text{ and } \tau_{xy_a} = \frac{V_a}{h}$	$\sigma_x = -f_p = -\frac{F_p}{h}, \sigma_y = 0, \text{ and } \tau_{xy_b} = \frac{V_b}{h}$

In both cases, a diagonal shear crack forms when the principal tensile stress at a location within the member reaches the tensile strength of concrete. To examine the effect of pre-compression on onset of shear cracking, the above equations are transformed into the principal axis as:

<u>Case a (CI = 0 mm/m)</u>	<u>Case b (CI > 0 mm/m)</u>
$\sigma_1 = \frac{\sigma_x + \sigma_y}{2} + \sqrt{\left(\frac{\sigma_x - \sigma_y}{2}\right)^2 + \tau_{xy}^2} = \tau_{xy_a}$ $\sigma_3 = \frac{\sigma_x + \sigma_y}{2} - \sqrt{\left(\frac{\sigma_x - \sigma_y}{2}\right)^2 + \tau_{xy}^2}$ $= -\tau_{xy_a}$	$\sigma_1 = \frac{-f_p}{2} + \sqrt{\frac{f_p^2}{4} + \tau_{xy_b}^2}$ $\sigma_3 = \frac{-f_p}{2} - \sqrt{\frac{f_p^2}{4} + \tau_{xy_b}^2}$

At the onset of shear cracking, the first principal stress (σ_1) reaches the cracking stress. To demonstrate the effect of ASR prestressing on shear strength, the following two assumptions are made for Case a (zero internal expansion):

- A single continuous, straight shear crack forms at failure
- Assume the shear stress τ_{xy_a} at failure reaches to $2\sqrt{f'_c}$ per ACI 318-71 ($\sigma_1 = \tau_{xy_a} = 2\sqrt{f'_c}$).

Considering the above assumptions, the ratio $\frac{\tau_{xy_b}}{\sqrt{f'_c}}$ is calculated for different CI values for a typical 2 ft thick member reinforced with #8@12 in. and the result is depicted in Figure 3. The figure implies that by increasing the CI value, the applied external load that causes the shear crack increases. This is consistent with the conclusion made in the MPR/FSEL Shear Test Program, both conceptually and quantitatively.

Although both the MPR findings and the analytical solution presented herein show an increase in ultimate shear capacity of a member affected by internal ASR, the SGH Methodology Document conservatively does not allow for an increase in ultimate shear capacity, and only accounts for such an effect in determining formation of shear cracks and calculating shear stiffness reduction.

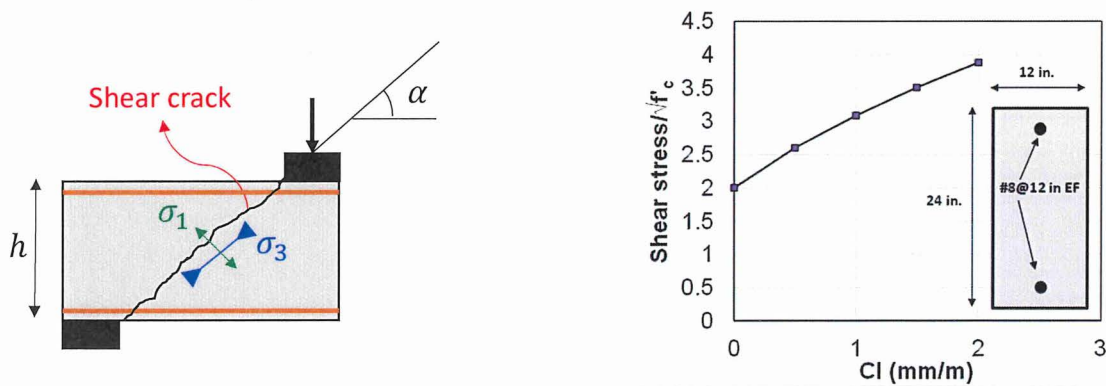


Figure 3: The effect of ASR prestressing on onset of shear cracking

Finally, since there is a one to one correspondence between stress and strain, using the strain values per the SGH Methodology Document to check the onset of shear cracking naturally captures the effect of pre-compression in the reinforced concrete section due to internal ASR expansion; and the calculated reduction in shear stiffness accounts for the effect of pre-compression.

2.3. REVISION TO THE METHODOLOGY DOCUMENT FOR SHEAR CRACKING

Revision 1 of the Methodology Document, Section 4.4.5 clarifies that the onset of cracking occurs when the strain overcomes the pre-straining (due to ASR prestressing) and reaches the cracking strain.

3. STIFFNESS REDUCTION DUE TO CRACKING FOR COMPLETED STRUCTURAL EVALUATIONS WITH ASR DEFORMATION

The structural evaluation including ASR loadings for the containment interior, and sixteen (16) other Seismic Category I structures have been completed. The completed structural evaluation calculations have been performed in accordance with Revision 0 of the Methodology Document. The completed calculations include Stage One, Two and Three evaluations. Revision 1 of the Methodology Document includes a modified equation to compute the flexural cracking moment that accounts for ASR-induced prestressing. This revision also clarifies that the strain for onset of cracking includes overcoming the pre-strain in concrete due to ASR-induced prestressing. Review of the completed calculations confirms that changes made for Revision 1 of the Methodology Document will not impact the previously-completed structural evaluations or the conclusions of the calculations, for one of the following reasons:

- No cracking was used to reduce member stiffness

The following completed evaluations did not consider any structural cracking:

- Equipment Hatch Missile Shield
 - CEVA and RCA Tunnel
 - Electrical Manholes (W01, W02, W09, W13 & W16)
 - Containment Internals
 - Electrical Cable Tunnel
 - Condensate Storage Tank Enclosure
 - Main Steam & Feedwater Pipe Chase -West & Personnel Hatch
 - Service Water Access Vault
- Stiffness reduction due to structural cracking is computed based on strain after overcoming the ASR pre-compression effects or is based on field observations

The evaluation of structures under this condition considers stiffness reduction and the onset of cracking based on: (a) strain in the element representing the concrete in the finite element model that already accounts for the pre-straining due to ASR prestressing per the modeling procedures described in the Methodology Document (CEB and FSB); and (b) strain for reducing the finite element stiffness is based on field measurement of structural crack widths (RHR building). The following structural evaluations consider the strain for cracking initiation:

- Containment Enclosure Building
 - RHR Equipment Vault
 - Fuel Storage Building
- Stiffness reduction due to flexural cracking is not impacted by ASR expansion

The calculations listed below use stiffness reduction due to flexural cracking based on the cracking moment defined in the Methodology Document, Section 4.4.5, Revision 0 (Equation 9.5 of ACI 318-71). The members where flexural stiffness reductions were considered either had: zero to negligible ASR expansion (less than $CI=0.1$ mm/m), or the cracking occurs at locations with net tension. When a member does not have ASR expansion or where flexural cracking is occurring when the section is in net tension, the modified cracking moment defined in Revision 1 of the Methodology Document will not change the calculations. When a member has negligible ASR expansion, the impact of using the pre-compression in the concrete per the modified cracking moment defined in Revision 1 of the Methodology Document is negligible or small and will not change the intent and conclusion of the calculation. The evaluations of the following structures use flexural cracking stiffness as discussed above:

- Pre-Action Valve Building
- Control Room Make-up Air Intake
- Main Steam & Feedwater Pipe Chase - East & Hydrogen Recombiner Room

The RHR and FSB structural calculations consider flexural stiffness reductions that are confirmed as described below to meet Revision 1 of the Methodology Document:

- RHR Equipment Vault

The RHR Vault calculation was completed prior to issuing the Methodology Document Revision 0, but this calculation conforms to this methodology except for calculating the flexural cracked stiffness about the vertical axis for exterior walls. The east exterior wall of the RHR at elevations close to the foundation level of the Primary Auxiliary Building (PAB) can crack for the static factored load combination (controlling load combination). The ASR expansion creates net compression in the concrete section. The RHR vault Calculation used the first equation (applicable to walls) in ACI 318-14 Table 6.6.3.1.1(b) to calculate the flexural cracking stiffness to be 35% of the gross section properties. Attachment 1 to this RAI response (See Enclosure 5) provides the calculation of the effective cracked section for this wall using the modified cracking moment equation provided in Section 4.4.5 of Revision 1 of the Methodology Document. The effective cracked section of the east wall of RHR building is 23% of the gross section, which is smaller than the value used in the Calculation. Therefore, the calculation does not require revision.

- Fuel Storage Building

The FSB calculation uses cracked section properties for pool walls that are in compression. The ASR expansion of the pool walls creates net compression in the concrete section in both horizontal and vertical directions. In the horizontal direction, the restraint from concrete backfill against pool walls ASR expansion and expansion of

concrete backfill creates net compression in some of the pool walls. Appendix I of this calculation uses the cracking moment equation defined in the Revision 0 of the Methodology Document for the static load combination but limits the section cracking to 25% of the gross section property. The original design calculations used fully cracked section properties for the fuel pool walls for operating thermal loading conditions, which are lower than the cracked section properties of 25% of the gross section properties used in this calculation. Attachment 2 to this RAI response (See Enclosure 5) provides the calculation of the effective cracked section using the modified cracking moment equation provided in Revision 1 of the Methodology Document. Results show that when considering operating thermal loading plus the compressive effects of ASR, the cracked section is 16% and 30% of the gross section properties in the vertical and horizontal directions, respectively. The pool walls are expected to crack more extensively in the vertical direction than 25% gross section properties used in the FSB calculation, therefore the computed demands were conservative. The pool walls are expected to crack less in the horizontal direction than the 25% gross section properties used in the FSB calculation. The highest D/C ratio reported in the FSB calculation for the horizontal direction of the pool walls is 0.5 due to interaction of axial compression and bending demands. Attachment 2 to this RAI response shows that the D/C ratio would increase from 0.5 to 0.6 when considering a cracked section stiffness of 30% of the gross section properties. In summary the calculated pool wall D/C for axial-flexure for moment about the horizontal axis, which is the governing wall evaluation, will not be changed by using the modified equation for the cracked moment defined in Revision 1. The small increase in the D/C for moment about vertical axis is still much less than the governing D/C for moment about the horizontal axis. Therefore, the conclusions for the FSB are not changed and the calculation does not require revision.

RAI-D11 (Follow-up to RAI-D8)

Background

- 1) 10 CFR Part 50.9, "Completeness and accuracy of information," requires, in part, that "information provided to the Commission by an applicant for a license or by a licensee ... shall be complete and accurate in all material aspects." Calculation results submitted in support of the RAI-D8 response (Tables 1 and 2 of Attachment 2 of Reference 3) included footnotes stating "preliminary results, may change during checking and approval," and "calculation pending final review."
- 2) Parametric Study 1, in response to RAI-D8 (Reference 3), in part concludes, "stresses and strains in steel rebar are less than the elastic limits at service load conditions, provided that ASR strain is less than 2 mm/m." The staff notes that this is consistent with the approximate strain level at which rebar is expected to yield (i.e., $f_y/E_s = 60 \text{ ksi}/29000 \text{ ksi} = 0.0021 \text{ mm/mm}$ or 2.1 mm/m). ASR in-plane expansion exceeding this magnitude could be indicative of rebar yielding or slip due to loss of bond between concrete and steel reinforcement. Potential yielding or slip of the reinforcement could be indicative of marked change in behavioral response of a structure, could impact structural capacity, or could

render assumptions of linear elastic behavior in the structural analyses incorrect (including UFSAR Section 3.7 seismic analysis).

Issue

- 1) It is not clear that the calculations submitted in support of RAI-D8 are finalized and thus are “complete and accurate in all material aspects.”
- 2) ASR in-plane expansion could increase with ASR progression under service conditions, and based on field monitoring; a structure may enter or include ASR Severity Zone 4 (CI greater than 2 mm/m). There is no criteria or upper limit of in-plane expansion in the method of evaluation that would trigger an action for evaluation of the implications of potential rebar yielding or slip under service conditions if field monitoring indicates a structure has entered Severity Zone 4. It is not clear if and how a structure will be evaluated for rebar yielding or slip if field monitoring data indicates a structure is in ASR Severity Zone 4.

Request

- 1) Confirm that the information provided in support of RAI-D8 is complete, final and accurate, or provide a finalized version of the supporting information.
- 2) Explain how a structure will be evaluated in the proposed method of evaluation for the implications of rebar yielding or slip under service conditions (as discussed in the background) if field monitoring data indicates a structure has entered, or includes, ASR Severity Zone 4 (CI greater than 2 mm/m) or provide a technical justification if no evaluation is planned.

NextEra Energy Seabrook’s Response to RAI D-11

- 1) Enclosure 4 provides the final Simpson Gumpertz & Heger Document No. 170444-L-003 Rev. 1, “Response to RAI-D8-Attachment 1 Example Calculation of Rebar Stress For a Section Subjected to Combined Effect of External Axial Moment and Internal ASR,” which had been previously submitted via SBK-L-17204 (Reference 5) as Enclosure 2. The conclusion and results of revised version remain unchanged and serves to finalize previous statements of preliminary information.
- 2) Sections 3.1.1 and 3.1.1.1 of the Methodology Document have been revised to address actions that should be performed when the CI or CCI value exceeds 2 mm/m (Zone 4). The revised Section 3.1.1 provides the requirements for Seismic Category I structures when CI or CCI value exceeds 2.0 mm/m, and Section 3.1.1.1 provides the requirements if the ASR in the Containment Building reaches Zone 4 as defined in Table 2 of the Methodology Document. The revised Methodology Document recommends consideration of performing petrography to confirm the status of ASR expansion prior to using the measured in-plane strain to characterize ASR expansion for structural analysis and evaluation. If the in-plane ASR strain as confirmed by petrography exceeds 2.0 mm/m, then the possibility that local yielding has occurred while the structural response

remains within elastic behavior shall be evaluated. If the in-plane ASR strain is confirmed to exceed 2.0 mm/m in a large region, then consider retrofit, repair to mitigate the possible reinforcement slippage due to near surface delamination, or further analysis to qualify the structure.

Rebar slip, which is a different failure mechanism than rebar yielding, is not expected to occur as a result of ASR expansion. Specifically, the MPR/FSEL Reinforcement Anchorage Test Program investigated this failure mode and concluded that ASR had no effect up to the maximum through-thickness and volumetric expansion levels in the test series. However, rebar slippage may occur if there is a near surface delamination (i.e., loss of reinforcement cover) over a large area due to structural deformation or distress.

RAI-D12

Background

Supplement 3 in the response to RAI-D2 (Reference 3) and Section 5.6 of the Methodology Document state, “the shear-friction capacity for members subjected to net compression can be calculated using procedures defined in Building Code Requirements for Structural Concrete (ACI 318-83 Section 11.7.7).”

With regard to use of portions of subsequent code editions or addenda, as a regulatory example, 10 CFR 50.55a(g)(4)(iv) requires that portions of editions or addenda may be used, provided all related requirements of the respective editions or addenda are met.

Issue

Code subsections often include caveats or related requirements that may impact other subsections within the same broader section. The technical basis for Supplement 3 compares ACI 318-83 Section 11.7.7 to the equivalent requirement in ACI 318-71 (Section 11.15); however, the basis does not address other portions of Section 11.7 or explain why Section 11.7 does not need to be used in its entirety.

Request

Provide a technical justification for the use of Section 11.7.7 that addresses why additional related requirements in 11.7 do not need to be included in Supplement 3, or update Supplement 3 to reference ACI 318-83 Section 11.7 in its entirety.

NextEra Energy Seabrook's Response to RAI D-12

Methodology Document, Revision 1, Supplement 3 has been updated to invoke Section 11.7 of ACI 318-83.

To limit the scope of changes to the original code design basis, Supplement 3 of the Methodology Document, Revision 0, invoked only ACI 318-83 Section 11.7.7 rather than the entirety of Section 11.7 because Section 11.7.7 was the only technical change to the shear-friction provisions of ACI 318-71 Section 11.15 [3] that was relevant to the evaluation of the Seismic Category I reinforced concrete structures at Seabrook Station. For completeness, Revision 1 of the Methodology Document invokes all of ACI 318-83 Section 11.7.

RAI-D13

Background

During a site audit the week of March 19, 2018, the staff reviewed calculation SGH 170443-CA- 01, Rev. 0 (Seabrook FP# 101166), which implements the guidance in the "Methodology Document" (MD) for a portion of the Electric Tunnel structure. The calculation determined that the structure (embedded wall against concrete backfill with no field observed signs of distress) is adequate for operability; however, when applying the procedure outlined in the MD to account for potential ASR expansion effects of concrete backfill in areas with no observed signs of ASR distress, the structure will not meet the ACI 318-71 code requirements. It appears either the structure needs to be modified to meet code requirements, or the MD needs to be revised to address cases with structures against concrete backfill that show no signs of distress.

Issue

It is unclear from reviewing the calculation if this will result in a change to the proposed method of evaluation related to structures against concrete backfill. It is also unclear if this situation is unique to the Electric Tunnel structure, or if other calculations concluded that the associated structures did not meet code requirements when analyzed with the proposed methodology to account for potential ASR expansion of concrete backfill for embedded structure segments with no observed signs of distress.

Request

Explain if the results of this calculation will result in a revision to the MD. If the MD will be revised, provide the revision with an explanation of the technical basis of the changes. Also, explain whether applicability of the revised proposed methodology is specific to the electrical tunnel structure, or whether it is generically applicable to any structure with embedded walls against concrete backfill with no observed signs of distress.

NextEra Energy Seabrook's Response to RAI D-13

Methodology Document Section 4.4.3.2 has been revised to provide an alternative approach to evaluate embedded walls which are expected to first form flexural cracks before shear cracks under increasing lateral load and currently show no sign of visible structural cracking. This alternate method defines the method for estimating the lateral pressure induced by ASR expansion of concrete backfill to be applied to these types of walls. This alternative method allows the concrete backfill pressure to be reduced under the following conditions:

- Limit the pressure to the lower value corresponding to any structural crack initiation (shear or flexure) for the factored load combinations with inclusion of threshold factor
- Increase the monitoring frequency (maximum 2-month interval)
- Design a retrofit or shoring for implementation after observation of any structural crack

This is an acceptable approach that provides sufficient margin for use with these types of walls of Seismic Category I structures, because:

- These walls when subjected to lateral pressure are expected to form flexural cracking before initiation of shear cracking for the in-situ condition. Flexural cracking is ductile behavior and is the expected behavior for flexural reinforced concrete members,
- The demand to capacity (D/C) ratios for shear may exceed the corresponding D/C ratio for flexure for factored load combinations when considering the larger load factor on ASR demands and lower shear strength reduction factor compared to flexure strength reduction factor,
- ASR growth is a displacement controlled slow process and as a wall deforms and cracks some of the pressure induced by concrete backfill pressure may be reduced,
- Increased inspection and having a designed retrofit or shoring provide assurance that any shear behavior can be contained in a timely manner.

RAI-D14

Background

10 CFR Part 50.34(b), "Final safety analysis report," describes what a licensee must include in a final safety analysis report. This includes "a description and analysis of the structures, systems and components of the facility, with emphasis upon performance requirements, the bases, with technical justification therefore, upon which such requirements have been established, and the evaluations required to show that safety function will be accomplished."

10 CFR Part 50.71(e), "Maintenance of records, making of reports," requires, in part, that licensees shall submit updates to the final safety analysis report (FSAR) to include "all the changes necessary to reflect information and analyses submitted to the Commission by the applicant or licensee ... since the last update to the FSAR."

- 1) The response to RAI-M2, Request 1, and RAI-M3, including Appendix B of the response (Reference 2), summarizes (i) corroboration studies of the correlation methodology in MPR-4153, and (ii) periodic assessment of ASR expansion behavior that will be conducted in the future to confirm that ASR expansion behavior in Seabrook structures is similar to that observed in the MPR/FSEL LSTP specimens.
- 2) The response to RAI-D2 (Reference 3) references a Methodology Document that defines the analysis and evaluation procedures for the analysis described in the original LAR. Sections 3.1, 4.2, 4.3 and 4.4 of the Methodology Document describe how the proposed ASR load is developed and Section 5.6 of identifies five 'supplements,' which are described as "deviations to the codes of record."

Issue

- 1) Verifying similar ASR expansion behavior between the MPR/FSEL LSTP specimens and Seabrook structures is part of the technical justification for the expansion limits and acceptance criteria developed in the MPR/FSEL LSTP. The future actions associated with the corroboration study and the periodic assessment of ASR behavior appear to be key aspects of this justification; however, these supporting actions are not described in the FSAR update markup for the LAR.
- 2) The codes of record, and any supplements or deviations, explain how structures are analyzed and how their safety functions will be accomplished and form an important part of the changes to the method of evaluation described in the FSAR; however, the development of the proposed ASR load and the 'supplements' to the Seabrook code of record are not described in the FSAR update markup for the LAR.

Request

- 1) Provide an UFSAR markup that includes a summary description of the proposed corroboration study and the periodic behavior assessment, including timeline, or explain why it is unnecessary to identify these items in the UFSAR as part of the proposed method of evaluation.
- 2) Provide an UFSAR markup that includes a summary description of how the ASR load, including the load due to expansion of concrete backfill, is determined and a complete description of the code 'supplements' identified in response to RAI-D2. Alternatively, explain why it is unnecessary to explain how this Seabrook unique load is developed and to identify the code deviations in the UFSAR as part of the proposed method of evaluation.

NextEra Energy Seabrook's Response to RAI D-14

- 1) The UFSAR markup of Table 3.8-18 that includes a summary description of the proposed corroboration study and the periodic behavior assessment is provided in Enclosure 2.
- 2) The UFSAR markup of Section 3.8.1.3(f) that describes how the ASR load is determined, including the load due to expansion of concrete backfill, is provided in Enclosure 2. The UFSAR markup to Section 3.8 that identifies the code deviations/supplements are also included in Enclosure 2.

Enclosure 2 to SBK-L-18074

NextEra Energy Seabrook Updated Final Safety Analyses Report Markup of Sections
1.8 and 3.8 – Design of Structures, Components, Equipment and Systems – Design of
Category I Structures

SEABROOK STATION	DESIGN OF STRUCTURES, COMPONENTS, EQUIPMENT AND SYSTEMS	Revision 19
UFSAR	Design of Category I Structures	Section 3.8 Page 109

Seismic Category I structures with concrete affected by ASR shall meet the acceptance criteria of the Codes of Record, with the following list of deviations which are considered as supplements to the Codes of Record.

<u>Supplement Number</u>	<u>Description</u>
	Reference NextEra Energy Seabrook FP# 101196
1	Consideration of ASR loads: The UFSAR load and load combinations Tables 3.8-1, 3.8-14, and 3.8-16 were modified in LAR 16-03 to consider the ASR load and load factors for calculating the total demands on structures affected by ASR.
2	Code acceptance criteria: Strength of reinforced concrete sections affected by ASR can be calculated using the Codes of Record (ASME 1975 and ACI 318-71) and the minimum specified design concrete strength, provided that ASR expansion is within the limits provided in Table 3.8-18 for through-thickness and volumetric expansion.
3	Shear-friction capacity for members subjected to net compression: The shear-friction capacity for members subjected to net compression can be calculated using procedures defined in Building Code Requirements for Reinforced Concrete (ACI 318-83 Section 11.7).
4	Flexural Cracked Section Properties: Reductions of the gross cross-sectional moment of inertia for analysis shall be computed considering the presence of cracking and the prestressing effects of ASR; alternatively, 50% of the gross cross-sectional moment of inertia can be used.
5	Axial and Shear Cracked Section Properties: Axial and shear cracking reduces the corresponding stiffness of a structural member. The effect of cracking on reducing the axial and shear stiffness of structural components may be considered in analysis.

SEABROOK STATION UFSAR	DESIGN OF STRUCTURES, COMPONENTS EQUIPMENT AND SYSTEMS	Revision: 9
	TABLE 3.8-18	Sheet: 1 of 1

TABLE 3.8-18 ASR EXPANSION LIMITS FOR STRUCTURAL LIMIT STATES

Structural Limit State	ASR Expansion Limit (4)
Shear	Through-thickness: See FP#101020 Section 2.1 (Ref 7) (2) (5) Volumetric: See FP#101050 Appendix B (Ref 8) (3)
Flexure	
Reinforcement Anchorage	
Anchors	See FP#101020 Section 2.1 (Ref 7)
Compression	(1)

- (1) Compressive load from ASR in the direction of reinforcement is combined and evaluated with other applied compressive loads.
- (2) The through-thickness expansion limit for shear, flexure and reinforcement anchorage presented in FP#101020 (Reference 7) are different. The most limiting value is applied as the acceptance criterion for through-thickness expansion monitoring among these structural limit states.
- (3) The maximum observed maximum volumetric expansion for shear, flexure and reinforcement anchorage identified in FP#101050 (Reference 8), Appendix B, Section 5 are different. The most limiting value is applied as the acceptance criterion for volumetric expansion monitoring among these structural limit states.
- (4) NextEra Energy Seabrook will perform the following actions to confirm that expansion behavior at Seabrook Station aligns with observations from the MPR/FSEL test programs and that the associated expansion limits are applicable:
 - a. Conduct assessments of expansion behavior to confirm that expansion behavior at Seabrook Station is comparable to what was observed in the MPR/FSEL test programs and to check margin for future expansion. Alignment confirms that the MPR/FSEL test program limits listed above are appropriate and applicable. NextEra Energy Seabrook completed the first expansion assessment in March 2018; subsequent expansion assessments will be performed every ten years, using the approach provided in FP#101050 (Reference 8) Appendix B.
 - b. Corroborate the modulus-expansion correlation used to calculate pre-instrument through-thickness expansion (FP#100918; Reference 9)) for 20 percent of extensometer locations no later than 2025 and 10 years thereafter, using the approach provided in FP#101050 (Reference 8) Appendix C. The corroboration study involves obtaining new cores from the vicinity of 20 percent of the extensometers, determining the elastic modulus, and using the correlation to estimate total through-thickness expansion. This value will be compared to the expansion determined using the sum of the differential expansion measured by the extensometer and the pre-instrument expansion (using the correlation) at the time the extensometer was installed. Corroboration between the expansion values

calculated using the modulus-expansion correlation with the expansion values determined from the extensometer and the original modulus-expansion result validates use of the correlation and confirms applicability of the MPR/FSEL test program limits.

- (5) Through-thickness expansion is determined as the sum of expansion measured using installed instrumentation (e.g. extensometers) and the expansion that occurred prior to installation of the instrumentation ("pre-instrument" expansion). Pre-instrument through-thickness expansion is determined using the methodology defined in FP#100918 (Reference 9).

SEABROOK STATION UFSAR	DESIGN OF STRUCTURES, COMPONENTS, EQUIPMENT AND SYSTEMS Design of Category I Structures	Revision 19 Section 3.8 Page 20
---------------------------------------	---	--

(Section 3.8.1.3 continued)

(f) Alkali Silica Reaction Loads (S_a)

These are structural effects caused by ASR expansion of concrete. ASR loads are passive and therefore occur during normal operation, shutdown conditions, and concurrently with all extreme environmental loads. For Containment, only the effects of ASR expansion occurring in reinforced concrete structural members are considered. (Expansion of concrete backfill is not considered as the concrete backfill does not interact directly with Containment.)

Calculation of the ASR demands are described below; detailed guidance on calculation of the loads is provided in "Methodology for the Analysis of Seismic Category I Structures with Concrete Affected by Alkali-Silica Reaction," (FP# 101196).

Demands associated with internal ASR expansion are applied to structural components as strain loads in the concrete model based on in-plane expansion measurements. The internal ASR expansion is applied uniformly through the cross-sectional thickness of the structural components (e.g., walls, slabs, foundations, etc.) unless otherwise justified. Application of ASR expansion to the concrete elements that are restrained by reinforcement elements results in compression of the concrete and tension in the reinforcement.

The in-plane ASR expansions can be adjusted when some or all of the cracks at an ASR monitoring grid are shown to be caused by a mechanism other than internal ASR in the reinforced concrete member (e.g., shrinkage, thermal, pressurization tests of Containment, etc.). The adjusted in-plane expansion values are computed by excluding the widths of cracks determined not to be caused by ASR.

SEABROOK STATION	DESIGN OF STRUCTURES, COMPONENTS, EQUIPMENT AND SYSTEMS	Revision 19 Section 3.8
UFSAR	Design of Category I Structures	Page 109

(Section 3.8.3.3 continued)

a. Design Loads

The definitions of the loads used in the design of the internal structures include the following:

1. Normal Plant Startup, Operation and Shutdown Loads

Normal loads are those loads encountered during normal plant start-up, operation and shutdown. They include the following:

(a) Dead Loads (D)

Dead loads are all permanent gravity loads including the weight of concrete walls and slabs, structural framing, piping, cable and cable trays, permanent equipment, and static pressures of liquids. **Concrete creep, shrinkage, and swelling are considered for structures affected by the expansion of concrete from alkali-silica reaction (ASR). See Subsection 3.8.4.6 for a description of the effects of ASR on concrete.**

(b) Live Loads (L)

Live loads include any movable equipment loads and other loads which vary in intensity and/or occurrence. Live loads are present only during shutdown conditions, and do not govern the design of any components.

(c) Operational Thermal Loads (T_o)

The temperature gradient through the walls under normal operating conditions is considered in the design. For a discussion of minimum and maximum operating temperatures, see Subsection 6.2.1.

(d) Operational Pipe Reactions (R_o)

These are pipe reactions due to thermal conditions existing in the piping during normal operation or shutdown. They are based on the most critical transient or steady-state condition.

(e) Alkali-Silica Reaction Loads

These are structural effects caused by ASR. These loads are considered if ASR is observed or identified in concrete structures internal to Containment. ASR loads are passive and therefore occur during normal operation, shutdown conditions,

and concurrently with all extreme environmental loads. For Containment internal structures, only the effects of ASR expansion occurring in reinforced concrete structural members are considered. (Expansion of concrete backfill is not considered as the concrete backfill does not interact with Containment internal structures.) Calculation of these demands is described below; detailed guidance on calculation of the loads is provided in "Methodology for the Analysis of Seismic Category I Structures with Concrete Affected by Alkali-Silica Reaction," (FP# 101196).

Demands associated with internal ASR expansion shall be applied to structural components as strain loads based on in-plane expansion measurements. The demands associated with internal ASR expansion shall be applied uniformly through the cross-sectional thickness of the structural components (e.g., walls, slabs, foundations, etc.) unless otherwise justified.

Large in-plane expansion measurement values may not necessarily imply large ASR expansions. If some or all of the cracks at an ASR monitoring grid are shown to be caused by a mechanism other than internal ASR in the reinforced concrete member (e.g., shrinkage, thermal, pressurization tests of Containment, structural cracks due to external loads, etc.), then the in-plane expansion measurements should be adjusted accordingly. The adjusted in-plane expansion value shall be computed by excluding the widths of cracks determined not to be caused by ASR.

SEABROOK STATION	DESIGN OF STRUCTURES, COMPONENTS, EQUIPMENT AND SYSTEMS	Revision 19
UFSAR	Design of Category I Structures	Section 3.8 Page 8

(b) Primary Equipment Supports

The primary equipment supports transmit loads to the fill mat, to the primary and secondary shield walls and to the operating floor slab. For a discussion of these loads and of the design criteria for the supports see Subsection 5.4.14.

(c) Load Considerations for Internal Structures

(1) Time dependent loads such as thermal effects, creep and shrinkage do not have any significant effects on the internal structures since the accident loads are generally resisted in tension by the reinforcing steel. In addition, the accident loads are short-term, once-occurring loads, which have negligible creep effects.

(2) The containment structure functions as an independent structure with complete physical separation from the internal structures, and therefore there are no loading interactions between the two.

(3) Compartmentalization is considered in the design of the internal structures by using the peak subcompartment differential pressures, plus a safety margin. This is further discussed in Subsection 6.2.1.2.

(4) Self-Straining Loads

The internal concrete structures are analyzed for deformation caused by ASR and are designed to withstand the effects of ASR expansion, creep, shrinkage, and swelling.

b. Load Combinations

Various load combinations are considered in design to determine the greatest strength requirements of the structure. Where varying loads occur, the combinations producing the most critical loading are used. Basic combinations in the design of the containment internal structures are given in Table 3.8-14. These load combinations are in agreement with Subsections II.3 and II.5 of the Standard Review Plan for Subsection 3.8.3 of the UFSAR. The factors which are to be applied to allowable stresses have been transposed and applied as load factors instead, resulting in acceptance criteria as indicated in the table. Two categories of loading conditions and criteria are used in the design of the containment internal structures as described below.

SEABROOK STATION UFSAR	DESIGN OF STRUCTURES, COMPONENTS, EQUIPMENT AND SYSTEMS Design of Category I Structures	Revision 19 Section 3.8 Page 114
---------------------------------------	---	--

1. Normal Load Conditions

Normal load conditions are those encountered during testing and normal operation. They include dead load, live load, **Alkali Silica Reaction (ASR) loads**, and anticipated transients or test conditions during normal and emergency startup and shutdown of the Nuclear Steam Supply, Safety and Auxiliary Systems. Normal loading also includes the effect of an Operating Basis Earthquake. Normal load conditions are referred to in Division 2 as service load conditions.

Under each of these loading conditions, the structure is designed so that stresses will be within the elastic limits. Design assumptions are presented in Subsection 3.8.3.4 and stress limitations are presented in Subsection 3.8.3.5.

2. Unusual Load Conditions

Unusual load conditions are those conditions resulting from combinations of the LOCA, SSE and OBE, high-energy pipe failures, and live and dead loads. They are referred to in Division 2 as factored load conditions.

For each of the unusual loading combinations, the internal structures are designed to remain below their ultimate capacity so that the behavior of structural components is in the small deformation elastic range. Design assumptions are presented in Subsection 3.8.3.4 and stress limitations are presented in Subsection 3.8.3.5.

SEABROOK STATION	DESIGN OF STRUCTURES, COMPONENTS, EQUIPMENT AND SYSTEMS	Revision 19
UFSAR	Design of Category I Structures	Section 3.8
		Page 136

(Section 3.8.4.3a.1 continued)

(a) Dead Loads (D)

Dead loads are all permanent gravity loads including, but not limited to, concrete walls and slabs, structural framing, piping, cable and cable trays, permanent equipment and miscellaneous building items. Hydrostatic pressures of liquids are also included in this category. **Concrete creep, shrinkage, and swelling are considered for structures affected by the expansion of concrete from alkali-silica reaction (ASR). See Subsection 3.8.4.6 for a description of the effects of ASR on concrete.**

(b) Live Loads (L)

Live loads are all temporary gravity loads including but not limited to normal snow loads, conventionally distributed and concentrated floor loads, and movable equipment loads, such as cranes and hoists.

Equipment operating loads and impact factors are the greater of those recommended by the manufacturer or the applicable building codes.

Unusual snow load (L_s), which is greater in magnitude than normal snow load, was also used where applicable. Lateral earth pressures due to soil backfill (H) were used where applicable. Three types of lateral earth pressure loading, active, at rest and passive, were considered, with pressures determined by acceptable theories of soil mechanics.

(c) Operational Thermal Loads (T_o)

These are the thermal effects and loads occurring during normal operating or shutdown conditions, based on the most critical transient or steady-state condition.

(d) Operational Pipe Reactions (R_o)

These are the pipe reactions occurring during normal operating or shutdown conditions, based on the most critical transient or steady-state condition.

(e) Alkali-Silica Reaction Loads

These are structural effects caused by ASR. ASR loads are passive and therefore occur during normal operation, shutdown conditions, and concurrently with all extreme environmental loads. The structural effects from ASR expansion include demands associated with internal ASR expansion of structural components, and, as applicable, the pressure exerted on embedded structures by ASR expansion of the concrete backfill. Calculation of these demands is described below; detailed guidance on calculation of the loads is provided in "Methodology for the Analysis of Seismic Category I Structures with Concrete Affected by Alkali-Silica Reaction," (FP# 101196).

Internal ASR Expansion of Structural Components

Demands associated with internal ASR expansion shall be applied to structural components as strain loads based on in-plane expansion measurements. The demands associated with internal ASR expansion shall be applied uniformly through the cross-sectional thickness of the structural components (e.g., walls, slabs, foundations, etc.) unless otherwise justified.

Large in-plane expansion measurement values may not necessarily imply large ASR expansions. If some or all of the cracks at an ASR monitoring grid are shown to be caused by a mechanism other than internal ASR in the reinforced concrete member (e.g., shrinkage, thermal, structural cracks due to external loads, etc.), then the in-plane expansion measurements should be adjusted accordingly. The adjusted in-plane expansion value shall be computed by excluding the widths of cracks determined not to be caused by ASR.

External Load from ASR Expansion of Concrete Backfill

ASR expansion of concrete backfill can create an external pressure on the walls and slabs of structures and can lead to structural deformation, rigid body displacement of structures, and relative displacements between adjacent structures. ASR expansion of concrete backfill cannot easily be measured directly. External pressure on the walls and slabs due to ASR expansion of concrete backfill is determined indirectly through field measurements of structural displacements and deformations, and/or through the use of conservative assumptions, as described in FP# 101196. The magnitude of concrete backfill pressure can be adjusted by correlating the structural analysis deformation under in-situ conditions to field observations.

ASR expansion of concrete backfill is considered for structures

embedded in concrete backfill without an isolation gap. This approach is conservative as shrinkage of the concrete backfill and structure and possible deterioration of the waterproofing backboard would result in separation.

SEABROOK STATION	DESIGN OF STRUCTURES, COMPONENTS, EQUIPMENT AND SYSTEMS	Revision 19
UFSAR	Design of Category I Structures	Section 3.8 Page 154

3.8.6 References

1. Wilson, E.L., "Structural Analysis of Axisymmetric Solids," AIAAJ. Vol. 3, No. 12 (1965) pp. 163-182.
2. Wilson, E.L., "A Digital Computer Program for the Finite Element Analysis of Axisymmetric Solids with Orthotropic, Nonlinear Material Properties," November 1969.
3. Duchon, N.B., "Analysis of Reinforced Concrete Membrane Subject to Tension and Shear," ACI Journal, September, 1972, pp. 578-583.
4. Wilson, E.L. and Nicholl, R.E., "Application of the Finite Element Method to Heat Conduction Analysis," Journal of Nuclear Engineering and Design, Vol. 4, 1966.
5. Alexandria, S. C., Effects of Irradiation of Concrete, Final Results, Research Reactor Division UKAEA, Harwell, AERE-R-4490, December 1963.
6. Foreign Print 100716, Impact of ASR on Structures.
7. MPR-4288, Revision 0, "Seabrook Station: Impact of Alkali-Silica Reaction on the Structural Design Evaluations," July 2016. FP#101020
8. MPR-4273, **Revision 1**, "Seabrook Station – Implications of Large-Scale Test Program Results on Reinforced Concrete Affected by Alkali-Silica Reaction." FP#101050
9. **MPR-4153, Revision 3, "Seabrook Station – Approach for Determining Through-Thickness Expansion from Alkali-Silica Reaction." FP#100918**
10. **SGH Document 170444-MD-01, Revision 1, "Methodology for the Analysis of Seismic Category I Structures with Concrete Affected By Alkali-Silica Reaction." FP#101196**

Enclosure 3 to SBK-L-18074

Simpson Gumpertz & Heger Document No. 170444-MD-01, Rev. 1, "Methodology for the Analysis of Seismic Category I Structures with Concrete Affected by Alkali-Silica Reaction" for Seabrook Station

DOCUMENT APPROVAL SHEET

SIMPSON GUMPERTZ & HEGER



Engineering of Structures
and Building Enclosures



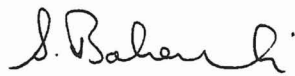
Client: NextEra Energy Seabrook Project No. 170444.00
Project: Susceptibility Evaluation of Category I Structures at Seabrook Station, Seabrook, NH

Document No.: 170444-MD-01
Document Type: Methodology Document
Title: Methodology for the Analysis of Seismic Category I Structures with
Concrete Affected By Alkali-Silica Reaction
Number of Pages Including This Page: 71

Descriptions:

This document provides methodology for analyzing and evaluating Seismic Category I structures with concrete affected by ASR.

<u>Revision</u>	<u>Descriptions</u>
0	Initial Document
1	Revised to address NRC questions and comments during March 2018 audit.

<u>Revision</u>	<u>Preparer / Date</u>	<u>Verifier / Date</u>	<u>Approver / Date</u>
0	Andrew Sarawit 12/7/2017	Michael Mudlock 12/7/2017	Said Bolourchi 12/7/2017
1	 Andrew Sarawit 5/31/2018	 Michael Mudlock 5/31/2018	 Said Bolourchi 5/31/2018

**METHODOLOGY FOR THE ANALYSIS OF SEISMIC CATEGORY I
STRUCTURES WITH CONCRETE AFFECTED BY ALKALI-SILICA
REACTION**

SGH Document No. 170444-MD-01

Revision No. 1

31 May 2018

TABLE OF CONTENTS

1.	INTRODUCTION.....	1
1.1	Purpose	1
1.2	Scope	2
1.3	Document Organization	3
1.4	Overview of Methodology	3
	1.4.1 Analytical and Evaluation Methods.....	3
	1.4.2 Effects of ASR on Reinforced Concrete Material Properties.....	4
2.	CHARACTERISTICS AND MEASUREMENT OF ASR	5
2.1	Cracking Index (CI).....	5
2.2	Pin-to-Pin In-Plane Expansion Measurements.....	6
3.	LOADS AND LOAD COMBINATIONS	7
3.1	ASR Loads	7
	3.1.1 ASR Expansion of Structural Components	7
	3.1.2 ASR Expansion of Concrete Backfill.....	9
3.2	ASR Load Factors and Load Combinations	10
	3.2.1 Containment Structure	10
	3.2.2 Containment Internal Structures.....	10
	3.2.3 Other Seismic Category I Structures	11
	3.2.4 Foundations for Seismic Category I Structures.....	11
3.3	Self-Straining Loads other than ASR	11
	3.3.1 Creep	11
	3.3.2 Shrinkage.....	12
	3.3.3 Swelling.....	13
4.	ANALYSIS APPROACH.....	14
4.1	Selection of Starting Stage	14
4.2	Stage One Screening Evaluation.....	14
	4.2.1 Field Observations to Support Stage One Analyses	14
	4.2.2 Non-ASR Demands for Stage One Analyses.....	15
	4.2.3 ASR Demands for Stage One Analyses	15
4.3	Stage Two Analytical Evaluation.....	17
	4.3.1 Field Observations to Support Stage Two Analyses.....	17
	4.3.2 Non-ASR Demands for Stage Two Analyses.....	18
	4.3.3 ASR Demands for Stage Two Analyses	18
4.4	Stage Three Detailed Evaluation	20
	4.4.1 Field Observations to Support Stage Three Analyses	20
	4.4.2 Non-ASR Demands for Stage Three Analyses	20
	4.4.3 ASR Demands for Stage Three Analyses.....	21
	4.4.4 Correlation of Analysis Model to Field Observations.....	26
	4.4.5 Refined Analytical Methods	26
5.	ACCEPTANCE CRITERIA	29
5.1	Containment Structure.....	30
	5.1.1 General	30

5.1.2	Concrete	30
5.1.3	Reinforcing Steel.....	30
5.1.4	Liner Plate and Liner Anchorage System	31
5.1.5	Stability	31
5.2	Containment Internal Structures	31
5.2.1	Normal Load Conditions	31
5.2.2	Unusual Load Conditions	31
5.2.3	Deformations.....	31
5.3	Other Seismic Category I Structures.....	32
5.3.1	Normal Load Conditions	32
5.3.2	Unusual Load Conditions	32
5.3.3	Deformations.....	32
5.3.4	Stability	32
5.4	Foundations for Seismic Category I Structures	32
5.5	Acceptance Criteria for Isolation Gaps.....	33
5.6	Supplement to Code of Record Acceptance Criteria.....	34
6.	ASR THRESHOLD LIMITS AND MONITORING	37
6.1	Methodology to Account for Potential Future ASR Expansion.....	37
6.2	ASR Threshold Monitoring for Stage One Evaluations.....	39
6.3	ASR Threshold Monitoring for Stage Two Evaluations.....	39
6.4	ASR Threshold Monitoring for Stage Three Evaluations	39
7.	EVALUATION FOR APPROACHING THRESHOLD LIMITS	41
7.1	Stage One Evaluation.....	41
7.2	Stage Two Evaluation.....	41
7.3	Stage Three Evaluation	42
8.	REFERENCES	43
9.	TABLES	45
10.	FIGURES.....	52

LIST OF APPENDICES

Appendix A Determination of Cracked Section Properties

LIST OF TABLES

Table 1 – Evaluation Criteria for Suspected ASR Cracking45
Table 2 – ASR Severity Zones [14]46
Table 3 – ASR-Related Strain Loads for Analysis of the Containment Structure [14]46
Table 4 – Load Combinations for Evaluation of Containment Structure (Modified from Table 3.8-1 of UFSAR).....47
Table 5 – Load Combinations for Evaluation of Containment Internal Structures (Modified from Table 3.8-14 of UFSAR to Include ASR Loads and Load Factors)48
Table 6 – Load Combinations for Evaluation of Seismic Category I Structures other Than Containment (Modified from Table 3.8-16 of UFSAR to Include ASR Loads and Load Factors)49
Table 7 – Structure Deformation Monitoring Requirements50
Table 8 – Acceptance Criteria for Stability against Overturning, Sliding and Flotation50
Table 9 – Field Observations and Measurements for Susceptibility Evaluations51

LIST OF FIGURES

Figure 1. Structural Cracks due to Differential ASR Expansion in the Structure.52
Figure 2. Structural Cracks due to Differential ASR Expansion in the Concrete Backfill.53
Figure 3. Structural Cracks due to Concrete Backfill Expansion.54
Figure 4. Flow Chart Schematic for Computing Lateral Concrete Backfill Pressure due to ASR.
.....55
Figure 5. Threshold Monitoring56

SYMBOLS AND ABBREVIATIONS

ACI	American Concrete Institute
AR	Action Request
ASME	American Society of Mechanical Engineers
ASR	Alkali-Silica Reaction
ASTM	American Society for Testing and Materials
CCI	Combined Cracking index
CI	Cracking Index
f_c'	Compressive strength of concrete
FSEL	Ferguson Structural Engineering Laboratory
LAR	License Amendment Request
LOCA	Loss-Of-Coolant Accident
MPR	MPR Associates, Inc.
NextEra	NextEra Energy Seabrook
NRC	Nuclear Regulatory Commission
OBE	Operating Basis Earthquake
SGH	Simpson Gumpertz & Heger Inc.
SMP	Structural Monitoring Program
SRSS	Square Root of the Sum of the Squares
SSE	Safe-Shutdown Earthquake
UFSAR	Updated Final Safety Analysis Report
WO	Work Order

REVISION HISTORY

- Revision 0: Initial document.
- Revision 1: Revised to address NRC questions and comments from the March 2018 audit. Revisions are identified by a vertical line in the left margin. Note that minor editorial changes are not identified by a vertical line in the left margin.

1. INTRODUCTION

1.1 Purpose

The purpose of this methodology document is to provide a method for analyzing and evaluating Seismic Category I structures with concrete affected by ASR. This analysis methodology is in accordance with the approach outlined in License Amendment Request 16-03 (LAR) [1], which NextEra Energy Seabrook (NextEra) submitted to the NRC in 2016. Details of these analysis and evaluation procedures permit all Seismic Category I structures to be evaluated using the same methodology, and provide clear guidance to engineers performing the structural evaluation with sufficient procedural details to be repeatable by other engineers.

NextEra initially identified pattern cracking typical of alkali-silica reaction (ASR) in the B Electrical Tunnel in 2009, and, subsequently, in several other Seismic Category I structures at Seabrook Station. NextEra informed the Nuclear Regulatory Commission (NRC) of this discovery and then performed a root cause investigation into the presence of ASR at Seabrook Station. The root cause investigation concluded that the original concrete mix designs used a coarse aggregate that was susceptible to ASR. An interim structural assessment was completed in 2012 [2]. The evaluation concluded that the reinforced concrete structures at Seabrook Station remain suitable for continued service for an interim period given the extent of ASR identified at that time. The evaluation noted that additional testing was required to verify that some structures satisfy ACI 318-71 [3] code requirements for shear and reinforcement anchorage (development and lap length). NextEra has since completed MPR/FSEL large-scale test programs [4] and used the test results and literature to develop guidance for evaluating ASR-affected reinforced concrete structures at Seabrook Station [5].

Seismic Category I structures other than the Containment Structure were originally designed to meet the requirements of ACI 318-71. The Containment Structure is a reinforced concrete structure that was designed in accordance with the requirements of Section III of the American Society of Mechanical Engineers (ASME) Boiler & Pressure Vessel Code (1975 Edition) [6]. Neither ACI 318-71 nor the ASME code include provisions for the analysis and evaluation of structures affected by ASR. The analysis approach established in this methodology document properly accounts for the effects of ASR when performing the building evaluations. Following the methodology and meeting the acceptance criteria that are established herein will demonstrate

that the structure meets the intent of the original design codes of record and achieves the structural safety reliability indices consistent with the original design. This methodology document also provides a list of deviations from the codes of record and justification that those deviations meet the intent of the original codes of record.

Development of ASR loads based on field measurements of in-plane ASR expansion within the structure and assessment of concrete backfill ASR expansion establishes a set of loads applicable to the time concurrent with the measurements. The potential for future ASR expansion is considered in the methodology by stipulating procedures for reevaluation of the structure for an increased ASR load to account for potential future ASR expansion. When the evaluation of a structure based on current ASR demands consistent with current inspection data indicates that remaining design margin exists, the evaluation to confirm the current design margin shall be performed with ASR loads amplified by a threshold factor such that the controlling demands on the structure are equal to (or slightly less than) the capacity of the structure.

The threshold factor represents the reserve design margin in the structure for accommodating increasing ASR future demands. Once the threshold factor is established, the structure is monitored, and quantitative measurements and qualitative observations are compared to the specified limit. If the quantitative measurements or qualitative observations approach the corresponding specified limits, then further structural evaluations in accordance with procedures specified in this methodology document are performed to reevaluate the structure in order to increase the threshold limit without decreasing code inherent safety factors, or structural modifications may be made to alleviate the concern for the approaching threshold limit.

1.2 Scope

The scope of this document is to define a methodology for consistent and repeatable evaluation of the concrete structures and foundations of Seismic Category I structures at Seabrook Station that are impacted by self-straining loads including ASR. This methodology for structural evaluation includes the use of dimensions, details, and notes on the structural design drawings. This document defines the material properties, loads and load combinations, analysis methods, acceptance criteria, threshold factor, and actions to follow when the structural monitoring program shows that the ASR growth is reaching the threshold limits. Because of flexibility and tolerances in structural steel construction, structural deformations due to ASR expansion are considered to be small enough to not impact the design or integrity of the steel structures supported on the

reinforced concrete structures or foundations affected by ASR. Possible impacts of concrete deformations due to ASR on equipment are beyond the scope of this document.

1.3 Document Organization

This methodology document is organized into following sections:

- Section 1: Introduction – Provides an overview of the analysis and evaluation methodology and defines the purpose and scope.
- Section 2: Characteristics and Measurement of ASR – Provides background information on effects of ASR on reinforced concrete material properties and measurement methods.
- Section 3: Loads and Load Combinations – Discusses the addition of self-straining loads (creep, shrinkage, and swelling) to the original design loads and the addition of ASR load to the design load combinations.
- Section 4: Analysis Approach – Provides methodologies for Stage One, Two, and Three analyses which include field observations to support the analysis, calculation for non-ASR and ASR demands, analysis method, and correlation of analysis results to field observations.
- Section 5: Acceptance Criteria – Defines the acceptance criteria for evaluation of Seismic Category I structures and identifies deviations from the original codes of record and the reason and justification for those deviations.
- Section 6: ASR Threshold Limits and Monitoring – Discusses methodology to account for potential future ASR expansion and determine the ASR threshold limit, and methods to monitor the structures.
- Section 7: Evaluation for Approaching Threshold Limits – Discusses the evaluation procedures and decision options to alleviate the concern for structures approaching ASR threshold limits.
- Section 8: References – Provides a complete list of cited references.

1.4 Overview of Methodology

1.4.1 Analytical and Evaluation Methods

A three-stage analysis approach shall be used for analyzing and evaluating Seismic Category I structures, as identified in the Seabrook LAR 16-03. Each stage applies more sophisticated methods and uses additional field measurement data of ASR expansion to improve the rigor of the analysis. The analysis and evaluation of each structure may begin at any stage and, if

necessary, shall progress to a higher analysis stage. The three analysis stages are described in Section 4.

Each structure shall be analyzed in accordance with the required stage of analysis. The total demands, including the ASR demands amplified by threshold limits, will be compared to the acceptance criteria described in Section 5. The threshold monitoring limits will be determined based on the structural evaluation calculations that are specific for each structure and shall be included in the Structural Monitoring Program (SMP), as discussed in Section 6. The evaluation for approaching the ASR threshold limits are discussed in Section 7.

1.4.2 Effects of ASR on Reinforced Concrete Material Properties

As reported in the technical literature [7] and observed in the MPR/FSEL test programs [4], one effect of ASR is that material properties of unreinforced concrete are reduced. Specifically, compressive strength exhibits a relatively shallow decrease as a function of ASR progression, while elastic modulus and tensile strength are much more sensitive. However, for reinforced concrete structures, this decrease in material properties may not result in a decrease in structural performance, due to the chemical prestressing effect that also results from ASR [7]. For the limit states of shear and flexure, results from the MPR/FSEL test programs suggest that the effects of confinement from the reinforcement more than compensate for degradation of material properties when ASR progression is within the range observed in the test specimens [5].

From the MPR studies referenced above, it is concluded that for analyses of reinforced concrete structures at Seabrook Station, the elastic modulus of concrete shall be computed using the minimum specified design compressive strength, and no reduction shall be taken for ASR-related damage. Material properties for analysis and evaluation of Seismic Category I reinforced concrete structures shall be consistent with those used in the original design calculations [8] and those defined in the project specifications and drawing notes.

2. CHARACTERISTICS AND MEASUREMENT OF ASR

Alkali-silica reaction (ASR) is a chemical reaction between the alkali content in cement paste and reactive silica minerals contained in some types of concrete aggregates. The reaction produces a gel that swells if moisture is present. Typical characteristics of ASR include some combination of expansion and displacement of elements, a characteristic pattern of interconnected and closely-spaced cracks (which can be influenced by the stress state of the concrete), surface discoloration of cracks, ASR gel exudations, and an environment conducive to the development of ASR. ASR can cause concrete cracking, structural deformations and stresses, changes in unreinforced concrete strength and/or stiffness, and external loads on other adjacent structures.

ASR can be identified in the field through qualitative visual observations of common symptoms as reported in industry guidelines [9] and [10]. These guidelines include a classification system for the Condition Survey, which establishes the correlation between ASR features and probability of ASR. The field evaluation of the “likelihood” of ASR can be classified as “No”, “Possible”, or “Likely”. The specific visual features that are suggestive or indicative of ASR are summarized in Table 1 (taken from Table 2 of CSA International document A864-00 [10]).

Field Inspectors shall use the above-mentioned industry guidelines to identify the likelihood of ASR. Locations for which the criteria indicate that ASR is “Possible” or “Likely” shall be accounted for in the structural evaluation unless petrographic examinations of concrete samples extracted from that location show otherwise. Petrographic investigation can confirm ASR features, such as identification of aggregate types and reactive components, general characterization of microcracking, presence of reaction and/or the presence of an alteration rim around aggregate particles, and presence of gel or other deposits in voids.

Quantitative measurement of ASR in-plane expansion can be made by summation of crack widths or by measurement of change in distance between two points as explained in the following subsections.

2.1 Cracking Index (CI)

The cracking Index (CI) is a quantitative measurement of ASR in-plane progression obtained by crack width summation and normalization. It includes measurement and summation of crack widths along a set of perpendicular reference lines on the surface of a concrete element being

investigated. The sum of crack widths is normalized by the length of the reference lines to determine the CI in-plane expansion. The CI measurement captures surface crack widths from all sources of cracking and thus can be influenced by cracks from phenomena other than from ASR. The Combined Cracking Index (CCI) is the weighted average of the CI in the two measured in-plane directions. A typical ASR-monitoring location produces two CI values (in-plane perpendicular directions) and one CCI value. CI and CCI values are typically reported in mm/m. The CCI provides a reasonable approximation of true engineering strain and is acceptable for monitoring in-plane strain [11] and [4]. Measurement of concrete expansion can be approximated by crack width summation because concrete has low capacity for expansion before cracking. While true engineering strain is represented by the sum of material elongation and crack widths, the crack width term generally dominates the overall expansion. The Seabrook SMP uses CI to establish baseline strain in ASR deformed concrete.

2.2 Pin-to-Pin In-Plane Expansion Measurements

In-plane expansion measurements are quantitative measurements of the distance between two points (pin-to-pin) installed on the surface of a concrete component using a removable strain gage. Pin-to-pin in-plane expansion is computed as the change in length-measurement values recorded at different times.

Pin-to-pin measurements determine changes in ASR expansion more precisely than CI measurements determine changes over the duration of the monitoring period, since they are performed using a calibrated mechanical device capable of measuring changes in length as small as 0.0001 in. However, pin-to-pin in-plane expansion measurements are only able to capture strains that occur after the gage points are installed in the concrete surface after initial (baseline) measurements are made. This makes pin-to-pin in-plane expansion measurements ideal for monitoring changes in strain, but they require the use of other measurements (such as CI in-plane expansion) to approximate the strains in the concrete prior to the baseline in-plane expansion measurements. Similar to CI measurements, pin-to-pin expansion measurements only define strains at the surface of the concrete and could be influenced by cracks or deformation from loads other than ASR unless these effects are excluded from the measurement.

Total in-plane expansion can be determined by combining expansion up to installation of the pins from CI measurements with the change in expansion from the pin-to-pin expansion measurements.

3. LOADS AND LOAD COMBINATIONS

The original design loads are defined in the UFSAR [12] and SD-66 [13], which provides the structural design criteria for Seabrook Station structures. Evaluation of Seismic Category I structures shall consider all original design loads plus loads due to ASR. Other self-straining loads, including creep, shrinkage, and swelling, shall also be considered, if significant. When the deformed shape due to sustained dead load is small, then the creep effect that is proportional to this deformation is also small. The swelling can be considered to be small when the waterproofing membrane effectively stops intrusion of water into the structure. Evaluation for the original construction loads is not required since the buildings have already been built.

ASR loads, including ASR expansion of structural components and expansion of concrete backfill, are discussed in Section 3.1. Load factors and load combinations including ASR loads are provided in Section 3.2. Other self-straining loads, including creep, shrinkage, and swelling, are discussed in Section 3.3.

3.1 ASR Loads

3.1.1 ASR Expansion of Structural Components

Demands associated with internal ASR expansion shall be applied to structural components as strain loads based on CI measurements and supplemented by pin-to-pin in-plane expansion measurements, if available. The demands associated with internal ASR expansion shall be applied uniformly through the cross-sectional thickness of the structural components (walls, slabs, foundations, etc.) unless otherwise justified. An average strain value may be used when ASR measurements are available on opposite sides of a structural component.

In the MPR/FSEL test programs, control over the loads imposed on the test specimens allowed isolation of ASR as the primary driver for expansion. At Seabrook Station, the cracking condition may be complex due to phenomena and loads other than ASR expansion such as:

- Concrete shrinkage,
- Thermal effects related to high temperatures during the initial concrete placement or during plant operation,
- Construction or equipment loads,
- Pressurization tests of the Containment Structure,

- Structural cracks not indicative of ASR cracking that are defined in Table 1,
- Structural cracks due to differential internal ASR expansions in different regions (see Figure 1 for example), and
- Structural cracks due to externally applied loads from concrete backfill expansion causing differential movements between adjacent buildings or regions of buildings (see Figures 2 and 3 for example).

Large CI measurement values therefore may not necessarily imply large ASR expansions. If some or all of the cracks at an ASR monitoring grid are shown to be caused by a mechanism other than internal ASR in the reinforced concrete member (such as crack types listed above), then the CI value or pin-to-pin expansion measurements should be adjusted accordingly. The adjusted CI value and pin-to-pin expansion shall be computed by excluding the widths of cracks determined not to be caused by ASR. This determination may be through petrography, detailed examination of cracking features, review of operating conditions and history, analytical evaluation for causes other than ASR (e.g. thermal, shrinkage), or other justified means. If the CI or CCI values, after adjustment to exclude structural cracks, exceed 2.0 mm/m, then petrography on extracted cores shall be considered to confirm the status of ASR expansion (if any) prior to using these values for ASR loading of concrete structural members. If CI or CCI values after adjustment and petrographic confirmation exceed 2.0 mm/m, then the possibility of local yielding while the overall structural response remains elastic should be evaluated as discussed in Section 5.3. If the in-plane ASR strain is confirmed to exceed 2.0 mm/m in a large region, then consider retrofit, repair to mitigate the possible reinforcement slippage due to near surface delamination, or further analysis to qualify the structure. ASR loads shall be applied to Seismic Category I structures with concrete affected by ASR as described in the following subsections.

3.1.1.1 Containment Structure

ASR in the Containment Structure shall be categorized into Severity Zones based on the magnitude of ASR, as defined in Table 2. CI values supplemented by pin-to-pin measurements (if available) that are used for severity zone categorization should be adjusted to exclude cracking due to repeated pressure testing of the Containment Structure. Although present cracking features may conform to some of the Table 1 definitions, review of the historical crack mapping after pressurization is important to better define the ASR cracking level. The adjusted CI for Containment is currently at Zone I of Table 2. The possibility that the Containment ASR CI value increases to Zone IV is very unlikely, but if it does, then the possibility of reinforcement yielding shall be evaluated as discussed in Section 5.1.1. The magnitude of the applied ASR strain loads

shall be based on the Severity Zone and the analysis stage, as provided in Table 3 with consideration of using bounding values.

3.1.1.2 Containment Internal Structures

For Containment Internal Structures (CIS), the CI values supplemented by pin-to-pin measurements (if available) shall be used for regions identified as having ASR expansion. The ASR in-plane expansion shall be used to calculate ASR demands for regions impacted by ASR (if any).

3.1.1.3 Other Seismic Category I Structures

For Seismic Category I structures other than the Containment Structure, the CI value supplemented by pin-to-pin measurements (if available) recorded within a particular region shall be used to compute the ASR strain loads from expansion of the structure for that particular region. ASR in-plane expansion can be adjusted when justified to exclude cracks determined not be caused by ASR as discussed in Section 3.1.1. If multiple measurement grids are located within a region, an average measurement value shall be used to compute the ASR strain loads for that region.

3.1.1.4 Foundations for Seismic Category I Structures

Similar to Seismic Category I structures other than the Containment Structure, foundations for Seismic Category I structures shall use the CI value supplemented by pin-to-pin measurements (if available) to represent the ASR strain loads, above. ASR in-plane expansion can be adjusted when justified to exclude cracks determined not be caused by ASR as discussed in Section 3.1.1. If multiple measurement grids are located within a region, an average measurement value shall be used to compute the ASR strain loads for that region. For regions that are not accessible for making field measurements or observations, bounding ASR strain loads shall be considered using available values from other regions within the foundation or within the structure in close proximity to the foundation.

3.1.2 ASR Expansion of Concrete Backfill

ASR expansion of the concrete backfill can create an external pressure on the walls and slabs of structures and lead to structural deformation, rigid body displacement of structures, and relative displacements between adjacent structures. The ASR expansion of the concrete backfill cannot easily be measured directly. External pressure on the walls and slabs due to concrete backfill

ASR expansion shall be determined indirectly through field measurements of structural displacements and deformations, and/or through the use of conservative assumptions, as discussed in more detail in Section 4.4.3.2. The magnitude of concrete backfill pressure can be adjusted by correlating the structural analysis deformation under in-situ conditions to field observations.

3.2 ASR Load Factors and Load Combinations

Load factors for ASR loads are based on the work presented in [14]. These load factors were developed to maintain the level of structural reliability provided by the original codes of record load combinations. ASR load factors and load combinations shall be used to compute demands for Seismic Category I structures with concrete affected by ASR as described in the following subsections.

3.2.1 Containment Structure

Load combinations for evaluation of the Containment Structure are provided in Table 4. This is the same table provided in the UFSAR (Table 3.8-1) but with revision to include load factors for ASR loading. The Containment Structure is designed using the ASME Boiler and Pressure Vessel Code [6], which generally implements a working stress design approach and uses load factors of 1.0 for service-level load combinations. Many loads, including ASR, are assigned a load factor of 1.0; however, load factors greater than 1.0 are used for some loads in severe environmental, extreme environmental, and abnormal load combinations. The Containment Structure is not exposed to earth pressures, wind loads, or snow loads, and therefore does not include such loads in its combinations.

3.2.2 Containment Internal Structures

Load combinations for evaluation of Containment Internal Structures are provided in Table 5. This is the same table provided in the UFSAR (Table 3.8-14) but with revision to include load factors for ASR loading. The Containment Internal Structures were designed using the strength design provisions of ACI 318-71, which uses load factors that are greater than 1.0 for normal load combinations as defined in the UFSAR for reinforced concrete structures. Load factors are generally equivalent to 1.0 for unusual load combinations (i.e., load combinations including LOCA, SSE, OBE, high-energy pipe failures, etc.). Containment Internal Structures are not exposed to earth pressures, wind loads, and snow loads, and therefore do not include such loads in their combinations.

3.2.3 Other Seismic Category I Structures

Load combinations for evaluation of Seismic Category I structures other than the Containment Structure are provided in Table 6. This is the same table provided in the UFSAR (Table 3.8-16) but with revision to include load factors for ASR loading. These structures were designed using the strength design provisions of ACI 318-71, which uses load factors that are greater than 1.0 for normal load combinations as defined in the UFSAR for reinforced concrete structures. Load factors are generally equivalent to 1.0 for unusual load combinations (i.e., load combinations including SSE or tornado loads) as defined in the UFSAR.

3.2.4 Foundations for Seismic Category I Structures

Load combinations for evaluation of foundations for Seismic Category I Structures, excluding the foundation of the Containment Structure, are provided in Table 6. These structures were designed using the strength design provisions of ACI 318-71, which uses load factors that are greater than 1.0 for normal load combinations as defined in the UFSAR for reinforced concrete foundations. Load factors are generally equivalent to 1.0 for unusual load combinations as defined in the UFSAR.

Load combinations for evaluation of the Containment Structure foundation are provided in Table 4. The Containment Structure foundation is designed using the ASME Boiler and Pressure Vessel Code [6], which generally implements a working stress design approach and uses load factors of 1.0 for service-level load combinations. Many loads, including ASR, are assigned a load factor of 1.0; however, load factors greater than 1.0 are used for some loads in severe environmental, extreme environmental, and abnormal load combinations.

3.3 Self-Straining Loads other than ASR

Self-straining loads, such as creep, shrinkage, and swelling, shall be considered as dead loads if field observations or analysis has identified that their load effects could be significant.

3.3.1 Creep

Creep due to sustained loads causes additional deflections beyond those which occur when loads are first placed on the structure. Such deflections are influenced by temperature, humidity, curing conditions, age at time of loading, quantity of compression reinforcement, magnitude of the sustained load, and other factors [3]. For most cases of long-term deflection in statically

determinate structures, the gradual time-change of stresses due to creep is negligible, but time changes of strains may be significant. In statically indeterminate structures, redistribution of internal forces may arise [15]. Creep does not apply any net forces on the reinforced concrete section but instead causes the stresses in the section to redistribute over time. The redistribution from creep causes a portion of the stress in concrete to relax and the stresses in the reinforcement to change proportionally.

The stress redistribution caused by creep can be excluded in the cases described below, when doing so is conservative for the specific conditions under evaluation.

- For sections where sustained loads cause net compression, creep causes a portion of the compression load to shift from the concrete to the reinforcement over time. In such cases, it is conservative to neglect this redistribution because it relieves compression demand in concrete and reduces the tensile demand in the reinforcement.
- For sections where sustained loads cause net tension, creep will cause a portion of the tension to shift from the concrete to the reinforcement over time. This redistribution does not impact this evaluation because ACI 318-71 and ASME already assume that concrete does not resist tension unless a section is specifically designed as a plain concrete section.

The general model for computation of the creep coefficient provided in ACI 209R-92 [15] shall be used.

3.3.2 Shrinkage

Shrinkage is the volume change that occurs during the hardening of concrete and is caused by the loss of water as the concrete cures. Shrinkage strains are independent of the sustained loads acting on a concrete section.

The stresses caused by shrinkage can be excluded from analysis in the cases described below, when doing so is conservative for the specific conditions under evaluation.

- Shrinkage generally acts in a direction opposite to ASR and therefore reduces the demand in sections that are undergoing ASR expansion (provided that the magnitude of ASR expansion is similar to or greater than the shrinkage strain).
- Shrinkage generally causes a small tensile demand in the concrete and a corresponding compression demand in the reinforcement in concrete structures without significant structural cracking or shrinkage restraint. These stresses are opposite from those typically resisted by the concrete and reinforcement and therefore can be conservatively excluded in most cases.

The general model for computation of concrete shrinkage provided in ACI 209R-92 shall be used.

3.3.3 Swelling

Concrete that is subjected to long-term water exposure exhibits a net increase in volume and mass over time due to swelling. Much like ASR expansion, concrete swelling will generally cause tension in the reinforcement and compression in the concrete.

Research has shown that reinforced concrete under conditions similar to those at Seabrook Station may have swelling expansion of 100×10^{-6} in./in. in the portions that are permanently exposed to groundwater [16].

4. ANALYSIS APPROACH

A three-stage analysis approach shall be used for analyzing Seismic Category I structures, as identified in the Seabrook LAR 16-03. Each stage applies increasingly sophisticated methods and uses additional field data to improve the rigor of the analysis, and without impacting the code inherent safety factors. The analysis of each structure may begin at any stage and, if necessary, shall progress to a higher analysis stage.

4.1 Selection of Starting Stage

The following criteria should be considered when selecting the starting stage for analysis.

1. Structures with simple geometry that permits structural analysis using closed-form solutions and/or simple finite element models
2. Structures with localized ASR expansion, or ASR expansion affecting the structure as a whole but with only minor indications of distress
3. Structures with an apparent robust original design leading to a reasonable amount of margin to accommodate ASR demands
4. Structures that do not exhibit significant signs of distress

Structures should start at Stage One if they meet all four criteria listed above. Structures should start at Stage Two if they meet two or three of the listed criteria. Structures should start at Stage Three if they meet one or none of the listed criteria.

Note that the above process for selection of starting stage is a guideline, and the starting stage may be adjusted after performing preliminary analysis/review. Stage One Screening Evaluation, Stage Two Analytical Evaluation, and Stage Three Detailed analyses are described in following Sections 4.2, 4.3, and 4.4, respectively.

4.2 Stage One Screening Evaluation

Structural evaluation should start at Stage One Screening Evaluation if the structure meets all four criteria listed in Section 4.1.

4.2.1 Field Observations to Support Stage One Analyses

Walkdowns of structures and plant equipment have been performed by NextEra to identify symptoms of ASR presence. Inspection data from these walkdowns shall be used in conjunction with other previous measurements to identify potential locations and directions of structural

movement and deformation. The previous data include measurements of relative building movements, equipment misalignments, and CI. Indications of deformation or ASR conditions documented in NextEra Action Requests (ARs), and Work Orders (WOs) shall be reviewed.

After reviewing previous field data, a walkthrough inspection shall be performed to verify field conditions and determine whether ASR expansion only affects localized regions of the structure or whether the structure has experienced global deformations. Previous field data that are older than three years shall be verified during this walkthrough inspection. Additional field measurements can be taken during these walkthrough inspections, but collection of extensive field data is not intended for this inspection.

Many of the existing ASR monitoring grids for measurement of CI that have been installed prior to the start of ASR susceptibility evaluation are at reasonably-accessible locations of most apparent ASR cracking identified by visual inspection. These measurements, when used in combination with pin-to-pin in-plane expansion measurements, provide a conservative estimate of the ASR strain in the structure. If a new ASR monitoring grid must be installed to support a Stage One analysis, it shall be installed at the location where cracking is most apparent, based on visual observation, within the region that requires additional data. Measurement data used for Stage One analysis shall be from measurements made within three years, in accordance with the Seabrook LAR 16-03 [1]. Monitoring requirements are listed in Table 7.

4.2.2 Non-ASR Demands for Stage One Analyses

The demands from the original design load calculations (non-ASR demands) shall be used. If required, when demands are either not calculated in the original design or the calculated demands are overly conservative, the non-ASR demands may be recalculated using methods that are generally consistent with the original design methodology.

Effects of creep, shrinkage, and swelling are considered small in the Stage One analysis methodology; therefore, structures being evaluated in this stage should have little to no sign of distress due to these self-straining loads.

4.2.3 ASR Demands for Stage One Analyses

Structural demands caused by ASR loads shall be computed by using conservative and simplified structural analysis methods similar to the original design calculations, or using simple finite

element models. Analysis shall consider the structure to be subject to ASR expansion of structural components on a conservative basis using the limited but conservative field inspection data. For structures embedded in concrete backfill, analysis shall also consider pressure on the structure due to concrete backfill ASR expansion.

4.2.3.1 ASR Expansion of Structural Components

Regions of the structure that exhibit features typical of ASR shall be analyzed for ASR expansion corresponding to the field measurement value obtained from one of the most severe cracking locations within the region. ASR loads shall be applied as uniform strain through the concrete thickness of the structural component to cause an expansion that is consistent with the assigned ASR expansion value or the assigned bounding value for the case of the Containment Structure as discussed in Subsection 3.1.1.1.

4.2.3.2 ASR Expansion of Concrete Backfill

For structures embedded in concrete backfill without an isolation gap, the structure and the backfill shall be considered to be in direct contact, even though shrinkage of the concrete backfill and structure and possible deterioration of the waterproofing backboard could result in a separation.

Pressures acting laterally on walls due to concrete backfill ASR expansion shall be taken as equal to the overburden pressure at the elevation under consideration. The overburden pressure is considered to be the approximate upper-limit for the unfactored lateral pressure. Once this pressure is reached, additional ASR expansion will occur preferentially in the vertical and/or other transverse directions. Lower concrete backfill pressure can be used when it is justified based on structural deformation or lack of distressed area by field observations. Concrete backfill ASR pressures acting laterally on walls shall be determined by the steps discussed in Section 4.4.3.2 and schematically shown in Figure 4.

4.2.3.3 Use of Cracked Section Properties in Stage One Analysis

Stage One analysis should generally use uncracked section properties for conservatism. Cracked section properties, however, may be used to account for the effects of structural cracking on flexural stiffness of a member provided both of the following conditions are met:

- Cracked section properties were used in the original design calculations.

- Using cracked section properties to represent flexural stiffness for calculating ASR demands would not affect the non-ASR demands calculated in the original design documents.

The flexural stiffness of members with structural cracks, or members expected to develop structural cracks, reduces compared to uncracked section properties. It should be noted that the structural cracks are those due to external loading and not microcracks associated with ASR behavior. The effective moment of inertia (I_e) can be determined using one of the following approaches:

- Calculate I_e using Equation 9-4 of ACI 318-71 considering the prestressing of the concrete due to ASR expansion which would delay the crack initiation or increase the cracking moment (M_{cr}) defined in Section 4.4.5.
- Set I_e equal to 50% of the gross moment of inertia, per Supplement 4 to ACI 318-71 discussed in Section 5.6.

4.3 Stage Two Analytical Evaluation

Structures should start at Stage Two Analytical Evaluation if they meet two or three criteria listed in Section 4.1. Structures that do not meet acceptance criteria using the conservative methods of the Stage One analysis can also be evaluated using Stage Two analysis.

Effects of creep, shrinkage, and swelling are considered small in the Stage Two analysis methodology; therefore, structures being evaluated in this stage should show little to no sign of distress due to these self-straining loads.

4.3.1 Field Observations to Support Stage Two Analyses

Stage Two analyses are supported by additional structural inspections and field measurements beyond those already performed for a Stage One analysis to provide a broader and more accurate assessment of ASR effects on the structure. Field observation may also require identifying structural distress areas (if any) and quantifying the structural deformations to correlate analysis results to field observations. Measurement data used for Stage Two analysis shall be from measurements made within the past 18 months, in accordance with the Seabrook LAR 16-03 [1]. Monitoring requirements are listed in Table 7.

4.3.2 Non-ASR Demands for Stage Two Analyses

The demands from the original design load calculations (non-ASR demands) shall be used. If the required demands are not calculated in the original design or if the calculated demands are overly conservative, then the demands may be recalculated using the same general approach as the original design methodology but improved to eliminate or reduce unnecessary conservatism.

4.3.3 ASR Demands for Stage Two Analyses

Structural demands caused by ASR loads shall be computed by performing finite element analysis of the structure subject to ASR expansion for regions showing ASR expansion. For structures embedded in concrete backfill, analysis shall also consider pressure on the structure due to concrete backfill ASR expansion.

4.3.3.1 ASR Expansion of Structural Components

Regions of the structure that exhibit features indicative of ASR shall be analyzed for ASR expansion corresponding to the average field measurement value from measurements made within the region and adjusted to account for structural cracking as discussed in Subsection 3.1.1. ASR loads shall be applied as uniform strain through the concrete thickness of the structural component within each region to cause an expansion that is consistent with the assigned ASR expansion value per Subsection 3.1.1.

Structural walls, for which the concrete is generally modeled in finite element analysis using shell elements, shall be subject to uniform imposed through-thickness strains to cause an expansion that is consistent with field measurements of ASR in-plane strain. In these locations where ASR expansion is applied, steel reinforcement shall also be modeled, and in the case of structural walls the reinforcement should be modeled using membrane elements with orthotropic properties to account for different quantities of steel in horizontal and vertical directions. Modeling of steel reinforcement shall take into consideration the development length required to be fully effective. Testing has shown that the adequacy of reinforcement development length is not impacted by ASR for the expansion up to the limit defined in MPR-4273 [4]. For sections with symmetric reinforcement, the steel membrane elements may be placed at the mid surface of the shell element and contribute only in axial stiffness. Otherwise, the effect of unsymmetrical reinforcement should be considered by accounting for rebar offset from the centroid.

In-plane gradients in ASR expansion may be used to transition between regions of different ASR expansion quantities. While the description above is specific to reinforced concrete structural walls modeled with a combination of shell and membrane elements, this methodology may be extended to other type of elements (beam, solid, etc.).

4.3.3.2 ASR Expansion of Concrete Backfill

For structures embedded in concrete backfill without an isolation gap, the structure and the backfill shall be considered to be in direct contact, even though shrinkage of the concrete backfill and structure, and possible deterioration of the waterproofing backboard, could result in a separation.

Concrete backfill ASR pressures acting laterally on walls shall be taken as equal to the overburden pressure at the elevation under consideration. The overburden pressure is considered to be the approximate upper-limit for the unfactored lateral pressure. Once this pressure is reached, additional ASR expansion will preferentially occur in the vertical and/or other transverse directions.

If field observations of the wall show no signs of distress, then the unfactored backfill pressure may be reduced and be limited to the pressure that would initiate observable distress in the wall. In most cases, distress would be observable as flexural cracking. Concrete backfill ASR pressures acting laterally on walls shall be determined by the steps discussed in Section 4.4.3.2 and schematically shown in Figure 4.

4.3.3.3 Use of Cracked Section Properties in Stage Two Analyses

Stage Two analysis may use cracked section properties as explained in Section 4.4.5 for Stage Three analysis provided that the use of cracked section properties does not adversely impact the original design demands calculation or change the load path for the original design loads.

For Stage Two evaluation, the iterative steps for calculating the effective section properties, see Section 4.4.5, may be stopped after a single iteration (initial step plus iterative step 1) if the structural responses of interest are forces and moments and not structural deformation. Limiting the number of iterations leads to stiffer section properties with less cracking, which results in conservative forces and moments. Calculation of the demand stress level for crack initiation should account for the prestressing of the concrete due to ASR expansion.

4.4 Stage Three Detailed Evaluation

Structures should start at Stage Three if they meet one or none of the criteria listed in Section 4.1. Structures that do not meet acceptance criteria using the conservative method of the Stage Two analysis can be evaluated using Stage Three analysis.

4.4.1 Field Observations to Support Stage Three Analyses

Stage Three analyses may need to be supported by additional inspections beyond those already performed for Stage Two to provide a broader and more accurate assessment of ASR effects on the structure. Structural deformation also shall be measured at sufficient locations for estimating deformed geometry of the structure or specific structural member(s). Field observation should also identify locations with structural distress, such as structural cracking and/or concrete cover delamination (if any), so that correlations can be made between the analytical results for the in-situ condition and field observations; this is discussed in more detail in Section 4.4.4. Measurement data used for Stage Three analysis shall be from measurements made within the past 6 months, in accordance with the Seabrook LAR 16-03 [1]. Monitoring requirements are listed in Table 7.

4.4.2 Non-ASR Demands for Stage Three Analyses

Finite element analysis shall be used to compute the non-ASR structural demand forces more rigorously than in the original design calculation. The non-ASR loads (i.e. - wind, seismic, hydrostatic pressure, etc.) from the original design calculations shall be applied to the finite element model unless otherwise justified. For example, reduced loads may be applied to the model if the original design used loads that enveloped both Unit 1 and Unit 2 conditions but the loading is shown to be conservative for Unit 1 which is of interest. Another justified circumstance is when the original design utilized conservative preliminary loading prior to defining the actual loading (e.g., equipment loading and thermal loading). The original design generally used simplified analysis methods or models to calculate structural responses, while the detailed finite element model used in Stage Three analysis more rigorously calculates the structural demands. Comparison between the design loads determined from the Stage Three finite element analysis and original design calculations should be made, and reason(s) for differences should be determined.

For seismic loads, the maximum seismic acceleration profiles in each direction (typically N-S, E-W, and vertical) provided in the original design calculations shall be applied to the finite element model independently. Because elements in Stage Three analytical models are typically more discretized than in the original design models, linear interpolation may be used to obtain the maximum acceleration at each node of the Stage Three finite element model. The seismic mass of the structure shall include all dead weight including fixed equipment, piping, and etc. The response of each directional input shall be combined using the SRSS method in accordance with Regulatory Guide 1.92 [18].

Creep, shrinkage, and swelling shall be considered in Stage Three analysis when comparing simulated deformations to field measurements if field observations or analysis has determined that their load effects could be significant.

4.4.3 ASR Demands for Stage Three Analyses

Structural demands caused by ASR loads shall be computed by performing finite element analysis of the structure subject to ASR expansion for regions affected by ASR. For structures embedded in concrete backfill, analysis shall also consider pressure on the structure due to concrete backfill ASR expansion. ASR expansions of the structural concrete and backfill concrete will produce stresses in one another. The interaction between ASR-induced expansion of the structure and stiffness of concrete fill restraining the expansion of the structure shall be considered as described in following subsections.

4.4.3.1 ASR Expansion of Structural Components

Structural members with significantly varying CI values will be divided into regions to better define the in-plane expansion variation for structural members. Each region of the structure that exhibits features indicative of ASR shall be assigned an average field measurement value from measurements made within that region. ASR loads shall be applied as uniform strain through the concrete thickness of the structural component to cause an expansion that is consistent with the assigned ASR expansion value as discussed in Subsection 3.1.1.

Structural walls, which are generally modeled in finite element analysis using shell elements or beam elements, shall be subject to uniform strain through the thickness to cause an expansion in the concrete model that is consistent with field measurements of ASR in-plane strain. In locations where ASR expansion is applied, steel reinforcement shall also be modeled, and in the case of

structural walls and slabs the reinforcement should be modeled using membrane elements with orthotropic properties to account for different quantities of steel in horizontal and vertical directions. Modeling of steel reinforcement shall take into consideration the development length required to be fully effective. Testing has shown that the performance of reinforcement development length is not impacted by ASR for the expansions up to the limit defined in MPR-4273 [4]. Additional discussion on finite element modeling is presented in Section 4.3.3.1.

In-plane gradients in ASR expansion may be used to transition between regions of different ASR expansion quantities. While the description above is specific to reinforced concrete structural walls modeled with a combination of shell and membrane elements, this methodology may be extended to other types of elements (beam, solid, etc.).

In locations where concrete backfill is adjacent to structural components without a seismic isolation gap, the stiffness of the concrete backfill shall be accounted for in the finite element model. The stiffness of the backfill elements shall be determined as follows:

- If the concrete backfill has sufficient stiffness to fully restrain a structural component (e.g., wall or slab) that is affected by ASR, then the total member strain will be limited due to the restraint. This restraint can be observed by reviewing if the pin-to-pin expansion measurement over time remained constant or increased slightly. The effective stiffness of the backfill concrete in these cases shall be quantified using the elastic modulus from the following equation.

$$E_{backfill} = E_c k_{r1}$$

Where:

E_c is the elastic modulus of backfill concrete per Section 8.3 of ACI 318-71 based on the original design specified compressive strength.

k_{r1} is a knockdown factor that represents the reduction in elastic modulus of unreinforced concrete due to ASR. Material testing indicates that a reduction in elastic modulus occurs in unreinforced concrete with ASR [19], [20], [7], [11], and [21]. In Stage Three analyses, a 70% stiffness reduction shall be used for backfill concrete with 0.35% expansion or higher, and the stiffness reduction shall decrease proportionally to 0% at zero expansion. This stiffness reduction is based on data reported in various sources ([19], [20], and [7][7]). The strain of concrete fill can be estimated based on CI expansion measured in adjacent structural members or observed structural deformation relative to the width of the concrete fill perpendicular to the plane of the below-grade wall.

- If pin-to-pin in-plane expansion measurements indicate that the total strain of the component is increasing over time, then the backfill must have a reduced stiffness to accommodate this strain. The stiffness of the backfill shall be quantified using the elastic modulus from the equation below.

$$E_{backfill} = E_c k_{r1} k_{r2}$$

where k_{r2} is a knockdown factor that represents additional reduction in backfill concrete elastic modulus due to shrinkage, compression of waterproofing backboard, and/or crushing. The k_{r2} knockdown factor shall only be used when field measurements indicate that backfill concrete does not restrain the ASR expansion of a structural component as much as analysis using the stiffness $E_c k_{r1}$ would indicate. The value of k_{r2} shall be determined empirically through finite element model simulations that compare the in-situ conditions of the structural component of interest, including the adjacent members, to field observations and to locations of distressed areas or lack of observed distressed areas.

4.4.3.2 ASR Expansion of Concrete Backfill

For structures embedded in concrete backfill without an isolation gap, the structure and the backfill shall be considered to be in contact, even though shrinkage of the concrete backfill and structure, and possible deterioration of the waterproofing backboard, would result in a separation. Concrete backfill ASR pressures acting laterally on walls shall be determined by following the steps described below and shown schematically in Figure 4. The lateral concrete backfill pressure for Steps One through Six shall correspond to unfactored sustained load combinations unless factored load conditions are explicitly specified.

- **Step One:** The maximum unfactored lateral pressure on walls from concrete backfill ASR expansion shall be taken as equal to the overburden pressure at the elevation under consideration.
- **Step Two:** If structural deformation measurements associated with backfill pressure are available, then the backfill pressure may be limited to the pressure that simulates the measured deformations. The simulated deformations calculated based on in-situ loading consist of unfactored sustained loads and unfactored ASR expansion of the structural components; therefore, limiting ASR pressure from concrete backfill should simulate the measured deformations. This limit may only be imposed if an assessment determines that the deformation measurements were, in part, caused by out-of-plane pressures imposed by ASR expansion of the concrete backfill.
- **Step Three:** If field observations of the wall show no signs of distress, such as flexural cracking, then the unfactored backfill pressure may be limited to the pressure that would initiate observable ductile distress (flexural cracking) in the wall.

The following alternate approach can be used for embedded walls which are expected to first form flexural cracking before shear cracking under increased lateral loading from ASR expansion of concrete backfill but that currently show no sign of visible structural cracking under in-situ conditions. When subjected to lateral pressure, these walls are expected to first form flexural cracking. However due to a lower strength reduction factor for shear compared to flexure and the higher load factor for ASR load compared to non-ASR loads, it is possible to determine that the controlling demand-to-capacity ratio for factored load combinations is governed by out-of-plane shear. Assuming an applied lateral pressure for these walls corresponding to flexural crack initiation due to sustained

loading can be too conservative. Therefore, the concrete backfill pressure can be reduced under the following conditions:

- a) Limit the pressure to the lower value corresponding to any structural crack initiation (shear or flexure) for the factored load combinations with inclusion of threshold factor
- b) Increase the monitoring frequency (maximum 2-month interval)
- c) Design a retrofit or shoring for implementation after observation of any structural crack

- **Step Four:** If field observations of the wall show signs of distress associated with concrete backfill pressure, and if the distress is a symptom of a ductile load effect (such as flexure), then the unfactored backfill pressure may be limited to the pressure that would cause the observed level of distress. Computation of this limiting pressure requires sufficient measurements to quantify the level of distress, and sufficiently detailed simulation to correlate the level of distress with concrete backfill pressure. The simulation shall consider unfactored sustained loads and unfactored ASR expansion of the structure acting in addition to the backfill pressure. Since distress is observed in the in-situ condition, stiffness reductions due to structural cracking in accordance with Section 4.4.5 may be used when simulating the backfill behavior.

Note: Step four may only be used in Stage Three analyses.

- **Step Five:** When the interfacial compressive stress between the concrete backfill and the structural wall reaches or exceeds the overburden compression stress, further expansion of the concrete backfill will occur preferentially in the vertical and/or other transverse directions. Therefore, the interfacial compressive stress determined from analysis with ASR expansion of structural components alone calculated per Section 4.4.3.1 can be subtracted from the pressure determined from Step 1.

Note: Step five may only be used in Stage Three analyses.

- **Step Six:** The unfactored pressure exerted on the structure due to concrete backfill ASR expansion, p_H , shall be computed as:

$$p_H = \min[p_{H3}, (p_{H1} - p_{H0}), \max(p_{H2}, p_{H4})] \geq 0 \text{ psi}$$

where, p_{H0} is the compressive stress applied to the concrete backfill by ASR expansion of the structural components calculated per Section 4.4.3.1, and p_{H1} , p_{H2} , p_{H3} , and p_{H4} are limiting backfill pressures from Steps 1, 2, 3, and 4, respectively. It should be noted that if Steps 2, 3, and 4 are not applicable, then p_{H2} , p_{H3} , and p_{H4} should be excluded from the above equation. If only one of Steps 2, 3, or 4 are performed, then the pressure associated with that step should be entered and the other two pressures should be excluded from the above equation. If Steps 2 and 3 are performed, then p_{H2} and p_{H3} should be entered and p_{H4} should be excluded from the above equation. If Steps 2 and 4 are performed then the maximum of p_{H2} and p_{H4} would govern but need not exceed $(p_{H1} - p_{H0})$.

In this equation, the overburden pressure is reduced by the compressive stress in the backfill due to other loads (expressed as $(p_{H1} - p_{H0})$). This is done to avoid double-counting of the pressures acting on the interface between the backfill and structure.

- **Step Seven:** For factored load conditions, p_H shall be amplified by the product of the load factor for ASR and the threshold factor as defined in Section 6. In lieu of applying concrete backfill pressure for cases where it would produce unrealistic deformation (due to structural cracking or structural movement), the concrete backfill ASR expansion (deformation) can be amplified by the product of the load factor for ASR and the threshold factor while considering increased cracking in the restraining structure.

Research has shown that ASR expansion occurs preferentially in directions with less compression stress [4], [19], [22], and [21][21]. In the above methodology, the overburden pressure is treated as an approximate upper-limit for the unfactored lateral pressure. Once this pressure is reached, additional ASR expansion will occur preferentially in the vertical and/or other transverse directions. When consideration is given to the load factor for ASR expansion, an out-of-plane pressure of up to twice the overburden pressure (load factor for static load combination) may be applied laterally to walls. This factor of 2 for pressure may be reduced, but not to less than the load factor for dead load when the field data confirms the rigid body vertical movement of the structure components such as base slabs that overlay the concrete backfill.

Overburden pressures include the weight of structures, soil, permanent equipment, and concrete backfill above a certain elevation. Overburden pressures can also include clamping pressures imposed by walls that are tensioned by vertical concrete backfill expansion, such as those shown in Figures 2 and 3. When concrete backfill is in a narrow region, such as that shown in Figure 2b, analysis may show that the overburden stress is partially reduced by the adjacent rock.

Concrete backfill ASR vertical expansion that creates uplift pressure below a base slab shall be determined by the following steps:

- **Step One:** Determine if the concrete backfill is in a confined region, such as those illustrated in Figures 2 and 3. When a confined region exists, vertical expansion of the fill also causes an axial tension in the confining walls in addition to uplift pressure on the base slab.
- **Step Two:** If the concrete backfill is in a confined region, then the expansion of the fill shall be modeled using a vertical-upward pressure acting on the base slab. When field measurements of vertical displacement and/or vertical strain in the connecting wall(s) are available, the magnitude of the upward pressure shall be adjusted to simulate measurements. The upward pressure is a function of the stiffness of the structure, which shall be adjusted in accordance with Section 4.4.5 to account for cracking. For factored load conditions, the upward pressure shall be amplified by the product of the ASR load factor and the threshold factor as defined in Section 6. Alternatively when the restraining structure is cracking, the vertical displacement/strain shall be amplified by the product of the ASR load factor and threshold factor, and then the upward pressure associated with this amplified displacement/strain shall be treated as the factored pressure.

- **Step Three:** If the concrete backfill is not in a confined region, then vertical expansion of the fill may cause upward rigid body movement of the structure with some possible rigid-body rotation. If there are discontinuities in the upward movement, then demands resembling differential settlement may occur; such effects shall be evaluated when apparent. As described in Section 5, the impact of ASR on global stability shall be assessed.

4.4.4 Correlation of Analysis Model to Field Observations

The finite element analysis results for in-situ conditions should correlate with the deformations, strains, and distressed areas (if any) observed onsite. Further refinement of modeling procedures or additional field observations may be required to improve the correlation between analysis results and field observations for locations and types of distress (such as crack type, crack direction, location of cracking region, etc.) and deformation. Deviations between analytical results and field observations could be from incorrect modeling assumptions, ASR load, ASR modeling steps discussed in Section 4.4.3, or other self-straining load that must be adjusted to improve the correlation between the finite element results and field observations. Considering cracked section properties, modifying the boundary conditions, and adjusting the ASR expansion pressure for concrete backfill, when justified, can be used to improve the analysis model. The analysis model is considered acceptable when the following conditions are consistent with field observations:

- Location of major structural cracks, as well as the type and direction of structural cracking regions,
- Structural deformation patterns and locations and magnitudes of critical deformation within the accuracy of the measurements and structural construction tolerances, and
- Relative movement between adjacent structures or between structures and components or piping at critical locations.

4.4.5 Refined Analytical Methods

The effect of structural cracking on reducing the axial, shear, and flexural stiffness of a structural component may be considered if at least one of the following two conditions is met:

- I. Field investigation indicates the formation of structural cracks, i.e. - flexural cracks, membrane/axial cracks, and/or shear cracks.
 - Flexural cracks are expected to be accompanied by out-of-plane movement.
 - Axial/membrane cracks are expected to form in the direction perpendicular to tensile stress direction.

- In-plane shear cracks are expected to be inclined to the primary directions of reinforcement, e.g., 45°.

II. Finite element analysis shows the stress or strain associated with flexure, tension, and/or shear cracking exceeds the corresponding limits discussed later in this section. For correlation of the analysis model to field observations (Section 4.4.4), the analysis should be performed for unfactored insitu loads including ASR. The effect of structural cracking due to factored load combinations may be considered when evaluating the structure for factored load conditions including ASR load.

- Finite element analysis shows that the out-of-plane bending moment of a concrete shell element (representing a wall or slab) or moment about the principal axis of a beam element (representing a beam or column) exceeds the flexural cracking moment, where the magnitude of cracking moment shall be computed using modified Equation 9-5 of ACI 318-71 to account for prestressing effects of ASR as:

$$M_{cr} = \frac{(f_r + f_p)I_g}{y_t}$$

where f_r is the concrete modulus of rupture, f_p is the concrete compressional stress due to ASR prestressing and other net compression loading on the section, I_g is the gross moment of inertia, and y_t is the distance between the extreme tensile fiber and the centerline of the cross-section. The value of f_r can be computed using Equation 9-5 of ACI 318-71 as:

$$f_r = 7.5\sqrt{f_c'}$$

where f_c' is the specified compressive strength of the concrete.

- Finite element analysis shows that the 1st principal mechanical strain of a concrete element with consideration of ASR prestressing and other net compressional forces on section (shell, solid or beam element) exceeds the cracking strain, ε_{cr} , computed from the following equation:

$$\varepsilon_{cr} = f_t/E_c$$

where E_c is the elastic modulus of concrete and f_t is the uniaxial tensile strength of concrete material. The value of f_t can be computed using the following equation which is within the value range recommended by [23]:

$$f_t = 5\sqrt{f_c'}$$

Flexural cracks are common in concrete structures, and are allowed to form by the code of record [3]. Cracked section properties due to flexural cracks were also used in the original design calculations of the structures at Seabrook Station.

Axial cracking caused by ASR expansion of structural components usually occurs at the intersection of two components or at boundaries of two regions with different magnitudes of ASR expansion. Any difference in ASR expansion between two regions will subject the region with higher ASR to compression while causing tension in the other region. This phenomenon is schematically depicted in Figure 1 for a sample wall-to-slab connection. Another example is the wall that connects two separate structural slabs with relative upward motion due to expansion of concrete backfill within a confined region as depicted in Figure 3.

To account for the effects of cracking, the axial rigidity (EA), shear rigidity (GA), and/or flexural rigidity (EI) of the cracked element must be reduced. In finite element modeling, the reduction in most cases cannot be applied merely to the E (modulus of elasticity) and/or G (shear modulus), because any reduction in E will affect both axial and flexural rigidities, i.e. - they are coupled. The reduction in axial rigidity should be applied only in the direction perpendicular to the cracks. Additionally, flexural cracks can form without the formation of axial cracks, or axial cracks can form only in one direction; therefore, it is necessary to formulate a decoupled set of equations that allow independent reduction in axial, shear, and flexural rigidities. This requires the use of orthotropic material properties combined with modified cross-sectional dimensions, as explained in the step-by-step procedure provided in Appendix A. Decoupling of rigidities is acceptable if there is only one predominate axial, shear, or flexure demand load on the structural component of interest.

5. ACCEPTANCE CRITERIA

The effect of ASR on the structural design basis of affected concrete structures at Seabrook Station is evaluated in MPR Report MPR-4288 [5]. It assesses the impact of ASR on structural limit states (flexure, shear, and compression capacities and that of attachments to concrete structures) as well as several additional design considerations. For the limit states of shear, flexure, and reinforcement development and lap length, results from the MPR/FSEL test programs suggest that the effects of confinement from the reinforcement more than compensate for degradation of material properties when ASR progression is within the range observed in the test specimens [5]. MPR-4288 concludes that the effects of ASR expansion on the structural behavior of reinforced concrete structures can be explained with basic structural mechanics and that these effects can be evaluated using the provisions of the structural design codes applicable to Seabrook Station. Based on this conclusion, acceptance criteria from the applicable Codes of Record, supplemented or modified as described in this document, shall be applied for meeting the intent of the Codes. Technical justification for the application of acceptance criteria not specified in the Codes of Record is provided elsewhere in this document and is based on structural mechanics and sound engineering practices consistent with the Codes of Record.

Acceptance criteria shall be calculated using material properties specified in the original design basis. The basis for the use of design material properties is provided in MPR-4288. The applicability of the conclusions provided in MPR-4288 and used herein is based on the large scale test program described in MPR-4273 [4] and is limited to the extent of ASR expansion documented in MPR-4273. Accordingly, for analyses of concrete structures at Seabrook Station, the elastic modulus of concrete shall be computed using the minimum design compressive strength, and no reduction shall be taken for ASR-related damage. Material properties for analysis and evaluation of Seismic Category I structures shall be consistent with those used in original design calculations and those defined in the project specifications and drawing notes.

Structural acceptance criteria for evaluation of Seismic Category I structures with concrete affected by ASR shall be in accordance with the applicable Codes of Record except for deviations listed in Section 5.6, which are considered as supplements to the Codes of Record. A summary of the acceptance criteria as defined in the UFSAR is provided in the following sections.

5.1 Containment Structure

Structural acceptance criteria for evaluation of the Containment Structure shall be in accordance with UFSAR Section 3.8.1.5.

5.1.1 General

The Containment Structure, including liner and penetrations, shall remain within elastic limits under service load conditions and under the mechanical loads of the factored load conditions. With thermal loads included, the reinforcing steel in some regions may yield, but the strain shall not exceed twice the yield strain. Gross deformations of the Containment Structure shall not cause the structure to contact other structures or components. Service load combinations include conditions encountered during testing, normal operation, shutdown, and severe environmental conditions; these are listed in Table 4. Factored load combinations include those conditions resulting from severe environmental, extreme environmental, abnormal, abnormal/severe environmental, and abnormal/extreme environmental loads, as defined in ASME and listed in Table 4.

The design limits imposed on the various parameters that serve to quantify the structural behavior and provide a margin of safety shall be in compliance with ASME Sec. III, Div. 2. The allowable limits on these parameters, for service and factored loads, are given in Table 3.8-2 of the UFSAR.

5.1.2 Concrete

The allowable compressive stresses, including membrane, membrane plus bending and localized stresses, and shear stresses under service loads and factored loads are as specified in ASME Sec. III, Div. 2, Article CC-3400, with the exceptions related to shear stresses as specified in UFSAR Section 3.8.1.5 (b).

5.1.3 Reinforcing Steel

The stress and strain limits for reinforcing steel under service and factored loads are as specified in ASME Sec. III, Div. 2, Articles CC-3432 and CC-3422, respectively.

If local yielding occurs under combined mechanical and thermal load, the net strain shall be less than twice the yield strain, as established in the 1977 Winter Addendum to ASME Sec. III, Div. 2,

Article CC-3422.1 (d). This strain limit insures that the yielding under thermal load does not result in concrete cracking which would cause deterioration of the Containment Structure.

5.1.4 Liner Plate and Liner Anchorage System

The evaluation of the liner plate and its anchorage system is not part of structural ASR susceptibility analysis described in this methodology document.

5.1.5 Stability

Acceptance criteria for stability against overturning, sliding, and flotation are as defined in Table 8.

5.2 Containment Internal Structures

Structural acceptance criteria for evaluation of Containment Internal Structures shall be in accordance with UFSAR Section 3.8.3.5. The basis for the development of the stress-strain criteria are the ACI 318-71 code. The reinforced concrete structures must meet ACI 318-71 with supplements as listed in Section 5.6.

5.2.1 Normal Load Conditions

Normal load conditions are those encountered during testing and normal operation as defined in UFSAR Subsection 3.8.3.3. They include dead load, live load, ASR load, and anticipated transients or test conditions during normal and emergency startup and shutdown of the Nuclear Steam Supply, Safety, and Auxiliary Systems. Normal loading also includes the effect of an Operating Basis Earthquake.

5.2.2 Unusual Load Conditions

Unusual load conditions are those conditions resulting from combinations of the LOCA, SSE and OBE, high-energy pipe failures, ASR, and live and dead loads as defined in UFSAR Subsection 3.8.3.3. The upper bound of elastic behavior is taken as the yield strength capacity of the load carrying components. The yield strength of structural and reinforcing steel is to be taken as the minimum guaranteed yield stress as given in the appropriate ASTM Specification.

5.2.3 Deformations

The deformation for each of the structures due to ASR (if any) is to remain small so that no gross deformations will occur and cause contact with other structures or pieces of equipment.

5.3 Other Seismic Category I Structures

Structural acceptance criteria for evaluation of other Seismic Category I concrete structures shall be in accordance with UFSAR section 3.8.4.5. The basis for the acceptance criteria is the ACI 318-71 Code. However, under the action of seismic or wind loadings, in accordance with the standard review plan (Section II.5), the 33 percent increase in allowable stresses is not permitted. The reinforced concrete structures must meet ACI 318-71 with supplements as listed in Section 5.6.

5.3.1 Normal Load Conditions

Normal load conditions are those encountered during testing and normal operation as defined in UFSAR Subsection 3.8.4.3 and are referred to in the standard review plan as service load conditions. They include dead load, live load, ASR load and anticipated transients, loads occurring during normal startup and shutdown, and loads occurring during emergency shutdown of the nuclear steam supply, safety, and auxiliary systems. Normal loading also includes the effect of an operating basis earthquake and normal wind load.

5.3.2 Unusual Load Conditions

The unusual load conditions include ASR load and those loads shown in Subsection 3.8.4.3 of UFSAR. The upper bound of elastic behavior is to be taken as the yield strength capacity of the load carrying components. The yield strength of reinforcing steel is to be taken as the minimum specified yield stress as given in the appropriate ASTM Specifications.

5.3.3 Deformations

The additional deformation due to ASR for each of the structures shall not cause contact with other structures or pieces of equipment in accordance with UFSAR Section 3.8.4.5.c.

5.3.4 Stability

Acceptance criteria for stability against overturning, sliding and flotation are as defined in Table 8.

5.4 Foundations for Seismic Category I Structures

Structural acceptance criteria for the evaluation of foundations for Seismic Category I structures shall be in accordance with UFSAR Section 3.8.5.4. The acceptance criteria relating to stress, strain, gross deformation, and shear loads are described in Subsections 3.8.1.5 and 3.8.4.5 of

the UFSAR for the Containment Structure and other Seismic Category I structure foundations, respectively. Safety factors for buoyancy, sliding, and overturning are given Section 5.1.5:

5.5 Acceptance Criteria for Isolation Gaps

The maximum displacements of adjacent structures due to a design seismic event, when combined with the deformations due to ASR (total ASR deformation including threshold value), shall not exceed the designed gap between these structures. Where the gap can be measured, then the maximum displacements of adjacent structures due to a design seismic event, when combined with the additional ASR threshold deformations, shall not exceed the field measured gap between these structures. The gap between two adjacent structures, A and B, shall satisfy the following equation:

$$\Delta_{Gap} \geq \Delta_{transient} + \Delta_{ASR}$$

Where:

$$\Delta_{transient} = \sqrt{\Delta_{Axis1}^2 + \Delta_{Axis2}^2}$$

$$\Delta_{Axis1} = \Delta_{Axis1,A} + \Delta_{Axis1,B}$$

$$\Delta_{Axis2} = \Delta_{Axis2,A} + \Delta_{Axis2,B}$$

$$\Delta_{ASR} = \Delta_{ASR,A}(k_{th,A}k_{Sa,A} - k_0) + \Delta_{ASR,B}(k_{th,B}k_{Sa,B} - k_0)$$

Δ_{Gap} is the design gap between structures A and B when the gap cannot be measured due to accessibility. When the gap can be measured Δ_{Gap} is the field measured gap between structures A and B.

$\Delta_{transient}$ is the movement of the structures due to factored transient loads. The equation for $\Delta_{transient}$ is used in existing evaluations performed by NextEra.

Δ_{Axis1} and Δ_{Axis2} are the absolute sum of the maximum elastically computed displacements in directions 1 and 2 of structures A and B due to factored transient loads. The two directions 1 and 2 are perpendicular horizontal axes (such as north-south and east-west) at the location under evaluation.

$\Delta_{Axis1,A}$ and $\Delta_{Axis2,A}$ are structure A displacements due to transient in directions 1 and 2;

$\Delta_{Axis1,B}$ and $\Delta_{Axis2,B}$ are structure B displacements due to transient in directions 1 and 2.

Δ_{ASR} is the movement of the structures at the evaluation location in the direction towards each other due to ASR expansion.

$\Delta_{ASR,A}$ and $\Delta_{ASR,B}$ are ASR deformations of structures A and B (based on structural analysis).

$k_{th,A}$ and $k_{th,B}$ are threshold factors associated with structures A and B.

$k_{Sa,A}$ and k_{SaBA} are the load factors for ASR for the load combination under consideration associated with structures A and B.

k_0 is equal to 0 (zero) when the gap can't be measured, and is equal to 1 when the gap is measured.

In the equation for Δ_{ASR} , the product of the threshold factor and load factor for each structure is reduced by $k_0 = 1$ for the condition when the gap width between structures is based on field measurements that already includes $\Delta_{ASR,A} + \Delta_{ASR,B}$. If the reduction in seismic gap width (as measured in the field prior to analysis) exceeds the ASR deformation simulated in analysis at a particular location, then the resulting impact of Δ_{ASR} shall be assessed.

5.6 Supplement to Code of Record Acceptance Criteria

Seismic Category I structures with concrete affected by ASR shall meet the acceptance criteria of the Codes of Record, with the following list of deviations which are considered as supplements to the Codes of Record:

- **Supplement 1** - Consideration of ASR Loads: The UFSAR load and load combinations Tables 3.8-1, 3.8-14, and 3.8-16 were modified in LAR 16-03 to consider the ASR load and load factors for calculating the total demands on structures affected by ASR.

Basis: ASME 1975 [6] and ACI 318-71 [3] codes do not address the requirement to consider any special loading for reinforced concrete structures that are impacted by ASR behavior. The concrete ASR growth causes stresses in reinforcement and concrete and member forces due to deformation compatibility between members expanding due to ASR. SGH Report 160268-R-01 [14][14] defines the ASR load and associated load factors to be combined with the original factored load combinations to provide safety margins comparable to those provided by the original factored loads in the original codes of record.

- **Supplement 2** – Code Acceptance Criteria: Strength of reinforced concrete sections affected by ASR can be calculated using the Codes of Record (ASME 1975 and ACI 318-71) and the minimum specified design concrete strength, provided that through-thickness ASR expansion is within the limits stated in report MPR-4273 [4] for through-thickness and volumetric expansion.

Basis: Report MPR-4288 [5] provides the basis for Supplement 2; the report conclusions are supported by the MPR/FSEL large scale test program described in report MPR-4273. MPR-4273 and MPR-4288 discuss expansion in terms of through-thickness expansion,

the correlating parameter used in evaluation of the MPR/FSEL large scale test program results. NextEra Energy Seabrook committed to apply a limit on volumetric expansion in NextEra Energy Seabrook, LLC Letter SBK-L-17156 [32]. Limits for through-thickness and volumetric expansion are provided in MPR-4273.

- **Supplement 3 – Shear-Friction Capacity for Members Subjected to net Compression:** The shear-friction capacity for members including the effect of net compression can be calculated using procedures defined in Building Code Requirements for Reinforced Concrete (ACI 318-83 Section 11.7) [24].

Basis: The shear-friction capacity defined by ACI 318-71 Section 11.15 does not address members subjected to sustained compression. Later versions of ACI 318 and ACI 349 provide provisions for members subject to permanent net compression when computing shear-friction capacity. The provisions for calculation of shear-friction capacity for members subject to net compression are provided in the following ACI Codes:

ACI 318-83 [31] and -02 Section 11.7.7, ACI 318-08 and -11 Section 11.6.7, ACI 318-14 Section 22.9.4.5 [24], and ACI 349-85 and -01 Section 11.7.7 [25]. In addition, each of the referenced ACI codes similarly limits the nominal shear stress (or strength), which, in effect, restricts the benefit of permanent net compression. ACI 318-71 Section 11.15.3 limits the maximum nominal shear stress to $0.2f_c'$ or 800 psi; more recent code editions such as ACI 318-02 Section 11.7.5 limit the maximum nominal shear strength to $0.2f_c'A_c$ or $800A_c$, where A_c is the area of concrete section resisting shear transfer. Both versions of ACI 318-71 and -83 also use the same strength reduction factors, Φ , for shear. To be consistent all provisions for shear-friction from ACI 318-83, Section 11.7 will be used instead of the corresponding section from ACI 318-71.

- **Supplement 4 – Flexural Cracked Section Properties:** Reduction of the gross cross-sectional moment of inertia for analysis shall be computed considering the presence of cracking and the prestressing effect of ASR; alternatively, 50% of the gross cross-sectional moment of inertia can be used.

Basis: The flexural stiffness of members with structural cracks or expected to develop structural cracks reduces compared to uncracked section properties. It should be noted that the structural cracks are those due to external loading and not microcracks associated with ASR behavior. The ratio of cracked to uncracked (gross) moment of inertia of 0.5 is consistent with provisions of ACI 318-14 Section 6.6.3.1.2 [17], ASCE 43-05 Table 3-1 [26], and ASCE 4-16 Table 3-2 [27]. Additionally, a review of 24 in. deep sections at Seabrook Station structures with 3 in. concrete cover and reinforcement configurations ranging from No. 8 bars at 12 in. spacing (ratio = 0.0032) to No. 11 bars at 6 in. spacing (ratio = 0.0128) indicates that the ratio of cracked to uncracked gross moment of inertia ranges from 16% to 47%. The first ratio represents minimum allowable flexural reinforcement per ACI 318-71 Section 10.5.1, and the second ratio represents 80% of the maximum allowable flexural reinforcement per ACI 318-71 Section 10.3.2. This review indicates that using a ratio of 50% for reinforced sections in analysis is reasonable or conservative, since flexural demands from ASR tend to decrease as the flexural stiffness decreases. The review also indicates that benefit can be achieved by explicitly calculating and using the cracked section moment of inertia in the analysis. While recent editions of ACI 318 limit the maximum reinforcement ratio via other

provisions than contained in ACI 318-71, the effect is similar, and therefore the comparison to the 50% ratio is justified.

- **Supplement 5 – Axial and Shear Cracked Section Properties:** Axial and shear cracking reduces the corresponding stiffness of a structural member. The effect of cracking on reducing the axial and shear stiffness of structural components may be considered in analysis.

Basis: As the net tension on a concrete section reaches or exceeds the concrete tensile stress limit, the tensile stiffness of concrete section is reduced gradually to account for possible aggregate interlocking behavior, which is conservative compared to abruptly reducing the concrete tensile strength to zero. Gradual reduction of concrete tension stiffness results in larger net tension on a section which is resisted by the rebar and results in conservative evaluation of rebar strength. The axially cracked section properties can be calculated based on the stress-strain relationship defined in Appendix A which is based on ACI 224.2R92 [28], and Lu and Panagiotou [29]. The shear cracked section properties can be calculated based on the shear retention factor defined in Appendix A which is based on Červenka V. [30].

6. ASR THRESHOLD LIMITS AND MONITORING

6.1 Methodology to Account for Potential Future ASR Expansion

To qualify a structure with margin, the code allowable limits must be larger than the factored design-basis loading plus factored current ASR loading. This margin is used for demands associated with future ASR expansion. The threshold factor is the design margin expressed as the amount which ASR loads can increase beyond values used in the calculations such that the structure or structural component will still meet the allowable limits of the code. Threshold factor is an outcome of the evaluation, not an input to the analysis methodology approach. Calculation of the threshold factor is done by back-calculating the threshold factor such that when the factored original design load is combined with factored ASR load multiplied by the threshold factor, the total demand is equal to or less than the code allowable limits. A unique threshold factor is calculated for each building based on the available margin, and is used to establish threshold limits for structural monitoring parameters. Threshold factor may be revised based on further analysis by using additional inspection and measurement data and/or a more refined structural analysis method without reducing the code inherent margin of safety.

The development of ASR loads based on field measurements of expansion establishes a set of loads that are applicable at the time the measurements are made. The potential for future internal ASR expansion and ASR expansion of the concrete backfill amplified by the threshold limits, as discussed above, shall be considered in the evaluation and design confirmation of Seismic Category I structures. The threshold limit is confirmed when the structural member demands calculated for total factored design loads plus the factored ASR loads amplified by threshold limit remain equivalent to (or slightly less than) the corresponding capacity of the structure.

Specific methods to monitor each structure shall be recommended to identify if there are noticeable changes in the distribution of ASR within a structure from different expansion rates for different regions, changes in boundaries of a region, new regions of ASR, etc. Specific methods to monitor each structure to identify when the selected threshold factor is being approached shall also be recommended. Guidelines for selection of threshold monitoring measurements are as follows:

1. A subset of the measurements listed in Table 9 should be recommended for threshold monitoring.

2. Threshold monitoring measurements should be performed at a frequency of 36, 18, or 6 months for Stages One, Two, and Three structural evaluations, respectively, in accordance with the monitoring intervals specified in Table 7 (consistent with LAR 16-03).
3. The selection of threshold monitoring measurements should be informed by the analysis/evaluation and should track the behaviors/symptoms that are correlated with ASR progression.
4. Threshold monitoring measurements shall be quantifiable, whenever possible. Qualitative monitoring may supplement quantifiable measurements. In such cases, quantitative aspects of the qualitative conditions should be identified for monitoring whenever possible.
5. Threshold monitoring measurements may be recommended in sets or individually. If a set of monitoring measures are used, the measurements within the set should be averaged and compared to a single threshold limit for the entire set. A measurement set should contain only similar types of measurements (e.g., a single measurement set cannot contain both strain measurements and displacement measurements).
6. The method used to perform threshold monitoring measurements shall be capable of detecting the progression of strains and/or deformations between the previous measurements and the threshold measurements. The measurement method should also be repeatable such that incidental variation between repeated measurements is small relative to the margin between the threshold and baseline conditions.

If threshold monitoring of in-plane strain of a member is recommended, then monitoring using pin-to-pin in-plane expansion measurements is preferred over CI measurements due to its higher precision and repeatability, except for locations where CI measurements are specified for monitoring the in-plane expansion.

7. If CI measurements instead of pin-to-pin expansion measurements are recommended for threshold monitoring, the monitoring should consist of a set with at least two ASR monitoring grids. This reduces the possibility of incidental spalling of a single crack from having a disproportionately large impact on the monitored cracking index relative to the established limit.

In addition to the above quantitative threshold measurements, qualitative threshold measurements can be specified to monitor the ASR growth. Qualitative measurements include observation of new structural cracks, near surface delamination, local crushing of concrete, structural deformation, etc. The locations of the qualitative measurements are generally identified from the analysis performed to qualify the structure. The purpose, type, and specific location of any qualitative measurement shall be clearly defined to enable reliable and repeatable data collection by field inspectors.

6.2 ASR Threshold Monitoring for Stage One Evaluations

Threshold monitoring measurements should be performed at a frequency of 36 months. Since the Stage One analyses are performed using a conservative approach based on several CI and/or pin-to-pin in-plane expansion locations and other structural deformation parameters, there will be a limited number of threshold monitoring quantitative measurements and several qualitative observation parameters. The quantitative measurements shall be compared to the corresponding specified limits from Stage One analysis evaluation. Similarly, the qualitative threshold measurements should be within the specified description and/or limits for these observations. When the observed variables are below the specified limits, the next threshold monitoring shall be performed within the monitoring frequency of 36 months. If a quantitative or qualitative observation variable approaches the corresponding specified limits, then further evaluations or structural modifications may be considered, as described in Section 7.

6.3 ASR Threshold Monitoring for Stage Two Evaluations

Threshold monitoring measurements should be performed at a frequency of 18 months. Quantitative measurements include in-plane expansion measurements and measurement of additional structural deformations. The quantitative threshold variable could be from one location or from an average of several locations with similar behavior. The quantitative measurement or average of several measurements as defined by the monitoring program shall be compared to the corresponding specified limits from Stage Two analysis evaluation. Similarly, the qualitative threshold measurements should be within the specified description and/or limits for these observations. When the observed variables are below the specified limits, then the next threshold monitoring shall be performed within the monitoring frequency of 18 months. If a quantitative or qualitative observation variable approaches the corresponding specified limits, then further evaluations or structural modifications may be considered, as described in Section 7.

6.4 ASR Threshold Monitoring for Stage Three Evaluations

Threshold monitoring measurements should be performed at a frequency of 6 months. Quantitative measurements include CI in-plane expansion measurements, pin-to-pin in-plane expansion measurements, crack width measurements, and measurement of other structural deformation variables. The quantitative threshold variable for each region could be from one location or from an average of several locations with similar behavior. The quantitative and qualitative measurements specified for each building shall be performed within the required

frequency of inspection. The quantitative measurement or average of several measurements, as defined by the structural monitoring program, shall be compared to the corresponding specified limits from Stage Three analysis evaluation. Similarly, the qualitative threshold measurements should be within the specified description and/or limits for these observations. When the observed variables are below the specified limits, then the next threshold monitoring shall be performed within the monitoring frequency of 6 months. If a quantitative or qualitative observation variable approaches the corresponding specified limits, then further evaluations or structural modifications may be considered, as described in Section 7. The structure may need to be re-analyzed if new ASR regions are observed during monitoring or a limiting analysis parameter, such as flexural cracking, that was limiting the backfill pressure is observed.

7. EVALUATION FOR APPROACHING THRESHOLD LIMITS

An administrative limit of 97% of the threshold limit is set in addition to reductions of 90%, 95%, and 100% set in LAR 16-03 for Stage One, Two, and Three threshold limits, respectively. The additional 3 percent margin plus the reduction to threshold factors for Stage One and Two analyses provide time to perform additional inspections to confirm that the limits are being approached and to initiate corrective actions. When the quantitative or qualitative threshold monitoring variables reach the administrative limits following the workflow shown in Figure 5, further structural evaluation in accordance with procedures specified in this methodology document shall be performed to re-evaluate the structure or to consider structural modification to alleviate the concern for the approaching variable(s) to the specified limit(s). More frequent ASR threshold monitoring may also be performed. If a structural modification approach is considered, the as-modified structure shall be evaluated using the procedures and acceptance criteria defined in this methodology document to confirm the as-modified structure meets the ASR susceptibility evaluation; and analysis shall be performed to calculate a new threshold factor for the as-modified structure.

7.1 Stage One Evaluation

The Stage One analysis and evaluation approach generally includes significant conservatism. When a threshold measurement reaches the administrative limits set for the Stage One threshold variables, the structure should retain sufficient reserve margin to allow reevaluation using more detailed analysis procedures defined in this methodology document. The reevaluation shall be performed using the more rigorous, higher Stage Two or Three analysis procedures described in this document. However if further evaluation cannot requalify the structure for higher threshold limits, a structural modification concept may be developed to mitigate the risk of exceeding the project acceptance criteria.

7.2 Stage Two Evaluation

The Stage Two analysis and evaluation approach generally includes some conservatism. When a threshold measurement reaches the administrative limits set for the Stage Two threshold variables, then the structure should retain sufficient reserve margin to allow reevaluation and requalification using more detailed analysis procedures defined in this methodology document. The reevaluation shall be performed using another Stage Two analysis with additional field measurements to better define the ASR affected regions used in the previous evaluation or could

be a Stage Three analysis. However if further evaluation cannot requalify the structure for higher threshold limits, a structural modification concept shall be developed to mitigate the risk of exceeding the project acceptance criteria.

7.3 Stage Three Evaluation

The Stage Three analysis and evaluation approach generally has considered most of the analysis approaches defined in this document. However, there is usually some conservatism in this evaluation that can be considered if the monitoring variable(s) reach the administrative limits set for the corresponding threshold variable(s). Further field inspections to better define the ASR impact on the structure may be used to reevaluate the building in accordance with the Stage Three procedures defined in this document. However if further evaluation cannot requalify the structure for higher threshold limits, a structural modification concept shall be developed to mitigate the risk of exceeding the project acceptance criteria; analysis shall be performed to calculate a new threshold factor for the as-modified structure.

8. REFERENCES

- [1] NextEra Energy Seabrook, *License Amendment Request 16-03*, SBK-L-16071, 31 July 2016.
- [2] MPR, *Seabrook Station: Impact of Alkali-Silica Reaction on Concrete Structures and Attachments*, MPR-3727, Revision 1 (FP100716), May 2012.
- [3] American Concrete Institute, ACI Committee 318, *Building Code Requirements for Reinforced Concrete*, ACI 318-71, Third Printing, 1972.
- [4] MPR, *Seabrook Station: Implications of Large-Scale Test Program Results on Reinforced Concrete Affected by Alkali-Silica Reaction*, MPR-4273, Revision 1 (FP101050), March 2018.
- [5] MPR, *Seabrook Station: Impact of Alkali-Silica Reaction on Structural Design Evaluations*, MPR-4288, Revision 0 (FP101020), July 2016.
- [6] ACI-ASME Joint Committee, American Concrete Institute, ASME Boiler and Pressure Vessel Code, Section III, Division 2/ACI Standard 359-74, *Code for Concrete Reactor Vessels and Containments*, Detroit, Michigan / American Society of Mechanical Engineers, New York, NY, 1975.
- [7] The Institution of Structural Engineers, *Structural Effects of Alkali-Silica Reaction*, 1992.
- [8] United Engineers & Constructors Inc., *Seabrook Station Structural Design Calculations*.
- [9] Federal Highway Administration, *Alkali-Silica Reactivity Field Identification Handbook*, FHWA-HIF-12-022, Washington D.C., December 2011.
- [10] CSA International, A864-00, *Guide to the Evaluation and Management of Concrete Structures Affected by Alkali Silicate Reaction*, Toronto, ON, Canada, 2000.
- [11] Mohammed T.U., Hamada H., and Yamaji, T., "Alkali-Silica Reaction-Induced Strains over Concrete Surface and Steel Bars in Concrete", *ACI Materials Journal*, Vol. 100, No. 2, Mar.-Apr. 2003.
- [12] Seabrook, *Updated Final Safety Analysis Report*, Revision 17.
- [13] Seabrook, *System Description For Structural Design Criteria For Public Service Company of New Hampshire Seabrook Station Unit Nos. 1 & 2*, 9763-SD-66, Revision 2, 2 Mar. 1984.
- [14] Simpson Gumpertz & Heger Inc., *Development of ASR Load Factors for Seismic Category I Structures (Including Containment) at Seabrook Station, Seabrook, NH*, Document No. 160268-R-01, Revision 0, (FP101039) Waltham, MA, Jul. 2016.
- [15] American Concrete Institute, ACI Committee 209, *Prediction of Creep, Shrinkage, and Temperature Effects in Concrete Structures*, ACI 209R-92, Reapproved 1997.
- [16] G.E. Troxell, J.M. Raphael, and R.E. Davis, "Long-Time Creep and Shrinkage Tests of Plain and Reinforced Concrete", *Proceeding of the American Society for Testing and Materials*, Vol. 58, 1958, pp 1101-1120.
- [17] American Concrete Institute, ACI Committee 318, *ACI 318-14 Building Code Requirements for Structural Concrete and Commentary*, 2014.

- [18] U.S. Nuclear Regulatory Commission, *Combining Modal Responses and Spatial Components in Seismic Response Analysis*, Regulatory Guide 1.92, Revision 1, 1976.
- [19] D. Wald, "ASR Expansion Behavior in Reinforced Concrete - Experimentation and Numerical Modeling for Practical Application, PhD Dissertation," Austin, TX, 2017.
- [20] Clark, L.A., "Critical Review of the Structural Implications of the Alkali Silica Reaction in Concrete", Transport and Road Research Laboratory Contractor Report 169, 1989.
- [21] K. Snyder and H. Lew, "Alkali-Silica Reaction Degradation of Nuclear Power Plant Concrete Structures: A Scoping Study," National Institute of Standards and Technology (NIST), 2013.
- [22] B. P. Gautam, D. K. Panesar, S. A. Sheikh, and F. J. Vecchio, "Multiaxial Expansion-Stress Relationship for Alkali Silica Reaction-Affected Concrete", ACI materials journal, , V. 114, No. 1, January-February 2017.
- [23] Nilson A. H., Darwin D., and Dolan C. W. *Design of Concrete Structures*, 14th Edition, 2010.
- [24] American Concrete Institute, ACI Committee 318, ACI 318 Building Code Requirements for Structural Concrete (ACI 318-02, ACI 318-08, ACI 318-11, ACI 318-14).
- [25] American Concrete Institute, ACI Committee 349, ACI 349 Code Requirements for Nuclear Safety Related Concrete Structures (ACI 349-85, ACI 349-01).
- [26] ASCE Standard ASCE/SEI 43-05, "Seismic Design Criteria for Structures, System, and Components in Nuclear Facilities."
- [27] ASCE Standard ASCE/SEI 4-16, "Seismic Analysis of Safety-Related Nuclear Structures."
- [28] ACI Committee 224, *Cracking of Concrete Members in Direct Tension*, ACI 224.2R-92, Reapproved 1997.
- [29] Lu, Yuan, and Marios Panagiotou. "Three-dimensional cyclic beam-truss model for nonplanar reinforced concrete walls." *Journal of Structural Engineering*, 2013, 140(3): 04013071.
- [30] Červenka V., Jendele L., and Červenka J., ATENA Program Documentation, Part 1, Theory. Dec. 2016, pp 29.
- [31] American Concrete Institute, ACI Committee 318, *Building Code Requirements for Reinforced Concrete*, ACI 318-83, First Printing, 1983.
- [32] NextEra Energy Seabrook, LLC Letter SBK-L-17156 to NRC, October 3, 2017.

9. TABLES

Table 1 – Evaluation Criteria for Suspected ASR Cracking

Visible Features Suggestive or Indicative of ASR Rating	ASR Classification		
	No	Possible	Likely
Expansion and/or displacement of elements	None	Some	Structure shows symptoms of increase in concrete volume leading to concrete spalling, displacement, and misalignment of elements
Cracking and crack pattern	None	Some cracking—pattern typical of ASR (i.e., map cracking or cracks aligned with major reinforcement or stress)	Extensive map cracking or cracking aligned with major reinforcement or stress
Surface discoloration	None	Slight surface discoloration associated with some cracks	Line or cracks having dark discoloration with an adjacent zone of light-colored concrete
Exudations	None	White exudations around some cracks	Colorless, jelly-like exudations readily identifiable as ASR gel associated with some cracks
Environment	Dry and sheltered	Outdoor exposure but sheltered from wetting	Parts of components frequently exposed to moisture such as rain, groundwater, or water due to natural function of the structure (e.g., hydraulic dam or bridge)
Overall	Based on reviewer experience, judgment, and information from the particular features listed above		

Table 2 – ASR Severity Zones [14]

Zone	CI / CCI Range (mm/m)
I	0.0 to 0.5*
II	0.5 to 1.0
III	1.0 to 2.0
IV	>2.0

* CI / CCI less than 0.1 mm/m can be excluded from Zone I in the Containment Structure evaluation [14]

Table 3 – ASR-Related Strain Loads for Analysis of the Containment Structure [14]

Zone	Strain Load (mm/m) for Stage 1 Screening Evaluation[#]		Strain Load (mm/m) for Stage 2 Analytical and Stage 3 Detailed Evaluation[#]	
	Low	High	Low	High
I	0.1	0.6	0.1	0.5
II	0.4	1.3	0.5	1.0
III	0.8	2.5	1.0	2.0
IV	1.5	*	2.0	**

[#] Strains presented as percentage in [14], but have been converted to mm/m in this document for consistency.

* The high strain load for Zone IV is to be 25% greater than the largest observed strain in the zone from CI measurements and/or visual inspection.

** The largest observed strain in the zone from CI measurements may be used.

Table 4 – Load Combinations for Evaluation of Containment Structure (Modified from Table 3.8-1 of UFSAR to Include ASR Loads and Load Factors)

TABLE 3.8-1 CONTAINMENT LOAD COMBINATIONS AND LOAD FACTORS(5)

Design Conditions	Category	Load Combination Number	LOADING ⁽⁶⁾																		
			Dead Load	Live Load	ASR Load	Test Pressure	Accident Pressure	Test Temperature	Normal Temperature	DBA Temperature	Operating Basis Earthquake	Safe Shutdown Earthquake	Wind Load	Tornado	Normal Pipe Reaction	DBA Thermal Pipe Reaction	R _e (DBA Local Effects)			Pressure Variations	Design Basis Flood
																	Reaction of Ruptured High Energy Pipe	Jet Impingement Loads	Impact of Ruptured High Energy Pipe		
Loading Notation	D	L	S _a	P _t	P _a	T _t	T _n	T _a ⁽¹⁾	E _o	E _{ss}	W	W _i	R _n	R _t	R _h	R _j	R _i	P _v ⁽²⁾	F ⁽³⁾		
Service Load	Test	1	1.0	1.0	1.0	1.0	-	1.0	-	-	-	-	-	-	-	-	-	-	-	-	
	Normal	2	1.0	1.0	1.0	-	-	-	1.0	-	-	-	-	-	1.0	-	-	-	-	1.0	
	Severe Environmental	3	1.0	1.0	1.0	-	-	-	1.0	-	-	-	-	-	1.0	-	-	-	-	1.0	
Factored Load	Severe Environmental	4	1.0	1.3	1.0	-	-	-	1.0	-	-	-	1.5	-	-	-	-	-	-	1.0	
	Extreme Environmental	5a	1.0	1.0	1.0	-	-	-	1.0	-	-	-	-	-	1.0 ⁽⁷⁾	-	-	-	-	1.0	
		5b	1.0	1.0	1.0	-	-	-	1.0	-	-	-	1.0	-	1.0 ^(7,8)	-	-	-	-	1.0	
	Abnormal	6a	1.0	1.0	1.0	-	1.5 ⁽⁴⁾	-	-	1.0 ⁽⁴⁾	-	-	-	-	-	1.0	-	-	-	-	
		6b	1.0	1.0	1.0	-	1.0 ⁽⁴⁾	-	-	1.0 ⁽⁴⁾	-	-	-	-	-	1.25	-	-	-	-	
	Abnormal/Severe Environmental	7	1.0	1.0	1.0	-	1.25 ⁽⁴⁾	-	-	1.0 ⁽⁴⁾	1.25	-	-	-	-	1.0	1.0	1.0	1.0	-	
	Abnormal/Extreme Environmental	8	1.0	1.0	1.0	-	1.0 ⁽⁴⁾	-	-	1.0 ⁽⁴⁾	-	1.0	-	-	-	1.0	1.0	1.0	1.0	-	

- (1) Includes effect of normal operating thermal loads and accident loads. For all abnormal load conditions, structure should be checked to assure that accident pressure load without thermal load can be resisted by the structure within the specified allowable stresses for this condition.
- (2) Negative pressure variations inside the structure shall not be considered simultaneously with outside negative pressure due to tornado loadings.
- (3) For this load case, the design basis flood elevation shall be the max. ground water elevation, i.e., El. +20'-0".
- (4) Load cases examined for maximum pressure and its coincident liner temperature and maximum liner temperature with its coincident pressure.
- (5) All load factors shall be taken as 1.0 for the design of steel liner.
- (6) See Subsection 3.8.1.3 for discussion of loadings.
- (7) W_i includes missile effects only.
- (8) For this load case, loadings from E_{ss} or W_i included individually.

Note: Section references made in the footnotes of this table refer to sections within the UFSAR [12].

Table 5 – Load Combinations for Evaluation of Containment Internal Structures (Modified from Table 3.8-14 of UFSAR to Include ASR Loads and Load Factors)

TABLE 3.8-14 INTERIOR CONTAINMENT STRUCTURES BASIC LOAD COMBINATIONS AND LOAD FACTORS

Design Conditions	Material		LOADING ⁽¹⁾														Stress Limit or Design Criteria			
	Loading Notations		Load Case Number	Dead Load and Hydrostatic Load	Live Load	ASR Loads	Accident Pressure	Operational Temperature	Accident Temperature	Operating Basis Earthquake	Safe Shutdown Earthquake	Operational Piping Loads	Accident Piping Loads	Jet Force Reaction	Jet Impingement Loads	Missile Impact Loads		Internal Missile Loads		
																			D	L
Normal Load	Structural Steel		1S	1.0	1.0	-	-	-	-	-	-	-	-	-	-	-	-	≤F _s Per AISC		
			2S	1.0	1.0	-	-	-	-	-	1.0	-	-	-	-	-	-	-		
			3S	0.67	0.67	-	-	-	0.67	-	-	-	0.67	-	-	-	-	-	-	
			4S	0.67	0.67	-	-	-	0.67	-	0.67	-	0.67	-	-	-	-	-	-	
	Concrete		1C	1.4	1.7	2.0	-	-	-	-	-	-	-	-	-	-	-	-	ACI 318-71	
			2C	1.4	1.7	1.3	-	-	-	-	1.9	-	-	-	-	-	-	-	-	
			3C	-	-	-	-	-	-	-	-	-	-	-	-	-	-	-	-	
Unusual Load	Structural Steel	Elastic	5S	0.63	0.63	-	-	0.63	-	-	-	0.63	0.63	-	-	-	-	-	≤F _s Per AISC	
			6S	0.63	0.63	-	0.63	-	0.63	-	-	-	-	0.63	-	-	-	-	-	
			7S	0.63	0.63	-	0.63	-	0.63	0.63	-	-	-	0.63	0.63	0.63	0.63	0.63	0.63	
			8S	0.59	0.59	-	0.59	-	0.59	-	0.59	-	0.59	0.59	0.59	0.59	0.59	0.59	0.59	
		Plastic	5S	1.1	1.1	-	-	-	1.1	-	-	-	1.1	-	-	-	-	-	-	AISC, Part II
			6S	1.1	1.1	-	1.7	-	1.1	-	-	-	-	1.1	-	-	-	-	-	-
			7S	1.1	1.1	-	1.4	-	1.1	1.4	-	-	-	1.1	1.1	1.1	1.1	1.1	1.1	-
			8S	1.1	1.1	-	1.1	-	1.1	-	1.1	-	1.1	1.1	1.1	1.1	1.1	1.1	1.1	-
	Concrete		5C	1.0	1.0	1.0	-	1.0	-	-	-	1.0	1.0	-	-	-	-	-	ACI 318-71	
			6C	1.0	1.0	1.0	1.5	-	1.0	-	-	-	-	1.0	-	-	-	-	-	
			7C	1.0	1.0	1.0	1.25	-	1.0	1.25	-	-	-	1.0	1.0	1.0	1.0	1.0	1.1	
			8C	1.0	1.0	1.0	1.0	-	1.0	-	1.0	-	1.0	-	1.0	1.0	1.0	1.0	1.0	

(F_s = Allowable Stress)

- (1) See Subsection 3.8.3.3 for discussion of loadings.
- (2) In above load combinations, the peak values of P_a, T_a, R_a, R_{ij}, R_{rr}, R_{rm} and M shall be combined (when they act concurrently) unless time history analysis is performed to justify otherwise.
- (3) For these load combinations either elastic or plastic design may be used.
- (4) Load combinations 7S, 8S, 7C and 8C are also checked without R_{rr}, R_{ij}, R_{rm}.
- (5) Where ASR strains are greater than 0.05% (0.5 mm/m), ASR load factors may be reduced by 20% but shall not be taken as less than 1.0.

Note: Section references made in the footnotes of this table refer to sections within the UFSAR [12].

Table 6 – Load Combinations for Evaluation of Seismic Category I Structures other Than Containment (Modified from Table 3.8-16 of UFSAR to Include ASR Loads and Load Factors)

TABLE 3.8-16 CATEGORY I, STRUCTURES OTHER THAN REACTOR CONTAINMENT STRUCTURE OR ITS INTERNALS BASIC LOAD COMBINATIONS AND LOAD FACTORS

Design Conditions		Material	All Structures														Concrete Only				Certain Structures, Where Appropriate										Stress Limit (5) or Design Criteria
			Required Strength	Dead Load and Hydrostatic Load	Live Load	Operational Temperature	Operating Basis Earthquake	Safe Shutdown Earthquake	Wind	Tornado Wind	Lateral Earth Pressures	Earth Pressure due to OBE	Earth Pressure due to SSE	ASR Loads (6)	Operational Piping Loads	Accident Pressure	Accident Piping Loads	Jet Impingement Loads	Missile Impact Loads	Jet Force Reaction	Internal Missile Loads	Accident Temperature	Design basis Flood	Unusual Snow Load							
Loading Notations			D	L	T _o	E _o	E _s	W	W _t	E	H _e	H _i	S _a	R _o	P _a	R _s	R _{ij}	R _{im}	R _{er}	M	T _a	F	Ls								
Normal Load	Structural Steel	S	1.0	1.0	-	-	-	-	-	-	-	-	-	-	-	-	-	-	-	-	-	-	-	-	≤F _a Per AISC						
			1.0	1.0	-	1.0	-	-	-	-	-	-	-	-	-	-	-	-	-	-	-	-	-	-	-						
			1.0	1.0	-	-	-	-	1.0	-	-	-	-	-	-	-	-	-	-	-	-	-	-	-	-	-					
			0.67	0.67	0.67	-	-	-	-	-	-	-	-	-	-	0.67	-	-	-	-	-	-	-	-	-	-					
			0.67	0.67	0.67	0.67	-	-	-	0.67	-	-	-	-	-	0.67	-	-	-	-	-	-	-	-	-	-					
	Concrete	U	1.4	1.7	-	-	-	-	-	-	1.7	-	-	2.0	-	-	-	-	-	-	-	-	-	-	-	ACI 318-71					
			1.4	1.7	-	1.9	-	-	-	-	1.7	1.9	-	1.3	-	-	-	-	-	-	-	-	-	-	-						
			1.4	1.7	-	-	-	1.7	-	-	1.7	-	-	1.7	-	-	-	-	-	-	-	-	-	-	-						
			1.05	1.28	1.28	-	-	-	-	-	1.28	-	-	1.5	1.28	-	-	-	-	-	-	-	-	-	-	-					
			1.05	1.28	1.28	1.43	-	-	-	-	1.28	1.43	-	1.0	1.28	-	-	-	-	-	-	-	-	-	-	-					
			1.05	1.28	1.28	-	-	-	1.3	-	1.28	-	-	1.28	1.28	-	-	-	-	-	-	-	-	-	-	-					
			1.2	-	-	-	-	1.7	-	-	1.7	-	-	1.7	-	-	-	-	-	-	-	-	-	-	-	-					
			1.2	-	-	1.9	-	-	-	-	1.7	1.9	-	1.3	-	-	-	-	-	-	-	-	-	-	-	-					
			Unusual Load	Structural Steel	Elastic	0.63	0.63	0.63	-	0.63	-	-	-	-	-	-	0.63	-	-	-	-	-	-	-	-	-	-	≤F _a Per AISC			
0.63	0.63	0.63				-	-	-	0.63	-	-	-	-	0.63	0.63	0.63	0.63	0.63	0.63	0.63	0.63	0.63	0.63	0.63							
0.63	0.63	-				0.63	-	-	-	-	-	-	-	-	-	0.63	0.63	0.63	0.63	0.63	0.63	0.63	0.63	0.63	0.63						
Plastic	Y	0.59			0.59	-	-	0.59	-	-	-	-	-	-	-	-	0.59	0.59	0.59	0.29	0.29	0.29	0.29	0.29	0.29	0.59	AISC, Part II				
		1.1			1.1	1.1	-	1.1	-	-	-	-	-	-	1.1	-	-	-	-	-	-	-	-	-	-	-					
		1.1			1.1	1.1	-	-	-	1.1	-	-	-	-	-	1.1	-	-	-	-	-	-	-	-	-	-	-				
		1.1			1.1	-	-	-	-	-	-	-	-	-	-	-	1.7	1.1	1.1	1.1	1.1	1.1	1.1	1.1	1.1	1.1					
Concrete	U	1.1		1.1	-	1.4	-	-	-	-	-	-	-	-	-	1.4	1.1	-	-	-	-	-	-	-	1.1						
		1.1		1.1	-	-	1.1	-	-	-	-	-	-	-	-	1.1	1.1	1.1	1.1	1.1	1.1	1.1	1.1	1.1	1.1						
		1.0		1.0	1.0	-	1.0	-	-	-	1.0	-	1.0	1.0	1.0	-	-	-	-	-	-	-	-	-	-	-	ACI 318-71				
		1.0		1.0	1.0	-	-	-	1.0	-	1.0	-	-	1.0	1.0	-	-	-	-	-	-	-	-	-	-	-					
		1.0		1.0	-	-	-	-	-	-	1.0	-	-	1.0	-	1.5	1.0	-	-	-	-	-	1.1	1.0	-	-					
		1.0		1.0	-	1.25	-	-	-	-	1.0	1.25	-	1.0	-	1.25	1.0	1.0	1.0	1.0	1.0	1.0	1.0	1.0	1.0	1.0					
		1.0		1.0	-	-	1.0	-	-	-	1.0	-	1.0	1.0	1.0	-	1.0	1.0	1.0	1.0	1.0	1.0	1.0	1.0	1.0	1.0					
1.0	1.0	1.0	-	-	1.0	-	1.0	-	-	-	1.0	1.0	-	-	-	-	-	-	-	-	-	-	(3)	1.0							
1.0	1.0	1.0	-	-	1.0	-	1.0	-	-	-	1.0	1.0	-	-	-	-	-	-	-	-	-	-	1.0	1.0							

(1) In above load combinations, the peak values of P_a, T_a, R_s, R_{ij}, R_{im}, R_{er}, and M shall be combined (when acting concurrently) unless time history analysis is performed to justify otherwise.
 (2) Elastic cases to be checked for overall stability by the plastic load combination cases as indicated by (*).
 (3) For design bases flood load case, elevation shall be the effective maximum ground water elevation i.e., El. + 20'-0".
 (4) See Subsection 3.8.4.3 for discussion of loadings.
 (5) (F_a = Allowable Stress)
 (6) Where ASR strains are greater than 0.05% (0.5 mm/m), ASR load factors may be reduced by 20% but shall not be taken as less than 1.0.

Note: Section references made in the footnotes of this table refer to sections within the UFSAR [12].

Table 7 – Structure Deformation Monitoring Requirements

Analysis Stage	Deformation Evaluation Stage	Monitoring Interval
1	Screening Evaluation	3 years
2	Analytical Evaluation	18 months
3	Detailed Evaluation	6 months

Table 8 – Acceptance Criteria for Stability against Overturning, Sliding and Flotation

Load	Factor of Safety		
	Overturning	Sliding	Flotation
Service/Normal load combinations	1.5	1.5	-
Factored/Unusual load combinations	1.1	1.1	-
Dead load and design basis flood load	-	-	1.5

Table 9 – Field Observations and Measurements for Susceptibility Evaluations

Label	Description
AC	<u>Cracking suspect of ASR (visual observations)</u> Qualitative visual observations made of cracking that exhibits visual indications of ASR and ASR-related features, using industry guidelines described in References [7] and [9][9].
NC	<u>Cracking not suspect of ASR (visual observations)</u> Qualitative visual observations made of cracking that does not exhibit indications of ASR. These cracks may be structural (i.e. caused by stresses acting on the structure) or caused by shrinkage or other mechanisms aside from ASR.
SD	<u>Other structural or material distress (visual observations)</u> Qualitative visual observations made of structural distress, such as buckled plates, broken welds, spalled concrete, delaminated concrete, displacement at embedded plates, damage to coatings, and chemical staining.
CI	<u>Cracking index</u> Quantitative measurement of in-plane cracking on a concrete structural component using the cracking index measurement procedure.
IP	<u>In-plane expansion</u> Quantitative measurement of distance between two points installed at the surface of a concrete component using a removable strain gage. In-plane expansion is computed as the change in length-measurement values recorded at different times.
TS	<u>Through-thickness expansion</u> Quantitative measurement in the through-thickness direction of a concrete component using an extensometer device. Through-thickness expansion is computed as the change in through-thickness measurement values recorded at different times.
CW	<u>Individual crack widths/lengths</u> Quantitative measurement of individual crack widths using either a crack card, an optical comparator, or any other instrument of sufficient resolution. Such measurements shall be accompanied by notes, sketches, or photographs that indicate the pattern of the cracks and their length. Also included in this category are tools that quantify the change in crack widths, such as mountable crack gages, extensometers, and invar wires.
SJ	<u>Seismic isolation joints</u> Quantitative measurement of the width of seismic joints that separate two adjacent structures. Also included in this category are qualitative observations of distress in seals covering or filling isolation joints, such as tears, wrinkles, and bubbles.
DM	<u>Structure dimensions</u> Quantitative measurement of a structure's dimensions or the distance between two adjacent structures. Included in this category are measurements of plumbness of walls, levelness of slabs, and bowing/bending of members.
EQ	<u>Equipment/conduit offsets</u> Quantitative measurement or visual observation of building deformation through the misalignment of equipment and/or the deformation of flexible conduit joints.
OT	<u>Other observations/measurements</u> Any other observations or measurements that can be used to characterize and/or quantify ASR conditions or other conditions of distress.

10. FIGURES

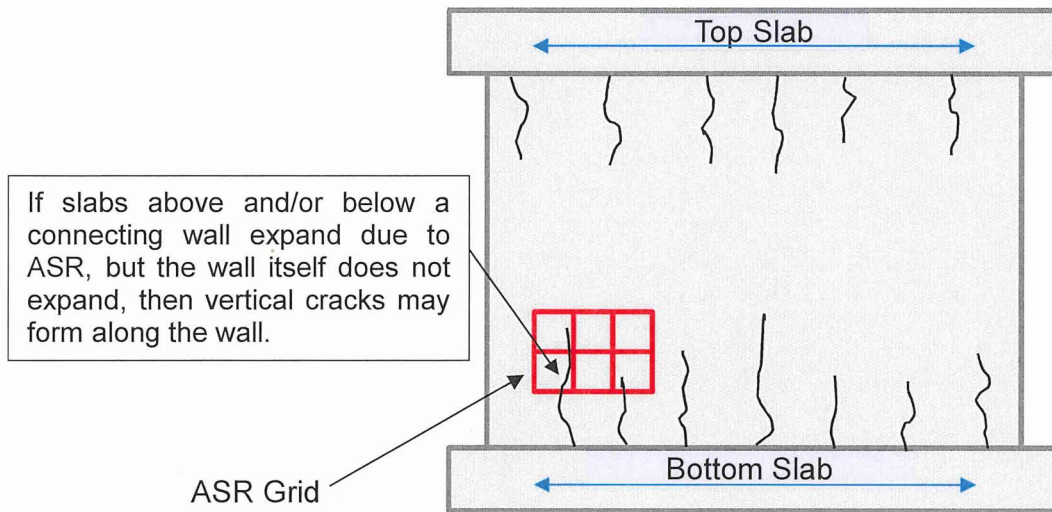
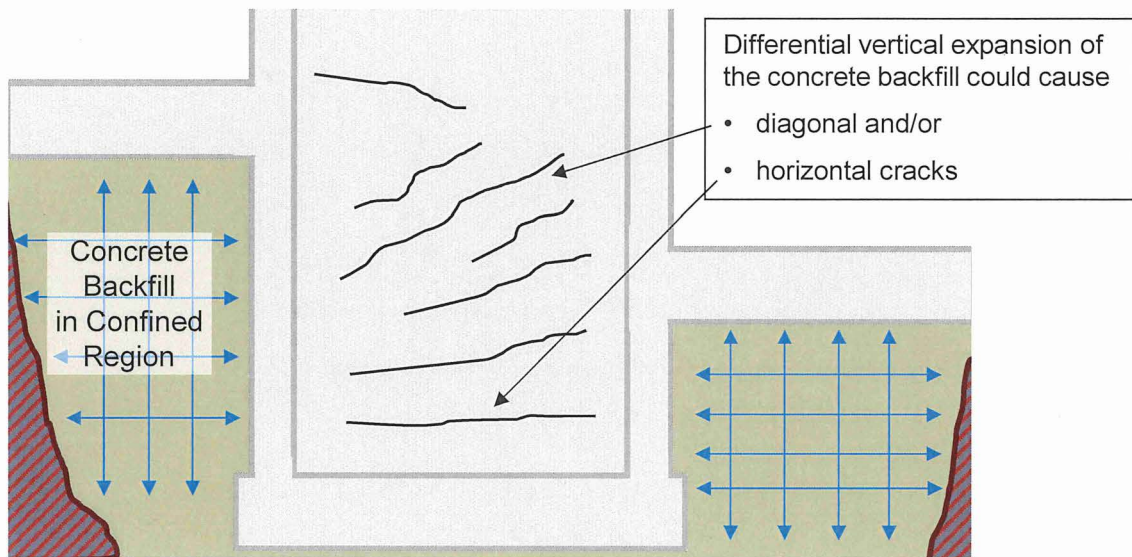
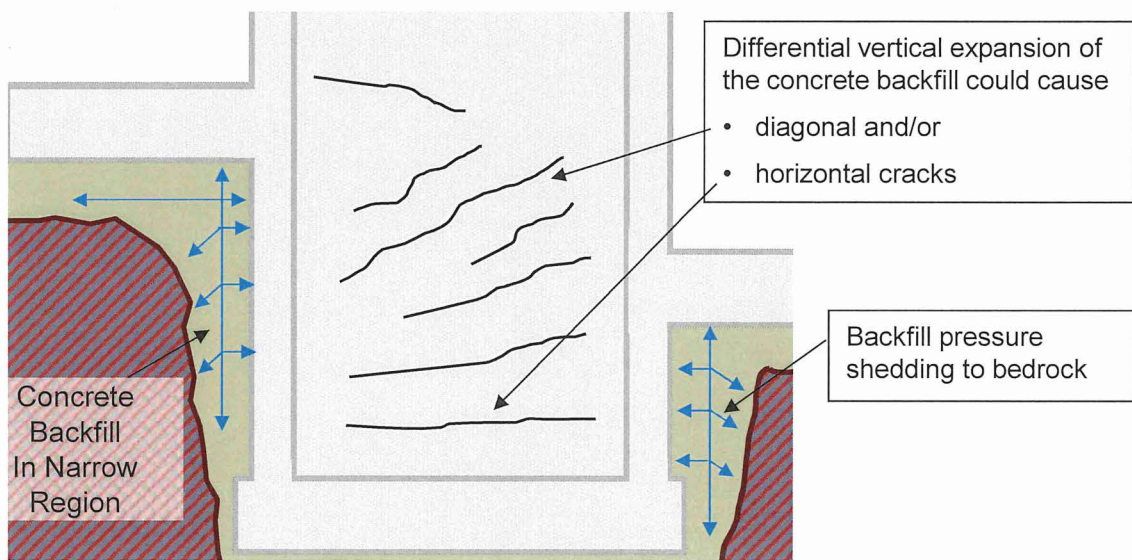


Figure 1. Structural Cracks due to Differential ASR Expansion in the Structure.



(a)



(b)

Figure 2. Structural Cracks due to Differential ASR Expansion in the Concrete Backfill.

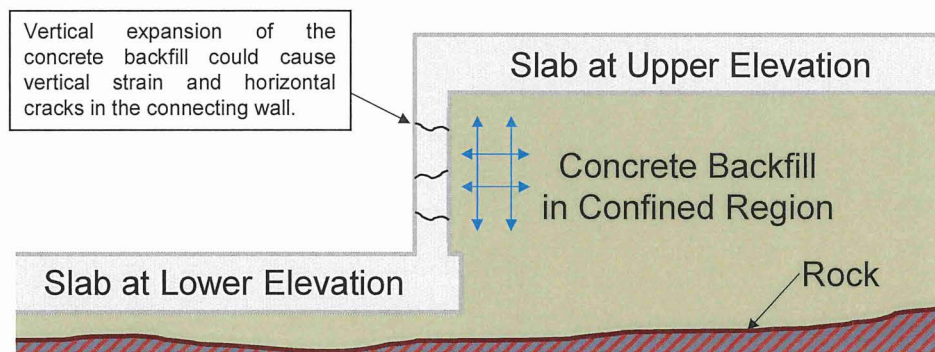


Figure 3. Structural Cracks due to Concrete Backfill Expansion.

Lateral Pressure Exerted by Concrete Fill

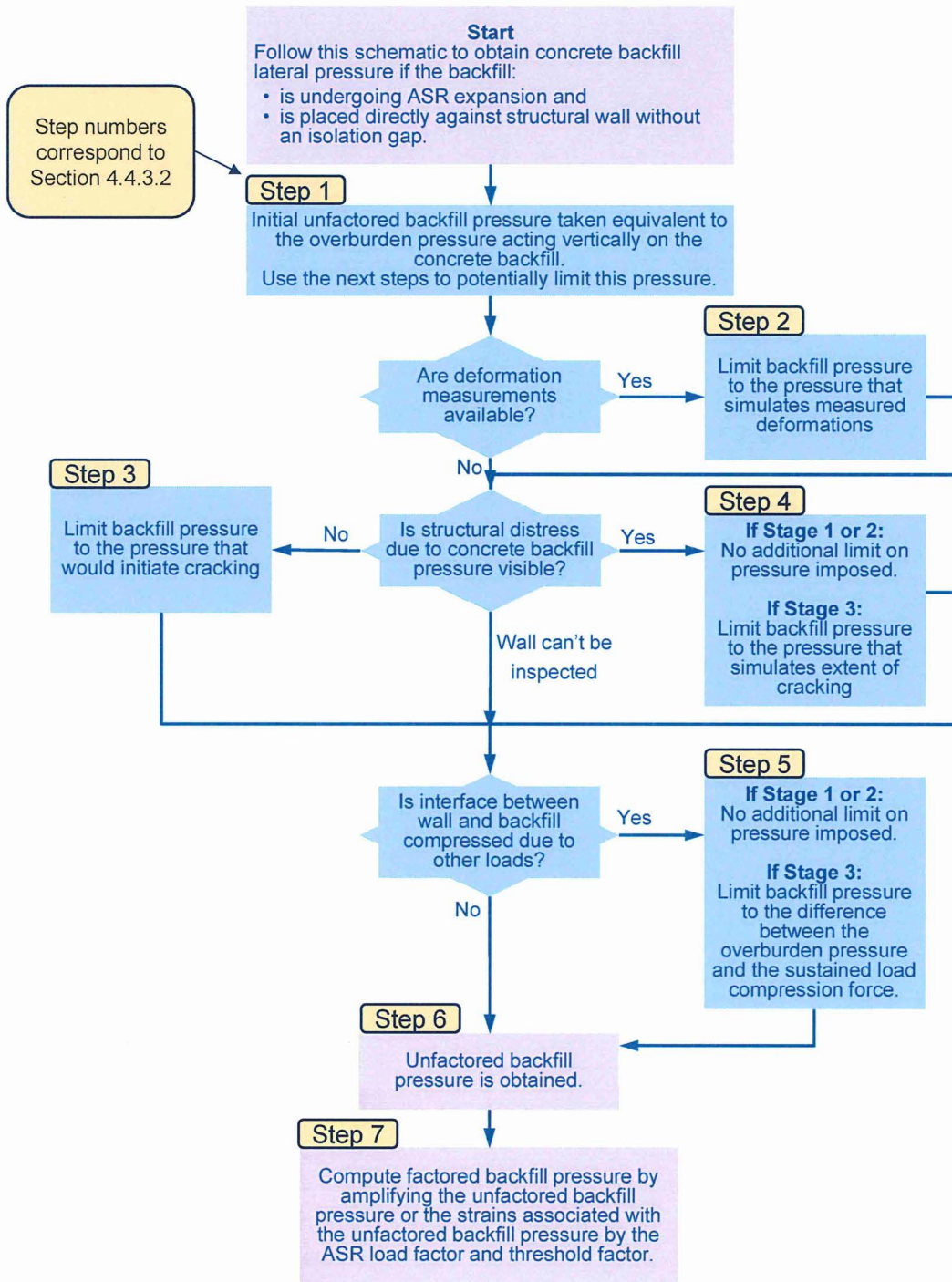


Figure 4. Flow Chart Schematic for Computing Lateral Concrete Backfill Pressure due to ASR.

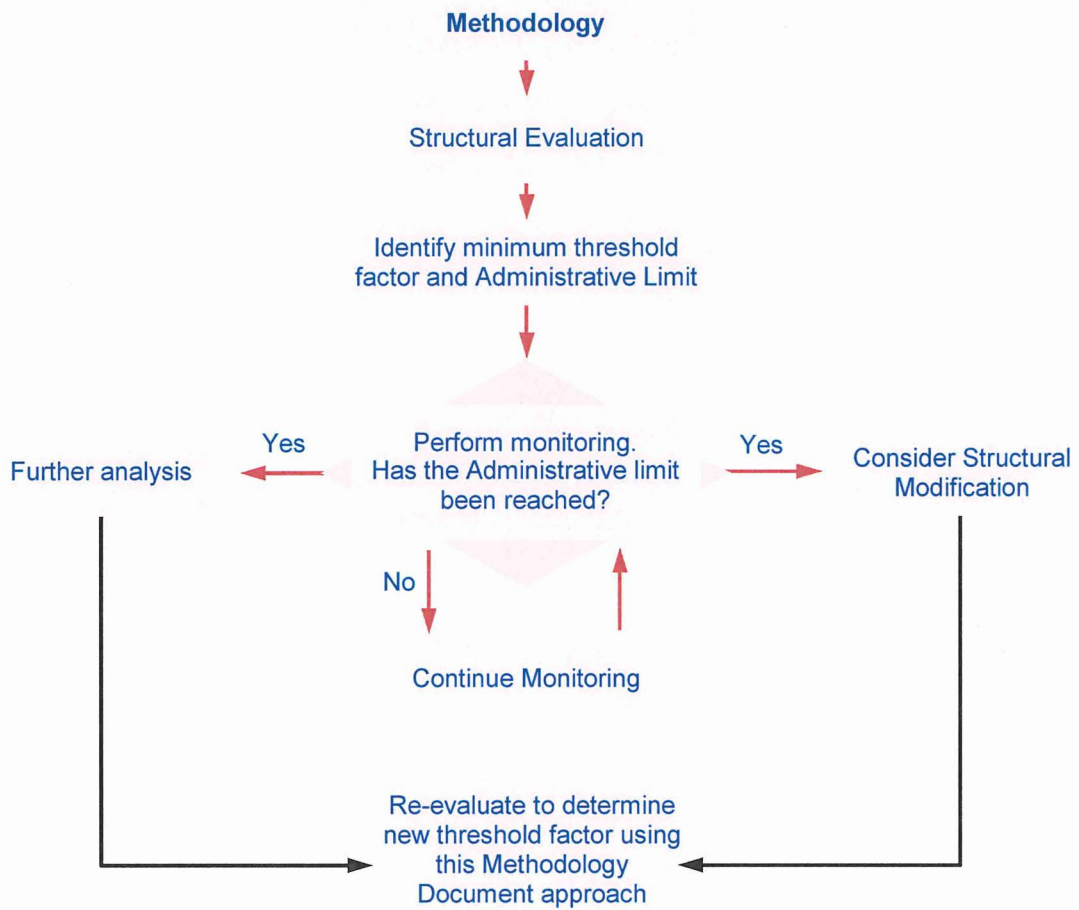


Figure 5. Threshold Monitoring

APPENDIX A

APPENDIX A – DETERMINATION OF CRACKED SECTION PROPERTIES

Reinforced concrete cracked section properties shall be determined by following the steps described below:

- **Step One:** Perform the finite element analysis using uncracked section properties.
- **Step Two:** Post-process the results and find the membrane/axial strain, in-plane shear strain, and the out-of-plane moment (M_a) if applicable for each group of elements, i.e. groups of elements that form a region, component, or a member. If the magnitude of moment exceeds the cracking moment and/or axial/membrane strain exceeds the cracking strain, then the elements of that group are cracked.
- **Step Three:** Knowing the bending moment, axial strain, and shear strain in concrete elements, calculate the required amount of reduction in flexural, axial, and shear rigidities as follows:
 - **Flexural rigidity:** Knowing the moment in the concrete elements, M_a , compute the effective moment of inertia, I_e , using Equation 9-4 of ACI 318-71 [A1] with the condition that the effective moment of inertia shall not exceed the gross moment of inertia:

$$I_e = \left(\frac{M_{cr}}{M_a}\right)^3 \cdot I_g + \left[1 - \left(\frac{M_{cr}}{M_a}\right)^3\right] \cdot I_{cr} \leq I_g$$

where M_a is the demanding moment from analysis, M_{cr} is cracking moment calculated accounting for the effect of precompression due to ASR expansion or other load effects, and I_g and I_{cr} are gross and cracked moment of inertias, respectively. This equation implies that as the moment demand (M_a) increases, the effective moment of inertia approaches the cracked moment of inertia.

To circumvent the need for iteration, the effective moment of inertia can be set equal to $0.5I_g$ but not less than I_{cr} per Supplement 4 to ACI 318-71 discussed in Section 5.6.

To consider the simultaneous effects of axial tension and bending moment, the value of M_{cr} and/or I_{cr} may be computed for a cross-section subjected to tension; however, excluding such an effect is conservative, and hence, is recommended.

Stiffness reduction coefficient in flexure (ratio of cracked to uncracked flexural rigidity) is:

$$K_f = \frac{(EI)_e}{(EI)} = \frac{I_e}{I_g}$$

- **Axial rigidity:** Knowing the axial/membrane mechanical strain in concrete element, ε , calculate the axial stress, σ , using either the procedure recommended

by ACI Committee 224 [A3] or the Steven's equation that accounts for tension stiffening [A4] by using an exponential decay function.

$$\sigma = f_t [(1 - M)e^{-\lambda_t(\varepsilon - \varepsilon_{cr})} + M]$$

Where:

$$M = 75 (mm) \frac{\rho}{d_b}$$

$$\lambda_t = \frac{540}{\sqrt{M}}$$

$$\varepsilon_{cr} = f_t / E_c$$

ε is the axial mechanical strain in concrete, σ is the tensile stress in concrete, d_b is the diameter of longitudinal rebar in mm, ρ is the longitudinal reinforcement ratio, f_t is the uniaxial tensile strength of concrete material defined in Section 4.4.5, and E_c is the elastic modulus of concrete. In the above equations, M determines the residual tensile strength, and λ_t controls the area under the softening portion of the curve which is related to Mode-I fracture energy. Note that by using the mechanical strain in concrete, the effect of prestressing due to ASR expansion or precompression due to other load effects is inherently captured. The effective concrete modulus is:

The

$$E_e = \frac{\sigma}{\varepsilon}$$

Stiffness reduction coefficient in axial (ratio of cracked over uncracked axial rigidity) is:

$$K_a = \frac{(EA)_e}{(EA)} = \frac{E_e}{E_c}$$

- **Shear rigidity:** Knowing the shear strain in concrete, ε_s , compute the stiffness reduction coefficient in shear (shear retention factor) for regions with or with expected shear cracks [A6] as follows:

$$K_s = \frac{(GA)_e}{GA} = -\frac{c_3}{c_2} \ln \left(\frac{1000\varepsilon_s}{c_1} \right)$$

Where:

$$c_1 = 7 + 333(\rho - 0.005)$$

$$c_2 = 10 - 167(\rho - 0.005)$$

$$c_3 = 1 \text{ (per [A6] recommendation)}$$

ε_s is the analytically computed mechanical shear strain, and ρ is the longitudinal reinforcement ratio.

- **Step Four:** Knowing the stiffness reduction coefficient in flexure (K_f), axial (K_a) and shear (K_s), calculate the cracked section properties for each type of element. Note that the following formulation accommodates any combinations of flexural, axial and shear cracks; for instance if no axial crack was observed (in the field and/or analysis), the equations remain valid by setting $K_a = 1$.
- **Shell elements:** There are five stiffnesses (K_{fx} , K_{fy} , K_{ax} , K_{ay} , K_s defined below) but only four input properties (t_{cr} , $E_{cr,x}$, $E_{cr,y}$, G_{cr} defined below) to an orthotropic shell element; therefore, a membrane element must be introduced. The orthotropic material properties and adjusted shell and membrane thicknesses shall be computed as:

$$t_{cr} = \sqrt{\frac{K_{fx}}{K_{ax}}} \times t$$

$$E_{cr,x} = K_{ax} \sqrt{\frac{K_{ax}}{K_{fx}}} \times E_c$$

$$E_{cr,y} = K_{fy} \left(\sqrt{\frac{K_{ax}}{K_{fx}}} \right)^3 \times E_c$$

$$G_{cr} = K_s \frac{t}{t_{cr}} \times G_c$$

$$E_{cr,y.add} = K_{ay} \frac{t}{t_{cr}} E_c - E_{cr,y}$$

where E_c and G_c are elastic and shear moduli of idealized homogenous concrete material, $E_{cr,x}$ and $E_{cr,y}$ correspond to the orthotropic material elastic moduli of the orthotropic shell element, G_{cr} is the cracked shear modulus of the shell element, t and t_{cr} are the uncracked and adjusted cracked thicknesses of the shell and membrane elements, K_{ax} and K_{ay} are the ratio of cracked to uncracked axial rigidities along two local axis of the shell element, K_{fx} (about y-axis) and K_{fy} (about x-axis) are the ratio of cracked over uncracked flexural rigidities about two local axes of the shell element, and $E_{cr,y.add}$ is the modulus of the additional membrane element along the y-local axis.

Note that the additional membrane element has axial stiffness only in the direction of the larger axial stiffness (parallel to the larger crack direction).

Since the thickness of the shell element is changed, the density must be adjusted to keep the self-weight unaltered. No weight density is needed in the additional membrane element.

$$Dens_{cr} = Dens \frac{t}{t_{cr}}$$

- **Solid elements:** There are six equations and six unknowns, and all equations are independent. The orthotropic material properties shall be calculated as:

$$E_{cr.x} = K_{ax} E_c$$

$$E_{cr.y} = K_{ay} E_c$$

$$E_{cr.z} = K_{az} E_c$$

$$G_{cr.xy} = K_{sxy} G_c$$

$$G_{cr.yz} = K_{syz} G_c$$

$$G_{cr.xz} = K_{sxz} G_c$$

- **Beam elements:** There are four equations and four unknowns, and therefore the orthotropic material properties shall be calculated as:

$$b_{cr} = b \sqrt{\frac{K_{fz}}{K_{ax}}}$$

$$h_{cr} = h \sqrt{\frac{K_{fy}}{K_{ax}}}$$

$$E_{cr.x} = K_{ax} \frac{b \times h}{b_{cr} \times h_{cr}} E_c$$

$$G_{cr} = K_s \frac{b \times h}{b_{cr} \times h_{cr}} G_c$$

$$Dens_{cr} = Dens \frac{b \times h}{b_{cr} \times h_{cr}}$$

where, b_{cr} and h_{cr} are adjusted cross-sectional width and height.

- **Step Five:** Modify the finite element model by assigning the calculated cracked section properties to the elements and rerun the analysis. The analysis is considered complete if the overall magnitude of the 1st principal mechanical tensile strain for the majority of cracked elements from two successive steps remain approximately unchanged. If this condition has not been satisfied, go to Step Two and repeat the process.

References for Appendix A

- [A1] American Concrete Institute, ACI Committee 318, *Building Code Requirements for Reinforced Concrete*, ACI 318-71, Third Printing, 1972.
- [A2] ACI 318-14 Building Code Requirements for Structural Concrete and Commentary, 2014
- [A3] ACI Committee 224, *Cracking of Concrete Members in Direct Tension*, ACI 224.2R-92, Reapproved 1997.
- [A4] Lu, Yuan, and Marios Panagiotou. "Three-dimensional cyclic beam-truss model for nonplanar reinforced concrete walls." *Journal of Structural Engineering*, 2013, 140(3): 04013071.
- [A5] Nilson A. H., Darwin D., and Dolan C. W. *Design of concrete structures*, 14th Edition, 2010.
- [A6] Červenka V., Jendele L., and Červenka J., ATENA Program Documentation, Part 1, Theory. Dec. 2016, pp 29.

Enclosure 4 to SBK-L-18074

Simpson Gumpertz & Heger Document No. 170444-L-003 Rev. 1, "Response to RAI-D8-Attachment 1 Example Calculation of Rebar Stress For a Section Subjected to Combined Effect of External Axial Moment and Internal ASR."



RESPONSE TO RAI-D8-ATTACHMENT 1

EXAMPLE CALCULATION OF REBAR STRESS FOR A SECTION SUBJECTED TO COMBINED EFFECT OF EXTERNAL AXIAL AND MOMENT AND INTERNAL ASR

1. REVISION HISTORY

Revision 0: Initial document.

2. OBJECTIVE OF CALCULATION

The objective of this calculation is to provide an example calculation of rebar stress used in parametric studies 1 and 2 in response to RAI-D8.

3. RESULTS AND CONCLUSIONS

Table 1 summarizes the tensile stress in rebars corresponding to constant axial force and moment with an increasing ASR expansion. The results are also plotted in Figure 1b. This data is used to draw diagrams similar to what presented in Figure 3b of parametric study 1.

4. DESIGN DATA / CRITERIA

Diagrams presented in the response to RAI-D8 are extracted for two extreme sections one with minimum reinforcement ratio and the other with maximum reinforcement ratio. There is no other criteria.

5. ASSUMPTIONS

5.1 Justified assumptions

The concrete material is represented by compression only elastoplastic material with compressive strain cutoff of 0.003. This simple constitutive model satisfactorily captures the response of concrete in compression because stresses are not near reaching the compressive strength. Attachment 2 Appendix H provides a comparison study between the stresses in rebars of the critical component of two structures (with high and low compressive stress in concrete) computed using two different constitutive models for concrete, namely:

- Accurate model that uses Kent and Park concrete response in compression
- Simple model/idealized model which is an elastoplastic model with compressive stress cutoff at compressive strain of 0.003

The concrete strength in tension is conservatively neglected.

5.2 Unverified assumptions

There are no unverified assumptions.

6. METHODOLOGY

As an example calculation, Case I for a section with high reinforcement ratio is considered. The section is 2ft thick with 3000psi concrete that is reinforced with #11@6in. on both faces. The point corresponding to case I is highlighted on P-M interaction diagram provided in Figure 1. The amount of axial force and moment for Case I are -128.5kip/ft and 174.2kip-ft/ft, respectively.

To calculate the diagram in parametric study 1, the axial force and moment are kept constant while the internal ASR load is increased. Such a diagram is presented in Figure 3 of the response to RAI-D8. For the second parametric study, specific ASR expansion is selected and the amount of moment is increased. The calculation presented here provides an example for both parametric studies. In fact, the loading sequence does not matter.

The stress in rebars is calculated considering the following steps:

- 1) The geometry including thickness, rebar size, spacing, etc. are provided.
- 2) The compatibility and equilibrium equations are satisfied for concrete and steel when the concrete undergoes expansion due to internal ASR. Consequently, the initial stresses in concrete and steel are calculated.
- 3) Appropriate material model are assigned for concrete and steel. Specifically, elastic material for steel and an elastoplastic material for concrete are used.
- 4) Section is discretized into 20 layers, and appropriate functions are developed to facilitate the calculation of strain and stress at middle of each layer. Steel layers are also used at the center of rebars at each faces.
- 5) By knowing the value of axial force "P" ($P = -128.5\text{kip/ft}$), the curvature value " ϕ " is iterated to minimize the difference between the target moment ($M = 174.2\text{kip-ft/ft}$) and the moment from sectional analysis based on inputted axial force and trial curvature.
- 6) Using the developed functions, the strain and consequently stress are calculated for each steel fiber and at the farthest edge of the concrete compressive fiber.

7. REFERENCES

There are no references

8. COMPUTATION

8.1. Strain in Steel and Concrete due to Internal ASR expansion

Input Data

ASR expansion

Measured crack index	$\epsilon_{CI} := 0.8 \frac{\text{mm}}{\text{m}}$
Threshold factor	$F_{thr} := 1$

Material properties

Compressive strength of concrete	$f_c := -3\text{ksi}$
Young's modulus of concrete	$E_c := 3120\text{ksi}$
Yield strength of steel	$f_y := 60\text{ksi}$
Young's modulus of steel	$E_s := 29000\text{ksi}$

Geometry

Width of fibers	$b := 12\text{in}$
Total thickness or height	$h := 24\text{in}$
Area of concrete	$A_c := b \cdot h = 288 \cdot \text{in}^2$
Area of tensile reinforcement (#8@12 in.)	$A_s := 2 \cdot 1.56\text{in}^2$
Number of reinforcement in row, e.g. equal to 2 for tensile and compressive	$\text{Steel}_{\text{Num}} := 2$
Depth to reinforcement	$d := 20.3\text{in}$

Finding the strain in steel and concrete by satisfying compatibility and equilibrium

	Initial Guess
Initial mechanical strain in concrete	$\epsilon_{o,\text{conc}} := 0$
Initial strain in steel	$\epsilon_{o,\text{steel}} := 0$
	Given
Compatibility equation	$F_{thr} \cdot \epsilon_{CI} = \epsilon_{o,\text{steel}} - \epsilon_{o,\text{conc}}$

Equilibrium equation

$$(E_c \cdot A_c) \cdot \epsilon_{o,conc} + (E_s \cdot A_s \cdot \text{Steel}_{\text{Num}}) \cdot \epsilon_{o,steel} = 0$$

$$\text{ans} := \text{Find}(\epsilon_{o,conc}, \epsilon_{o,steel})$$

Initial strain in concrete and steel

$$\epsilon_{o,conc} := \text{ans}_1 = -1.341 \times 10^{-4}$$
$$\epsilon_{o,steel} := \text{ans}_2 = 6.659 \times 10^{-4}$$

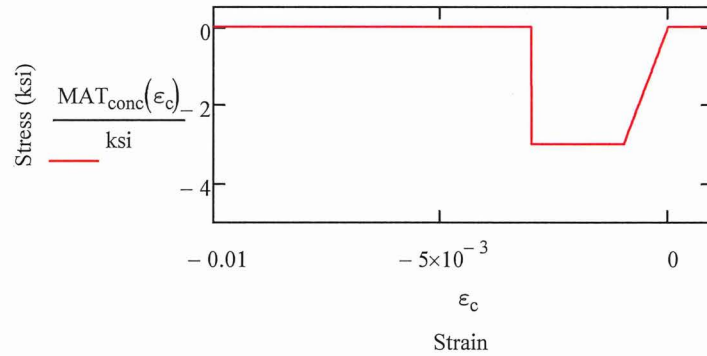
8.2. Sectional Analysis

Input Data

Concrete Material Model

Constitutive model for concrete

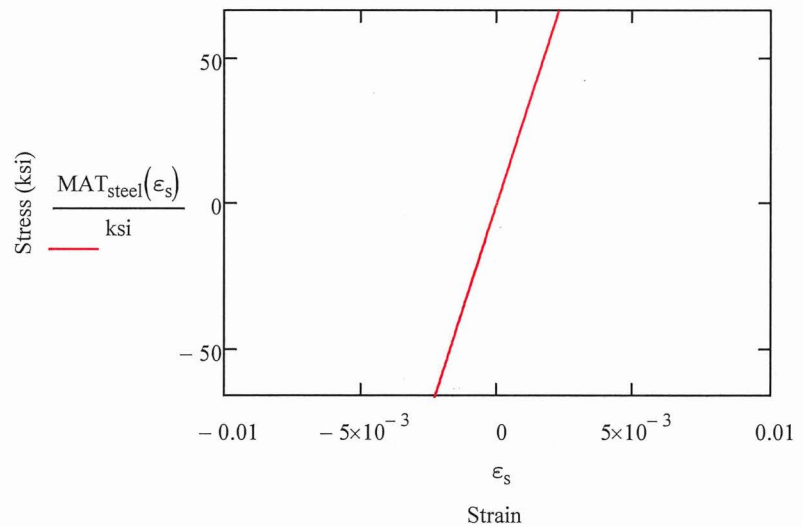
$$\text{MAT}_{\text{conc}}(\epsilon) := \begin{cases} 0 & \text{if } \epsilon > 0 \\ f_c & \text{if } -0.003 \leq \epsilon < \frac{f_c}{E_c} \\ 0 & \text{if } \epsilon < -0.003 \\ (E_c \cdot \epsilon) & \text{otherwise} \end{cases}$$



Steel Material Model

Constitutive model for steel

$$\text{MAT}_{\text{steel}}(\epsilon) := E_s \cdot \epsilon$$



Concrete Fibers

Number of fibers

$$\text{Conc}_{\text{Num}} := 20$$

Height of fibers

$$\text{Conc}_H := \frac{h}{\text{Conc}_{\text{Num}}} = 1.2 \cdot \text{in}$$

Concrete fiber coordinates

$$\text{Conc}_y := \begin{cases} \text{for } i \in 1.. \text{Conc}_{\text{Num}} \\ \text{ans}_i \leftarrow -\frac{h}{2} + \frac{\text{Conc}_H}{2} + (i-1) \cdot \text{Conc}_H \\ \text{ans} \end{cases}$$

Concrete fiber strain

$$\text{Conc}_\varepsilon(\varepsilon_{o.\text{conc}}, \varepsilon, \varphi) := \begin{cases} \text{for } i \in 1.. \text{Conc}_{\text{Num}} \\ \text{ans}_i \leftarrow \varepsilon_{o.\text{conc}} + \varepsilon - \varphi \cdot \text{Conc}_{y_i} \\ \text{ans} \end{cases}$$

Concrete fiber stress

$$\text{Conc}_\sigma(\varepsilon_{o.\text{conc}}, \varepsilon, \varphi) := \begin{cases} \text{for } i \in 1.. \text{Conc}_{\text{Num}} \\ \text{ans}_i \leftarrow \text{MAT}_{\text{conc}}(\text{Conc}_\varepsilon(\varepsilon_{o.\text{conc}}, \varepsilon, \varphi)_i) \\ \text{ans} \end{cases}$$

Concrete fiber force

$$\text{Conc}_F(\varepsilon_{o.\text{conc}}, \varepsilon, \varphi) := \begin{cases} \text{for } i \in 1.. \text{Conc}_{\text{Num}} \\ \text{ans}_i \leftarrow \text{Conc}_\sigma(\varepsilon_{o.\text{conc}}, \varepsilon, \varphi)_i \cdot (b \cdot \text{Conc}_H) \\ \text{ans} \end{cases}$$

Reinforcement/Steel fibers

Depth to reinforcement fiber

$$\text{Steel}_{y_1} := -\left(d - \frac{h}{2}\right) = -8.3 \cdot \text{in}$$

$$\text{Steel}_{y_2} := d - \frac{h}{2} = 8.3 \cdot \text{in}$$

Area of reinforcement fiber

$$\text{Steel}_{A_{s_1}} := A_s = 3.12 \cdot \text{in}^2$$

$$\text{Steel}_{A_{s_2}} := A_s = 3.12 \cdot \text{in}^2$$

Steel fiber strain

$$\text{Steel}_\varepsilon(\varepsilon_{o.\text{steel}}, \varepsilon, \varphi) := \begin{cases} \text{for } i \in 1.. \text{Steel}_{\text{Num}} \\ \text{ans}_i \leftarrow \varepsilon_{o.\text{steel}} + \varepsilon - \varphi \cdot \text{Steel}_{y_i} \\ \text{ans} \end{cases}$$

Steel fiber stress

$$\text{Steel}_\sigma(\varepsilon_{o.\text{steel}}, \varepsilon, \varphi) := \begin{cases} \text{for } i \in 1.. \text{Steel}_{\text{Num}} \\ \text{ans}_i \leftarrow \text{MAT}_{\text{steel}}(\text{Steel}_\varepsilon(\varepsilon_{o.\text{steel}}, \varepsilon, \varphi)_i) \\ \text{ans} \end{cases}$$

Steel fiber force

$$\text{Steel}_F(\varepsilon_{o.\text{steel}}, \varepsilon, \varphi) := \begin{cases} \text{for } i \in 1.. \text{Steel}_{\text{Num}} \\ \text{ans}_i \leftarrow \text{Steel}_\sigma(\varepsilon_{o.\text{steel}}, \varepsilon, \varphi)_i \cdot \text{Steel}_{A_{s_i}} \\ \text{ans} \end{cases}$$

Initial Stress State

Initial stress in concrete

$$\text{Concrete}_{\sigma} := \text{Conc}_{\sigma}(\varepsilon_{o,\text{conc}}, 0, 0)$$

$$\text{Concrete}_{\sigma_i} = -0.418 \cdot \text{ksi}$$

Initial stress in steel

$$\text{Rebar}_{\sigma} := \text{Steel}_{\sigma}(\varepsilon_{o,\text{steel}}, 0, 0)$$

$$\text{Rebar}_{\sigma_i} = 19.311 \cdot \text{ksi}$$

Axial Equilibrium

$$\text{Force}(\varepsilon_{o,\text{conc}}, \varepsilon_{o,\text{steel}}, \varepsilon, \varphi) := \left| \begin{array}{l} \text{ans1} \leftarrow 0 \\ \text{for } i \in 1.. \text{ConcNum} \\ \quad \text{ans1} \leftarrow \text{ans1} + \text{Conc}_F(\varepsilon_{o,\text{conc}}, \varepsilon, \varphi)_i \\ \text{ans2} \leftarrow 0 \\ \text{for } i \in 1.. \text{SteelNum} \\ \quad \text{ans2} \leftarrow \text{ans2} + \text{Steel}_F(\varepsilon_{o,\text{steel}}, \varepsilon, \varphi)_i \\ \text{ans} \leftarrow \text{ans1} + \text{ans2} \end{array} \right.$$

Moment Equilibrium

$$\text{Moment}(\varepsilon_{o,\text{conc}}, \varepsilon_{o,\text{steel}}, \varepsilon, \varphi) := \left| \begin{array}{l} \text{ans1} \leftarrow 0 \\ \text{for } i \in 1.. \text{ConcNum} \\ \quad \text{ans1} \leftarrow \text{ans1} + -1 \cdot \text{Conc}_F(\varepsilon_{o,\text{conc}}, \varepsilon, \varphi)_i \cdot \text{Conc}_{y_i} \\ \text{ans2} \leftarrow 0 \\ \text{for } i \in 1.. \text{SteelNum} \\ \quad \text{ans2} \leftarrow \text{ans2} + -1 \cdot \text{Steel}_F(\varepsilon_{o,\text{steel}}, \varepsilon, \varphi)_i \cdot \text{Steel}_{y_i} \\ \text{ans} \leftarrow \text{ans1} + \text{ans2} \end{array} \right.$$

Solution

Known parameters

Axial force $P := -128.52 \text{ kip}$

Iteration

Curvature $\phi := 0.000046 \cdot \frac{1}{\text{in}}$ Requires iteration

Solve for strain at centroid

Axial strain at centroid (initial guess) $x_0 := 0.0$

Axial force equilibrium $f(x) := \text{Force}(\epsilon_{o.\text{conc}}, \epsilon_{o.\text{steel}}, x, \phi) - P$
 $\epsilon_{\text{cent}} := \text{root}(f(x_0), x_0) = -7.471 \times 10^{-5}$

Sectional forces

$\text{Force}(\epsilon_{o.\text{conc}}, \epsilon_{o.\text{steel}}, \epsilon_{\text{cent}}, \phi) = -128.52 \cdot \text{kip}$
 $\text{Moment}(\epsilon_{o.\text{conc}}, \epsilon_{o.\text{steel}}, \epsilon_{\text{cent}}, \phi) = \blacksquare \cdot \text{kip} \cdot \text{ft}$

Stress and strain in concrete and steel

Steel fiber stress and strain

$$\text{Rebar}_\epsilon := \text{Steel}_\epsilon(\epsilon_{o.\text{steel}}, \epsilon_{\text{cent}}, \phi) = \begin{pmatrix} 9.73 \times 10^{-4} \\ 2.094 \times 10^{-4} \end{pmatrix}$$

$$\text{Rebar}_\sigma := \text{Steel}_\sigma(\epsilon_{o.\text{steel}}, \epsilon_{\text{cent}}, \phi) = \begin{pmatrix} 28.217 \\ 6.072 \end{pmatrix} \cdot \text{ksi}$$

$$\text{Steel}_p(\epsilon_{o.\text{steel}}, \epsilon_{\text{cent}}, \phi) = \begin{pmatrix} 88.036 \\ 18.946 \end{pmatrix} \cdot \text{kip}$$

$\text{Concrete}_y := \text{Conc}_y$

Concrete fiber stress and strain

$$\text{Concrete}_\epsilon := \text{Conc}_\epsilon(\epsilon_{o.\text{conc}}, \epsilon_{\text{cent}}, \phi)$$

$$\text{Concrete}_\sigma := \text{Conc}_\sigma(\epsilon_{o.\text{conc}}, \epsilon_{\text{cent}}, \phi)$$

Maximum compressive strain in concrete

$$\epsilon_{\text{max.comp}} := \frac{\text{Concrete}_\epsilon_{\text{ConcNum}} - \text{Concrete}_\epsilon_{\text{ConcNum-1}}}{\text{Conc}_y_{\text{ConcNum}} - \text{Conc}_y_{\text{ConcNum-1}}} \cdot \left(\frac{h}{2} - \text{Conc}_y_{\text{ConcNum-1}} \right) + \text{Concrete}_\epsilon_{\text{ConcNum-1}} \dots = -7.608 \times 10^{-4}$$

Maximum compressive stress in concrete

$$\sigma_{\text{max.comp}} := \text{MAT}_{\text{conc}}(\epsilon_{\text{max.comp}}) = -2.374 \text{ ksi}$$

9. TABLES

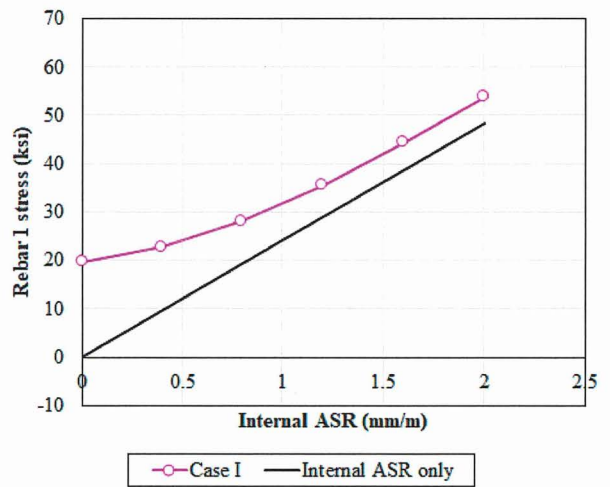
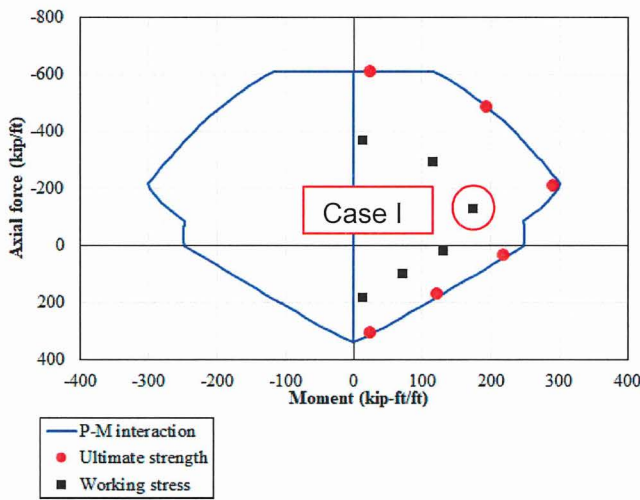
Table 1: Stress in rebars of 2ft thick section with high reinforcement ratio for $P=-128.52\text{kip/ft}$ and $M=174.24\text{kip-ft/ft}$

Cl (mm/m)	initial stress in concrete (ksi)	Curvature, ϕ (1/in)*	Total stress in steel (ksi)		Maximum compressive stress in concrete (ksi)
			Rebar 1	Rebar 1	
0	0	0.00007	19.737	-13.961	-2.31
0.4	9.655	0.000056	22.869	-4.089	-2.334
0.8	19.311	0.000046	28.217	6.072	-2.374
1.2	28.966	0.00004	35.511	16.255	-2.457
1.6	38.622	0.000038	44.377	26.084	-2.624
2	48.277	0.0000375	53.851	35.799	-2.821

*The curvature needs to be found iteratively to satisfy the moment equilibrium

Example in Section 8

10. FIGURES



(b) Location of Case I in P-M interaction

(b) Stress in the critical rebar of Case I

Figure 1: Results for Case I



RESPONSE TO RAI-D8-ATTACHMENT 2

EVALUATION OF MAXIMUM STRESS IN REBARS OF SEABROOK STRUCTURES

1. REVISION HISTORY

Revision 0: Initial document.

Revision 1: Revised pages 9, 10, 11 and 12 from Revision 0 to 1. The revision was made to remove footnotes 'a' and 'b' which identified CEB results to be preliminary, and WPC/PH and EMH results to be pending final review. Revised pages 1 to update Revision history section. Revised page 13 to update revision of references 7 and 8.

2. OBJECTIVE OF CALCULATION AND SCOPE

The objective of this calculation is to evaluate the stress in rebars of the structures at NextEra Energy (NEE) Seabrook Station in Seabrook, New Hampshire for in-situ load combinations considering unfactored normal operating loads when adding the loads due to ASR. All demands are from the ASR susceptibility evaluation of each structure.

The scope of this calculation includes the following structures:

- Control Room Makeup Air Intake structure (CRMAI)
- Residual Heat Removal Equipment Vault structure (RHR)
- Containment Enclosure Building (CEB)
- Enclosure for Condensate Storage Tank (CSTE)
- Main steam and feed water west pipe chase and Personnel Hatch (WPC/PH)
- Containment Equipment Hatch Missile Shield structure (CEHMS)
- Containment Enclosure Ventilation Area (CEVA)
- Safety-Related Electrical Duct Banks and Manholes (EMH) W01, W02, W09, and W13 through W16



3. RESULTS AND CONCLUSIONS

Stress evaluation results are listed below:

- The structure is evaluated for the load combinations listed in Section 4. The load combination listed below controls the calculation of maximum stress in rebars.
 - $D + L + E + T_o + E_o + H_e + F_{THR}.S_a$ (LC2)
- The stress in rebars of all structural components remain below yield strength. The following components give the highest stress in rebars:
 - Rebars along the horizontal strip of east exterior wall of the RHR structure at approximate elevation of -30 ft are stressed to 56.5 ksi subjected to LC2. The high stress is expected to occur in localized area, and therefore, the moment can distributed to mid span in susceptibility evaluation of the structure [3]. In addition, the stresses are expected to less because of the conservatism including a limited model of PAB as connected to RHR as explained in Section 6.3.
 - The maximum axial stress of 55.6 ksi is expected in rebars of the wall above east corner of Electrical Penetration at EL +45 ft subjected to LC2 in CEB.
 - Rebars along the horizontal strip at east wall of CRMAI structure are expected to experience tensile stress as high as 43.3ksi. The CI/CCI value over the walls of the structure is zero, and the induced demands are mainly due to relative expansion of the base mat with respect to walls.
 - Rebars in the east-west direction at the base slab of CEVA are expected to be stressed to 44 ksi if the CI value increases 200% beyond the current state. As explained in Section 6.6, the actual value is expected to be less because of the conservatism in computing unfactored demands due to original loads.

4. DESIGN DATA / CRITERIA

In response to RAI-D8 request, the maximum stress in the rebars of Seabrook structures is calculated and compared with yielding strength of rebars ($f_y = 60\text{ksi}$). In this evaluation, the following in-situ load combinations (also called service load and unfactored normal operating load) are considered:

- $D + L + E + T_o + S_a$ (In-situ condition, LC1)
- $D + L + E + T_o + E_o + H_e + F_{THR}.S_a$ (In-situ condition plus seismic load, LC2)

where D is dead load, L is live load, E is lateral earth pressure, T_o is operating temperature, E_o is the operating basis earthquake (OBE), H_e is dynamic earth pressure due to OBE, and S_a is ASR load. Operating temperature T_o is only applicable to the WPC/PH. For the second in-situ load combination, ASR loads are further amplified by a threshold factor (F_{THR}) to account for the future ASR expansion.

5. METHODOLOGY

To calculate the stress in rebars of structural components subjected to in-situ load combinations, sectional analysis based on fiber section method is used. In this method, the cross section is discretized into fibers (or layers), and an appropriate material model is assigned to each fiber. Figure 1 demonstrates a typical fiber section discretization. The total moment and axial force are calculated by integrating force over all fibers.

The concrete material is represented by compression only elastoplastic material with compressive strain cutoff of 0.003. This simple constitutive model satisfactorily captures the response of concrete in compression because stresses are not near reaching the compressive strength. Appendix H provides a comparison study between the stresses in rebars of the critical component of two structures (with high and low compressive stress in concrete) computed using two different constitutive models for concrete, namely:

- Accurate model that uses Kent and Park concrete response in compression
- Simple model/idealized model which is an elastoplastic model with compressive stress cutoff at compressive strain of 0.003

Both models are schematically depicted in Figure 2a. The concrete strength in tension is conservatively neglected. Reinforcing steel bars are modeled using elastic perfectly plastic material in compression and tension. Figure 2b demonstrates the steel material model used for the section analysis. The initial slope (Young modules) are 29,000 ksi for steel and $57,000\sqrt{f'_c}$ for concrete.

In this evaluation the ASR load effect causes:

- The axial force and bending moment that are induced by ASR expansion of other components (adjacent structural component)
- The internal stress in rebars due to ASR expansion of the component itself

The latter induces tensile stress in rebars and compressive stress in concrete that is called initial stress state. The effect of internal ASR expansion is considered by adding autogenous strain to the concrete and steel material. The input strain magnitude is set to be the ASR strain value measured over the specific component, and the output strains (initial strain in concrete and steel after application of ASR strain) are calculated by satisfying equilibrium and compatibility equations. If a member does not show any sign of internal ASR or the internal ASR expansion of the member was conservatively set equal to zero during ASR susceptibility evaluation of the structure, the initial stress in concrete and rebar are set to zero.

The critical sections that governed the calculation of threshold factor of each structure are selected for the evaluation, and demands due to combined effects of internal ASR expansion and induced ASR expansion of other components are computed with methods used in susceptibility evaluation of the structures. Appendix J provides Run ID logs. These demands are added to the demands subjected to original design loads, and the stress in rebars are calculated.

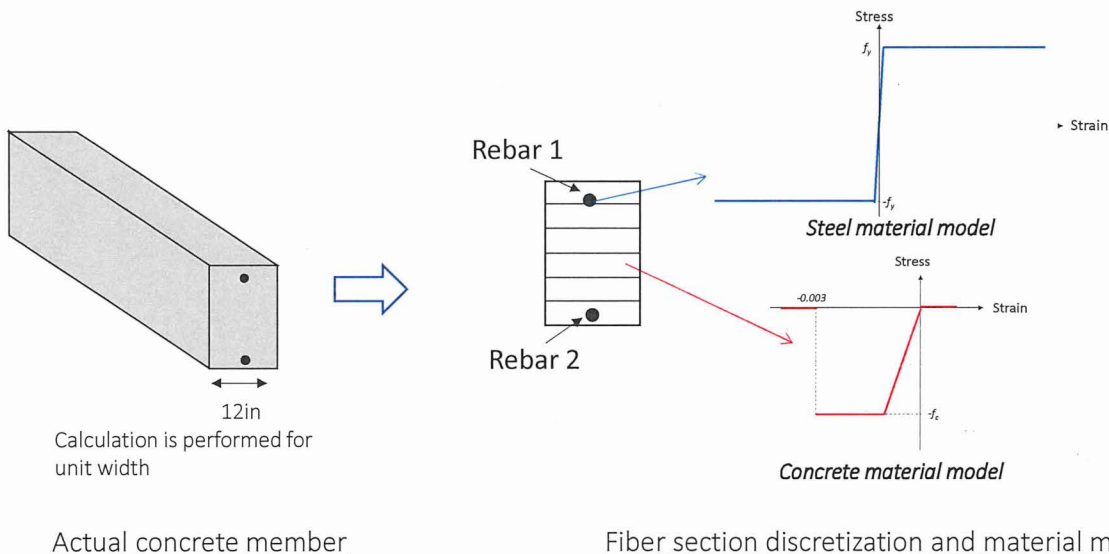


Figure 1 – Schematic representation of fiber section method

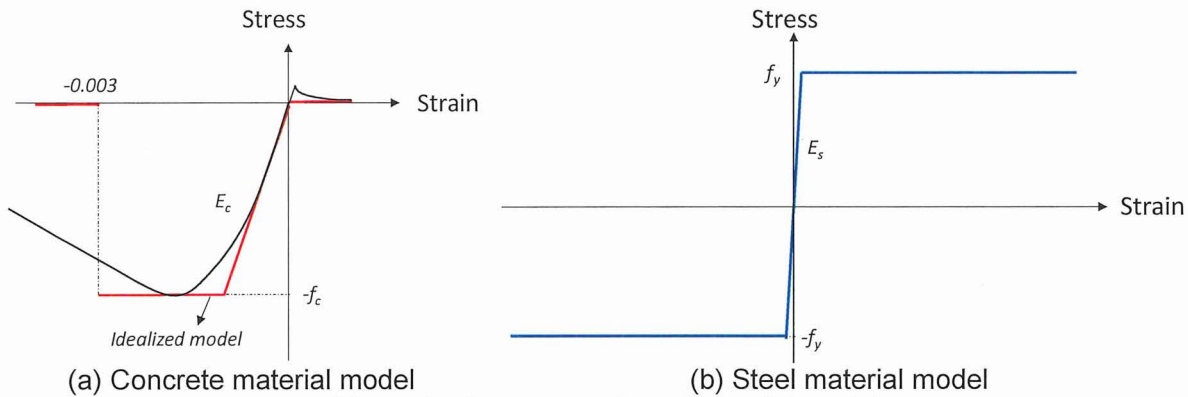


Figure 2 – Concrete and steel material model

6. ANALYSIS AND EVALUATION COMPUTATIONS

This section summarizes the maximum stress that are computed in rebars and concrete of several Seabrook structures at critical sections.

6.1 Control Room Makeup Air Intake structure

The stress in rebars of the critical components of CRMAI structure that governed the calculation of threshold factor is calculated and presented in Appendix A. Calculation of the threshold factor for the CRMAI structure is primarily governed by axial-flexure interaction along the horizontal strip of the east wall that occurs at the middle of the wall [1]. A threshold factor of 1.4 was determined from evaluation of the CRMAI structure, which indicates that ASR-related demands are amplified by 40% beyond the factored values.

Tables 1 and 2 summarize the stress in rebars of east wall and base mat of CRMAI structure. As can be seen from the table, the maximum axial stress is 43.3 ksi expected to form in a horizontal rebar of the walls close to the interior of the structure. The maximum stress in base mat that has highest ASR expansion within the structure is 39.1 ksi. Both stresses are below the yield strength of rebars.



6.2 Containment Enclosure Building

The stress in rebars at the critical section of the CEB structures is calculated and presented in Appendix B. The calculated threshold factor was 1.3 [2]. Tables 1 and 2 summarize the stress in rebars at two critical locations. The maximum axial stress of 55.6 ksi is expected in rebars of the wall above east corner of Electrical Penetration.

6.3 Residual Heat Removal Equipment Vault

The stress in rebars of the critical components of RHR structure that governed the calculation of threshold factor is calculated and presented in Appendix C. Calculation of the threshold factor for the RHR structure is primarily governed by axial-flexure interaction along the horizontal strip along the south side of the east exterior wall [3]. A threshold factor of 1.2 was determined from evaluation of the RHR structure, which indicates that ASR-related demands are amplified by 20% beyond the factored values.

Tables 1 and 2 list the stress in horizontal rebars of east exterior wall, and the stress in vertical rebars in west and east interior walls of RHR structure. As can be seen from the table, the maximum tensile stress of 59.5 ksi is expected in the vertical rebars of the east interior wall due to LC2. However, the RHR walls are designed to span horizontally between intersecting walls; and therefore, the vertical rebars are not part of the main load path for the RHR. Figure C1 shows the contour plots of vertical strains in the interior walls due to LC1. The contour plots show that the overall vertical strains are reasonable compared to the yielding strain of rebars. Localized strain concentration is observed close to the door openings at approximate El. (-) 30 ft. and El. (-) 45 ft.

The next highest tensile stress is 56.5 ksi calculated for the horizontal rebars of exterior east wall. The specific section also governed the determination of threshold factor for the RHR structure. As explained in the susceptibility evaluation of RHR [3], moment can distribute to mid span and along the width of the wall, therefore, localized strain concentration is not of concern. The majority of the stresses that develop at this location are due to the RHR connection to PAB. The PAB foundation locally stiffens the connection between the RHR and the PAB which attracts the moment demand about the vertical axis in the east exterior wall of the RHR. In addition, the PAB base slab is subject to uplift pressure from backfill expansion which in turns



induces forces in the RHR external walls near the connection. The stresses in the RHR evaluation and as reported here are conservative due to only including a limited model of PAB as connected to RHR which introduces extra overturning moment as well as the expected vertical shear force at this connection.

6.4 Condensate Storage Tank Enclosure

The stress in rebars of the critical components of CSTE structure that governed the calculation of threshold factor is calculated and presented in Appendix D. Selection of threshold factor for the CSTE structure is primarily governed by hoop tension at the top of the tank enclosure wall and vertical moment at the base of the tank enclosure wall [4]. A threshold factor of 1.6 was determined from evaluation of the CSTE structure, which indicates that ASR-related demands are amplified by 60% beyond the factored values.

Tables 1 and 2 summarize the stress in rebars of the tank enclosure wall of the CSTE structure. As can be seen from the table, the maximum axial stress of 26.7 ksi is expected to form in vertical rebars at the bottom of the tank enclosure wall.

6.5 Containment Equipment Hatch Missile Shield

The stress in rebars of the critical components of CEHMS structure that governed the calculation of threshold factor is calculated and presented in Appendix E. Selection of threshold factor for the CEHMS structure is primarily governed by out-of-plane moment at the base of east wing wall [5]. A threshold factor of 1.5 was determined from evaluation of the CEHMS structure, which indicates that ASR-related demands are amplified by 50% beyond the factored values.

Tables 1 and 2 summarize the stress in rebars of east wing wall of CEHMS structure. The maximum axial stress is 41.6 ksi expected to form in vertical rebars of the east wing wall at top of the column.

6.6 Containment Enclosure Ventilation Area

The stress in rebars of the critical components of CEVA structure that governed the calculation of threshold factor is calculated and presented in Appendix F. Selection of threshold factor for the CEVA is primarily governed by out-of-plane moment at the base slab located in Area 3 (Areas are defined in Ref. 6). A threshold factor of 3.0 was determined from evaluation of the



CEVA structure, which indicates that ASR-related demands are amplified by 200% beyond the factored values.

Tables 1 and 2 summarize the stress in rebars at the base slab. The maximum computed axial stress in rebars of the base mat is 44 ksi. However, as explained in Appendix F, the original design calculation did not provide demands due to unfactored load cases/combinations; hence, a conservative value was selected for the evaluation of rebar stress presented in Appendix F.

6.7 West Pipe Chase and Personnel Hatch

The stress in rebars at the critical flexural section of the WPC/PH structures is calculated and presented in Appendix I. The threshold factor of 1.8 was calculated based on out-of-plane shear of the WPC west wall [7]. Tables 1 and 2 summarize the stress in rebars at the base of the WPC north wall, the critical tensile stress location. A maximum tensile stress of 44.4 ksi develops in horizontal rebars of the WPC north wall.

6.8 Electrical Manholes

The stress in rebars at the critical flexural section of the EMH W13 and W15 is calculated and presented in Appendix G. The calculated threshold factor was 3.7 [8]. Tables 1 and 2 summarize the stress in rebars in EMH W13 and W15. A maximum tensile stress of 27.0 ksi develops in the horizontal rebars of EMH W13 and W15.

Table 1 – Stress in rebars of structural components subjected to LC1

	Component	Item		Internal ASR (mm/m)	Location	Total stress in steel (ksi)		Maximum compressive stress in concrete (ksi)	Maximum compressive mechanical strain in concrete
						Rebar 1	Rebar 2		
CRMAI	East Wall	M = 5.2	(kip-ft/ft)	0	East wall, horizontal strip, at the middle of the wall	36.2	26.8	0	>0
		P = 49.8	(kip/ft)						
	Base mat	M = 20.8	(kip-ft/ft)	0.99	North-south strip, at intersection with south walls	27.8	26.4	-0.28	-8.96e-5
		P = -28.4	(kip/ft)						
CEB	Wall	M = 459.5	(kip-ft/ft)	0.60	Between Mechanical & Electrical Penetration at Elev. -30ft.	27.1	5.60	-2.21	-6.61e-4
		P = -141.2	(kip/ft)						
	Wall	M = -39.6	(kip-ft/ft)	0.10	Wall between Mechanical & Electrical Penetration, below personal hatch	24.6	2.73	-0.71	-1.88e-4
		P = 14.1	(kip/ft)						
RHR	East exterior wall	M = -98.5	(kip-ft/ft)	0.75	East exterior wall, horizontal strip, at the approximate El. (-) 30 ft	46.9	11.4	-1.9	-6.09e-4
		P = -35.0	(kip/ft)						
	East interior wall	M = 28.6	(kip-ft/ft)	0.0	East interior wall, vertical strip, at the approximate El. (-) 45 ft	41.6	5.5	0.0	>0
		P = 37.2	(kip/ft)						
	West interior wall	M = 11.0	(kip-ft/ft)	0.0	West interior wall, vertical strip, at the approximate El. (-) 30 ft	26.5	12.5	0.0	>0
		P = 30.8	(kip/ft)						

Table 1 – (Continue)

	Component	Item		Internal ASR (mm/m)	Location	Total stress in steel (ksi)		Maximum compressive stress in concrete (ksi)	Maximum compressive mechanical strain in concrete
						Rebar 1	Rebar 2		
CSTE	Tank Enclosure Wall	M = 41.0	(kip-ft/ft)	0.43	Bottom of tank enclosure wall, vertical direction	15.8	8.6	-0.68	-1.89e-4
		P = -12.9	(kip/ft)						
CEHMS	East wing walls	M = 159.6	(kip-ft/ft)	0.72	East wing wall, at intersection with column	23.4	15.0	-0.78	-2.50e-4
		P = -8.3	(kip/ft)						
CEVA	Base slab	M = 83.7	(kip-ft/ft)	0.31	Base slab rebar along east-west direction	32.8	5.1	-0.89	-2.8e-4
		P = 1.7	(kip/ft)						
WPC/PH	North wall	M = 3.8	(kip-ft/ft)	0.24	North wall below pipe break beam	7.8	6.6	-0.07	-0.22e-4
		P = 19.1	(kip/ft)						
EMH	W13/W15	M = 7.4	(kip-ft/ft)	0.25	W13/W15 walls	11.2	5.6	-0.28	-9.61e-6
		P = -3.2	(kip/ft)						

Table 2 – Stress in rebars of structural components subjected to LC2

	Component	Item		F _{THR}	Internal ASR (mm/m)	Location	Total stress in steel (ksi)		Maximum compressive stress in concrete (ksi)	Maximum compressive mechanical strain in concrete
							Rebar 1	Rebar 2		
CRMAI	East Wall	M = 7.7	(kip-ft/ft)	1.4	0**	East wall, horizontal strip, at the middle of the wall	43.3	29.6	0	>0
		P = 57.6	(kip/ft)							
	Base mat	M = 26.5	(kip-ft/ft)		0.99	North-south strip, at intersection with south walls	39.1	37.3	-0.33	-1.06e-4
		P = -32.3	(kip/ft)							
CEB	Wall	M = 614.7	(kip-ft/ft)	1.3	0.60	Between Mechanical & Electrical Penetration at Elev. -30ft.	42.5	1.97	-2.68	-8.51e-4
		P = 10.5	(kip/ft)							
	Wall	M = 22.8	(kip-ft/ft)	1.3	0.10	East side of Electrical Penetration at Elev. 45ft.	55.6	12.9	-1.33	-3.67e-4
		P = 52.8	(kip/ft)							
RHR	East exterior wall	M = -119.5	(kip-ft/ft)	1.2	0.75	East exterior wall, horizontal strip, at the approximate El. (-) 30 ft	56.5	13.8	-2.1	-6.73e-4
		P = -40.8	(kip/ft)							
	East interior wall	M = 33.0	(kip-ft/ft)		0.0**	East interior wall, vertical strip, at the approximate El. (-) 45 ft	59.5*	17.7	0.0	>0
		P = 60.9	(kip/ft)							
	West interior wall	M = 13.4	(kip-ft/ft)		0.0**	West interior wall, vertical strip, at the approximate El. (-) 30 ft	36.6*	19.6	0.0	>0
		P = 44.4	(kip/ft)							

Table 2 – (Continued)

	Component	Item		F _{THR}	Internal ASR (mm/m)	Location	Total stress in steel (ksi)		Maximum compressive stress in concrete (ksi)	Maximum compressive mechanical strain in concrete
							Rebar 1	Rebar 2		
CSTE	Tank Enclosure Wall	M = 65.7	(kip-ft/ft)	1.6	0.43	Bottom of tank enclosure wall, vertical direction	26.7	13.9	-1.11	-3.08e-4
		P = -12.9	(kip/ft)							
CEHMS	East wing walls	M = 311.6	(kip-ft/ft)	1.5	0.72	East wing wall, at intersection with column	41.6	20.8	-1.52	-4.87e-4
		P = -0.7	(kip/ft)							
CEVA	Base slab	M = 83.7	(kip-ft/ft)	3.0	0.31	Base slab rebar along east-west direction	44.0	20.6	-1.08	-3.46e-4
		P = 1.7	(kip/ft)							
WPC/PH	North wall	M = 78.8	(kip-ft/ft)	1.8	0.24	North wall below pipe break beam	44.4	8.0	-1.36	-4.37e-4
		P = 34.4	(kip/ft)							
EMH	W13/W15	M = 0	(kip-ft/ft)	3.7	0.25	W13/W15 walls	27.0	24.5	-0.30	-9.69e-5
		P = 23.6	(kip/ft)							

* Vertical strips (strips that engage vertical rebars) are not part of primary load path for RHR, and therefore, are not designed following ACI 318 strength design method. These members do not need to be considered for the evaluation of stress in rebars.

** Members with zero internal ASR expansion that satisfy the ACI 318 requirements for strength design method do not yield subjected to unfactored normal operating load condition.



7. REFERENCES

- [1] Simpson Gumpertz & Heger Inc., *Evaluation of Control Room Makeup Air Intake Structure*, 160268-CA-08 Rev. 0, Waltham, MA, May 2017.
- [2] Simpson Gumpertz & Heger, Inc., *Evaluation and Design Confirmation of As-designed CEB 150252-CA-02 Rev 1*, Waltham, MA, Dec. 2017.
- [3] Simpson Gumpertz & Heger Inc., *Evaluation of Residual Heat Removal Equipment Vault*, 160268-CA-06 Rev. 0, Waltham, MA, Dec 2016.
- [4] Simpson Gumpertz & Heger Inc., *Evaluation of Condensate Storage Tank Enclosure Structure*, 160268-CA-03 Rev. 0, Waltham, MA, Dec. 2016.
- [5] Simpson Gumpertz & Heger Inc., *Evaluation of Containment Equipment Hatch Missile Shield Structure*, 160268-CA-02 Rev. 0, Waltham, MA, Oct. 2016.
- [6] Simpson Gumpertz & Heger Inc., *Evaluation of Containment Enclosure Ventilation Area*, 160268-CA-05 Rev. 0, Waltham, MA, Mar. 2017.
- [7] Simpson Gumpertz & Heger, Inc., *Evaluation of Main Steam and Feedwater West Pipe Chase & Personnel Hatch Structures 170443-CA-04 Rev. 0*, Waltham, MA, Jan. 2018.
- [8] Simpson Gumpertz & Heger, Inc., *Evaluation of Seismic Category I Electrical Manholes – Stage 1 160268-CA-12 Rev. 0*, Waltham, MA, Jan. 2018.

**APPENDIX A****TENSILE STRESS IN REBARS OF CONTROL ROOM MAKEUP AIR INTAKE STRUCTURE****A1. REVISION HISTORY**

Revision 0: Initial document.

A2. OBJECTIVE OF CALCULATION

The objective of this calculation is to compute the maximum tensile stress that can form in the rebars of Control Room Makeup Air Intake (CRMAI) structure.

A3. RESULTS AND CONCLUSIONS

Table A1 summarizes the tensile stress in rebars of the CRMAI structure calculated at critical locations. The maximum tensile stress is 43.3 ksi computed for the horizontal rebar of east wall close to the interior of the structure and subjected to the second In Situ load combination.

Besides, although the stress due to internal ASR expansion is high for the base mat, the stress due to loading is small. Therefore, base mat does not govern the calculation of the maximum stress in rebars.

A4. DESIGN DATA / CRITERIA

See Section 4 of the calculation main body (Calc. 160268-CA-08 Rev. 0).

A5. ASSUMPTIONS**A5.1 Justified assumptions**

There are no justified assumptions.

A5.2 Unverified assumptions

There are no unverified assumptions.

A6. METHODOLOGY

The critical demand that controlled the selection of threshold factor of the CRMAI structure was axial-flexure interaction along the horizontal strip of the east wall and close to the middle which is considered for evaluation. Additionally, the north-south strip of the base mat is also considered to check a location with high internal ASR expansion. Finite element analyses are conducted to calculate the axial force and bending moment at critical sections of the structure. The FE model and analysis method are similar to what explained in susceptibility evaluation of CRMAI structure [A1]. The axial force and bending moments are calculated using section cuts method. The computed demands are:

- LC1 for the walls: $M = 5.2$ kip-ft/ft, $P = 49.8$ kip/ft
- LC1 for the base mat: $M = 20.8$ kip-ft/ft, $P = -28.4$ kip/ft
- LC2 for the walls: $M = 7.7$ kip-ft/ft, $P = 57.6$ kip/ft
- LC2 for the base mat: $M = 26.5$ kip-ft/ft, $P = -32.3$ kip/ft

To calculate the stress in rebars subjected to a combination of axial force and bending moment, sectional analysis based on fiber section method, as explained in calculation main body, is used. The calculation is conducted per 1 foot width of the walls/slabs, and each section is discretized into 20 fibers. An example calculation that evaluates the stress in rebars of the east wall is presented in Section A8. The CI value for the base mat was 0.99 mm/m which included in the analysis to find the initial stress state due to internal ASR alone. Value of zero internal ASR is used for the walls as it leads to conservative demands.

A7. REFERENCES

- [A1] Simpson Gumpertz & Heger Inc., *Evaluation of Control Room Makeup Air Intake structure*, 160268-CA-08 Rev. 0, Waltham, MA, May 2017.
- [A2] United Engineers & Constructors Inc., *Seabrook Station Structural Design Drawings*.
- [A3] United Engineers & Constructors Inc., *Design of Makeup Air Intake Structure, MT-28-Calc Rev. 2*, Feb. 1984.

A8. COMPUTATION

A8.1. Strain in Steel and Concrete due to Internal ASR expansion

Input Data

ASR expansion

Measured crack index	$\epsilon_{CI} := 0 \frac{\text{mm}}{\text{m}}$
Threshold factor	$F_{thr} := 1.4$

Material properties

Compressive strength of concrete	$f_c := -3\text{ksi}$	Ref. [A1]
Young's modulus of concrete	$E_c := 3120\text{ksi}$	
Yield strength of steel	$f_y := 60\text{ksi}$	
Young's modulus of steel	$E_s := 29000\text{ksi}$	

Geometry

Width of fibers	$b := 12\text{in}$	Ref. [A2]
Total thickness or height	$h := 24\text{in}$	
Area of concrete	$A_c := b \cdot h = 288 \cdot \text{in}^2$	
Area of tensile reinforcement (#8@12 in.)	$A_s := 0.79\text{in}^2$	
Number of reinforcement in row, e.g. equal to 2 for tensile and compressive	$\text{Steel}_{\text{Num}} := 2$	
Depth to reinforcement	$d := 20.5\text{in}$	

Finding the strain in steel and concrete by satisfying compatibility and equilibrium

	Initial Guess
Initial mechanical strain in concrete	$\epsilon_{o,\text{conc}} := 0$
Initial strain in steel	$\epsilon_{o,\text{steel}} := 0$
	Given
Compatibility equation	$F_{thr} \cdot \epsilon_{CI} = \epsilon_{o,\text{steel}} - \epsilon_{o,\text{conc}}$
Equilibrium equation	$(E_c \cdot A_c) \cdot \epsilon_{o,\text{conc}} + (E_s \cdot A_s \cdot \text{Steel}_{\text{Num}}) \cdot \epsilon_{o,\text{steel}} = 0$
	$\text{ans} := \text{Find}(\epsilon_{o,\text{conc}}, \epsilon_{o,\text{steel}})$

Initial strain in concrete and steel

$$\epsilon_{o,concrete} := ans_1 = 0$$

$$\epsilon_{o,steel} := ans_2 = 0$$

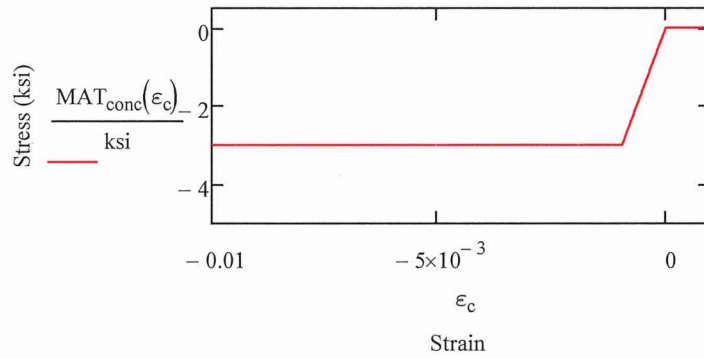
A8.2. Sectional Analysis

Input Data

Concrete Material Model

Constitutive model for concrete

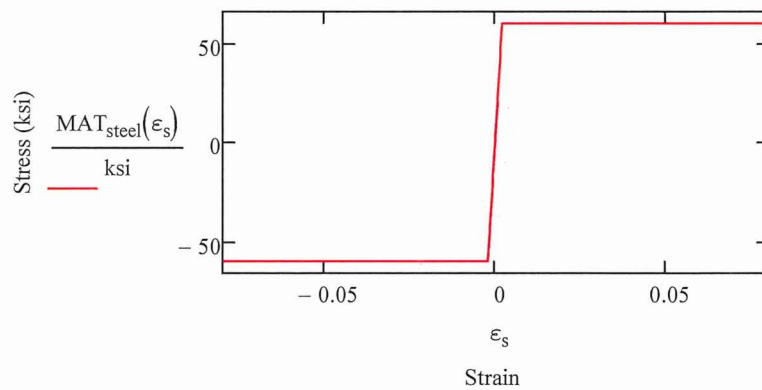
$$MAT_{conc}(\epsilon) := \begin{cases} 0 & \text{if } \epsilon > 0 \\ f_c & \text{if } \epsilon < \frac{f_c}{E_c} \\ (E_c \cdot \epsilon) & \text{otherwise} \end{cases}$$



Steel Material Model

Constitutive model for steel

$$MAT_{steel}(\epsilon) := \begin{cases} f_y & \text{if } \epsilon > \frac{f_y}{E_s} \\ -f_y & \text{if } \epsilon < \frac{-f_y}{E_s} \\ (E_s \cdot \epsilon) & \text{otherwise} \end{cases}$$



Concrete Fibers

Number of fibers	$\text{Conc}_{\text{Num}} := 20$
Height of fibers	$\text{Conc}_H := \frac{h}{\text{Conc}_{\text{Num}}} = 1.2 \cdot \text{in}$
Concrete fiber coordinates	$\text{Conc}_y := \left \begin{array}{l} \text{for } i \in 1.. \text{Conc}_{\text{Num}} \\ \text{ans}_i \leftarrow -\frac{h}{2} + \frac{\text{Conc}_H}{2} + (i-1) \cdot \text{Conc}_H \\ \text{ans} \end{array} \right.$
Concrete fiber strain	$\text{Conc}_\varepsilon(\varepsilon_{o,\text{conc}}, \varepsilon, \varphi) := \left \begin{array}{l} \text{for } i \in 1.. \text{Conc}_{\text{Num}} \\ \text{ans}_i \leftarrow \varepsilon_{o,\text{conc}} + \varepsilon - \varphi \cdot \text{Conc}_{y_i} \\ \text{ans} \end{array} \right.$
Concrete fiber stress	$\text{Conc}_\sigma(\varepsilon_{o,\text{conc}}, \varepsilon, \varphi) := \left \begin{array}{l} \text{for } i \in 1.. \text{Conc}_{\text{Num}} \\ \text{ans}_i \leftarrow \text{MAT}_{\text{conc}}(\text{Conc}_\varepsilon(\varepsilon_{o,\text{conc}}, \varepsilon, \varphi)_i) \\ \text{ans} \end{array} \right.$
Concrete fiber force	$\text{Conc}_F(\varepsilon_{o,\text{conc}}, \varepsilon, \varphi) := \left \begin{array}{l} \text{for } i \in 1.. \text{Conc}_{\text{Num}} \\ \text{ans}_i \leftarrow \text{Conc}_\sigma(\varepsilon_{o,\text{conc}}, \varepsilon, \varphi)_i \cdot (b \cdot \text{Conc}_H) \\ \text{ans} \end{array} \right.$

Reinforcement/Steel fibers

Depth to reinforcement fiber	$\text{Steel}_{y_1} := -\left(d - \frac{h}{2}\right) = -8.5 \cdot \text{in}$ $\text{Steel}_{y_2} := d - \frac{h}{2} = 8.5 \cdot \text{in}$
Area of reinforcement fiber	$\text{Steel}_{A_{s_1}} := A_s = 0.79 \cdot \text{in}^2$ $\text{Steel}_{A_{s_2}} := A_s = 0.79 \cdot \text{in}^2$
Steel fiber strain	$\text{Steel}_\varepsilon(\varepsilon_{o,\text{steel}}, \varepsilon, \varphi) := \left \begin{array}{l} \text{for } i \in 1.. \text{Steel}_{\text{Num}} \\ \text{ans}_i \leftarrow \varepsilon_{o,\text{steel}} + \varepsilon - \varphi \cdot \text{Steel}_{y_i} \\ \text{ans} \end{array} \right.$
Steel fiber stress	$\text{Steel}_\sigma(\varepsilon_{o,\text{steel}}, \varepsilon, \varphi) := \left \begin{array}{l} \text{for } i \in 1.. \text{Steel}_{\text{Num}} \\ \text{ans}_i \leftarrow \text{MAT}_{\text{steel}}(\text{Steel}_\varepsilon(\varepsilon_{o,\text{steel}}, \varepsilon, \varphi)_i) \\ \text{ans} \end{array} \right.$
Steel fiber force	$\text{Steel}_F(\varepsilon_{o,\text{steel}}, \varepsilon, \varphi) := \left \begin{array}{l} \text{for } i \in 1.. \text{Steel}_{\text{Num}} \\ \text{ans}_i \leftarrow \text{Steel}_\sigma(\varepsilon_{o,\text{steel}}, \varepsilon, \varphi)_i \cdot \text{Steel}_{A_{s_i}} \\ \text{ans} \end{array} \right.$

Initial Stress State

Initial stress in concrete

$$\text{Concrete}_{\sigma} := \text{Conc}_{\sigma}(\varepsilon_{o,\text{conc}}, 0, 0)$$

$$\text{Concrete}_{\sigma_1} = 0 \cdot \text{ksi}$$

Initial stress in steel

$$\text{Rebar}_{\sigma} := \text{Steel}_{\sigma}(\varepsilon_{o,\text{steel}}, 0, 0)$$

$$\text{Rebar}_{\sigma_1} = 0 \cdot \text{ksi}$$

Axial Equilibrium

$$\text{Force}(\varepsilon_{o,\text{conc}}, \varepsilon_{o,\text{steel}}, \varepsilon, \varphi) := \begin{array}{l} \text{ans1} \leftarrow 0 \\ \text{for } i \in 1.. \text{ConcNum} \\ \quad \text{ans1} \leftarrow \text{ans1} + \text{Conc}_F(\varepsilon_{o,\text{conc}}, \varepsilon, \varphi)_i \\ \text{ans2} \leftarrow 0 \\ \text{for } i \in 1.. \text{SteelNum} \\ \quad \text{ans2} \leftarrow \text{ans2} + \text{Steel}_F(\varepsilon_{o,\text{steel}}, \varepsilon, \varphi)_i \\ \text{ans} \leftarrow \text{ans1} + \text{ans2} \end{array}$$

Moment Equilibrium

$$\text{Moment}(\varepsilon_{o,\text{conc}}, \varepsilon_{o,\text{steel}}, \varepsilon, \varphi) := \begin{array}{l} \text{ans1} \leftarrow 0 \\ \text{for } i \in 1.. \text{ConcNum} \\ \quad \text{ans1} \leftarrow \text{ans1} + -1 \cdot \text{Conc}_F(\varepsilon_{o,\text{conc}}, \varepsilon, \varphi)_i \cdot \text{Conc}_{y_i} \\ \text{ans2} \leftarrow 0 \\ \text{for } i \in 1.. \text{SteelNum} \\ \quad \text{ans2} \leftarrow \text{ans2} + -1 \cdot \text{Steel}_F(\varepsilon_{o,\text{steel}}, \varepsilon, \varphi)_i \cdot \text{Steel}_{y_i} \\ \text{ans} \leftarrow \text{ans1} + \text{ans2} \end{array}$$

Solution

Known parameters

Axial force $P := 57.6 \text{ kip}$

Iteration

Curvature $\phi := 0.0000279 \cdot \frac{1}{\text{in}}$ Requires iteration

Solve for strain at centroid

Axial strain at centroid (initial guess) $x_0 := 0.0$

Axial force equilibrium $f(x) := \text{Force}(\epsilon_{o.\text{conc}}, \epsilon_{o.\text{steel}}, x, \phi) - P$

$$\epsilon_{\text{cent}} := \text{root}(f(x_0), x_0) = 1.257 \times 10^{-3}$$

Sectional forces

$$\text{Force}(\epsilon_{o.\text{conc}}, \epsilon_{o.\text{steel}}, \epsilon_{\text{cent}}, \phi) = 57.6 \cdot \text{kip}$$

$$\text{Moment}(\epsilon_{o.\text{conc}}, \epsilon_{o.\text{steel}}, \epsilon_{\text{cent}}, \phi) = 7.697 \cdot \text{kip}\cdot\text{ft}$$

Stress and strain in concrete and steel

Steel fiber stress and strain

$$\text{Rebar}_\epsilon := \text{Steel}_\epsilon(\epsilon_{o.\text{steel}}, \epsilon_{\text{cent}}, \phi) = \begin{pmatrix} 1.494 \times 10^{-3} \\ 1.02 \times 10^{-3} \end{pmatrix}$$

$$\text{Rebar}_\sigma := \text{Steel}_\sigma(\epsilon_{o.\text{steel}}, \epsilon_{\text{cent}}, \phi) = \begin{pmatrix} 43.333 \\ 29.578 \end{pmatrix} \cdot \text{ksi}$$

$$\text{Steel}_F(\epsilon_{o.\text{steel}}, \epsilon_{\text{cent}}, \phi) = \begin{pmatrix} 34.233 \\ 23.367 \end{pmatrix} \cdot \text{kip}$$

$$\text{Concrete}_y := \text{Conc}_y$$

Concrete fiber stress and strain

$$\text{Concrete}_\epsilon := \text{Conc}_\epsilon(\epsilon_{o.\text{conc}}, \epsilon_{\text{cent}}, \phi)$$

$$\text{Concrete}_\sigma := \text{Conc}_\sigma(\epsilon_{o.\text{conc}}, \epsilon_{\text{cent}}, \phi)$$

Maximum compressive strain in concrete

$$\epsilon_{\text{max.comp}} := \frac{\text{Concrete}_\epsilon_{\text{ConcNum}} - \text{Concrete}_\epsilon_{\text{ConcNum}-1}}{\text{Conc}_y_{\text{ConcNum}} - \text{Conc}_y_{\text{ConcNum}-1}} \cdot \left(\frac{h}{2} - \text{Conc}_y_{\text{ConcNum}-1} \right) + \text{Concrete}_\epsilon_{\text{ConcNum}-1} \dots = 9.223 \times 10^{-4}$$

Maximum compressive stress in concrete

$$\sigma_{\text{max.comp}} := \text{MAT}_{\text{conc}}(\epsilon_{\text{max.comp}}) = 0 \cdot \text{ksi}$$

A9. TABLES

Table A1: Stress in rebars at critical locations of CRMAI structure subjected to LC1

Component	Item	Total demands for sustained load (In Situ condition, LC1)		Total stress in steel (ksi)		Maximum compressive stress in concrete (ksi)
		Demand	Location	Rebar 1	Rebar 2	
Walls	Out-of-plane moment (kip-ft/ft)	5.2	East wall, horizontal strip, at the middle of the wall	36.2	26.8	0
	Axial force (kip/ft)	49.8				
Base mat	Out-of-plane moment (kip-ft/ft)	20.8	North-south strip, at intersection with south walls	27.8	26.4	-0.28
	Axial force (kip/ft)	-28.4				

Table A2: Stress in rebars at critical locations of CRMAI structure subjected to LC2

Component	Item	Total demands for sustained loads plus OBE amplified with threshold factor (In Situ condition, LC2)		Total stress in steel (ksi)		Maximum compressive stress in concrete (ksi)
		Demand	Location	Rebar 1	Rebar 2	
Walls	Out-of-plane moment (kip-ft/ft)	7.7	East wall, horizontal strip, at the middle of the wall	43.3	29.6	0
	Axial force (kip/ft)	57.6				
Base mat	Out-of-plane moment (kip-ft/ft)	26.5	North-south strip, at intersection with south walls	39.1	37.3	-0.33
	Axial force (kip/ft)	-32.3				

Example in Section A8

A10. FIGURES

There are no figures.



APPENDIX B
TENSILE STRESS IN REBAR AND CONCRETE OF CONTAINMENT ENCLOSURE
BUILDING STRUCTURE

B1. REVISION HISTORY

Revision 0: Initial document.

B2. OBJECTIVE OF CALCULATION

The objective of this calculation is to compute the maximum tensile stress that can form in the rebars and the maximum compressive stress that can form in concrete sections of the Containment Enclosure Building (CEB) structure.

B3. RESULTS AND CONCLUSIONS

Table B1 through B4 summarizes the stress results in rebar and concrete sections of the CEB structure calculated at critical locations. The Maximum tensile stress is 55.6 ksi in the wall at the east side of electrical penetration at Elev. 45 ft subjected to the second in-situ load combination (LC2).

B4. DESIGN DATA / CRITERIA

See Section 4 of the calculation main body (Calc. 150252-CA-02 Rev. 1).

B5. ASSUMPTIONS

B5.1 Justified assumptions

There are no justified assumptions.

B5.2 Unverified assumptions

There are no unverified assumptions.

B6. METHODOLOGY

The critical demands that control the selection of the threshold factor for the CEB structure are out-of-plane moment and axial load interaction at various sections of the wall surface. Finite element analyses were conducted to calculate the axial force and bending moment at these locations due to ASR load [B1].

To calculate the stress in rebars subjected to a combination of axial force and bending moment, sectional analysis based on fiber section method, as explained in calculation main body, is used. The calculation is conducted per 1 foot width of the walls, and each section is discretized into 20 fibers. An example calculation that evaluates the stress in the vertical rebars at the section of the wall on the east side of the electrical penetration and at Elev. 45 ft. is presented in Section B8. The ASR expansion of the CEB wall is included in the analysis to find the initial stress state due to internal ASR alone.

B7. REFERENCES

- [B1] Simpson Gumpertz & Heger Inc., *Evaluation of Containment Enclosure Building Structure*, 150252-CA-02 Rev. 1, Waltham, MA, Dec 2017.
- [B2] United Engineers & Constructors Inc., *Seabrook Station Structural Design Drawings*.

B8. COMPUTATION

B8.1. Strain in Steel and Concrete due to Internal ASR expansion

Input Data

ASR expansion

Measured crack index	$\epsilon_{CI} := 0.10 \frac{\text{mm}}{\text{m}}$
Threshold factor	$F_{thr} := 1.3$

Material properties

Compressive strength of concrete	$f_c := -4\text{ksi}$	Ref. [B1]
Young's modulus of concrete	$E_c := 3605\text{ksi}$	
Yield strength of steel	$f_y := 60\text{ksi}$	
Young's modulus of steel	$E_s := 29000\text{ksi}$	

Geometry

Width of fibers	$b := 12\text{in}$	Ref. [B2]
Total thickness or height	$h := 15\text{in}$	
Area of concrete	$A_c := b \cdot h = 180 \cdot \text{in}^2$	
Area of tensile reinforcement	$A_s := 1.00\text{in}^2$	
Number of reinforcement in row, e.g. equal to 2 for tensile and compressive	$\text{Steel}_{\text{Num}} := 2$	
Depth to reinforcement	$d := 15\text{in} - 3.60\text{in} = 11.4\text{in}$	

Finding the strain in steel and concrete by satisfying compatibility and equilibrium

	Initial Guess
Initial mechanical strain in concrete	$\epsilon_{o,conc} := 0$
Initial strain in steel	$\epsilon_{o,steel} := 0$
	Given
Compatibility equation	$F_{thr} \cdot \epsilon_{Cl} = \epsilon_{o,steel} - \epsilon_{o,conc}$
Equilibrium equation	$(E_c \cdot A_c) \cdot \epsilon_{o,conc} + (E_s \cdot A_s \cdot Steel_{Num}) \cdot \epsilon_{o,steel} = 0$
	$ans := Find(\epsilon_{o,conc}, \epsilon_{o,steel})$
Initial strain in concrete and steel	$\epsilon_{o,conc} := ans_1 = -1.217 \times 10^{-5}$ $\epsilon_{o,steel} := ans_2 = 1.178 \times 10^{-4}$

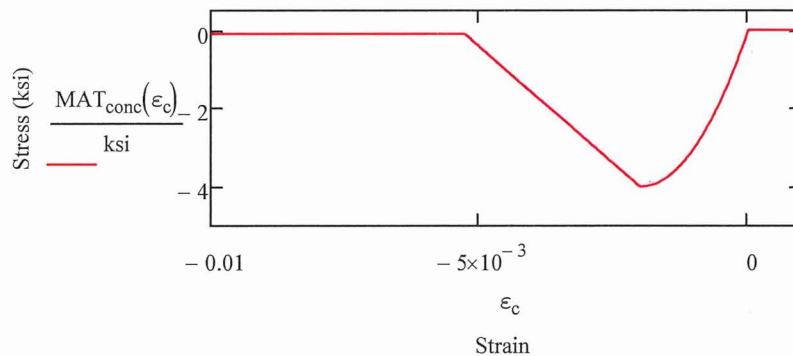
B8.2. Sectional Analysis

Input Data

Concrete Material Model

Kent & Park Model

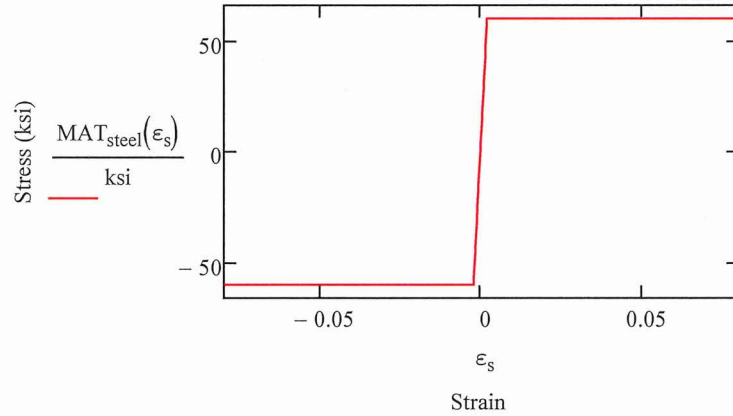
Strain at Peak compressive strength	$\epsilon_{co} := -0.002$
Strain at 50% compressive strength	$\epsilon_{50u} := \frac{3 - 0.002 \cdot \frac{f_c}{psi}}{\frac{f_c}{psi} + 1000} = -3.667 \times 10^{-3}$
Model parameter	$Z := \frac{0.5}{\epsilon_{50u} - \epsilon_{co}} = -300$
Residual compressive strength	$f_{c,res} := f_c \cdot 0.025 = -100 \cdot psi$
Constitutive model for concrete	$MAT_{conc}(\epsilon) := \begin{cases} \min[f_{c,res}, f_c \cdot [1 - Z \cdot (\epsilon - \epsilon_{co})]] & \text{if } \epsilon < \epsilon_{co} \\ f_c \cdot \left[\frac{2 \cdot \epsilon}{\epsilon_{co}} - \left(\frac{\epsilon}{\epsilon_{co}} \right)^2 \right] & \text{if } \epsilon_{co} \leq \epsilon < 0 \\ 0 & \text{if } 0 \leq \epsilon \end{cases}$



Steel Material Model

Constitutive model for steel

$$\text{MAT}_{\text{steel}}(\varepsilon) := \begin{cases} f_y & \text{if } \varepsilon > \frac{f_y}{E_s} \\ -f_y & \text{if } \varepsilon < -\frac{f_y}{E_s} \\ (E_s \cdot \varepsilon) & \text{otherwise} \end{cases}$$



Concrete Fibers

Number of fibers

$$\text{Conc}_{\text{Num}} := 20$$

Height of fibers

$$\text{Conc}_H := \frac{h}{\text{Conc}_{\text{Num}}} = 0.75 \cdot \text{in}$$

Concrete fiber coordinates

$$\text{Conc}_y := \begin{cases} \text{for } i \in 1.. \text{Conc}_{\text{Num}} \\ \text{ans}_i \leftarrow -\frac{h}{2} + \frac{\text{Conc}_H}{2} + (i-1) \cdot \text{Conc}_H \\ \text{ans} \end{cases}$$

Concrete fiber strain

$$\text{Conc}_\varepsilon(\varepsilon_{o,\text{conc}}, \varepsilon, \varphi) := \begin{cases} \text{for } i \in 1.. \text{Conc}_{\text{Num}} \\ \text{ans}_i \leftarrow \varepsilon_{o,\text{conc}} + \varepsilon - \varphi \cdot \text{Conc}_{y_i} \\ \text{ans} \end{cases}$$

Concrete fiber stress

$$\text{Conc}_\sigma(\varepsilon_{o,\text{conc}}, \varepsilon, \varphi) := \begin{cases} \text{for } i \in 1.. \text{Conc}_{\text{Num}} \\ \text{ans}_i \leftarrow \text{MAT}_{\text{conc}}(\text{Conc}_\varepsilon(\varepsilon_{o,\text{conc}}, \varepsilon, \varphi)_i) \\ \text{ans} \end{cases}$$

Concrete fiber force

$$\text{Conc}_F(\varepsilon_{o,\text{conc}}, \varepsilon, \varphi) := \begin{cases} \text{for } i \in 1.. \text{Conc}_{\text{Num}} \\ \text{ans}_i \leftarrow \text{Conc}_\sigma(\varepsilon_{o,\text{conc}}, \varepsilon, \varphi)_i \cdot (b \cdot \text{Conc}_H) \\ \text{ans} \end{cases}$$

Reinforcement/Steel fibers

Depth to reinforcement fiber

$$\text{Steel}_{y_1} := -\left(d - \frac{h}{2}\right) = -3.9 \cdot \text{in}$$

$$\text{Steel}_{y_2} := d - \frac{h}{2} = 3.9 \cdot \text{in}$$

Area of reinforcement fiber

$$\text{Steel}_{A_{s_1}} := A_s = 1 \cdot \text{in}^2$$

$$\text{Steel}_{A_{s_2}} := A_s = 1 \cdot \text{in}^2$$

Steel fiber strain

$$\text{Steel}_\epsilon(\epsilon_{o,\text{steel}}, \epsilon, \varphi) := \left| \begin{array}{l} \text{for } i \in 1.. \text{SteelNum} \\ \text{ans}_i \leftarrow \epsilon_{o,\text{steel}} + \epsilon - \varphi \cdot \text{Steel}_{y_i} \\ \text{ans} \end{array} \right.$$

Steel fiber stress

$$\text{Steel}_\sigma(\epsilon_{o,\text{steel}}, \epsilon, \varphi) := \left| \begin{array}{l} \text{for } i \in 1.. \text{SteelNum} \\ \text{ans}_i \leftarrow \text{MAT}_{\text{steel}}(\text{Steel}_\epsilon(\epsilon_{o,\text{steel}}, \epsilon, \varphi)_i) \\ \text{ans} \end{array} \right.$$

Steel fiber force

$$\text{Steel}_F(\epsilon_{o,\text{steel}}, \epsilon, \varphi) := \left| \begin{array}{l} \text{for } i \in 1.. \text{SteelNum} \\ \text{ans}_i \leftarrow \text{Steel}_\sigma(\epsilon_{o,\text{steel}}, \epsilon, \varphi)_i \cdot \text{Steel}_{A_{s_i}} \\ \text{ans} \end{array} \right.$$

Initial Stress State

Initial stress in concrete

$$\text{Concrete}_\sigma := \text{Conc}_\sigma(\epsilon_{o,\text{conc}}, 0, 0)$$

$$\text{Concrete}_{\sigma_1} = -0.049 \cdot \text{ksi}$$

Initial stress in steel

$$\text{Rebar}_\sigma := \text{Steel}_\sigma(\epsilon_{o,\text{steel}}, 0, 0)$$

$$\text{Rebar}_{\sigma_1} = 3.417 \cdot \text{ksi}$$

Axial Equilibrium

$$\text{Force}(\epsilon_{o,\text{conc}}, \epsilon_{o,\text{steel}}, \epsilon, \varphi) := \left| \begin{array}{l} \text{ans1} \leftarrow 0 \\ \text{for } i \in 1.. \text{ConcNum} \\ \text{ans1} \leftarrow \text{ans1} + \text{Conc}_F(\epsilon_{o,\text{conc}}, \epsilon, \varphi)_i \\ \text{ans2} \leftarrow 0 \\ \text{for } i \in 1.. \text{SteelNum} \\ \text{ans2} \leftarrow \text{ans2} + \text{Steel}_F(\epsilon_{o,\text{steel}}, \epsilon, \varphi)_i \\ \text{ans} \leftarrow \text{ans1} + \text{ans2} \end{array} \right.$$

Moment Equilibrium

$$\text{Moment}(\epsilon_{o,\text{conc}}, \epsilon_{o,\text{steel}}, \epsilon, \phi) := \begin{cases} \text{ans1} \leftarrow 0 \\ \text{for } i \in 1.. \text{ConcNum} \\ \text{ans1} \leftarrow \text{ans1} + -1 \cdot \text{Conc}_F(\epsilon_{o,\text{conc}}, \epsilon, \phi)_i \cdot \text{Conc}_{y_i} \\ \text{ans2} \leftarrow 0 \\ \text{for } i \in 1.. \text{SteelNum} \\ \text{ans2} \leftarrow \text{ans2} + -1 \cdot \text{Steel}_F(\epsilon_{o,\text{steel}}, \epsilon, \phi)_i \cdot \text{Steel}_{y_i} \\ \text{ans} \leftarrow \text{ans1} + \text{ans2} \end{cases}$$

Solution

Known parameters

Axial force

$$P := 52.80 \text{ kip}$$

Iteration

Curvature

$$\phi := 0.000189 \cdot \frac{1}{\text{in}}$$

Requires iteration

Solve for strain at centroid

Axial strain at centroid (initial guess)

$$x_0 := 0.0$$

Axial force equilibrium

$$f(x) := \text{Force}(\epsilon_{o,\text{conc}}, \epsilon_{o,\text{steel}}, x, \phi) - P$$

$$\epsilon_{\text{cent}} := \text{root}(f(x_0), x_0) = 1.063 \times 10^{-3}$$

Sectional forces

$$\text{Force}(\epsilon_{o,\text{conc}}, \epsilon_{o,\text{steel}}, \epsilon_{\text{cent}}, \phi) = 52.8 \cdot \text{kip}$$

$$\text{Moment}(\epsilon_{o,\text{conc}}, \epsilon_{o,\text{steel}}, \epsilon_{\text{cent}}, \phi) = 22.807 \cdot \text{kip} \cdot \text{ft}$$

Stress and strain in concrete and steel

Steel fiber stress and strain

$$\text{Rebar}_\epsilon := \text{Steel}_\epsilon(\epsilon_{o,\text{steel}}, \epsilon_{\text{cent}}, \phi) = \begin{pmatrix} 1.918 \times 10^{-3} \\ 4.434 \times 10^{-4} \end{pmatrix}$$

$$\text{Rebar}_\sigma := \text{Steel}_\sigma(\epsilon_{o,\text{steel}}, \epsilon_{\text{cent}}, \phi) = \begin{pmatrix} 55.61 \\ 12.858 \end{pmatrix} \cdot \text{ksi}$$

$$\text{Steel}_F(\epsilon_{o,\text{steel}}, \epsilon_{\text{cent}}, \phi) = \begin{pmatrix} 55.61 \\ 12.858 \end{pmatrix} \cdot \text{kip}$$

$$\text{Concrete}_y := \text{Conc}_y$$

Concrete fiber stress and strain

$$\text{Concrete}_\epsilon := \text{Conc}_\epsilon(\epsilon_{o,\text{conc}}, \epsilon_{\text{cent}}, \phi)$$

$$\text{Concrete}_\sigma := \text{Conc}_\sigma(\epsilon_{o,\text{conc}}, \epsilon_{\text{cent}}, \phi)$$

Maximum compressive strain in concrete

$$\epsilon_{\max.\text{comp}} := \frac{\text{Concrete}\epsilon_{\text{ConcNum}} - \text{Concrete}\epsilon_{\text{ConcNum-1}}}{\text{Conc}_y_{\text{ConcNum}} - \text{Conc}_y_{\text{ConcNum-1}}} \cdot \left(\frac{h}{2} - \text{Conc}_y_{\text{ConcNum-1}} \right) + \text{Concrete}\epsilon_{\text{ConcNum-1}} \dots = -3.67 \times 10^{-4}$$

Maximum compressive stress in concrete

$$\sigma_{\max.\text{comp}} := \text{MAT}_{\text{conc}}(\epsilon_{\max.\text{comp}}) = -1.333 \text{ ksi}$$

B9. TABLES

Table B1. Stress in Rebar and Concrete of Structural Components Subjected to LC1 Standard Case

Comp.	Demand		Location	Total stress in steel (ksi)		Maximum stress and strain in concrete (ksi) [in./in.]
				Rebar 1	Rebar 2	
Wall 36 in.	M = 459.5	(kip-ft/ft)	Wall near foundation. Horz. cut.	27.1	5.60	-2.21 [-6.61e-4]
	P = -141.2	(kip/ft)				
Wall 15 in.	M = 1.94	(kip-ft/ft)	Wall above Elec. Penetration. Horz. cut.	13.2	7.18	0.0 [2.25e-5]
	P = 20.33	(kip/ft)				
Wall 27 in.	M = -39.58	(kip-ft/ft)	Below personal hatch. Vert. cut.	24.6	2.73	-0.71 [-1.88e-4]
	P = 14.07	(kip/ft)				
Wall 27 in.	M = -34.00	(kip-ft/ft)	Side of personal hatch. Vert. cut.	19.5	2.78	-0.57 [-1.49e-4]
	P = 11.05	(kip/ft)				

Table B2. Stress in Rebar and Concrete of Structural Components subjected to LC2 Standard Case

Comp.	Demand		Location	Total stress in steel (ksi)		Maximum stress and strain in concrete (ksi) [in./in.]
				Rebar 1	Rebar 2	
Wall 36 in.	M = 614.7	(kip-ft/ft)	Wall near foundation. Horz. cut.	42.5	1.97	-2.68 [-8.507e-4]
	P = 10.48	(kip/ft)				
Wall 36 in.	M = 432.1	(kip-ft/ft)	Wall near foundation. Horz. cut.	20.6	2.16	-2.48 [-7.69e-4]
	P = -391.3	(kip/ft)				
Wall 15 in.	M = 22.81	(kip-ft/ft)	Wall above Elec. Penetration. Horz. cut.	55.6	12.9	-1.33 [-3.67e-4]
	P = 52.80	(kip/ft)				
Wall 15 in.	M = -12.92	(kip-ft/ft)	Wall above Elec. Penetration. Horz. cut.	17.2	3.96	-0.78 [-2.042e-4]
	P = 4.70	(kip/ft)				
Wall 27 in.	M = -6.57	(kip-ft/ft)	Below personal hatch. Vert. cut.	25.9	19.7	0.0 [5.05e-4]
	P = 57.80	(kip/ft)				
Wall 27 in.	M = -92.23	(kip-ft/ft)	Below personal hatch. Vert. cut.	37.0	-1.17	-1.54 [-4.32e-4]
	P = -15.28	(kip/ft)				
Wall 27 in.	M = -1.18	(kip-ft/ft)	Side of personal hatch. Vert. cut.	22.5	21.4	0.0 [6.00e-4]
	P = 55.82	(kip/ft)				
Wall 27 in.	M = -80.76	(kip-ft/ft)	Side of personal hatch. Vert. cut.	27.8	-0.83	-1.29 [-3.55e-4]
	P = -21.38	(kip/ft)				

**Table B3. Stress in Rebar and Concrete of Structural Components Subjected to LC1
Standard-Plus Case**

Comp.	Demand		Location	Total stress in steel (ksi)		Maximum stress and strain in concrete (ksi) [in./in.]
				Rebar 1	Rebar 2	
Wall 36 in.	M = 459.2	(kip-ft/ft)	Wall near foundation. Horz. cut.	27.1	5.58	-2.21 [-6.61e-4]
	P = -142.2	(kip/ft)				
Wall 15 in.	M = 1.69	(kip-ft/ft)	Wall above Elec. Penetration. Horz. cut.	12.5	7.34	0.0 [4.03e-5]
	P = 19.88	(kip/ft)				
Wall 27 in.	M = -39.25	(kip-ft/ft)	Below personal hatch. Vert. cut.	24.6	2.73	-0.71 [-1.88e-4]
	P = 13.92	(kip/ft)				
Wall 27 in.	M = -33.66	(kip-ft/ft)	Side of personal hatch. Vert. cut.	19.3	2.79	-0.57 [-1.47e-4]
	P = 11.03	(kip/ft)				

Table B4. Stress in Rebar and Concrete of Structural Components Subjected to LC2 Standard-Plus Case

Comp.	Demand		Location	Total stress in steel (ksi)		Maximum stress and strain in concrete (ksi) [in./in.]
				Rebar 1	Rebar 2	
Wall 36 in.	M = 614.4	(kip-ft/ft)	Wall near foundation. Horz. cut.	42.4	1.97	-2.68 [-8.51e-4]
	P = 9.38	(kip/ft)				
Wall 36 in.	M = 431.8	(kip-ft/ft)	Wall near foundation. Horz. cut.	20.6	2.19	-2.48 [-7.67e-4]
	P = -392.3	(kip/ft)				
Wall 15 in.	M = 22.45	(kip-ft/ft)	Wall above Elec. Penetration. Horz. cut.	54.9	12.8	-1.32 [-3.62e-4]
	P = 52.29	(kip/ft)				
Wall 15 in.	M = -13.08	(kip-ft/ft)	Wall above Elec. Penetration. Horz. cut.	17.1	3.90	-0.78 [-2.06e-4]
	P = 4.25	(kip/ft)				
Wall 27 in.	M = -6.24	(kip-ft/ft)	Below personal hatch. Vert. cut.	25.9	19.7	0.0 [5.05e-4]
	P = 57.62	(kip/ft)				
Wall 27 in.	M = -91.80	(kip-ft/ft)	Below personal hatch. Vert. cut.	37.0	-1.17	-1.54 [-4.32e-4]
	P = -15.46	(kip/ft)				
Wall 27 in.	M = -0.85	(kip-ft/ft)	Side of personal hatch. Vert. cut.	22.4	21.5	0.0 [6.07e-4]
	P = 55.76	(kip/ft)				
Wall 27 in.	M = -80.25	(kip-ft/ft)	Side of personal hatch. Vert. cut.	27.5	-0.81	-1.29 [-3.52e-4]
	P = -21.39	(kip/ft)				

B9. Figures

There are no figures

**APPENDIX C****TENSILE STRESS IN REBARS OF RESIDUAL HEAT REMOVAL EQUIPMENT VAULT STRUCTURE****C1. REVISION HISTORY**

Revision 0: Initial document.

C2. OBJECTIVE OF CALCULATION

The objective of this calculation is to compute the maximum tensile stress that can form in the reinforcing steel rebars of Residual Heat Removal Equipment Vault (RHR) structure.

C3. RESULTS AND CONCLUSIONS

Table C1 summarizes the tensile stress in rebars of the RHR structure calculated at critical locations. The maximum tensile stress is 59.5 ksi computed for the vertical rebar of east interior wall at approximate El. (-) 45 ft. and subjected to the second in situ load combination. However, per RHR susceptibility evaluation [C1] and original design calculation [C3], the vertical rebars are not the primary load path. Essentially, the wall were designed to span horizontally. The next highest stress value is 56.5 ksi that is computed for the east exterior wall.

C4. DESIGN DATA / CRITERIA

See Section 4 of the calculation main body (Calc. 160268-CA-06 Rev. 0).

C5. ASSUMPTIONS**C5.1 Justified assumptions**

There are no justified assumptions.

C5.2 Unverified assumptions

There are no unverified assumptions.

C6. METHODOLOGY

The most critical stress demand in the horizontal rebars of the RHR structure is primarily due to the axial-flexure interaction along the vertical section cut in the south side of the east exterior wall. The highest stress demand in the vertical rebars of the RHR structure is primarily due to tension in the east and west interior walls.

Finite element analyses are conducted to calculate the axial force and bending moment at critical sections of the structure. The FE model and analysis method are similar to what explained in susceptibility evaluation of RHR structure [C1]. The axial force and bending moments are calculated using the method of section cuts.

Sectional analysis based on fiber section method is used to calculate the stress in the rebars of a section of a wall subjected to a combination of axial force and bending moment, as explained in calculation main body. Each wall section is discretized into 20 fibers of 1 ft width. An example calculation that evaluates the stress in the rebars of the east exterior wall is presented in Section C8. The CI value for the exterior wall was 0.75 mm/m which included in the analysis to find the initial stress state due to internal ASR alone. Zero internal ASR is used for the interior walls.

Figure C1 shows the contour plots of vertical strains in the interior walls due to LC1. The contour plots show that the overall vertical strains are reasonable compared to the yielding strain of rebars (i.e., 0.02% in/in). Localized strain concentration is observed close to the door openings at approximate El. (-) 30 ft. and El. (-) 45 ft.. Ductile distribution of local demands along the width of the interior walls is possible. As a result, localized strain concentration is not of concern.

C7. REFERENCES

- [C1] Simpson Gumpertz & Heger Inc., *Evaluation of Residual Heat Removal Equipment Vault*, 160268-CA-06 Rev. 0, Waltham, MA, August 2017.
- [C2] United Engineers & Constructors Inc., *Seabrook Station Structural Design Drawings*.
- [C3] United Engineers & Constructors Inc., *Analysis and Design of Vault Walls up to El. 23 ft., PB-30 Calc Rev. 9*, Dec. 2002.

C8. COMPUTATION

C8.1 Strain in Steel and Concrete due to Internal ASR expansion

Input Data

ASR expansion

Measured crack index	$\epsilon_{CI} := 0.75 \frac{\text{mm}}{\text{m}}$
Threshold factor	$F_{thr} := 1.0$

Material properties

Compressive strength of concrete	$f_c := -3\text{ksi}$	Ref. [C1]
Young's modulus of concrete	$E_c := 3120\text{ksi}$	
Yield strength of steel	$f_y := 60\text{ksi}$	
Young's modulus of steel	$E_s := 29000\text{ksi}$	

Geometry

Width of fibers	$b := 12\text{in}$	Ref. [C2]
Total thickness or height	$h := 24\text{in}$	
Area of concrete	$A_c := b \cdot h = 288 \cdot \text{in}^2$	
Area of tensile reinforcement (#8@9 in.)	$A_s := 0.79 \cdot \frac{12}{9} \text{in}^2 = 1.053 \cdot \text{in}^2$	
Number of reinforcement in row, e.g. equal to 2 for tensile and compressive	$\text{Steel}_{\text{Num}} := 2$	
Depth to reinforcement	$d := 20.5\text{in}$	

Finding the strain in steel and concrete by satisfying compatibility and equilibrium

	Initial Guess
Initial mechanical strain in concrete	$\epsilon_{o,\text{conc}} := 0$
Initial strain in steel	$\epsilon_{o,\text{steel}} := 0$
	Given
Compatibility equation	$F_{thr} \cdot \epsilon_{CI} = \epsilon_{o,\text{steel}} - \epsilon_{o,\text{conc}}$
Equilibrium equation	$(E_c \cdot A_c) \cdot \epsilon_{o,\text{conc}} + (E_s \cdot A_s \cdot \text{Steel}_{\text{Num}}) \cdot \epsilon_{o,\text{steel}} = 0$
	$\text{ans} := \text{Find}(\epsilon_{o,\text{conc}}, \epsilon_{o,\text{steel}})$
Initial strain in concrete and steel	$\epsilon_{o,\text{conc}} := \text{ans}_1 = -4.775 \times 10^{-5}$
	$\epsilon_{o,\text{steel}} := \text{ans}_2 = 7.023 \times 10^{-4}$

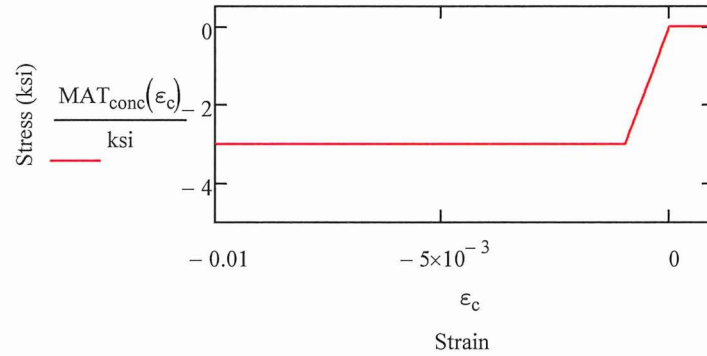
C8.2 Sectional Analysis

Input Data

Concrete Material Model

Constitutive model for concrete

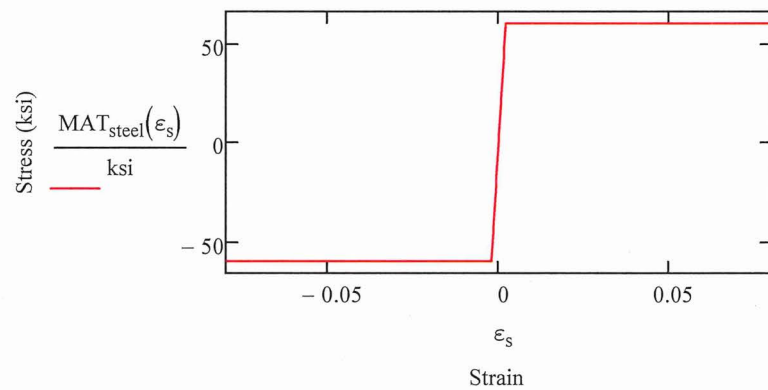
$$\text{MAT}_{\text{conc}}(\epsilon) := \begin{cases} 0 & \text{if } \epsilon > 0 \\ f_c & \text{if } \epsilon < \frac{f_c}{E_c} \\ (E_c \cdot \epsilon) & \text{otherwise} \end{cases}$$



Steel Material Model

Constitutive model for steel

$$\text{MAT}_{\text{steel}}(\epsilon) := \begin{cases} f_y & \text{if } \epsilon > \frac{f_y}{E_s} \\ -f_y & \text{if } \epsilon < \frac{-f_y}{E_s} \\ (E_s \cdot \epsilon) & \text{otherwise} \end{cases}$$



Concrete Fibers

Number of fibers

$$\text{Conc}_{\text{Num}} := 20$$

Height of fibers

$$\text{Conc}_H := \frac{h}{\text{Conc}_{\text{Num}}} = 1.2 \cdot \text{in}$$

Concrete fiber coordinates

$$\text{Conc}_y := \left| \begin{array}{l} \text{for } i \in 1.. \text{Conc}_{\text{Num}} \\ \text{ans}_i \leftarrow -\frac{h}{2} + \frac{\text{Conc}_H}{2} + (i-1) \cdot \text{Conc}_H \\ \text{ans} \end{array} \right.$$

Concrete fiber strain

$$\text{Conc}_\epsilon(\epsilon_{o,\text{conc}}, \epsilon, \varphi) := \left| \begin{array}{l} \text{for } i \in 1.. \text{Conc}_{\text{Num}} \\ \text{ans}_i \leftarrow \epsilon_{o,\text{conc}} + \epsilon - \varphi \cdot \text{Conc}_{y_i} \\ \text{ans} \end{array} \right.$$

Concrete fiber stress

$$\text{Conc}_\sigma(\epsilon_{o,\text{conc}}, \epsilon, \varphi) := \left| \begin{array}{l} \text{for } i \in 1.. \text{Conc}_{\text{Num}} \\ \text{ans}_i \leftarrow \text{MAT}_{\text{conc}}(\text{Conc}_\epsilon(\epsilon_{o,\text{conc}}, \epsilon, \varphi)_i) \\ \text{ans} \end{array} \right.$$

Concrete fiber force

$$\text{Conc}_F(\epsilon_{o,\text{conc}}, \epsilon, \varphi) := \left| \begin{array}{l} \text{for } i \in 1.. \text{Conc}_{\text{Num}} \\ \text{ans}_i \leftarrow \text{Conc}_\sigma(\epsilon_{o,\text{conc}}, \epsilon, \varphi)_i \cdot (b \cdot \text{Conc}_H) \\ \text{ans} \end{array} \right.$$

Reinforcement/Steel fibers

Depth to reinforcement fiber

$$\text{Steel}_{y_1} := -\left(d - \frac{h}{2}\right) = -8.5 \cdot \text{in}$$

$$\text{Steel}_{y_2} := d - \frac{h}{2} = 8.5 \cdot \text{in}$$

Area of reinforcement fiber

$$\text{Steel}_{A_{s_1}} := A_s = 1.053 \cdot \text{in}^2$$

$$\text{Steel}_{A_{s_2}} := A_s = 1.053 \cdot \text{in}^2$$

Steel fiber strain

$$\text{Steel}_\epsilon(\epsilon_{o,\text{steel}}, \epsilon, \varphi) := \left| \begin{array}{l} \text{for } i \in 1.. \text{Steel}_{\text{Num}} \\ \text{ans}_i \leftarrow \epsilon_{o,\text{steel}} + \epsilon - \varphi \cdot \text{Steel}_{y_i} \\ \text{ans} \end{array} \right.$$

Steel fiber stress

$$\text{Steel}_\sigma(\epsilon_{o,\text{steel}}, \epsilon, \varphi) := \left| \begin{array}{l} \text{for } i \in 1.. \text{Steel}_{\text{Num}} \\ \text{ans}_i \leftarrow \text{MAT}_{\text{steel}}(\text{Steel}_\epsilon(\epsilon_{o,\text{steel}}, \epsilon, \varphi)_i) \\ \text{ans} \end{array} \right.$$

Steel fiber force

$$\text{Steel}_F(\epsilon_{o,\text{steel}}, \epsilon, \varphi) := \left| \begin{array}{l} \text{for } i \in 1.. \text{Steel}_{\text{Num}} \\ \text{ans}_i \leftarrow \text{Steel}_\sigma(\epsilon_{o,\text{steel}}, \epsilon, \varphi)_i \cdot \text{Steel}_{A_{s_i}} \\ \text{ans} \end{array} \right.$$

Initial Stress State

Initial stress in concrete

$$\text{Concrete}_{\sigma} := \text{Conc}_{\sigma}(\varepsilon_{o,\text{conc}}, 0, 0)$$

$$\text{Concrete}_{\sigma_1} = -0.149 \text{ ksi}$$

Initial stress in steel

$$\text{Rebar}_{\sigma} := \text{Steel}_{\sigma}(\varepsilon_{o,\text{steel}}, 0, 0)$$

$$\text{Rebar}_{\sigma_1} = 20.365 \text{ ksi}$$

Axial Equilibrium

$$\text{Force}(\varepsilon_{o,\text{conc}}, \varepsilon_{o,\text{steel}}, \varepsilon, \varphi) := \left| \begin{array}{l} \text{ans1} \leftarrow 0 \\ \text{for } i \in 1.. \text{Conc}_{\text{Num}} \\ \quad \text{ans1} \leftarrow \text{ans1} + \text{Conc}_F(\varepsilon_{o,\text{conc}}, \varepsilon, \varphi)_i \\ \\ \text{ans2} \leftarrow 0 \\ \text{for } i \in 1.. \text{Steel}_{\text{Num}} \\ \quad \text{ans2} \leftarrow \text{ans2} + \text{Steel}_F(\varepsilon_{o,\text{steel}}, \varepsilon, \varphi)_i \\ \\ \text{ans} \leftarrow \text{ans1} + \text{ans2} \end{array} \right.$$

Moment Equilibrium

$$\text{Moment}(\varepsilon_{o,\text{conc}}, \varepsilon_{o,\text{steel}}, \varepsilon, \varphi) := \left| \begin{array}{l} \text{ans1} \leftarrow 0 \\ \text{for } i \in 1.. \text{Conc}_{\text{Num}} \\ \quad \text{ans1} \leftarrow \text{ans1} + -1 \cdot \text{Conc}_F(\varepsilon_{o,\text{conc}}, \varepsilon, \varphi)_i \cdot \text{Conc}_{y_i} \\ \\ \text{ans2} \leftarrow 0 \\ \text{for } i \in 1.. \text{Steel}_{\text{Num}} \\ \quad \text{ans2} \leftarrow \text{ans2} + -1 \cdot \text{Steel}_F(\varepsilon_{o,\text{steel}}, \varepsilon, \varphi)_i \cdot \text{Steel}_{y_i} \\ \\ \text{ans} \leftarrow \text{ans1} + \text{ans2} \end{array} \right.$$

Solution

Known parameters

Axial force

$$P := -35 \text{ kip}$$

Iteration

Curvature

$$\phi := -0.000072 \cdot \frac{1}{\text{in}}$$

Requires iteration

Solve for strain at centroid

Axial strain at centroid (initial guess)

$$x_0 := 0.0$$

Axial force equilibrium

$$f(x) := \text{Force}(\epsilon_{o.\text{conc}}, \epsilon_{o.\text{steel}}, x, \phi) - P$$

$$\epsilon_{\text{cent}} := \text{root}(f(x_0), x_0) = 3.028 \times 10^{-4}$$

Sectional forces

$$\text{Force}(\epsilon_{o.\text{conc}}, \epsilon_{o.\text{steel}}, \epsilon_{\text{cent}}, \phi) = -35 \cdot \text{kip}$$

$$\text{Moment}(\epsilon_{o.\text{conc}}, \epsilon_{o.\text{steel}}, \epsilon_{\text{cent}}, \phi) = -100.015 \cdot \text{kip} \cdot \text{ft}$$

Stress and strain in concrete and steel

Steel fiber stress and strain

$$\text{Rebar}_{\epsilon} := \text{Steel}_{\epsilon}(\epsilon_{o.\text{steel}}, \epsilon_{\text{cent}}, \phi) = \begin{pmatrix} 3.931 \times 10^{-4} \\ 1.617 \times 10^{-3} \end{pmatrix}$$

$$\text{Rebar}_{\sigma} := \text{Steel}_{\sigma}(\epsilon_{o.\text{steel}}, \epsilon_{\text{cent}}, \phi) = \begin{pmatrix} 11.399 \\ 46.895 \end{pmatrix} \cdot \text{ksi}$$

$$\text{Steel}_F(\epsilon_{o.\text{steel}}, \epsilon_{\text{cent}}, \phi) = \begin{pmatrix} 12.007 \\ 49.396 \end{pmatrix} \cdot \text{kip}$$

$$\text{Concrete}_y := \text{Conc}_y$$

Concrete fiber stress and strain

$$\text{Concrete}_{\epsilon} := \text{Conc}_{\epsilon}(\epsilon_{o.\text{conc}}, \epsilon_{\text{cent}}, \phi)$$

$$\text{Concrete}_{\sigma} := \text{Conc}_{\sigma}(\epsilon_{o.\text{conc}}, \epsilon_{\text{cent}}, \phi)$$

Maximum compressive stress in concrete

$$\sigma_{\text{max.comp}} := \text{MAT}_{\text{conc}} \left(\text{Concrete}_{\epsilon_1} + \phi \cdot \frac{\text{Conc}_H}{2} \right) = -1.9 \cdot \text{ksi}$$

C9. TABLES

Table C1: Stress in rebars at critical locations of RHR structure subjected to LC1

Component	Item	Total demands for sustained load (In Situ condition, LC1)		Total stress in steel (ksi)		Maximum compressive stress in concrete (ksi)
		Demand	Location	Rebar 1	Rebar 2	
Wall	Moment about the vertical global axis (kip-ft/ft)	-98.5	East exterior wall, vertical strip, at the approximate El. (-) 30 ft	46.9	11.4	-1.9
	Axial force (kip/ft)	-35.0				
Wall	Moment about the horizontal global axis (kip-ft/ft)	28.6	East interior wall, horizontal strip, at the approximate El. (-) 45 ft	41.6	5.5	0.0
	Axial force (kip/ft)	37.2				
Wall	Moment about the horizontal global axis (kip-ft/ft)	11.0	West interior wall, horizontal strip, at the approximate El. (-) 30 ft	26.5	12.5	0.0
	Axial force (kip/ft)	30.8				

Table C2: Stress in rebars at critical locations of RHR structure subjected to LC2

Component	Item	Total demands for sustained load (In Situ condition, LC1)		Total stress in steel (ksi)		Maximum compressive stress in concrete (ksi)
		Demand	Location	Rebar 1	Rebar 2	
Wall	Moment about the vertical global axis (kip-ft/ft)	-119.5	East exterior wall, vertical strip, at the approximate El. (-) 30 ft	56.5	13.8	-2.1
	Axial force (kip/ft)	-40.8				
Wall	Moment about the horizontal global axis (kip-ft/ft)	33.0	East interior wall, horizontal strip, at the approximate El. (-) 45 ft	59.5	17.7	0.0
	Axial force (kip/ft)	60.9				
Wall	Moment about the horizontal global axis (kip-ft/ft)	13.4	West interior wall, horizontal strip, at the approximate El. (-) 30 ft	36.6	19.6	0.0
	Axial force (kip/ft)	44.4				

C10. FIGURES

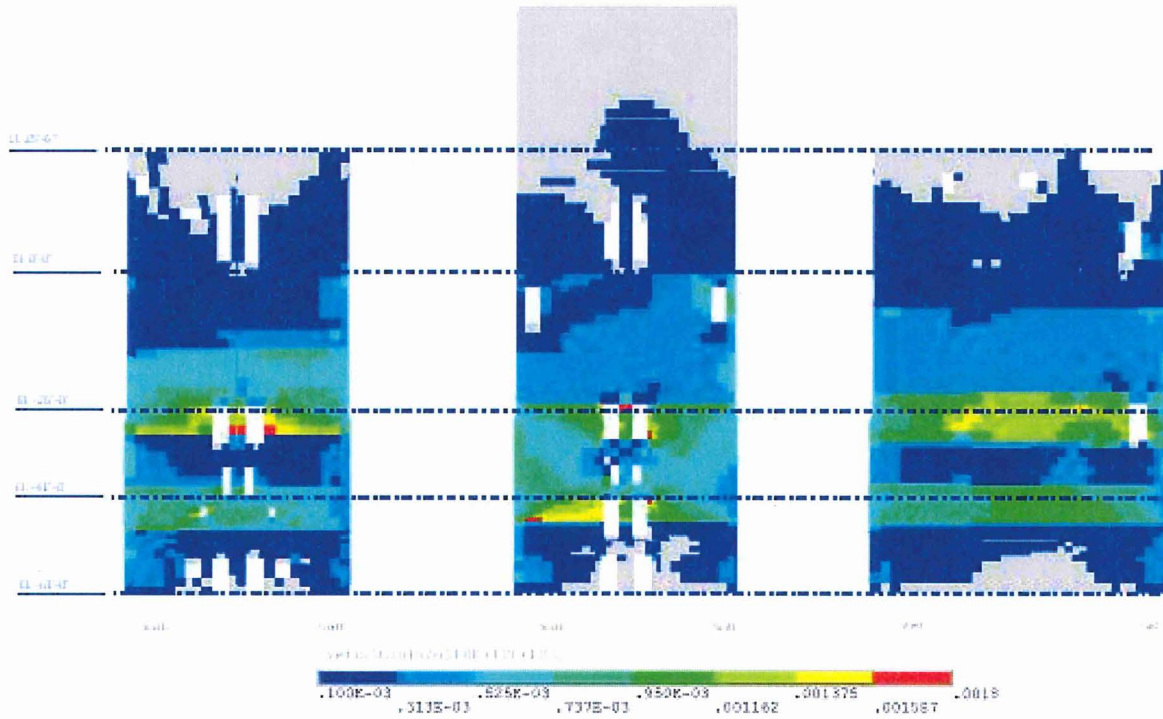


Figure C1: Contour plots of vertical strains in the interior walls due to LC1

**APPENDIX D****TENSILE STRESS IN REBARS OF CONDENSATE STORAGE TANK ENCLOSURE STRUCTURE****D1. REVISION HISTORY**

Revision 0: Initial document.

D2. OBJECTIVE OF CALCULATION

The objective of this calculation is to compute the maximum tensile stress that can form in the rebars of the Condensate Storage Tank Enclosure (CSTE) structure.

D3. RESULTS AND CONCLUSIONS

Table D1 summarizes the tensile stress in rebars of the CSTE structure calculated at critical locations. The Maximum tensile stress is 26.7 ksi at the bottom of the tank enclosure wall subjected to the second in situ load combination (LC2).

D4. DESIGN DATA / CRITERIA

See Section 4 of the calculation main body (Calc. 160268-CA-03 Rev. 0).

D5. ASSUMPTIONS**D5.1 Justified assumptions**

There are no justified assumptions.

D5.2 Unverified assumptions

There are no unverified assumptions.

D6. METHODOLOGY

The critical demands that control the selection of the threshold factor for the CSTE structure are hoop tension at the top of the tank enclosure wall, and vertical moment at the base of the tank enclosure wall. Finite element analyses were conducted to calculate the axial force and bending moment at these locations due to ASR load [D1].

To calculate the stress in rebars subjected to a combination of axial force and bending moment, sectional analysis based on fiber section method, as explained in calculation main body, is used. The calculation is conducted per 1 foot width of the walls, and each section is discretized into 20 fibers. An example calculation that evaluates the stress in the vertical rebars at the base of the tank enclosure wall is presented in Section D8. The ASR expansion of the tank enclosure is included in the analysis to find the initial stress state due to internal ASR alone.

D7. REFERENCES

- [D1] Simpson Gumpertz & Heger Inc., *Evaluation of Condensate Storage Tank Enclosure Structure*, 160268-CA-03 Rev. 0, Waltham, MA, Dec 2016.
- [D2] United Engineers & Constructors Inc., *Seabrook Station Structural Design Drawings*.
- [D3] United Engineers & Constructors Inc., *Condensate Storage Tank Mat and Wall Reinforcement*, MT-21, Rev. 3, Jan. 1984.

D8. COMPUTATION

D8.1. Strain in Steel and Concrete due to Internal ASR expansion

Input Data

ASR expansion

Measured crack index	$\epsilon_{CI} := 0.43 \frac{\text{mm}}{\text{m}}$
Threshold factor	$F_{thr} := 1.6$

Material properties

Compressive strength of concrete	$f_c := -4\text{ksi}$	Ref. [D1]
Young's modulus of concrete	$E_c := 3605\text{ksi}$	
Yield strength of steel	$f_y := 60\text{ksi}$	
Young's modulus of steel	$E_s := 29000\text{ksi}$	

Geometry

Width of fibers	$b := 12\text{in}$	Ref. [D2]
Total thickness or height	$h := 24\text{in}$	
Area of concrete	$A_c := b \cdot h = 288 \cdot \text{in}^2$	
Area of tensile reinforcement (#11@12 in.)	$A_s := 1.56\text{in}^2$	
Number of reinforcement in row, e.g. equal to 2 for tensile and compressive	$\text{Steel}_{Num} := 2$	
Depth to reinforcement	$d := 20.3\text{in}$	

Finding the strain in steel and concrete by satisfying compatibility and equilibrium

	Initial Guess
Initial mechanical strain in concrete	$\epsilon_{o,conc} := 0$
Initial strain in steel	$\epsilon_{o,steel} := 0$
	Given
Compatibility equation	$F_{thr} \cdot \epsilon_{CI} = \epsilon_{o,steel} - \epsilon_{o,conc}$
Equilibrium equation	$(E_c \cdot A_c) \cdot \epsilon_{o,conc} + (E_s \cdot A_s \cdot \text{Steel}_{Num}) \cdot \epsilon_{o,steel} = 0$
	$\text{ans} := \text{Find}(\epsilon_{o,conc}, \epsilon_{o,steel})$

Initial strain in concrete and steel

$$\epsilon_{0,conc} := ans_1 = -5.515 \times 10^{-5}$$

$$\epsilon_{0,steel} := ans_2 = 6.328 \times 10^{-4}$$

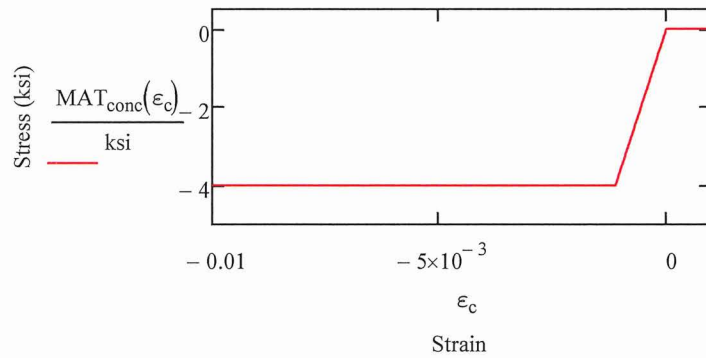
D8.2. Sectional Analysis

Input Data

Concrete Material Model

Constitutive model for concrete

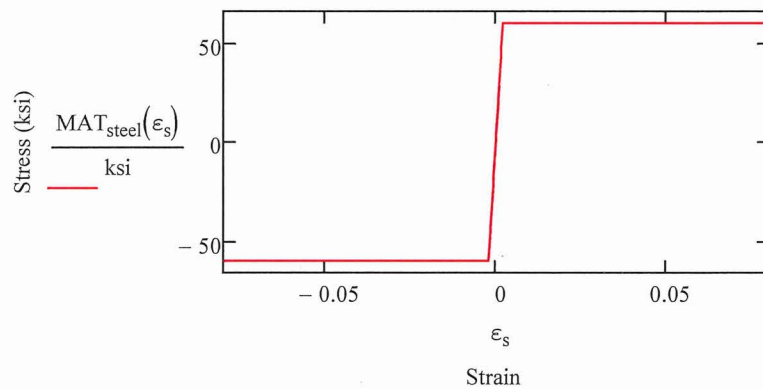
$$MAT_{conc}(\epsilon) := \begin{cases} 0 & \text{if } \epsilon > 0 \\ f_c & \text{if } \epsilon < \frac{f_c}{E_c} \\ (E_c \cdot \epsilon) & \text{otherwise} \end{cases}$$



Steel Material Model

Constitutive model for steel

$$MAT_{steel}(\epsilon) := \begin{cases} f_y & \text{if } \epsilon > \frac{f_y}{E_s} \\ -f_y & \text{if } \epsilon < \frac{-f_y}{E_s} \\ (E_s \cdot \epsilon) & \text{otherwise} \end{cases}$$



Concrete Fibers

Number of fibers

$$\text{Conc}_{\text{Num}} := 20$$

Height of fibers

$$\text{Conc}_H := \frac{h}{\text{Conc}_{\text{Num}}} = 1.2 \cdot \text{in}$$

Concrete fiber coordinates

$$\text{Conc}_y := \left| \begin{array}{l} \text{for } i \in 1.. \text{Conc}_{\text{Num}} \\ \text{ans}_i \leftarrow -\frac{h}{2} + \frac{\text{Conc}_H}{2} + (i-1) \cdot \text{Conc}_H \\ \text{ans} \end{array} \right.$$

Concrete fiber strain

$$\text{Conc}_\varepsilon(\varepsilon_{0,\text{conc}}, \varepsilon, \varphi) := \left| \begin{array}{l} \text{for } i \in 1.. \text{Conc}_{\text{Num}} \\ \text{ans}_i \leftarrow \varepsilon_{0,\text{conc}} + \varepsilon - \varphi \cdot \text{Conc}_{y_i} \\ \text{ans} \end{array} \right.$$

Concrete fiber stress

$$\text{Conc}_\sigma(\varepsilon_{0,\text{conc}}, \varepsilon, \varphi) := \left| \begin{array}{l} \text{for } i \in 1.. \text{Conc}_{\text{Num}} \\ \text{ans}_i \leftarrow \text{MAT}_{\text{conc}}(\text{Conc}_\varepsilon(\varepsilon_{0,\text{conc}}, \varepsilon, \varphi)_i) \\ \text{ans} \end{array} \right.$$

Concrete fiber force

$$\text{Conc}_F(\varepsilon_{0,\text{conc}}, \varepsilon, \varphi) := \left| \begin{array}{l} \text{for } i \in 1.. \text{Conc}_{\text{Num}} \\ \text{ans}_i \leftarrow \text{Conc}_\sigma(\varepsilon_{0,\text{conc}}, \varepsilon, \varphi)_i \cdot (b \cdot \text{Conc}_H) \\ \text{ans} \end{array} \right.$$

Reinforcement/Steel fibers

Depth to reinforcement fiber

$$\text{Steel}_{y_1} := -\left(d - \frac{h}{2}\right) = -8.3 \cdot \text{in}$$

$$\text{Steel}_{y_2} := d - \frac{h}{2} = 8.3 \cdot \text{in}$$

Area of reinforcement fiber

$$\text{Steel}_{A_{s_1}} := A_s = 1.56 \cdot \text{in}^2$$

$$\text{Steel}_{A_{s_2}} := A_s = 1.56 \cdot \text{in}^2$$

Steel fiber strain

$$\text{Steel}_\varepsilon(\varepsilon_{0,\text{steel}}, \varepsilon, \varphi) := \left| \begin{array}{l} \text{for } i \in 1.. \text{Steel}_{\text{Num}} \\ \text{ans}_i \leftarrow \varepsilon_{0,\text{steel}} + \varepsilon - \varphi \cdot \text{Steel}_{y_i} \\ \text{ans} \end{array} \right.$$

Steel fiber stress

$$\text{Steel}_\sigma(\varepsilon_{0,\text{steel}}, \varepsilon, \varphi) := \left| \begin{array}{l} \text{for } i \in 1.. \text{Steel}_{\text{Num}} \\ \text{ans}_i \leftarrow \text{MAT}_{\text{steel}}(\text{Steel}_\varepsilon(\varepsilon_{0,\text{steel}}, \varepsilon, \varphi)_i) \\ \text{ans} \end{array} \right.$$

Steel fiber force

$$\text{Steel}_F(\varepsilon_{0,\text{steel}}, \varepsilon, \varphi) := \left| \begin{array}{l} \text{for } i \in 1.. \text{Steel}_{\text{Num}} \\ \text{ans}_i \leftarrow \text{Steel}_\sigma(\varepsilon_{0,\text{steel}}, \varepsilon, \varphi)_i \cdot \text{Steel}_{A_{s_i}} \\ \text{ans} \end{array} \right.$$

Initial Stress State

Initial stress in concrete

$$\text{Concrete}_{\sigma} := \text{Conc}_{\sigma}(\varepsilon_{o,\text{conc}}, 0, 0)$$

$$\text{Concrete}_{\sigma_1} = -0.199 \text{ ksi}$$

Initial stress in steel

$$\text{Rebar}_{\sigma} := \text{Steel}_{\sigma}(\varepsilon_{o,\text{steel}}, 0, 0)$$

$$\text{Rebar}_{\sigma_1} = 18.353 \text{ ksi}$$

Axial Equilibrium

$$\text{Force}(\varepsilon_{o,\text{conc}}, \varepsilon_{o,\text{steel}}, \varepsilon, \varphi) := \left. \begin{array}{l} \text{ans1} \leftarrow 0 \\ \text{for } i \in 1.. \text{Conc}_{\text{Num}} \\ \quad \text{ans1} \leftarrow \text{ans1} + \text{Conc}_F(\varepsilon_{o,\text{conc}}, \varepsilon, \varphi)_i \\ \\ \text{ans2} \leftarrow 0 \\ \text{for } i \in 1.. \text{Steel}_{\text{Num}} \\ \quad \text{ans2} \leftarrow \text{ans2} + \text{Steel}_F(\varepsilon_{o,\text{steel}}, \varepsilon, \varphi)_i \\ \\ \text{ans} \leftarrow \text{ans1} + \text{ans2} \end{array} \right|$$

Moment Equilibrium

$$\text{Moment}(\varepsilon_{o,\text{conc}}, \varepsilon_{o,\text{steel}}, \varepsilon, \varphi) := \left. \begin{array}{l} \text{ans1} \leftarrow 0 \\ \text{for } i \in 1.. \text{Conc}_{\text{Num}} \\ \quad \text{ans1} \leftarrow \text{ans1} + -1 \cdot \text{Conc}_F(\varepsilon_{o,\text{conc}}, \varepsilon, \varphi)_i \cdot \text{Conc}_{y_i} \\ \\ \text{ans2} \leftarrow 0 \\ \text{for } i \in 1.. \text{Steel}_{\text{Num}} \\ \quad \text{ans2} \leftarrow \text{ans2} + -1 \cdot \text{Steel}_F(\varepsilon_{o,\text{steel}}, \varepsilon, \varphi)_i \cdot \text{Steel}_{y_i} \\ \\ \text{ans} \leftarrow \text{ans1} + \text{ans2} \end{array} \right|$$

Solution

Known parameters

Axial force

$$P := -12.9 \text{ kip}$$

Iteration

Curvature

$$\phi := 0.0000266 \cdot \frac{1}{\text{in}}$$

Requires iteration

Solve for strain at centroid

Axial strain at centroid (initial guess)

$$x_0 := 0.0$$

Axial force equilibrium

$$f(x) := \text{Force}(\epsilon_{o,\text{conc}}, \epsilon_{o,\text{steel}}, x, \phi) - P$$

$$\epsilon_{\text{cent}} := \text{root}(f(x_0), x_0) = 6.778 \times 10^{-5}$$

Sectional forces

$$\text{Force}(\epsilon_{o,\text{conc}}, \epsilon_{o,\text{steel}}, \epsilon_{\text{cent}}, \phi) = -12.9 \cdot \text{kip}$$

$$\text{Moment}(\epsilon_{o,\text{conc}}, \epsilon_{o,\text{steel}}, \epsilon_{\text{cent}}, \phi) = 65.634 \cdot \text{kip} \cdot \text{ft}$$

Stress and strain in concrete and steel

Steel fiber stress and strain

$$\text{Rebar}_\epsilon := \text{Steel}_\epsilon(\epsilon_{o,\text{steel}}, \epsilon_{\text{cent}}, \phi) = \begin{pmatrix} 9.214 \times 10^{-4} \\ 4.799 \times 10^{-4} \end{pmatrix}$$

$$\text{Rebar}_\sigma := \text{Steel}_\sigma(\epsilon_{o,\text{steel}}, \epsilon_{\text{cent}}, \phi) = \begin{pmatrix} 26.721 \\ 13.916 \end{pmatrix} \cdot \text{ksi}$$

$$\text{Steel}_F(\epsilon_{o,\text{steel}}, \epsilon_{\text{cent}}, \phi) = \begin{pmatrix} 41.685 \\ 21.709 \end{pmatrix} \cdot \text{kip}$$

$$\text{Concrete}_y := \text{Conc}_y$$

Concrete fiber stress and strain

$$\text{Concrete}_\epsilon := \text{Conc}_\epsilon(\epsilon_{o,\text{conc}}, \epsilon_{\text{cent}}, \phi)$$

$$\text{Concrete}_\sigma := \text{Conc}_\sigma(\epsilon_{o,\text{conc}}, \epsilon_{\text{cent}}, \phi)$$

Maximum compressive strain in concrete

$$\epsilon_{\text{max.comp}} := \frac{\text{Concrete}_\epsilon_{\text{ConcNum}} - \text{Concrete}_\epsilon_{\text{ConcNum}-1}}{\text{Conc}_y_{\text{ConcNum}} - \text{Conc}_y_{\text{ConcNum}-1}} \cdot \left(\frac{h}{2} - \text{Conc}_y_{\text{ConcNum}-1} \right) + \text{Concrete}_\epsilon_{\text{ConcNum}-1} \dots = -3.066 \times 10^{-4}$$

Maximum compressive stress in concrete

$$\sigma_{\text{max.comp}} := \text{MAT}_{\text{conc}}(\epsilon_{\text{max.comp}}) = -1.105 \cdot \text{ksi}$$

D9. TABLES

Table D1: Stress in rebars at critical locations of CSTE structure subjected to LC1

Component	Item	Total demands for sustained load (In Situ condition, LC1)		Total stress in steel (ksi)		Maximum compressive stress in concrete (ksi)
		Demand	Location	Rebar 1	Rebar 2	
Tank Enclosure Wall	Out-of-plane moment (kip-ft/ft)	0	Top of tank enclosure wall, horizontal direction	16.3	16.3	-0.14
	Axial force (kip/ft)	41.4				
	Out-of-plane moment (kip-ft/ft)	41	Bottom of tank enclosure wall, vertical direction	15.8	8.6	-0.68
	Axial force (kip/ft)	-12.9				

Table D2: Stress in rebars at critical locations of CSTE structure subjected to LC2

Component	Item	Total demands for sustained loads plus OBE amplified with threshold factor (In Situ condition, LC2)		Total stress in steel (ksi)		Maximum compressive stress in concrete (ksi)
		Demand	Location	Rebar 1	Rebar 2	
Tank Enclosure Wall	Out-of-plane moment (kip-ft/ft)	0	Top of tank enclosure wall, horizontal direction	26.0	26.0	-0.23
	Axial force (kip/ft)	66.2				
	Out-of-plane moment (kip-ft/ft)	65.7	Bottom of tank enclosure wall, vertical direction	26.7	13.9	-1.11
	Axial force (kip/ft)	-12.9				

Example in Section D8

D10. FIGURES

There are no figures.

APPENDIX E
TENSILE STRESS IN REBARS OF CONTAINMENT EQUIPMENT HATCH MISSILE SHIELD
STRUCTURE

E1. REVISION HISTORY

Revision 0: Initial document.

Revision 1: Revised page E-1 to update Revision history section. Revised page E-2 from Revision 0 to 1 to make editorial correction references to Section A8 to E8.

E2. OBJECTIVE OF CALCULATION

The objective of this calculation is to compute the maximum tensile stress that can form in the rebars of Containment Equipment Hatch Missile Shield (CEHMS) structure.

E3. RESULTS AND CONCLUSIONS

Table E1 summarizes the tensile stress in rebars of the CEHMS structure calculated at critical locations. The maximum tensile stress is 41.2 ksi computed for the eat wing wall at the intersection with the column.

E4. DESIGN DATA / CRITERIA

See Section 4 of the calculation main body (Calc. 160268-CA-02 Rev. 0).

E5. ASSUMPTIONS**E5.1 Justified assumptions**

There are no justified assumptions.

E5.2 Unverified assumptions

There are no unverified assumptions.

E6. METHODOLOGY

The critical demand that governed the computation of the threshold factor of CEHMS structure was bending of east wind wall at the intersection with column. At this location the demands are:

- ASR load with threshold factor: $M = 168$ kip-ft/ft, $P = 2.06$ kip/ft (Appendix C of Ref. E1)
- Unfactored ASR load: $M = 112.1$ kip-ft/ft, $P = 1.4$ kip/ft (threshold factor was 1.5)
- Original unfactored demands excluding the OBE: $M = 47.5$ kip-ft/ft, $P = -9.7$ kip/ft (Sheet 30 to 45 of Ref. E3)
- Original unfactored demands including the OBE: $M = 143.6$ kip-ft/ft, $P = -2.72$ kip/ft (Sheet 30 to 45 of Ref. E3)

To calculate the stress in rebars subjected to a combination of axial force and bending moment, sectional analysis based on fiber section method, as explained in calculation main body, is used. The calculation is conducted per 1 foot width of the wall, and each section is discretized into 20 fibers. An example calculation that evaluates the stress in rebars of the east wing wall is presented in Section E8. The CI value of the wall was 0.72 mm/m which included in the analysis to find the initial stress state due to internal ASR alone.

E7. REFERENCES

- [E1] Simpson Gumpertz & Heger Inc., *Evaluation of Containment Equipment Hatch Missile Shield structure*, 160268-CA-02 Rev. 0, Waltham, MA, Oct 2016.
- [E2] United Engineers & Constructors Inc., *Seabrook Station Structural Design Drawings*.
- [E3] United Engineers & Constructors Inc., *Equipment Hatch Shield Wall, CE-6-Calc Rev. 3*, Aug. 1998.

E8. COMPUTATION

E8.1. Strain in Steel and Concrete due to Internal ASR expansion

Input Data

ASR expansion

Measured crack index	$\epsilon_{CI} := 0.72 \frac{\text{mm}}{\text{m}}$
Threshold factor	$F_{thr} := 1.5$

Material properties

Compressive strength of concrete	$f_c := -3\text{ksi}$	Ref. [E1]
Young's modulus of concrete	$E_c := 3120\text{ksi}$	
Yield strength of steel	$f_y := 60\text{ksi}$	
Young's modulus of steel	$E_s := 29000\text{ksi}$	

Geometry

Width of fibers	$b := 12\text{in}$	Ref. [E2]
Total thickness or height	$h := 42\text{in}$	
Area of concrete	$A_c := b \cdot h = 504 \cdot \text{in}^2$	
Area of tensile reinforcement (#11@6 in.)	$A_s := 2 \cdot 1.56\text{in}^2$	
Number of reinforcement in row, e.g. equal to 2 for tensile and compressive	$\text{Steel}_{\text{Num}} := 2$	
Depth to reinforcement	$d := 36.88\text{in}$	

Finding the strain in steel and concrete by satisfying compatibility and equilibrium

	Initial Guess
Initial mechanical strain in concrete	$\epsilon_{o,\text{conc}} := 0$
Initial strain in steel	$\epsilon_{o,\text{steel}} := 0$
	Given
Compatibility equation	$F_{thr} \cdot \epsilon_{CI} = \epsilon_{o,\text{steel}} - \epsilon_{o,\text{conc}}$
Equilibrium equation	$(E_c \cdot A_c) \cdot \epsilon_{o,\text{conc}} + (E_s \cdot A_s \cdot \text{Steel}_{\text{Num}}) \cdot \epsilon_{o,\text{steel}} = 0$
	$\text{ans} := \text{Find}(\epsilon_{o,\text{conc}}, \epsilon_{o,\text{steel}})$

Initial strain in concrete and steel

$$\epsilon_{0,conc} := \text{ans}_1 = -1.115 \times 10^{-4}$$

$$\epsilon_{0,steel} := \text{ans}_2 = 9.685 \times 10^{-4}$$

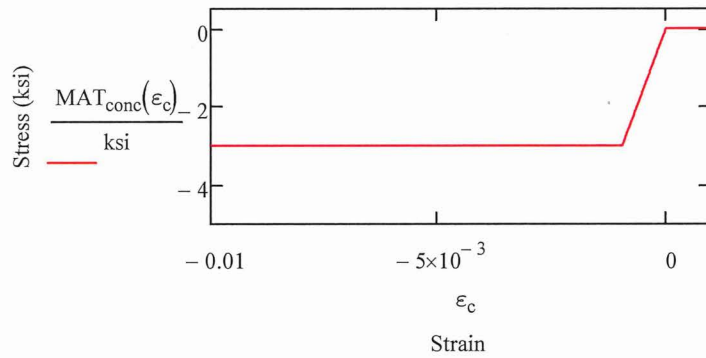
E8.2. Sectional Analysis

Input Data

Concrete Material Model

Constitutive model for concrete

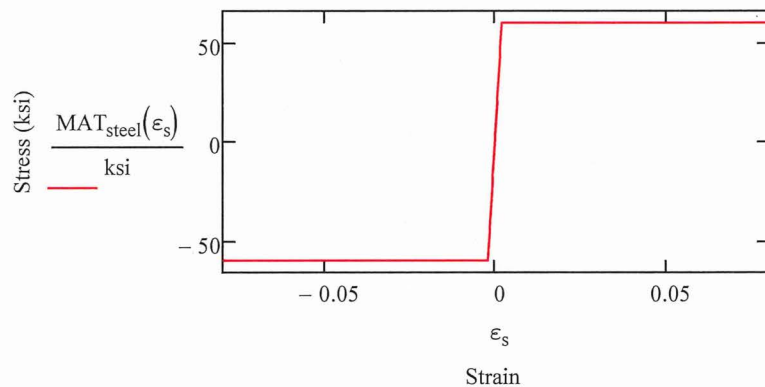
$$\text{MAT}_{conc}(\epsilon) := \begin{cases} 0 & \text{if } \epsilon > 0 \\ f_c & \text{if } \epsilon < \frac{f_c}{E_c} \\ (E_c \cdot \epsilon) & \text{otherwise} \end{cases}$$



Steel Material Model

Constitutive model for steel

$$\text{MAT}_{steel}(\epsilon) := \begin{cases} f_y & \text{if } \epsilon > \frac{f_y}{E_s} \\ -f_y & \text{if } \epsilon < \frac{-f_y}{E_s} \\ (E_s \cdot \epsilon) & \text{otherwise} \end{cases}$$



Concrete Fibers

Number of fibers

$$\text{Conc}_{\text{Num}} := 20$$

Height of fibers

$$\text{Conc}_H := \frac{h}{\text{Conc}_{\text{Num}}} = 2.1 \cdot \text{in}$$

Concrete fiber coordinates

$$\text{Conc}_y := \begin{cases} \text{for } i \in 1.. \text{Conc}_{\text{Num}} \\ \text{ans}_i \leftarrow -\frac{h}{2} + \frac{\text{Conc}_H}{2} + (i-1) \cdot \text{Conc}_H \\ \text{ans} \end{cases}$$

Concrete fiber strain

$$\text{Conc}_\varepsilon(\varepsilon_{o,\text{conc}}, \varepsilon, \varphi) := \begin{cases} \text{for } i \in 1.. \text{Conc}_{\text{Num}} \\ \text{ans}_i \leftarrow \varepsilon_{o,\text{conc}} + \varepsilon - \varphi \cdot \text{Conc}_{y_i} \\ \text{ans} \end{cases}$$

Concrete fiber stress

$$\text{Conc}_\sigma(\varepsilon_{o,\text{conc}}, \varepsilon, \varphi) := \begin{cases} \text{for } i \in 1.. \text{Conc}_{\text{Num}} \\ \text{ans}_i \leftarrow \text{MAT}_{\text{conc}}(\text{Conc}_\varepsilon(\varepsilon_{o,\text{conc}}, \varepsilon, \varphi)_i) \\ \text{ans} \end{cases}$$

Concrete fiber force

$$\text{Conc}_F(\varepsilon_{o,\text{conc}}, \varepsilon, \varphi) := \begin{cases} \text{for } i \in 1.. \text{Conc}_{\text{Num}} \\ \text{ans}_i \leftarrow \text{Conc}_\sigma(\varepsilon_{o,\text{conc}}, \varepsilon, \varphi)_i \cdot (b \cdot \text{Conc}_H) \\ \text{ans} \end{cases}$$

Reinforcement/Steel fibers

Depth to reinforcement fiber

$$\text{Steel}_{y_1} := -\left(d - \frac{h}{2}\right) = -15.88 \cdot \text{in}$$

$$\text{Steel}_{y_2} := d - \frac{h}{2} = 15.88 \cdot \text{in}$$

Area of reinforcement fiber

$$\text{Steel}_{A_{s_1}} := A_s = 3.12 \cdot \text{in}^2$$

$$\text{Steel}_{A_{s_2}} := A_s = 3.12 \cdot \text{in}^2$$

Steel fiber strain

$$\text{Steel}_\varepsilon(\varepsilon_{o,\text{steel}}, \varepsilon, \varphi) := \begin{cases} \text{for } i \in 1.. \text{Steel}_{\text{Num}} \\ \text{ans}_i \leftarrow \varepsilon_{o,\text{steel}} + \varepsilon - \varphi \cdot \text{Steel}_{y_i} \\ \text{ans} \end{cases}$$

Steel fiber stress

$$\text{Steel}_\sigma(\varepsilon_{o,\text{steel}}, \varepsilon, \varphi) := \begin{cases} \text{for } i \in 1.. \text{Steel}_{\text{Num}} \\ \text{ans}_i \leftarrow \text{MAT}_{\text{steel}}(\text{Steel}_\varepsilon(\varepsilon_{o,\text{steel}}, \varepsilon, \varphi)_i) \\ \text{ans} \end{cases}$$

Steel fiber force

$$\text{Steel}_F(\varepsilon_{o,\text{steel}}, \varepsilon, \varphi) := \begin{cases} \text{for } i \in 1.. \text{Steel}_{\text{Num}} \\ \text{ans}_i \leftarrow \text{Steel}_\sigma(\varepsilon_{o,\text{steel}}, \varepsilon, \varphi)_i \cdot \text{Steel}_{A_{s_i}} \\ \text{ans} \end{cases}$$

Initial Stress State

Initial stress in concrete

$$\text{Concrete}_{\sigma} := \text{Conc}_{\sigma}(\varepsilon_{o,\text{conc}}, 0, 0)$$

$$\text{Concrete}_{\sigma_1} = -0.348 \cdot \text{ksi}$$

Initial stress in steel

$$\text{Rebar}_{\sigma} := \text{Steel}_{\sigma}(\varepsilon_{o,\text{steel}}, 0, 0)$$

$$\text{Rebar}_{\sigma_1} = 28.088 \cdot \text{ksi}$$

Axial Equilibrium

$$\text{Force}(\varepsilon_{o,\text{conc}}, \varepsilon_{o,\text{steel}}, \varepsilon, \varphi) := \left. \begin{array}{l} \text{ans1} \leftarrow 0 \\ \text{for } i \in 1.. \text{Conc}_{\text{Num}} \\ \quad \text{ans1} \leftarrow \text{ans1} + \text{Conc}_{\text{F}}(\varepsilon_{o,\text{conc}}, \varepsilon, \varphi)_i \\ \text{ans2} \leftarrow 0 \\ \text{for } i \in 1.. \text{Steel}_{\text{Num}} \\ \quad \text{ans2} \leftarrow \text{ans2} + \text{Steel}_{\text{F}}(\varepsilon_{o,\text{steel}}, \varepsilon, \varphi)_i \\ \text{ans} \leftarrow \text{ans1} + \text{ans2} \end{array} \right|$$

Moment Equilibrium

$$\text{Moment}(\varepsilon_{o,\text{conc}}, \varepsilon_{o,\text{steel}}, \varepsilon, \varphi) := \left. \begin{array}{l} \text{ans1} \leftarrow 0 \\ \text{for } i \in 1.. \text{Conc}_{\text{Num}} \\ \quad \text{ans1} \leftarrow \text{ans1} + -1 \cdot \text{Conc}_{\text{F}}(\varepsilon_{o,\text{conc}}, \varepsilon, \varphi)_i \cdot \text{Conc}_{y_i} \\ \text{ans2} \leftarrow 0 \\ \text{for } i \in 1.. \text{Steel}_{\text{Num}} \\ \quad \text{ans2} \leftarrow \text{ans2} + -1 \cdot \text{Steel}_{\text{F}}(\varepsilon_{o,\text{steel}}, \varepsilon, \varphi)_i \cdot \text{Steel}_{y_i} \\ \text{ans} \leftarrow \text{ans1} + \text{ans2} \end{array} \right|$$

Solution

Known parameters

Axial force

$$P := -0.7 \text{ kip}$$

Iteration

Curvature

$$\phi := 0.00002285 \cdot \frac{1}{\text{in}}$$

Requires iteration

Solve for strain at centroid

Axial strain at centroid (initial guess)

$$x_0 := 0.0$$

Axial force equilibrium

$$f(x) := \text{Force}(\epsilon_{o.\text{conc}}, \epsilon_{o.\text{steel}}, x, \phi) - P$$

$$\epsilon_{\text{cent}} := \text{root}(f(x_0), x_0) = 1.037 \times 10^{-4}$$

Sectional forces

$$\text{Force}(\epsilon_{o.\text{conc}}, \epsilon_{o.\text{steel}}, \epsilon_{\text{cent}}, \phi) = -0.7 \cdot \text{kip}$$

$$\text{Moment}(\epsilon_{o.\text{conc}}, \epsilon_{o.\text{steel}}, \epsilon_{\text{cent}}, \phi) = 311.755 \cdot \text{kip} \cdot \text{ft}$$

Stress and strain in concrete and steel

Steel fiber stress and strain

$$\text{Rebar}_{\epsilon} := \text{Steel}_{\epsilon}(\epsilon_{o.\text{steel}}, \epsilon_{\text{cent}}, \phi) = \begin{pmatrix} 1.435 \times 10^{-3} \\ 7.094 \times 10^{-4} \end{pmatrix}$$

$$\text{Rebar}_{\sigma} := \text{Steel}_{\sigma}(\epsilon_{o.\text{steel}}, \epsilon_{\text{cent}}, \phi) = \begin{pmatrix} 41.618 \\ 20.572 \end{pmatrix} \cdot \text{ksi}$$

$$\text{Steel}_P(\epsilon_{o.\text{steel}}, \epsilon_{\text{cent}}, \phi) = \begin{pmatrix} 129.848 \\ 64.186 \end{pmatrix} \cdot \text{kip}$$

$$\text{Concrete}_y := \text{Conc}_y$$

Concrete fiber stress and strain

$$\text{Concrete}_{\epsilon} := \text{Conc}_{\epsilon}(\epsilon_{o.\text{conc}}, \epsilon_{\text{cent}}, \phi)$$

$$\text{Concrete}_{\sigma} := \text{Conc}_{\sigma}(\epsilon_{o.\text{conc}}, \epsilon_{\text{cent}}, \phi)$$

Maximum compressive strain in concrete

$$\epsilon_{\text{max.comp}} := \frac{\text{Concrete}_{\epsilon_{\text{ConcNum}}} - \text{Concrete}_{\epsilon_{\text{ConcNum}-1}}}{\text{Conc}_y_{\text{ConcNum}} - \text{Conc}_y_{\text{ConcNum}-1}} \cdot \left(\frac{h}{2} - \text{Conc}_y_{\text{ConcNum}-1} \right) \dots = -4.876 \times 10^{-4}$$

$$+ \text{Concrete}_{\epsilon_{\text{ConcNum}-1}}$$

Maximum compressive stress in concrete

$$\sigma_{\text{max.comp}} := \text{MAT}_{\text{conc}}(\epsilon_{\text{max.comp}}) = -1.521 \cdot \text{ksi}$$

E9. TABLES

Table E1: Stress in rebars at critical locations of CEHMS structure subjected to LC1

Component	Item	Total demands for sustained load (In Situ condition, LC1)		Total stress in steel (ksi)		Maximum compressive stress in concrete (ksi)
		Demand	Location	Rebar 1	Rebar 2	
East wing walls	Out-of-plane moment (kip-ft/ft)	159.6	East wing wall, at intersection with column	23.4	15.0	-0.78
	Axial force (kip/ft)	-8.3				

Table E2: Stress in rebars at critical locations of CEHMS structure subjected to LC2

Component	Item	Total demands for sustained loads plus OBE amplified with threshold factor (In Situ condition, LC2)		Total stress in steel (ksi)		Maximum compressive stress in concrete (ksi)
		Demand	Location	Rebar 1	Rebar 2	
East wing wall	Out-of-plane moment (kip-ft/ft)	311.6	East wall, horizontal strip, at the middle of the wall	41.6	20.8	-1.52
	Axial force (kip/ft)	-0.7				

Example in Section E8

E10. FIGURES

There are no figures.

**APPENDIX F****TENSILE STRESS IN REBARS OF CONTAINMENT ENCLOSURE VENTILATION AREA****F1. REVISION HISTORY**

Revision 0: Initial document.

F2. OBJECTIVE OF CALCULATION

The objective of this calculation is to compute the maximum tensile stress that can form in the rebars of Containment Enclosure Ventilation Area (CEVA) structure.

F3. RESULTS AND CONCLUSIONS

Table F1 summarizes the tensile stress in rebars of the CEVA structure calculated at critical locations. The maximum tensile stress is 44.0 ksi computed for the rebars of the base slab along east-west direction.

F4. DESIGN DATA / CRITERIA

See Section 4 of the calculation main body (Calc. 160268-CA-05 Rev. 0).

F5. ASSUMPTIONS**F5.1 Justified assumptions**

There are no justified assumptions.

F5.2 Unverified assumptions

There are no unverified assumptions.

F6. METHODOLOGY

The critical demand that governed the computation of the threshold factor of CEVA structure was bending moment of the base slab in Area 3 subjected to seismic load combinations that act parallel to east-west direction [F1]. The original calculation of CEVA structure [F3] does not provide unfactored demand values; therefore, in this evaluation, the factored load is conservatively divided by the minimum load factor in the load combination and used in calculating rebar stress:

- ASR load with threshold factor: $M = 28.7$ kip-ft/ft $P = 0$ (Appendix C of Ref. F1)
- Unfactored ASR load: $M = 9.56$ kip-ft/ft, $P = 0$ (threshold factor was 3.0)
- Original unfactored demands including the OBE: $M = 77/1.4 = 55$ kip-ft/ft, $P = 2.44/1.4 = 1.43$ kip/ft (Sheet 16 of Ref. F3). Note that the value of 1.4 was the load factor applied to the dead load in the combination (minimum load factor)

To calculate the stress in rebars subjected to a combination of axial force and bending moment, sectional analysis based on fiber section method, as explained in calculation main body, is used. The calculation is conducted per 1 foot width, and each section is discretized into 20 fibers. An example calculation that evaluates the stress in rebars of the base slab is presented in Section F8. The CI value of all components was set equal to 0.31 mm/m which included in the analysis to find the initial stress state due to internal ASR alone.

F7. REFERENCES

- [F1] Simpson Gumpertz & Heger Inc., *Evaluation of Containment Enclosure Ventilation Area*, 160268-CA-05 Rev. 0, Waltham, MA, Mar. 2017.
- [F2] United Engineers & Constructors Inc., *Seabrook Station Structural Design Drawings*.
- [F3] United Engineers & Constructors Inc., *Containment Enclosure Ventilation Area, EM-33-Calc Rev. 4*, Jan. 1986.

F8. COMPUTATION

F8.1. Strain in Steel and Concrete due to Internal ASR expansion

Input Data

ASR expansion

Measured crack index	$\epsilon_{CI} := 0.31 \frac{\text{mm}}{\text{m}}$
Threshold factor	$F_{thr} := 3$

Material properties

Compressive strength of concrete	$f_c := -3\text{ksi}$	Ref. [F1]
Young's modulus of concrete	$E_c := 3120\text{ksi}$	
Yield strength of steel	$f_y := 60\text{ksi}$	
Young's modulus of steel	$E_s := 29000\text{ksi}$	

Geometry

Width of fibers	$b := 12\text{in}$	Ref. [F2]
Total thickness or height	$h := 30\text{in}$	
Area of concrete	$A_c := b \cdot h = 360 \cdot \text{in}^2$	
Area of tensile reinforcement (#9@12 in.)	$A_s := 1 \text{in}^2$	
Number of reinforcement in row, e.g. equal to 2 for tensile and compressive	$\text{Steel}_{\text{Num}} := 2$	
Depth to reinforcement	$d := 26.4\text{in}$	

Finding the strain in steel and concrete by satisfying compatibility and equilibrium

	Initial Guess
Initial mechanical strain in concrete	$\epsilon_{o,\text{conc}} := 0$
Initial strain in steel	$\epsilon_{o,\text{steel}} := 0$
	Given
Compatibility equation	$F_{thr} \cdot \epsilon_{CI} = \epsilon_{o,\text{steel}} - \epsilon_{o,\text{conc}}$
Equilibrium equation	$(E_c \cdot A_c) \cdot \epsilon_{o,\text{conc}} + (E_s \cdot A_s \cdot \text{Steel}_{\text{Num}}) \cdot \epsilon_{o,\text{steel}} = 0$
	$\text{ans} := \text{Find}(\epsilon_{o,\text{conc}}, \epsilon_{o,\text{steel}})$

Initial strain in concrete and steel

$$\epsilon_{0,\text{conc}} := \text{ans}_1 = -4.567 \times 10^{-5}$$

$$\epsilon_{0,\text{steel}} := \text{ans}_2 = 8.843 \times 10^{-4}$$

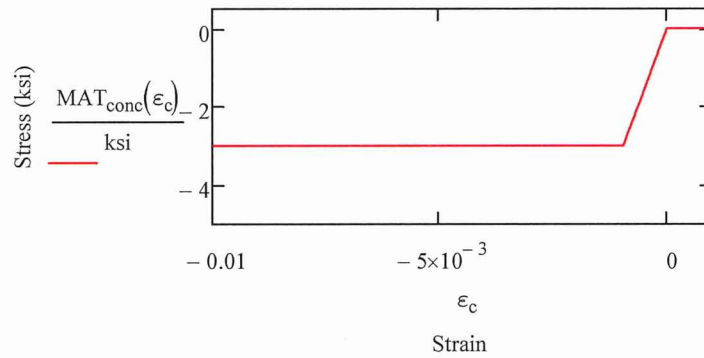
F8.2. Sectional Analysis

Input Data

Concrete Material Model

Constitutive model for concrete

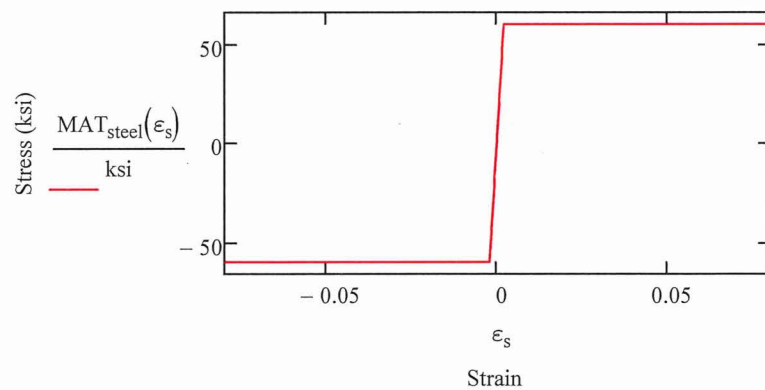
$$\text{MAT}_{\text{conc}}(\epsilon) := \begin{cases} 0 & \text{if } \epsilon > 0 \\ f_c & \text{if } \epsilon < \frac{f_c}{E_c} \\ (E_c \cdot \epsilon) & \text{otherwise} \end{cases}$$



Steel Material Model

Constitutive model for steel

$$\text{MAT}_{\text{steel}}(\epsilon) := \begin{cases} f_y & \text{if } \epsilon > \frac{f_y}{E_s} \\ -f_y & \text{if } \epsilon < \frac{-f_y}{E_s} \\ (E_s \cdot \epsilon) & \text{otherwise} \end{cases}$$



Concrete Fibers

Number of fibers

$$\text{Conc}_{\text{Num}} := 20$$

Height of fibers

$$\text{Conc}_H := \frac{h}{\text{Conc}_{\text{Num}}} = 1.5 \cdot \text{in}$$

Concrete fiber coordinates

$$\text{Conc}_y := \begin{cases} \text{for } i \in 1.. \text{Conc}_{\text{Num}} \\ \text{ans}_i \leftarrow -\frac{h}{2} + \frac{\text{Conc}_H}{2} + (i-1) \cdot \text{Conc}_H \\ \text{ans} \end{cases}$$

Concrete fiber strain

$$\text{Conc}_\varepsilon(\varepsilon_{o,\text{conc}}, \varepsilon, \varphi) := \begin{cases} \text{for } i \in 1.. \text{Conc}_{\text{Num}} \\ \text{ans}_i \leftarrow \varepsilon_{o,\text{conc}} + \varepsilon - \varphi \cdot \text{Conc}_{y_i} \\ \text{ans} \end{cases}$$

Concrete fiber stress

$$\text{Conc}_\sigma(\varepsilon_{o,\text{conc}}, \varepsilon, \varphi) := \begin{cases} \text{for } i \in 1.. \text{Conc}_{\text{Num}} \\ \text{ans}_i \leftarrow \text{MAT}_{\text{conc}}(\text{Conc}_\varepsilon(\varepsilon_{o,\text{conc}}, \varepsilon, \varphi)_i) \\ \text{ans} \end{cases}$$

Concrete fiber force

$$\text{Conc}_F(\varepsilon_{o,\text{conc}}, \varepsilon, \varphi) := \begin{cases} \text{for } i \in 1.. \text{Conc}_{\text{Num}} \\ \text{ans}_i \leftarrow \text{Conc}_\sigma(\varepsilon_{o,\text{conc}}, \varepsilon, \varphi)_i \cdot (b \cdot \text{Conc}_H) \\ \text{ans} \end{cases}$$

Reinforcement/Steel fibers

Depth to reinforcement fiber

$$\text{Steel}_{y_1} := -\left(d - \frac{h}{2}\right) = -11.4 \cdot \text{in}$$

$$\text{Steel}_{y_2} := d - \frac{h}{2} = 11.4 \cdot \text{in}$$

Area of reinforcement fiber

$$\text{Steel}_{A_{s_1}} := A_s = 1 \cdot \text{in}^2$$

$$\text{Steel}_{A_{s_2}} := A_s = 1 \cdot \text{in}^2$$

Steel fiber strain

$$\text{Steel}_\varepsilon(\varepsilon_{o,\text{steel}}, \varepsilon, \varphi) := \begin{cases} \text{for } i \in 1.. \text{Steel}_{\text{Num}} \\ \text{ans}_i \leftarrow \varepsilon_{o,\text{steel}} + \varepsilon - \varphi \cdot \text{Steel}_{y_i} \\ \text{ans} \end{cases}$$

Steel fiber stress

$$\text{Steel}_\sigma(\varepsilon_{o,\text{steel}}, \varepsilon, \varphi) := \begin{cases} \text{for } i \in 1.. \text{Steel}_{\text{Num}} \\ \text{ans}_i \leftarrow \text{MAT}_{\text{steel}}(\text{Steel}_\varepsilon(\varepsilon_{o,\text{steel}}, \varepsilon, \varphi)_i) \\ \text{ans} \end{cases}$$

Steel fiber force

$$\text{Steel}_F(\varepsilon_{o,\text{steel}}, \varepsilon, \varphi) := \begin{cases} \text{for } i \in 1.. \text{Steel}_{\text{Num}} \\ \text{ans}_i \leftarrow \text{Steel}_\sigma(\varepsilon_{o,\text{steel}}, \varepsilon, \varphi)_i \cdot \text{Steel}_{A_{s_i}} \\ \text{ans} \end{cases}$$

Initial Stress State

Initial stress in concrete

$$\text{Concrete}_{\sigma} := \text{Conc}_{\sigma}(\varepsilon_{0,\text{conc}}, 0, 0)$$

$$\text{Concrete}_{\sigma_1} = -0.142 \text{ ksi}$$

Initial stress in steel

$$\text{Rebar}_{\sigma} := \text{Steel}_{\sigma}(\varepsilon_{0,\text{steel}}, 0, 0)$$

$$\text{Rebar}_{\sigma_1} = 25.646 \text{ ksi}$$

Axial Equilibrium

$$\text{Force}(\varepsilon_{0,\text{conc}}, \varepsilon_{0,\text{steel}}, \varepsilon, \varphi) := \left\{ \begin{array}{l} \text{ans1} \leftarrow 0 \\ \text{for } i \in 1.. \text{ConcNum} \\ \quad \text{ans1} \leftarrow \text{ans1} + \text{Conc}_F(\varepsilon_{0,\text{conc}}, \varepsilon, \varphi)_i \\ \\ \text{ans2} \leftarrow 0 \\ \text{for } i \in 1.. \text{SteelNum} \\ \quad \text{ans2} \leftarrow \text{ans2} + \text{Steel}_F(\varepsilon_{0,\text{steel}}, \varepsilon, \varphi)_i \\ \\ \text{ans} \leftarrow \text{ans1} + \text{ans2} \end{array} \right.$$

Moment Equilibrium

$$\text{Moment}(\varepsilon_{0,\text{conc}}, \varepsilon_{0,\text{steel}}, \varepsilon, \varphi) := \left\{ \begin{array}{l} \text{ans1} \leftarrow 0 \\ \text{for } i \in 1.. \text{ConcNum} \\ \quad \text{ans1} \leftarrow \text{ans1} + -1 \cdot \text{Conc}_F(\varepsilon_{0,\text{conc}}, \varepsilon, \varphi)_i \cdot \text{Conc}_{y_i} \\ \\ \text{ans2} \leftarrow 0 \\ \text{for } i \in 1.. \text{SteelNum} \\ \quad \text{ans2} \leftarrow \text{ans2} + -1 \cdot \text{Steel}_F(\varepsilon_{0,\text{steel}}, \varepsilon, \varphi)_i \cdot \text{Steel}_{y_i} \\ \\ \text{ans} \leftarrow \text{ans1} + \text{ans2} \end{array} \right.$$

Solution

Known parameters

Axial force $P := 1.74 \text{ kip}$

Iteration

Curvature $\phi := 0.0000353 \cdot \frac{1}{\text{in}}$ Requires iteration

Solve for strain at centroid

Axial strain at centroid (initial guess) $x_0 := 0.0$

Axial force equilibrium $f(x) := \text{Force}(\epsilon_{o,\text{conc}}, \epsilon_{o,\text{steel}}, x, \phi) - P$
 $\epsilon_{\text{cent}} := \text{root}(f(x_0), x_0) = 2.299 \times 10^{-4}$

Sectional forces

$\text{Force}(\epsilon_{o,\text{conc}}, \epsilon_{o,\text{steel}}, \epsilon_{\text{cent}}, \phi) = 1.74 \cdot \text{kip}$
 $\text{Moment}(\epsilon_{o,\text{conc}}, \epsilon_{o,\text{steel}}, \epsilon_{\text{cent}}, \phi) = 83.675 \cdot \text{kip} \cdot \text{ft}$

Stress and strain in concrete and steel

Steel fiber stress and strain

$$\text{Rebar}_\epsilon := \text{Steel}_\epsilon(\epsilon_{o,\text{steel}}, \epsilon_{\text{cent}}, \phi) = \begin{pmatrix} 1.517 \times 10^{-3} \\ 7.118 \times 10^{-4} \end{pmatrix}$$

$$\text{Rebar}_\sigma := \text{Steel}_\sigma(\epsilon_{o,\text{steel}}, \epsilon_{\text{cent}}, \phi) = \begin{pmatrix} 43.982 \\ 20.642 \end{pmatrix} \cdot \text{ksi}$$

$$\text{Steel}_F(\epsilon_{o,\text{steel}}, \epsilon_{\text{cent}}, \phi) = \begin{pmatrix} 43.982 \\ 20.642 \end{pmatrix} \cdot \text{kip}$$

$\text{Concrete}_y := \text{Conc}_y$

Concrete fiber stress and strain

$$\text{Concrete}_\epsilon := \text{Conc}_\epsilon(\epsilon_{o,\text{conc}}, \epsilon_{\text{cent}}, \phi)$$

$$\text{Concrete}_\sigma := \text{Conc}_\sigma(\epsilon_{o,\text{conc}}, \epsilon_{\text{cent}}, \phi)$$

Maximum compressive strain in concrete

$$\epsilon_{\text{max,comp}} := \frac{\text{Concrete}_\epsilon_{\text{ConcNum}} - \text{Concrete}_\epsilon_{\text{ConcNum-1}}}{\text{Conc}_y_{\text{ConcNum}} - \text{Conc}_y_{\text{ConcNum-1}}} \cdot \left(\frac{h}{2} - \text{Conc}_y_{\text{ConcNum-1}} \right) + \text{Concrete}_\epsilon_{\text{ConcNum-1}} \dots = -3.453 \times 10^{-4}$$

Maximum compressive stress in concrete

$$\sigma_{\text{max,comp}} := \text{MAT}_{\text{conc}}(\epsilon_{\text{max,comp}}) = -1.077 \cdot \text{ksi}$$

F9. TABLES

Table F1: Stress in rebars at critical locations of CEVA structure subjected to LC1

Component	Item	Total demands for sustained load (In Situ condition, LC1)		Total stress in steel (ksi)		Maximum compressive stress in concrete (ksi)
		Demand	Location	Rebar 1	Rebar 2	
Base slab	Out-of-plane moment (kip-ft/ft)	64.5*	Base slab at Area 3	32.8	5.1	-0.89
	Axial force (kip/ft)	1.74*				

**These demands are computed conservatively by including OBE and dividing the total factor demand by the minimum load factor in the load combination in the original design calculation.*

Table F2: Stress in rebars at critical locations of CEVA structure subjected to LC2

Component	Item	Total demands for sustained load (In Situ condition, LC1)		Total stress in steel (ksi)		Maximum compressive stress in concrete (ksi)
		Demand	Location	Rebar 1	Rebar 2	
Base slab	Out-of-plane moment (kip-ft/ft)	83.7	Base slab at Area 3	44.0	20.6	-1.08
	Axial force (kip/ft)	1.74				

Example in Section F8

F10. FIGURES

There are no figures.



APPENDIX G

TENSILE STRESS IN REBARS OF STAGE 1 ELECTRICAL MANHOLES

G1. REVISION HISTORY

Revision 0: Initial document.

Revision 1: Revised pages G-1 and G-2 from Revision 0 to 1 to update references of calculation revision from A to 0. Revised page G-1 to update Revision history section.

G2. OBJECTIVE OF CALCULATION

The objective of this calculation is to compute the maximum tensile stress that can form in the rebars of the Stage 1 Electrical Manhole (EMH) structures.

G3. RESULTS AND CONCLUSIONS

Table G1 summarizes the tensile stress in rebars of the EMH calculated at critical locations. The maximum tensile stress is 27 ksi in EMH W13/W15 subjected to the second in situ load combination (LC2).

G4. DESIGN DATA / CRITERIA

See Section 4 of the calculation main body (Calc. 160268-CA-12 Rev. 0).

G5. ASSUMPTIONS

G5.1 Justified assumptions

There are no justified assumptions.

G5.2 Unverified assumptions

There are no unverified assumptions.

G6. METHODOLOGY

The critical demands that control rebar tension in the Stage 1 EMH are horizontal moment and horizontal tension in EMH W13 and W15. Finite element analyses were conducted to calculate the axial force and bending moment at these locations due to ASR load [G1].

To calculate the stress in rebars subjected to a combination of axial force and bending moment, sectional analysis based on fiber section method, as explained in calculation main body, is used. The calculation is conducted per 1 foot width of the walls, and each section is discretized into 20 fibers. An example calculation that evaluates the stress in the horizontal rebars in the walls of EMH W13 and W15 is presented in Section G8. The ASR expansion of the EMH is included in the analysis to find the initial stress state due to internal ASR alone.

G7. REFERENCES

- [G1] Simpson Gumpertz & Heger Inc., *Evaluation of Seismic Category I Electrical Manholes – Stage 1*, 160268-CA-12 Rev. 0, Waltham, MA, Jan 2018.
- [G2] United Engineers & Constructors Inc., Seabrook Station Structural Design Drawings.

G8. COMPUTATION

G8.1. Strain in Steel and Concrete due to Internal ASR expansion

Input Data

ASR expansion

Measured crack index	$\epsilon_{CI} := 0.25 \frac{\text{mm}}{\text{m}}$
Threshold factor	$F_{thr} := 3.7$

Material properties

Compressive strength of concrete	$f_c := -3\text{ksi}$	Ref. [G1]
Young's modulus of concrete	$E_c := 3120\text{ksi}$	
Yield strength of steel	$f_y := 60\text{ksi}$	
Young's modulus of steel	$E_s := 29000\text{ksi}$	

Geometry

Width of fibers	$b := 12\text{in}$	Ref. [G2]
Total thickness or height	$h := 18\text{in}$	
Area of concrete	$A_c := b \cdot h = 216 \cdot \text{in}^2$	
Area of tensile reinforcement (#6@12 in.)	$A_s := 0.44\text{in}^2$	
Number of reinforcement in row, e.g. equal to 2 for tensile and compressive	$\text{Steel}_{\text{Num}} := 2$	
Depth to reinforcement	$d := 15.625\text{in}$	

Finding the strain in steel and concrete by satisfying compatibility and equilibrium

	Initial Guess
Initial mechanical strain in concrete	$\epsilon_{o,\text{conc}} := 0$
Initial strain in steel	$\epsilon_{o,\text{steel}} := 0$
	Given
Compatibility equation	$F_{thr} \cdot \epsilon_{CI} = \epsilon_{o,\text{steel}} - \epsilon_{o,\text{conc}}$
Equilibrium equation	$(E_c \cdot A_c) \cdot \epsilon_{o,\text{conc}} + (E_s \cdot A_s \cdot \text{Steel}_{\text{Num}}) \cdot \epsilon_{o,\text{steel}} = 0$
	$\text{ans} := \text{Find}(\epsilon_{o,\text{conc}}, \epsilon_{o,\text{steel}})$

Initial strain in concrete and steel

$$\epsilon_{0,conc} := \text{ans}_1 = -3.375 \times 10^{-5}$$

$$\epsilon_{0,steel} := \text{ans}_2 = 8.913 \times 10^{-4}$$

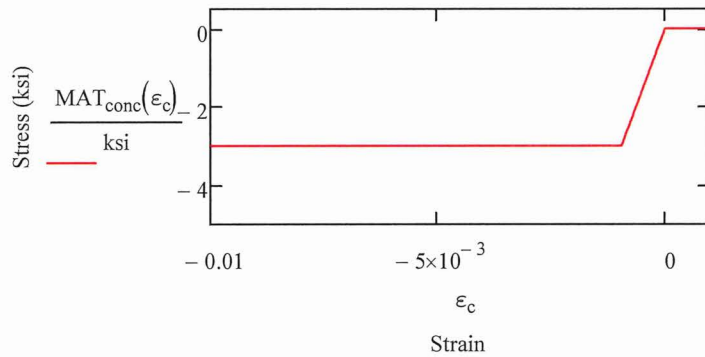
G8.2. Sectional Analysis

Input Data

Concrete Material Model

Constitutive model for concrete

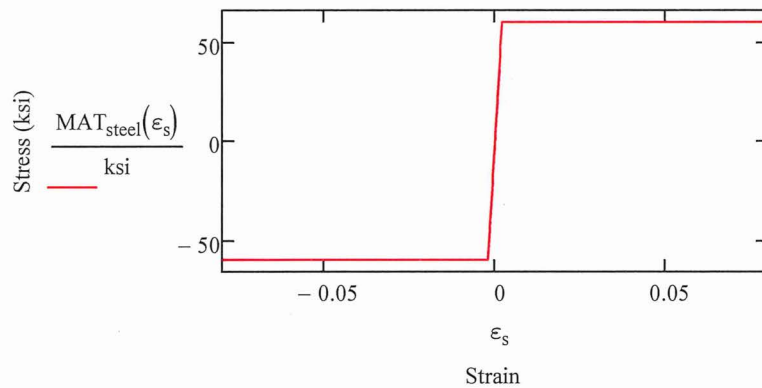
$$\text{MAT}_{\text{conc}}(\epsilon) := \begin{cases} 0 & \text{if } \epsilon > 0 \\ f_c & \text{if } \epsilon < \frac{f_c}{E_c} \\ (E_c \cdot \epsilon) & \text{otherwise} \end{cases}$$



Steel Material Model

Constitutive model for steel

$$\text{MAT}_{\text{steel}}(\epsilon) := \begin{cases} f_y & \text{if } \epsilon > \frac{f_y}{E_s} \\ -f_y & \text{if } \epsilon < \frac{-f_y}{E_s} \\ (E_s \cdot \epsilon) & \text{otherwise} \end{cases}$$



Concrete Fibers

Number of fibers

$$\text{Conc}_{\text{Num}} := 20$$

Height of fibers

$$\text{Conc}_H := \frac{h}{\text{Conc}_{\text{Num}}} = 0.9 \cdot \text{in}$$

Concrete fiber coordinates

$$\text{Conc}_y := \left| \begin{array}{l} \text{for } i \in 1.. \text{Conc}_{\text{Num}} \\ \text{ans}_i \leftarrow -\frac{h}{2} + \frac{\text{Conc}_H}{2} + (i-1) \cdot \text{Conc}_H \\ \text{ans} \end{array} \right.$$

Concrete fiber strain

$$\text{Conc}_\epsilon(\epsilon_{0,\text{conc}}, \epsilon, \varphi) := \left| \begin{array}{l} \text{for } i \in 1.. \text{Conc}_{\text{Num}} \\ \text{ans}_i \leftarrow \epsilon_{0,\text{conc}} + \epsilon - \varphi \cdot \text{Conc}_{y_i} \\ \text{ans} \end{array} \right.$$

Concrete fiber stress

$$\text{Conc}_\sigma(\epsilon_{0,\text{conc}}, \epsilon, \varphi) := \left| \begin{array}{l} \text{for } i \in 1.. \text{Conc}_{\text{Num}} \\ \text{ans}_i \leftarrow \text{MAT}_{\text{conc}}(\text{Conc}_\epsilon(\epsilon_{0,\text{conc}}, \epsilon, \varphi)_i) \\ \text{ans} \end{array} \right.$$

Concrete fiber force

$$\text{Conc}_F(\epsilon_{0,\text{conc}}, \epsilon, \varphi) := \left| \begin{array}{l} \text{for } i \in 1.. \text{Conc}_{\text{Num}} \\ \text{ans}_i \leftarrow \text{Conc}_\sigma(\epsilon_{0,\text{conc}}, \epsilon, \varphi)_i \cdot (b \cdot \text{Conc}_H) \\ \text{ans} \end{array} \right.$$

Reinforcement/Steel fibers

Depth to reinforcement fiber

$$\text{Steel}_{y_1} := -\left(d - \frac{h}{2}\right) = -6.625 \cdot \text{in}$$

$$\text{Steel}_{y_2} := d - \frac{h}{2} = 6.625 \cdot \text{in}$$

Area of reinforcement fiber

$$\text{Steel}_{A_{s_1}} := A_s = 0.44 \cdot \text{in}^2$$

$$\text{Steel}_{A_{s_2}} := A_s = 0.44 \cdot \text{in}^2$$

Steel fiber strain

$$\text{Steel}_\epsilon(\epsilon_{0,\text{steel}}, \epsilon, \varphi) := \left| \begin{array}{l} \text{for } i \in 1.. \text{Steel}_{\text{Num}} \\ \text{ans}_i \leftarrow \epsilon_{0,\text{steel}} + \epsilon - \varphi \cdot \text{Steel}_{y_i} \\ \text{ans} \end{array} \right.$$

Steel fiber stress

$$\text{Steel}_\sigma(\epsilon_{0,\text{steel}}, \epsilon, \varphi) := \left| \begin{array}{l} \text{for } i \in 1.. \text{Steel}_{\text{Num}} \\ \text{ans}_i \leftarrow \text{MAT}_{\text{steel}}(\text{Steel}_\epsilon(\epsilon_{0,\text{steel}}, \epsilon, \varphi)_i) \\ \text{ans} \end{array} \right.$$

Steel fiber force

$$\text{Steel}_F(\epsilon_{0,\text{steel}}, \epsilon, \varphi) := \left| \begin{array}{l} \text{for } i \in 1.. \text{Steel}_{\text{Num}} \\ \text{ans}_i \leftarrow \text{Steel}_\sigma(\epsilon_{0,\text{steel}}, \epsilon, \varphi)_i \cdot \text{Steel}_{A_{s_i}} \\ \text{ans} \end{array} \right.$$

Initial Stress State

Initial stress in concrete

$$\text{Concrete}_{\sigma} := \text{Conc}_{\sigma}(\varepsilon_{o,\text{conc}}, 0, 0)$$

$$\text{Concrete}_{\sigma_1} = -0.105 \cdot \text{ksi}$$

Initial stress in steel

$$\text{Rebar}_{\sigma} := \text{Steel}_{\sigma}(\varepsilon_{o,\text{steel}}, 0, 0)$$

$$\text{Rebar}_{\sigma_1} = 25.846 \cdot \text{ksi}$$

Axial Equilibrium

$$\text{Force}(\varepsilon_{o,\text{conc}}, \varepsilon_{o,\text{steel}}, \varepsilon, \varphi) := \left| \begin{array}{l} \text{ans1} \leftarrow 0 \\ \text{for } i \in 1.. \text{Conc}_{\text{Num}} \\ \quad \text{ans1} \leftarrow \text{ans1} + \text{Conc}_F(\varepsilon_{o,\text{conc}}, \varepsilon, \varphi)_i \\ \text{ans2} \leftarrow 0 \\ \text{for } i \in 1.. \text{Steel}_{\text{Num}} \\ \quad \text{ans2} \leftarrow \text{ans2} + \text{Steel}_F(\varepsilon_{o,\text{steel}}, \varepsilon, \varphi)_i \\ \text{ans} \leftarrow \text{ans1} + \text{ans2} \end{array} \right.$$

Moment Equilibrium

$$\text{Moment}(\varepsilon_{o,\text{conc}}, \varepsilon_{o,\text{steel}}, \varepsilon, \varphi) := \left| \begin{array}{l} \text{ans1} \leftarrow 0 \\ \text{for } i \in 1.. \text{Conc}_{\text{Num}} \\ \quad \text{ans1} \leftarrow \text{ans1} + -1 \cdot \text{Conc}_F(\varepsilon_{o,\text{conc}}, \varepsilon, \varphi)_i \cdot \text{Conc}_{y_i} \\ \text{ans2} \leftarrow 0 \\ \text{for } i \in 1.. \text{Steel}_{\text{Num}} \\ \quad \text{ans2} \leftarrow \text{ans2} + -1 \cdot \text{Steel}_F(\varepsilon_{o,\text{steel}}, \varepsilon, \varphi)_i \cdot \text{Steel}_{y_i} \\ \text{ans} \leftarrow \text{ans1} + \text{ans2} \end{array} \right.$$

Solution

Known parameters

Axial force $P := -4.4 \text{ kip}$

Iteration

Curvature $\phi := 0.0000065 \cdot \frac{1}{\text{in}}$ Requires iteration

Solve for strain at centroid

Axial strain at centroid (initial guess) $x_0 := 0.0$

Axial force equilibrium $f(x) := \text{Force}(\epsilon_{o.\text{conc}}, \epsilon_{o.\text{steel}}, x, \phi) - P$
 $\epsilon_{\text{cent}} := \text{root}(f(x_0), x_0) = -4.655 \times 10^{-6}$

Sectional forces

$\text{Force}(\epsilon_{o.\text{conc}}, \epsilon_{o.\text{steel}}, \epsilon_{\text{cent}}, \phi) = -4.4 \text{ kip}$
 $\text{Moment}(\epsilon_{o.\text{conc}}, \epsilon_{o.\text{steel}}, \epsilon_{\text{cent}}, \phi) = 9.679 \cdot \text{kip} \cdot \text{ft}$

Stress and strain in concrete and steel

Steel fiber stress and strain

$$\text{Rebar}_\epsilon := \text{Steel}_\epsilon(\epsilon_{o.\text{steel}}, \epsilon_{\text{cent}}, \phi) = \begin{pmatrix} 9.297 \times 10^{-4} \\ 8.435 \times 10^{-4} \end{pmatrix}$$

$$\text{Rebar}_\sigma := \text{Steel}_\sigma(\epsilon_{o.\text{steel}}, \epsilon_{\text{cent}}, \phi) = \begin{pmatrix} 26.96 \\ 24.462 \end{pmatrix} \cdot \text{ksi}$$

$$\text{Steel}_F(\epsilon_{o.\text{steel}}, \epsilon_{\text{cent}}, \phi) = \begin{pmatrix} 11.862 \\ 10.763 \end{pmatrix} \cdot \text{kip}$$

$\text{Concrete}_y := \text{Conc}_y$

Concrete fiber stress and strain

$$\text{Concrete}_\epsilon := \text{Conc}_\epsilon(\epsilon_{o.\text{conc}}, \epsilon_{\text{cent}}, \phi)$$

$$\text{Concrete}_\sigma := \text{Conc}_\sigma(\epsilon_{o.\text{conc}}, \epsilon_{\text{cent}}, \phi)$$

Maximum compressive strain in concrete

$$\epsilon_{\text{max.comp}} := \frac{\text{Concrete}_\epsilon_{\text{ConcNum}} - \text{Concrete}_\epsilon_{\text{ConcNum}-1}}{\text{Conc}_y_{\text{ConcNum}} - \text{Conc}_y_{\text{ConcNum}-1}} \cdot \left(\frac{h}{2} - \text{Conc}_y_{\text{ConcNum}-1} \right) + \text{Concrete}_\epsilon_{\text{ConcNum}-1} \dots = -9.69 \times 10^{-5}$$

Maximum compressive stress in concrete

$$\sigma_{\text{max.comp}} := \text{MAT}_{\text{conc}}(\epsilon_{\text{max.comp}}) = -0.302 \cdot \text{ksi}$$

G9. TABLES

Table G1: Stress in rebars at critical locations of EMH subjected to LC1

Component	Item	Total demands for sustained load (In Situ condition, LC1)		Total stress in steel (ksi)		Maximum compressive stress in concrete (ksi)
		Demand	Location	Rebar 1	Rebar 2	
EMH W13/W15	Out-of-plane moment (kip-ft/ft)	7.4	W13/W15 wall	11.2	5.6	-0.28
	Axial force (kip/ft)	-3.2				

Table G2: Stress in rebars at critical locations of EMH subjected to LC2

Component	Item	Total demands for sustained loads plus OBE amplified with threshold factor (In Situ condition, LC2)		Total stress in steel (ksi)		Maximum compressive stress in concrete (ksi)
		Demand	Location	Rebar 1	Rebar 2	
EMH W13/W15	Out-of-plane moment (kip-ft/ft)	9.3	W13/W15 wall	27.0	24.5	-0.30
	Axial force (kip/ft)	-4.4				

Example in Section G8

G10. FIGURES

There are no figures.



APPENDIX H

EVALUATING THE PERFORMANCE OF A SIMPLE ELASTO-PLASTIC MATERIAL MODEL FOR CONCRETE TO BE USED FOR EVALUATION OF REBAR STRESS

H1. REVISION HISTORY

Revision 0: Initial document.

H2. OBJECTIVE OF CALCULATION

The objective of this calculation is to compare the rebar stresses computed by using two different constitutive models for concrete, and justify the simple material model provides a satisfactory results.

H3. RESULTS AND CONCLUSIONS

The stress in rebars are computed using two constitutive models for concrete. The stress in rebars obtained using both models are very close indicating the simple model captures the concrete behavior satisfactorily. This is due to steel ratios in the components of Seabrook structures which is less than the maximum ratio allowed by the code. Therefore concrete crushing and post-linear response of the concrete does not impact the response noticeably.

CRMAI:

- Stress in Rebar 1: 39.1 (simple model, Appendix A) and 39.01 (accurate model)
- Stress in Rebar 2: 37.3 (simple model, Appendix A) and 37.16 (accurate model)
- Stress in concrete: -0.33 (simple model, Appendix A) and -0.328 (accurate model)

CEHMS:

- Stress in Rebar 1: 41.6 (simple model, Appendix E) and 42.1 (accurate model)
- Stress in Rebar 2: 20.8 (simple model, Appendix E) and 19.3 (accurate model)
- Stress in concrete: -1.5 (simple model, Appendix E) and -1.4 (accurate model)

H4. DESIGN DATA / CRITERIA

There are no design data.

H5. ASSUMPTIONS

H5.1 Justified assumptions

There are no justified assumptions.

H5.2 Unverified assumptions

There are no unverified assumptions.

H6. METHODOLOGY

Stress in rebars at the base mat of CRMAI and at the east wing wall of CEHMS structures are computed using a more accurate constitutive model of Kent and Park [H4] in compression, and the results are compared with the stresses obtained from the simple model as explained in the main body. The stresses in rebars from the simple model are provided in Appendix A and E for CRMAI and CEHMS structures respectively. Section H8 provides a sample calculation for the base mat of CRMAI structures.

H7. REFERENCES

- [H1] Simpson Gumpertz & Heger Inc., *Evaluation of Control Room Makeup Air Intake structure*, 160268-CA-08 Rev. 0, Waltham, MA, May 2017.
- [H2] United Engineers & Constructors Inc., *Seabrook Station Structural Design Drawings*.
- [H3] United Engineers & Constructors Inc., *Design of Makeup Air Intake Structure, MT-28-Calc Rev. 2*, Feb. 1984.
- [H4] Dudley. C. Kent, and Robert Park, Flexural members with confined concrete, *ASCE Journal of Structural Division*, 97 (ST7), 1969-1990, 1971.

H8. COMPUTATION

H8.1. Strain in Steel and Concrete due to Internal ASR expansion

Input Data

ASR expansion

Measured crack index	$\epsilon_{CI} := 0.99 \frac{\text{mm}}{\text{m}}$
Threshold factor	$F_{thr} := 1.4$

Material properties

Compressive strength of concrete	$f_c := -3\text{ksi}$	Ref. [H1]
Young's modulus of concrete	$E_c := 3120\text{ksi}$	

Yield strength of steel $f_y := 60\text{ksi}$
 Young's modulus of steel $E_s := 29000\text{ksi}$

Geometry

Width of fibers $b := 12\text{in}$ Ref. [H2]
 Total thickness or height $h := 36\text{in}$
 Area of concrete $A_c := b \cdot h = 432 \cdot \text{in}^2$
 Area of tensile reinforcement (#8@12 in.) $A_s := 0.79\text{in}^2$
 Number of reinforcement in row, e.g. equal to 2 for tensile and compressive $\text{Steel}_{\text{Num}} := 2$
 Depth to reinforcement $d := 32.5\text{in}$

Finding the strain in steel and concrete by satisfying compatibility and equilibrium

Initial Guess
 Initial mechanical strain in concrete $\epsilon_{o,\text{conc}} := 0$
 Initial strain in steel $\epsilon_{o,\text{steel}} := 0$
 Given
 Compatibility equation $F_{\text{thr}} \cdot \epsilon_{\text{Cl}} = \epsilon_{o,\text{steel}} - \epsilon_{o,\text{conc}}$
 Equilibrium equation $(E_c \cdot A_c) \cdot \epsilon_{o,\text{conc}} + (E_s \cdot A_s \cdot \text{Steel}_{\text{Num}}) \cdot \epsilon_{o,\text{steel}} = 0$
 $\text{ans} := \text{Find}(\epsilon_{o,\text{conc}}, \epsilon_{o,\text{steel}})$
 Initial strain in concrete and steel
 $\epsilon_{o,\text{conc}} := \text{ans}_1 = -4.557 \times 10^{-5}$
 $\epsilon_{o,\text{steel}} := \text{ans}_2 = 1.34 \times 10^{-3}$

H8.2. Sectional Analysis

Input Data

Concrete Material Model

Kent & Park Model

Strain at Peak compressive strength $\epsilon_{c0} := -0.002$

Strain at 50% compressive strength

$$\epsilon_{50u} := \frac{3 - 0.002 \cdot \frac{f_c}{\text{psi}}}{\frac{f_c}{\text{psi}} + 1000} = -4.5 \times 10^{-3}$$

Model parameter

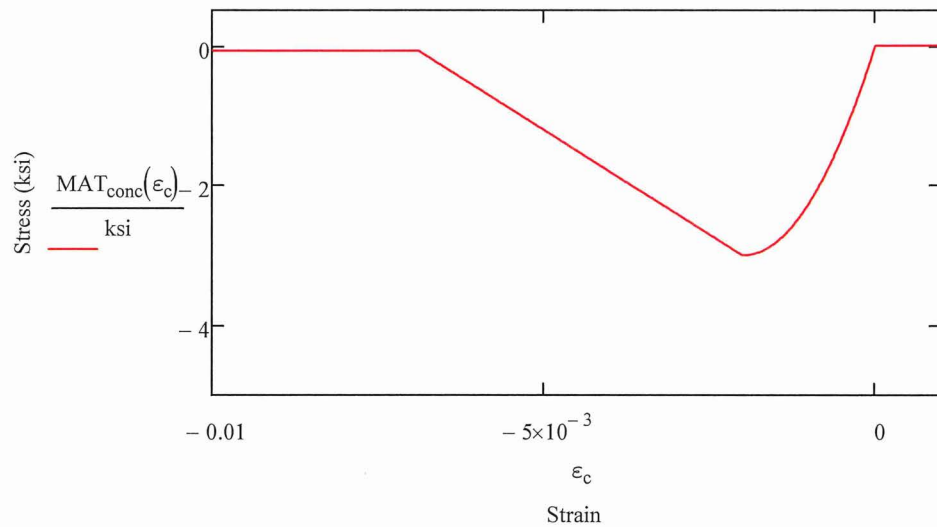
$$Z := \frac{0.5}{\epsilon_{50u} - \epsilon_{c0}} = -200$$

Residual compressive strength

$$f_{c.res} := f_c \cdot 0.025 = -75 \text{ psi}$$

Constitutive model for concrete

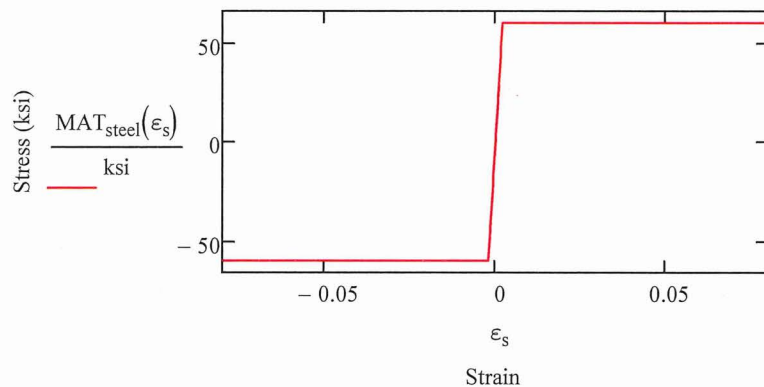
$$MAT_{conc}(\epsilon) := \begin{cases} \min[f_{c.res}, f_c \cdot [1 - Z \cdot (\epsilon - \epsilon_{c0})]] & \text{if } \epsilon < \epsilon_{c0} \\ f_c \cdot \left[\frac{2 \cdot \epsilon}{\epsilon_{c0}} - \left(\frac{\epsilon}{\epsilon_{c0}} \right)^2 \right] & \text{if } \epsilon_{c0} \leq \epsilon < 0 \\ 0 & \text{if } 0 \leq \epsilon \end{cases}$$



Steel Material Model

Constitutive model for steel

$$MAT_{steel}(\epsilon) := \begin{cases} f_y & \text{if } \epsilon > \frac{f_y}{E_s} \\ -f_y & \text{if } \epsilon < \frac{-f_y}{E_s} \\ (E_s \cdot \epsilon) & \text{otherwise} \end{cases}$$



Concrete Fibers

Number of fibers	$Conc_{Num} := 20$
Height of fibers	$Conc_H := \frac{h}{Conc_{Num}} = 1.8 \cdot \text{in}$
Concrete fiber coordinates	$Conc_y := \left \begin{array}{l} \text{for } i \in 1..Conc_{Num} \\ \text{ans}_i \leftarrow \frac{h}{2} + \frac{Conc_H}{2} + (i-1) \cdot Conc_H \\ \text{ans} \end{array} \right.$
Concrete fiber strain	$Conc_\epsilon(\epsilon_{o,conc}, \epsilon, \varphi) := \left \begin{array}{l} \text{for } i \in 1..Conc_{Num} \\ \text{ans}_i \leftarrow \epsilon_{o,conc} + \epsilon - \varphi \cdot Conc_{y_i} \\ \text{ans} \end{array} \right.$
Concrete fiber stress	$Conc_\sigma(\epsilon_{o,conc}, \epsilon, \varphi) := \left \begin{array}{l} \text{for } i \in 1..Conc_{Num} \\ \text{ans}_i \leftarrow MAT_{conc}(Conc_\epsilon(\epsilon_{o,conc}, \epsilon, \varphi)_i) \\ \text{ans} \end{array} \right.$
Concrete fiber force	$Conc_F(\epsilon_{o,conc}, \epsilon, \varphi) := \left \begin{array}{l} \text{for } i \in 1..Conc_{Num} \\ \text{ans}_i \leftarrow Conc_\sigma(\epsilon_{o,conc}, \epsilon, \varphi)_i \cdot (b \cdot Conc_H) \\ \text{ans} \end{array} \right.$

Reinforcement/Steel fibers

Depth to reinforcement fiber	$Steel_{y_1} := -\left(d - \frac{h}{2}\right) = -14.5 \cdot \text{in}$ $Steel_{y_2} := d - \frac{h}{2} = 14.5 \cdot \text{in}$
Area of reinforcement fiber	$Steel_{As_1} := A_s = 0.79 \cdot \text{in}^2$ $Steel_{As_2} := A_s = 0.79 \cdot \text{in}^2$
Steel fiber strain	$Steel_\epsilon(\epsilon_{o,steel}, \epsilon, \varphi) := \left \begin{array}{l} \text{for } i \in 1..Steel_{Num} \\ \text{ans}_i \leftarrow \epsilon_{o,steel} + \epsilon - \varphi \cdot Steel_{y_i} \\ \text{ans} \end{array} \right.$
Steel fiber stress	$Steel_\sigma(\epsilon_{o,steel}, \epsilon, \varphi) := \left \begin{array}{l} \text{for } i \in 1..Steel_{Num} \\ \text{ans}_i \leftarrow MAT_{steel}(Steel_\epsilon(\epsilon_{o,steel}, \epsilon, \varphi)_i) \\ \text{ans} \end{array} \right.$
Steel fiber force	$Steel_F(\epsilon_{o,steel}, \epsilon, \varphi) := \left \begin{array}{l} \text{for } i \in 1..Steel_{Num} \\ \text{ans}_i \leftarrow Steel_\sigma(\epsilon_{o,steel}, \epsilon, \varphi)_i \cdot Steel_{As_i} \\ \text{ans} \end{array} \right.$

Initial Stress State

Initial stress in concrete

$$\text{Concrete}_{\sigma} := \text{Conc}_{\sigma}(\epsilon_{o,\text{conc}}, 0, 0)$$

$$\text{Concrete}_{\sigma_1} = -0.135 \cdot \text{ksi}$$

Initial stress in steel

$$\text{Rebar}_{\sigma} := \text{Steel}_{\sigma}(\epsilon_{o,\text{steel}}, 0, 0)$$

$$\text{Rebar}_{\sigma_1} = 38.873 \cdot \text{ksi}$$

Axial Equilibrium

$$\text{Force}(\epsilon_{o,\text{conc}}, \epsilon_{o,\text{steel}}, \epsilon, \varphi) := \left| \begin{array}{l} \text{ans1} \leftarrow 0 \\ \text{for } i \in 1.. \text{ConcNum} \\ \quad \text{ans1} \leftarrow \text{ans1} + \text{Conc}_F(\epsilon_{o,\text{conc}}, \epsilon, \varphi)_i \\ \text{ans2} \leftarrow 0 \\ \text{for } i \in 1.. \text{SteelNum} \\ \quad \text{ans2} \leftarrow \text{ans2} + \text{Steel}_F(\epsilon_{o,\text{steel}}, \epsilon, \varphi)_i \\ \text{ans} \leftarrow \text{ans1} + \text{ans2} \end{array} \right.$$

Moment Equilibrium

$$\text{Moment}(\epsilon_{o,\text{conc}}, \epsilon_{o,\text{steel}}, \epsilon, \varphi) := \left| \begin{array}{l} \text{ans1} \leftarrow 0 \\ \text{for } i \in 1.. \text{ConcNum} \\ \quad \text{ans1} \leftarrow \text{ans1} + -1 \cdot \text{Conc}_F(\epsilon_{o,\text{conc}}, \epsilon, \varphi)_i \cdot \text{Conc}_{y_i} \\ \text{ans2} \leftarrow 0 \\ \text{for } i \in 1.. \text{SteelNum} \\ \quad \text{ans2} \leftarrow \text{ans2} + -1 \cdot \text{Steel}_F(\epsilon_{o,\text{steel}}, \epsilon, \varphi)_i \cdot \text{Steel}_{y_i} \\ \text{ans} \leftarrow \text{ans1} + \text{ans2} \end{array} \right.$$

Solution

Known parameters

Axial force $P := -32.3 \text{ kip}$

Iteration

Curvature $\phi := 0.0000022 \cdot \frac{1}{\text{in}}$ Requires iteration

Solve for strain at centroid

Axial strain at centroid (initial guess) $x_0 := 0.0$

Axial force equilibrium $f(x) := \text{Force}(\epsilon_{o.\text{conc}}, \epsilon_{o.\text{steel}}, x, \phi) - P$
 $\epsilon_{\text{cent}} := \text{root}(f(x_0), x_0) = -2.724 \times 10^{-5}$

Sectional forces

$\text{Force}(\epsilon_{o.\text{conc}}, \epsilon_{o.\text{steel}}, \epsilon_{\text{cent}}, \phi) = -32.3 \cdot \text{kip}$
 $\text{Moment}(\epsilon_{o.\text{conc}}, \epsilon_{o.\text{steel}}, \epsilon_{\text{cent}}, \phi) = 26.431 \cdot \text{kip} \cdot \text{ft}$

Stress and strain in concrete and steel

Steel fiber stress and strain

$$\text{Rebar}_\epsilon := \text{Steel}_\epsilon(\epsilon_{o.\text{steel}}, \epsilon_{\text{cent}}, \phi) = \begin{pmatrix} 1.345 \times 10^{-3} \\ 1.281 \times 10^{-3} \end{pmatrix}$$

$$\text{Rebar}_\sigma := \text{Steel}_\sigma(\epsilon_{o.\text{steel}}, \epsilon_{\text{cent}}, \phi) = \begin{pmatrix} 39.008 \\ 37.158 \end{pmatrix} \cdot \text{ksi}$$

$$\text{Steel}_F(\epsilon_{o.\text{steel}}, \epsilon_{\text{cent}}, \phi) = \begin{pmatrix} 30.816 \\ 29.354 \end{pmatrix} \cdot \text{kip}$$

$$\text{Concrete}_y := \text{Conc}_y$$

Concrete fiber stress and strain

$$\text{Concrete}_\epsilon := \text{Conc}_\epsilon(\epsilon_{o.\text{conc}}, \epsilon_{\text{cent}}, \phi)$$

$$\text{Concrete}_\sigma := \text{Conc}_\sigma(\epsilon_{o.\text{conc}}, \epsilon_{\text{cent}}, \phi)$$

Maximum compressive strain in concrete

$$\epsilon_{\text{max.comp}} := \frac{\text{Concrete}_\epsilon_{\text{ConcNum}} - \text{Concrete}_\epsilon_{\text{ConcNum-1}}}{\text{Conc}_y_{\text{ConcNum}} - \text{Conc}_y_{\text{ConcNum-1}}} \cdot \left(\frac{h}{2} - \text{Conc}_y_{\text{ConcNum-1}} \right) + \text{Concrete}_\epsilon_{\text{ConcNum-1}} \dots = -1.124 \times 10^{-4}$$

Maximum compressive stress in concrete

$$\sigma_{\text{max.comp}} := \text{MAT}_{\text{conc}}(\epsilon_{\text{max.comp}}) = -0.328 \cdot \text{ksi}$$

H9. TABLES

There are no tables.

H10. FIGURES

There are no figures.



APPENDIX I

TENSILE STRESS IN REBARS OF WEST PIPE CHASE STRUCTURE

11. REVISION HISTORY

Revision 0: Initial document.

Revision 1: Revised pages I-1 and I-2 from Revision 0 to 1 to update references of calculations revision from A to 0. Revised I-1 to update Revision history section.

12. OBJECTIVE OF CALCULATION

The objective of this calculation is to compute the maximum tensile stress that can form in the rebars of the West Pipe Chase (WPC) structure.

13. RESULTS AND CONCLUSIONS

Table I1 summarizes the tensile stress in rebars of the WPC structure calculated at critical locations. The Maximum tensile stress is 44 ksi at the base of the WPC north wall subjected to the second in situ load combination (LC2).

14. DESIGN DATA / CRITERIA

See Section 4 of the calculation main body (Calc. 170443-CA-04 Rev. 0).

15. ASSUMPTIONS

15.1 Justified assumptions

There are no justified assumptions.

15.2 Unverified assumptions

There are no unverified assumptions.

16. METHODOLOGY

The critical demands that control rebar tension in the WPC structure are horizontal moment and horizontal tension near the base of the WPC north wall. Finite element analyses were conducted to calculate the axial force and bending moment at these locations due to ASR load [11].

To calculate the stress in rebars subjected to a combination of axial force and bending moment, sectional analysis based on fiber section method, as explained in calculation main body, is used. The calculation is conducted per 1 foot width of the walls, and each section is discretized into 20 fibers. An example calculation that evaluates the stress in the horizontal rebars at the base of the WPC north wall is presented in Section I8. The ASR expansion of the WPC north wall is included in the analysis to find the initial stress state due to internal ASR alone.

17. REFERENCES

- [11] Simpson Gumpertz & Heger Inc., *Evaluation of the Main Steam and Feedwater West Pipe Chase and Personnel Hatch Structures*, 170443-CA-04 Rev. 0, Waltham, MA, Jan 2018.
- [12] United Engineers & Constructors Inc., *Seabrook Station Structural Design Drawings*.
- [13] United Engineers & Constructors Inc., *Analysis and Design of MS&FW Pipe Chase - West*, EM-20, Rev. 7, February 1986

18. COMPUTATION

18.1. Strain in Steel and Concrete due to Internal ASR expansion

Input Data

ASR expansion

Measured crack index	$\epsilon_{CI} := 0.24 \frac{\text{mm}}{\text{m}}$
Threshold factor	$F_{thr} := 1.0$

Material properties

Compressive strength of concrete	$f_c := -3\text{ksi}$	Ref. [1]
Young's modulus of concrete	$E_c := 3120\text{ksi}$	
Yield strength of steel	$f_y := 60\text{ksi}$	
Young's modulus of steel	$E_s := 29000\text{ksi}$	

Geometry

Width of fibers	$b := 12\text{in}$	Ref. [2]
Total thickness or height	$h := 24\text{in}$	
Area of concrete	$A_c := b \cdot h = 288 \cdot \text{in}^2$	
Area of tensile reinforcement (#11@12 in.)	$A_s := 1.56\text{in}^2$	
Number of reinforcement in row, e.g. equal to 2 for tensile and compressive	$\text{Steel}_{\text{Num}} := 2$	
Depth to reinforcement	$d := 20.3\text{in}$	

Finding the strain in steel and concrete by satisfying compatibility and equilibrium

	Initial Guess
Initial mechanical strain in concrete	$\epsilon_{o,\text{conc}} := 0$
Initial strain in steel	$\epsilon_{o,\text{steel}} := 0$
	Given
Compatibility equation	$F_{thr} \cdot \epsilon_{CI} = \epsilon_{o,\text{steel}} - \epsilon_{o,\text{conc}}$
Equilibrium equation	$(E_c \cdot A_c) \cdot \epsilon_{o,\text{conc}} + (E_s \cdot A_s \cdot \text{Steel}_{\text{Num}}) \cdot \epsilon_{o,\text{steel}} = 0$
	$\text{ans} := \text{Find}(\epsilon_{o,\text{conc}}, \epsilon_{o,\text{steel}})$

Initial strain in concrete and steel

$$\epsilon_{0,\text{conc}} := \text{ans}_1 = -2.196 \times 10^{-5}$$

$$\epsilon_{0,\text{steel}} := \text{ans}_2 = 2.18 \times 10^{-4}$$

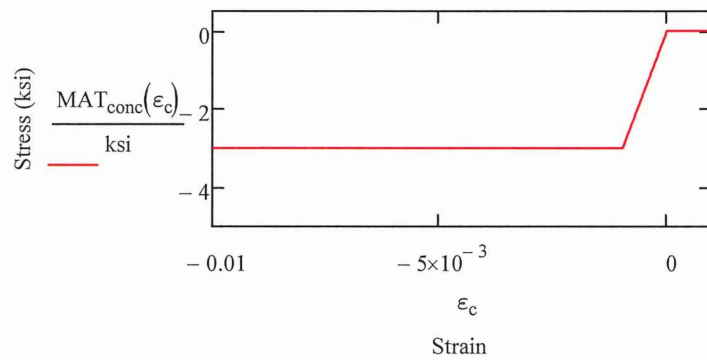
18.2. Sectional Analysis

Input Data

Concrete Material Model

Constitutive model for concrete

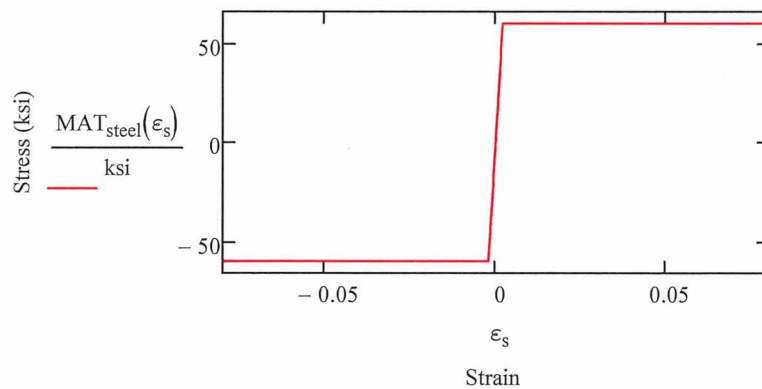
$$\text{MAT}_{\text{conc}}(\epsilon) := \begin{cases} 0 & \text{if } \epsilon > 0 \\ f_c & \text{if } \epsilon < \frac{f_c}{E_c} \\ (E_c \cdot \epsilon) & \text{otherwise} \end{cases}$$



Steel Material Model

Constitutive model for steel

$$\text{MAT}_{\text{steel}}(\epsilon) := \begin{cases} f_y & \text{if } \epsilon > \frac{f_y}{E_s} \\ -f_y & \text{if } \epsilon < \frac{-f_y}{E_s} \\ (E_s \cdot \epsilon) & \text{otherwise} \end{cases}$$



Concrete Fibers

Number of fibers

$$\text{Conc}_{\text{Num}} := 20$$

Height of fibers

$$\text{Conc}_H := \frac{h}{\text{Conc}_{\text{Num}}} = 1.2 \cdot \text{in}$$

Concrete fiber coordinates

$$\text{Conc}_y := \begin{cases} \text{for } i \in 1.. \text{Conc}_{\text{Num}} \\ \text{ans}_i \leftarrow -\frac{h}{2} + \frac{\text{Conc}_H}{2} + (i-1) \cdot \text{Conc}_H \\ \text{ans} \end{cases}$$

Concrete fiber strain

$$\text{Conc}_\varepsilon(\varepsilon_{o.\text{conc}}, \varepsilon, \varphi) := \begin{cases} \text{for } i \in 1.. \text{Conc}_{\text{Num}} \\ \text{ans}_i \leftarrow \varepsilon_{o.\text{conc}} + \varepsilon - \varphi \cdot \text{Conc}_{y_i} \\ \text{ans} \end{cases}$$

Concrete fiber stress

$$\text{Conc}_\sigma(\varepsilon_{o.\text{conc}}, \varepsilon, \varphi) := \begin{cases} \text{for } i \in 1.. \text{Conc}_{\text{Num}} \\ \text{ans}_i \leftarrow \text{MAT}_{\text{conc}}(\text{Conc}_\varepsilon(\varepsilon_{o.\text{conc}}, \varepsilon, \varphi)_i) \\ \text{ans} \end{cases}$$

Concrete fiber force

$$\text{Conc}_F(\varepsilon_{o.\text{conc}}, \varepsilon, \varphi) := \begin{cases} \text{for } i \in 1.. \text{Conc}_{\text{Num}} \\ \text{ans}_i \leftarrow \text{Conc}_\sigma(\varepsilon_{o.\text{conc}}, \varepsilon, \varphi)_i \cdot (b \cdot \text{Conc}_H) \\ \text{ans} \end{cases}$$

Reinforcement/Steel fibers

Depth to reinforcement fiber

$$\text{Steel}_{y_1} := -\left(d - \frac{h}{2}\right) = -8.3 \cdot \text{in}$$

$$\text{Steel}_{y_2} := d - \frac{h}{2} = 8.3 \cdot \text{in}$$

Area of reinforcement fiber

$$\text{Steel}_{A_{s_1}} := A_s = 1.56 \cdot \text{in}^2$$

$$\text{Steel}_{A_{s_2}} := A_s = 1.56 \cdot \text{in}^2$$

Steel fiber strain

$$\text{Steel}_\varepsilon(\varepsilon_{o.\text{steel}}, \varepsilon, \varphi) := \begin{cases} \text{for } i \in 1.. \text{Steel}_{\text{Num}} \\ \text{ans}_i \leftarrow \varepsilon_{o.\text{steel}} + \varepsilon - \varphi \cdot \text{Steel}_{y_i} \\ \text{ans} \end{cases}$$

Steel fiber stress

$$\text{Steel}_\sigma(\varepsilon_{o.\text{steel}}, \varepsilon, \varphi) := \begin{cases} \text{for } i \in 1.. \text{Steel}_{\text{Num}} \\ \text{ans}_i \leftarrow \text{MAT}_{\text{steel}}(\text{Steel}_\varepsilon(\varepsilon_{o.\text{steel}}, \varepsilon, \varphi)_i) \\ \text{ans} \end{cases}$$

Steel fiber force

$$\text{Steel}_F(\varepsilon_{o.\text{steel}}, \varepsilon, \varphi) := \begin{cases} \text{for } i \in 1.. \text{Steel}_{\text{Num}} \\ \text{ans}_i \leftarrow \text{Steel}_\sigma(\varepsilon_{o.\text{steel}}, \varepsilon, \varphi)_i \cdot \text{Steel}_{A_{s_i}} \\ \text{ans} \end{cases}$$

Initial Stress State

Initial stress in concrete

$$\text{Concrete}_{\sigma} := \text{Conc}_{\sigma}(\epsilon_{o,\text{conc}}, 0, 0)$$

$$\text{Concrete}_{\sigma_1} = -0.069 \cdot \text{ksi}$$

Initial stress in steel

$$\text{Rebar}_{\sigma} := \text{Steel}_{\sigma}(\epsilon_{o,\text{steel}}, 0, 0)$$

$$\text{Rebar}_{\sigma_1} = 6.323 \cdot \text{ksi}$$

Axial Equilibrium

$$\text{Force}(\epsilon_{o,\text{conc}}, \epsilon_{o,\text{steel}}, \epsilon, \varphi) := \begin{array}{l} \text{ans1} \leftarrow 0 \\ \text{for } i \in 1.. \text{ConcNum} \\ \quad \text{ans1} \leftarrow \text{ans1} + \text{Conc}_F(\epsilon_{o,\text{conc}}, \epsilon, \varphi)_i \\ \text{ans2} \leftarrow 0 \\ \text{for } i \in 1.. \text{SteelNum} \\ \quad \text{ans2} \leftarrow \text{ans2} + \text{Steel}_F(\epsilon_{o,\text{steel}}, \epsilon, \varphi)_i \\ \text{ans} \leftarrow \text{ans1} + \text{ans2} \end{array}$$

Moment Equilibrium

$$\text{Moment}(\epsilon_{o,\text{conc}}, \epsilon_{o,\text{steel}}, \epsilon, \varphi) := \begin{array}{l} \text{ans1} \leftarrow 0 \\ \text{for } i \in 1.. \text{ConcNum} \\ \quad \text{ans1} \leftarrow \text{ans1} + -1 \cdot \text{Conc}_F(\epsilon_{o,\text{conc}}, \epsilon, \varphi)_i \cdot \text{Conc}_{y_i} \\ \text{ans2} \leftarrow 0 \\ \text{for } i \in 1.. \text{SteelNum} \\ \quad \text{ans2} \leftarrow \text{ans2} + -1 \cdot \text{Steel}_F(\epsilon_{o,\text{steel}}, \epsilon, \varphi)_i \cdot \text{Steel}_{y_i} \\ \text{ans} \leftarrow \text{ans1} + \text{ans2} \end{array}$$

Solution

Known parameters

Axial force $P := 19.1 \text{ kip}$

Iteration

Curvature $\phi := 0.0000024 \cdot \frac{1}{\text{in}}$ Requires iteration

Solve for strain at centroid

Axial strain at centroid (initial guess) $x_0 := 0.0$

Axial force equilibrium $f(x) := \text{Force}(\epsilon_{o,\text{conc}}, \epsilon_{o,\text{steel}}, x, \phi) - P$

$$\epsilon_{\text{cent}} := \text{root}(f(x_0), x_0) = 3.004 \times 10^{-5}$$

Sectional forces

$$\text{Force}(\epsilon_{o,\text{conc}}, \epsilon_{o,\text{steel}}, \epsilon_{\text{cent}}, \phi) = 19.1 \cdot \text{kip}$$

$$\text{Moment}(\epsilon_{o,\text{conc}}, \epsilon_{o,\text{steel}}, \epsilon_{\text{cent}}, \phi) = 3.784 \cdot \text{kip} \cdot \text{ft}$$

Stress and strain in concrete and steel

Steel fiber stress and strain

$$\text{Rebar}_\epsilon := \text{Steel}_\epsilon(\epsilon_{o,\text{steel}}, \epsilon_{\text{cent}}, \phi) = \begin{pmatrix} 2.68 \times 10^{-4} \\ 2.282 \times 10^{-4} \end{pmatrix}$$

$$\text{Rebar}_\sigma := \text{Steel}_\sigma(\epsilon_{o,\text{steel}}, \epsilon_{\text{cent}}, \phi) = \begin{pmatrix} 7.772 \\ 6.617 \end{pmatrix} \cdot \text{ksi}$$

$$\text{Steel}_F(\epsilon_{o,\text{steel}}, \epsilon_{\text{cent}}, \phi) = \begin{pmatrix} 12.124 \\ 10.322 \end{pmatrix} \cdot \text{kip}$$

$$\text{Concrete}_y := \text{Conc}_y$$

Concrete fiber stress and strain

$$\text{Concrete}_\epsilon := \text{Conc}_\epsilon(\epsilon_{o,\text{conc}}, \epsilon_{\text{cent}}, \phi)$$

$$\text{Concrete}_\sigma := \text{Conc}_\sigma(\epsilon_{o,\text{conc}}, \epsilon_{\text{cent}}, \phi)$$

Maximum compressive strain in concrete

$$\epsilon_{\text{max.comp}} := \frac{\text{Concrete}_\epsilon_{\text{ConcNum}} - \text{Concrete}_\epsilon_{\text{ConcNum}-1} \cdot \left(\frac{h}{2} - \text{Conc}_y_{\text{ConcNum}-1} \right)}{\text{Conc}_y_{\text{ConcNum}} - \text{Conc}_y_{\text{ConcNum}-1} + \text{Concrete}_\epsilon_{\text{ConcNum}-1}} \dots = -2.072 \times 10^{-5}$$

Maximum compressive stress in concrete

$$\sigma_{\text{max.comp}} := \text{MAT}_{\text{conc}}(\epsilon_{\text{max.comp}}) = -0.065 \cdot \text{ksi}$$

19. TABLES

Table I1: Stress in rebars at critical locations of WPC structure subjected to LC1

Component	Item	Total demands for sustained load (In Situ condition, LC1)		Total stress in steel (ksi)		Maximum compressive stress in concrete (ksi)
		Demand	Location	Rebar 1	Rebar 2	
WPC North Wall	Out-of-plane moment (kip-ft/ft)	3.8	Base of wall, horizontal direction	7.8	6.6	-0.07
	Axial force (kip/ft)	19.1				

Example in Section I8

Table I2: Stress in rebars at critical locations of WPC structure subjected to LC2

Component	Item	Total demands for sustained loads plus OBE amplified with threshold factor (In Situ condition, LC2)		Total stress in steel (ksi)		Maximum compressive stress in concrete (ksi)
		Demand	Location	Rebar 1	Rebar 2	
WPC North Wall	Out-of-plane moment (kip-ft/ft)	78.8	Base of wall, horizontal direction	44.4	8.0	-1.36
	Axial force (kip/ft)	34.4				

110. FIGURES

There are no figures.

APPENDIX J

COMPUTER RUN IDENTIFICATION LOG

Client: NextEra Energy Seabrook Page 1 of 4

Project: Evaluation of maximum stress in rebars of Seabrook structures

Project No.: 170444 Subcontract No.: N/A Calculation No.: RAI-D8 Attachment 2

Run No.	Title	Program/Ver. ^A	Hardware	Date	Files
1	CRMAI subjected to unfactored load (sustained loading) including ASR load	ANSYS 15.0 Structural	Cluster3g ^B	10/12/2017	Note C
2	CRMAI subjected to unfactored load (sustained loading) plus OBE including ASR load that has been amplified by threshold factor	ANSYS 15.0 Structural	Cluster3g ^B	10/12/2017	Note C
3	CEB Standard Case subjected to unfactored loads (sustained loading) including ASR and OBE. For OBE load case, ASR loads are amplified by threshold factor.	ANSYS 15.0 Structural	Cluster3g ^B	11/22/2017	Note C
4	CEB Standard-Plus Case subjected to unfactored loads (sustained loading) including ASR and OBE. For OBE load case, ASR loads are amplified by threshold factor.	ANSYS 15.0 Structural	Cluster3g ^B	11/22/2017	Note C
5	RHR subjected to unfactored sustained loads (i.e., non ASR loads), unfactored ASR loads, and unfactored seismic loads considering unit acceleration (i.e., 1 g).	ANSYS 15.0 Structural	Cluster3g ^B	10/12/2017	Note C
6	CSTE subjected to ASR load	ANSYS 15.0 Structural	Cluster3g ^B	11/11/2016	Note C

SIMPSON GUMPERTZ & HEGEREngineering of Structures
and Building EnclosuresPROJECT NO: 170444DATE: Dec. 2017CLIENT: NextEra Energy SeabrookBY: MR. M. GargariSUBJECT: Evaluation of maximum stress in rebars of Seabrook structuresVERIFIER: A.T. Sarawit

Run No.	Title	Program/Ver. ^A	Hardware	Date	Files
7	WPC/PH subjected to ASR load	ANSYS 15.0 Structural	Cluster3g ^B	11/09/2017	Note C

Notes:

- A ANSYS 15.0 Structural is QA verified
- B Cluster3g information is provided below:
Model: Compute Blade E55A2
Serial Number: 4600E70 T201000293
Manufacturer: American Megatrends Inc.
Operating System: Microsoft Windows NT Server 6.2 (x64)
- C Input and output files for ANSYS computer runs are listed in Table J1.

Table J1. Input and output files for ANSYS computer runs

Run No.	Input Files ^A	Output Files ^A
1	CRMAI_SUS.db ^B	CRMAI_SUS.rst
2	CRMAI_SUS_OBE.db ^B	CRMAI_SUS_OBE.rst
3	SR_Rebar_Stress_A10_r0.db ^B	SR_Rebar_Stress_A10_r0.lxx
4	SR_Rebar_Stress_B7_r0.db ^B	SR_Rebar_Stress_B7_r0.lxx
5	<u>Non ASR Loads</u>	<u>Non ASR Loads</u>
	<ul style="list-style-type: none"> • RHR_ILC_02.db • RHR_ILC_03.db • RHR_ILC_05.db • RHR_ILC_16.db 	<ul style="list-style-type: none"> • RHR_ILC_02.rst • RHR_ILC_03.rst • RHR_ILC_05.rst • RHR_ILC_16.rst
	<u>ASR Loads</u>	<u>ASR Loads</u>
	<ul style="list-style-type: none"> • RHR_ILC_09.db • RHR_ILC_10.db 	<ul style="list-style-type: none"> • RHR_ILC_09.rst • RHR_ILC_10.rst
	<u>Seismic 1g</u>	<u>Seismic 1g</u>
	<ul style="list-style-type: none"> • RHR_ILC_06.db • RHR_ILC_07.db • RHR_ILC_08.db • RHR_ILC_13.db • RHR_ILC_14.db 	<ul style="list-style-type: none"> • RHR_ILC_06.rst • RHR_ILC_07.rst • RHR_ILC_08.rst • RHR_ILC_13.rst • RHR_ILC_14.rst
6	CST_024.db ^C	CST_024.rst
7	WPC.db ^C	WPC.rst

Notes:

- A Input and output files are provided on RAI-Attachment-CD. File type descriptions are as follows.
 *.db = ANSYS database file containing the model (nodes, elements, properties, boundary conditions, loads, etc.).
 *.rst = ANSYS result file containing forces, moments, reactions, displacements, etc.
 *.lxx = ANSYS load case file containing forces, moments, reactions, displacements, and other structural response output for load cases and load combinations.
- B Each structure has been analyzed for two load combination as follows:
 • D + L + E + To + Sa (In-situ condition, LC1)
 • D + L + E + To + Eo + He + F_{THR}.Sa (In-situ condition plus seismic load, LC2)
- C Each structure is analyzed for ASR load only. The original design demands are extracted from original design calculation.
- D The description of the input and output files for Run No. 5 is following:
 RHR_ILC_02: Self-Weight;
 RHR_ILC_03: Hydrostatic Pressure Outside
 RHR_ILC_05: Live Load
 RHR_ILC_06: Seismic North-South with 1g acceleration
 RHR_ILC_07: Seismic East-West with 1g acceleration
 RHR_ILC_08: Seismic Vertical with 1g acceleration
 RHR_ILC_09: In structure ASR

SIMPSON GUMPERTZ & HEGER



Engineering of Structures
and Building Enclosures

PROJECT NO: 170444

DATE: Dec. 2017

CLIENT: NextEra Energy Seabrook

BY: MR. M. Gargari

SUBJECT: Evaluation of maximum stress in rebars of Seabrook structures

VERIFIER: A.T. Sarawit

- RHR_ILC_10: Concrete fill
- RHR_ILC_13: Seismic South-North with 1g acceleration
- RHR_ILC_14: Seismic West-East with 1g acceleration
- RHR_ILC_16: Backfill Soil Static Pressure

Enclosure 5 to SBK-L-18074

Simpson Gumpertz & Heger calculations supporting the response provided to RAI D10 regarding cracked section properties used for the evaluation of the RHR vault and Spent fuel pool walls.

CLIENT NextEra Energy SeabrookSUBJECT Verification of cracked section properties: RHR structurePROJECT NO. 170444DATE 31 May 2018BY Georgios TsamprasCHECKED BY MR. M. Gargari

Calculation attachment Flexural Cracking of 2 ft. thick east exterior wall

1.0 Revision History

Revision 0. Initial document.

2.0 Objective of Calculation

The objective of this calculation attachment is to verify current cracked section properties used for the evaluation of the Residual Heat Removal (RHR) structure east exterior wall when considering ASR loading pre-compressive effect on the cracking moment calculation and to determine if such results affect negatively the current results for the evaluation of the RHR.

3.0 Assumptions

No assumptions are considered in this calculation attachment.

4.0 Methodology

The highest demand-to-capacity (D/C) ratio in the RHR walls is reported at the east exterior wall due to interaction of horizontal axial compression and bending about the vertical axis (see Appendix E of 160268-CA-06 [1]). Therefore, RHR east exterior wall is selected for the verification.

In Appendix E of 160268-CA-06 [1] Section E6.4.1 the bending moment demand was calculated considering uncracked section properties for bending about the vertical axis. In Appendix E of 160268-CA-06 Section E6.4.3 [1] the effective moment of inertia of cracked concrete is calculated according to ACI318-14 Table 6.6.3.1.1(b) [2] considering the factored moment and axial load demands. The ratio of effective over gross moment of inertia calculated in Appendix E of 160268-CA-06 Section E6.4.3 [1] is compared with the ratio of effective over gross moment of inertia calculated considering the modified ACI 318-71 Eqn 9-4 [3, 4] including the compressive stress due to ASR expansion effects.

5.0 Results and Conclusions

The effective moment of inertia of cracked concrete calculated in Appendix E of 160268-CA-06 [1] Section E6.4.3 is equal to 35% of the gross moment of inertia of uncracked concrete. The effective moment of inertia of cracked concrete calculated using the modified ACI 318-71 Eqn 9-4 [3, 4] including the compressive stress due to ASR expansion effects is equal to 23% of the gross moment of inertia of uncracked concrete. Thus, the demands are expected to reduce when the modified ACI 318-71 Eqn 9-4 [3, 4] is used to calculate the effective moment of inertia. As a result, the evaluation of the RHR structure presented in 160268-CA-06 is conservative and it is not affected.

6.0 Computations


Below are the demands at the support of the East exterior wall - 2 ft thick wall between El. (-) 32 ft to (-) 40 ft with uncracked section properties in flexure about the vertical axis from Section E6.4.1 160268-CA-06 [1].

Horizontal axial load due to 1.0Sa	$N_{B01} := 4.8031E+02 \cdot \frac{\text{lb} \cdot \text{f}}{\text{in}}$
Horizontal axial load due to 1.4D+ 1.7L+1.7E	$N_{C02} := -5.6331E+03 \cdot \frac{\text{lb} \cdot \text{f}}{\text{in}}$
ASR effects load combination multiplier	$SFSa := 1.6$
Threshold factor	$k_{th} := 1.2$
Total horizontal axial load	$N_{sup_u_2} := N_{C02} + k_{th} \cdot SFSa \cdot N_{B01} = -4.7109 \times 10^3 \cdot \frac{\text{lb} \cdot \text{f}}{\text{in}}$
Bending Moment about the vertical axis due to 1.0Sa	$M_{B01} := -1.1382E+05 \cdot \frac{\text{lb} \cdot \text{f} \cdot \text{in}}{\text{in}}$
Bending Moment about the vertical axis due to 1.4D+ 1.7L+1.7E	$M_{C02} := -2.4120E+04 \cdot \frac{\text{lb} \cdot \text{f} \cdot \text{in}}{\text{in}}$
Total bending Moment about the vertical axis	$M_{sup_u_2} := M_{C02} + k_{th} \cdot SFSa \cdot M_{B01} = -242.6544 \cdot \text{kip} \cdot \frac{\text{ft}}{\text{ft}}$

Calculation of effective moment of inertia of cracked concrete using the modified ACI 318-71 Eqn 9-4 [3, 4] including the compressive stress due to ASR expansion effects.

Wall thickness	$t_w := 2 \text{ft}$
Gross moment of inertia of uncracked concrete	$I_g := \frac{t_w^3}{12} = 1.152 \times 10^3 \cdot \frac{\text{in}^4}{\text{in}}$
One foot long section width	$b := 12 \text{in}$
Compressive stress due to compressive load	$c := \frac{-N_{sup_u_2}}{b} = 392.5754 \text{psi}$
Concrete Strength	$f_c := 3000 \text{psi}$
Cracking stress	$f_r := 7.5 \cdot \sqrt{f_c} \text{psi} = 410.7919 \text{psi}$

Size of reinforcing bar in the wall at the section cut

$$A_{rb} :=$$


Reinforcing bar area

$$(A_{rb} \cdot \text{in}^2) = 0.79 \cdot \text{in}^2$$

Reinforcing bar spacing

$$(s_w := 9 \text{ in})$$

Total reinforcing bar area per length in the wall at the location of the section cut

$$A_s := \frac{(A_{rb} \cdot \text{in}^2)}{\frac{s}{b}} = 1.0533 \cdot \text{in}^2$$

Depth of concrete section

$$d := 20.5 \text{ in}$$

Steel modulus

$$E_s := 29000 \text{ ksi}$$

Concrete modulus

$$E_c := 57000 \cdot \sqrt{f_c} \cdot \text{psi}$$

Ratio of steel modulus over concrete modulus

$$\left(n := \frac{E_s}{E_c} = 9.2889 \right)$$

$$B := \frac{b}{n \cdot A_s} = 1.2265 \cdot \text{in}^{-1}$$

$$kd := \frac{(\sqrt{2 \cdot d \cdot B + 1} - 1)}{B} = 5.0237 \cdot \text{in}$$

Cracked moment of inertia

$$I_{cr} := \frac{\frac{b \cdot kd^3}{3} + n \cdot A_s \cdot (d - kd)^2}{b} = 237.5526 \cdot \frac{\text{in}^4}{\text{in}}$$

Cracking moment

$$M_{cr} := \frac{I_g \cdot (f_r + c)}{\frac{t_w}{2}} = 77.1233 \cdot \frac{\text{kip} \cdot \text{ft}}{\text{ft}}$$

Reference [4]

Effective cracked moment of inertia [ACI 318-71 Eqn 9-4] (defined as a function of M_a)

$$I_{crsup_MD} := \left(\frac{M_{cr}}{|M_{sup_u_2}|} \right)^3 \cdot I_g + \left[1 - \left(\frac{M_{cr}}{|M_{sup_u_2}|} \right)^3 \right] \cdot I_{cr} = 266.9122 \cdot \frac{\text{in}^4}{\text{in}}$$

$$\frac{I_{crsup_MD}}{I_g} = 0.2317$$

7.0 References

[1] Simpson Gumpertz & Heger Inc., Appendix E: Evaluation of Residual Heat Removal Equipment Vault, Report 160268-CA-06, August 2017, Waltham, Revision 0

[2] American Concrete Institute, Building Code Requirements for Structural Concrete and Commentary, ACI 318-14, 2014

[3] American Concrete Institute, Building Code Requirements for Structural Concrete and Commentary, ACI 318-71, 1972

[4] Simpson Gumpertz & Heger Inc., Methodology for the analysis of seismic category I structures with concrete affected by Alkali-Silica Reaction, Methodology Document 170444-MD-01, Waltham, Revision 1



Calculation Attachment Flexural Cracking of 6ft Thick SFP Walls

1.0 Revision History

Revision 0. Initial document.

2.0 Objective of Calculation

The objective of this calculation attachment is to verify the cracked section properties used for the evaluation of the Spent Fuel Pool (SFP) walls in the Fuel Storage Building (FSB) when taking into account the ASR pre-compression effect has on delaying the onset of flexural cracking and determine if such effect negatively impact the current FSB evaluation results.

3.0 Assumptions

No assumptions are considered in this calculation attachment.

4.0 Methodology

The highest demand-to-capacity (D/C) ratio in the SFP walls is reported at the north wall due to interaction of vertical axial compression and bending about the horizontal axis. This SFP north wall is selected for the verification. For completeness, cracked section properties of this SFP north wall due to interaction of horizontal axial compression and bending about the vertical axis are also verified. The highest D/C ratio due to bending about horizontal axis is 0.9 and corresponds to load combination C03 (Table 10, Calculation 160268-CA-09). The highest D/C ratio due to bending about vertical axis is 0.5 and corresponds to load combination C03. Load combination C03 considers an ASR load factor of 2.0 and a threshold factor of 1.2 to account for potential future ASR expansion.

Field inspection of accessible SFP walls show that they are already cracked. Cracking can be initiated by factors other than flexural loads, such as thermal gradients. Original design calculation for the SFP mat and walls uses fully-cracked moment of inertia (I_{cr}) for the calculation of demands due to thermal gradients in the SFP walls.

The ratio of I_{cr} to the gross moment of inertia (I_g) is 0.13 when evaluating bending about the horizontal axis. The ratios of the effective moment of inertia (I_e) to I_g corresponding to the un-cracked section moment due to operational and accidental thermal gradients are 0.15 and 0.14, respectively. The above results justify the use of I_{cr} in the original design calculation for the evaluation of temperature bending demands about the horizontal axis in the SFP walls.

The ratio of I_{cr} to I_g is 0.09 when evaluating bending about the vertical axis. The ratios of I_e to I_g corresponding to the un-cracked section moment due to operational and accidental thermal gradients are 0.11 and 0.10, respectively. The above results justify the use of I_{cr} in the original design calculation for the evaluation of temperature bending demands about the vertical axis in the SFP walls.

The evaluation of the SFP walls in CA-09 is performed based on a ratio of I_e to I_g of 0.25. To verify the use of this ratio, the cracking moment (M_{cr}) is re-calculated taking into account the ASR pre-compression effect has on delaying the onset of flexural cracking. The I_e to I_g ratio is then calculated based on this re-calculated M_{cr} for the un-cracked section moment due to operational and accidental thermal gradients.

5.0 Results and Conclusions

The ratios of I_e to I_g about the horizontal axis due to operational and accidental thermal gradients when taking into account the ASR loading pre-compressive effect due to load combination C03 are 0.16 and 0.15, respectively. These ratio values do not exceed the used ratio value of 0.25.

The ratios of I_e to I_g about the vertical axis due to operational and accidental thermal gradients when taking into account the ASR loading pre-compressive effect due to load combination C03 are 0.30 and 0.21, respectively. The ratio value due operational thermal gradient slightly exceed the used ratio value of 0.25. The associated current D/C ratio is 0.5. Section 6.3 estimates the corresponding D/C ratio when I_e/I_g has a value of 0.30. The moment demand is estimated by amplifying the current moment demand by the ratio of I_e/I_g value of 0.30 to I_e/I_g value of 0.25. The updated D/C ratio is calculated as 0.6.

Based on the above results, it is concluded that accounting for the ASR loading pre-compression effect in calculating the M_{cr} does not impact negatively the current results for the evaluation of the FSB.

6.0 Computations

6.1 Bending About Horizontal Axis

Inputs

Section properties are obtained from Page I-06 of Calculation 160268-CA-09 Appendix I

thickness of cross section	$h := (6 \cdot 12) \text{in} = 6 \text{ft}$
depth to reinforcement	$d := h - 3.5 \text{in} - 1.128 \text{in} - \frac{1.41 \text{in}}{2} = 66.7 \cdot \text{in}$
unit width	$b := 1 \text{ft}$
concrete compressive strength	$f_{pc} := 3000 \text{psi}$
area of tension steel (#11 @ 12 in)	$A_s := 1.56 \text{in}^2$
yield strength of tension steel	$f_y := 60000 \text{psi}$
concrete elastic modulus	$E_c := 3120000 \text{psi}$
steel elastic modulus	$E_s := 29000000 \text{psi}$

ASR Loading Demands

The controlling combination load for the evaluation of the SFP North Wall is C03 (Section Cut 40 in Table 10, Calculation 160268-CA-09). Factored ASR axial compression demand and including the threshold factor of 1.2 applied in the vertical direction of the SFP north wall are obtained from FSB_UC model of the FSB (Section 6.2, Calculation 160268-CA-09). Axial compression demand due to the thermal gradient is not considered since the wall is free to translate in the upward direction.

Threshold factor	$TF := 1.2$
ASR loading factor of 2.0 for combination load C03 and affected by 20% reduction in ASR load (Table 6 of Methodology Document170444-MD-01)	$ASR_F := 1.6$

Unfactored ASR compression force.

$$P_u := 3737.5 \frac{\text{lbf}}{\text{in}} = 44.9 \frac{\text{kip}}{\text{ft}}$$

Factored ASR compressive stress due to combination load C03

$$f_{\text{initial}} := \frac{\text{ASR}_F \cdot \text{TF} \cdot P_u}{h} = 100 \text{ psi}$$

Temperature Loading Demands

The temperature moment demands for the un-cracked section of the wall are calculated based on thermal gradients defined in the original design calculation for the SFP mat and walls (FB-17) and considering fixed-fixed boundary conditions. Modeling as fixed-pinned boundary conditions leads to bending demands that are up to 1.5 times larger than that obtained using fixed-fixed boundary conditions. Therefore, the use of fixed-fixed boundary conditions for bending about the horizontal direction is conservative.

Operational Temperature:

Temperature at top

$$T_t := 175 \cdot \text{ } ^\circ\text{F}$$

Temperature at bottom

$$T_b := -10 \cdot \text{ } ^\circ\text{F}$$

Coefficient of Thermal Expansion for concrete

$$:= 5.5 \cdot 10^{-6} \cdot \left(\frac{1}{\text{ } ^\circ\text{F}} \right)$$

Gross moment of inertia

$$I_g := \frac{b \cdot h^3}{12} = 3.732 \times 10^5 \cdot \text{in}^4$$

Operational thermal moment based on un-cracked section

$$M_{\text{tgo}} := \frac{E_c \cdot (I_g) \cdot \left(\frac{T_t - T_b}{2} \right)}{0.5 \cdot h} = 1371.4 \cdot \text{kip} \cdot \text{ft}$$

Accidental Temperature:

Temperature at top

$$T_t := 212 \cdot \text{ } ^\circ\text{F}$$

Temperature at bottom

$$T_b := -10 \cdot \text{ } ^\circ\text{F}$$

Accidental thermal moment based on un-cracked section

$$M_{\text{tga}} := \frac{E_c \cdot (I_g) \cdot \left(\frac{T_t - T_b}{2} \right)}{0.5 \cdot h} = 1645.7 \cdot \text{kip} \cdot \text{ft}$$

Determine M_{cr}

Ratio of steel to concrete elastic moduli

$$n := \text{round} \left(\frac{E_s}{E_c} \right) = 9$$

modulus of rupture
[ACI 318-71 Section 9.5.2.2]

$$f_r := 7.5 \cdot \sqrt{\frac{f_{\text{pc}}}{\text{psi}}} \cdot \text{psi} = 410.792 \cdot \text{psi}$$

Cracking moment [ACI 318-71 Eqn 9-5]

$$M_{\text{cr}} := \frac{(f_r + f_{\text{initial}}) \cdot I_g}{0.5 \cdot h} = 441 \cdot \text{kip} \cdot \text{ft}$$

Compute Cracked Moment of Inertia

Distance to neutral axis
of cracked section

$$kd := \left(\sqrt{1 + \frac{2b \cdot d}{n \cdot A_s}} - 1 \right) \cdot \frac{n \cdot A_s}{b} = 11.375 \cdot \text{in}$$

Fully cracked moment of
inertia

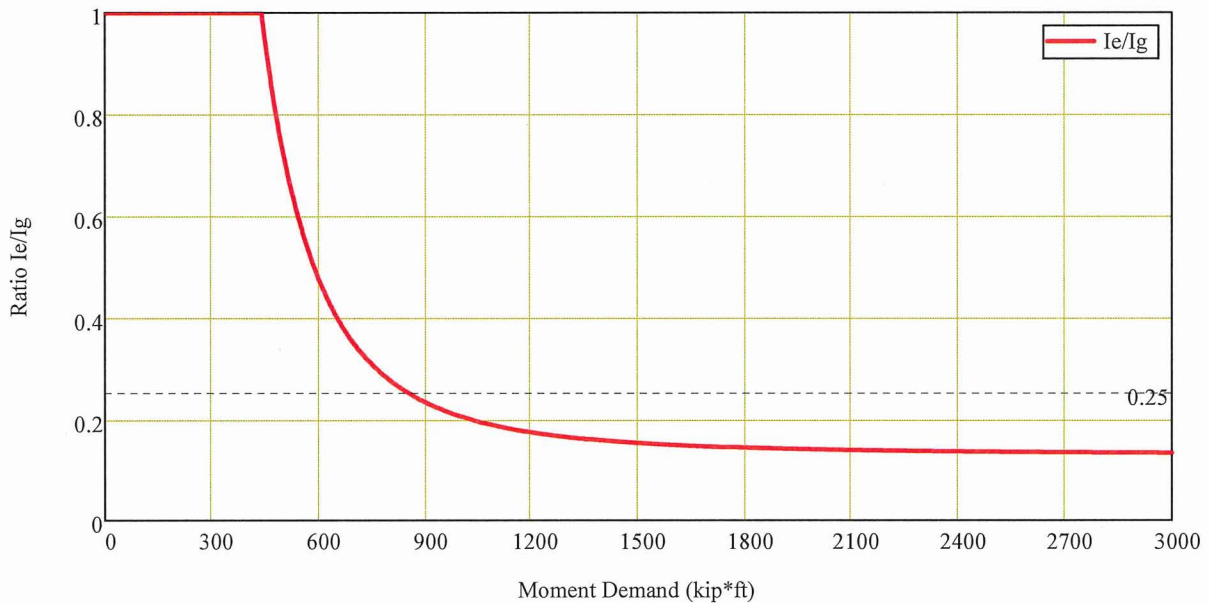
$$I_{cr} := \frac{b \cdot kd^3}{3} + n \cdot A_s \cdot (d - kd)^2 = 4.881 \times 10^4 \cdot \text{in}^4$$

Ratio of fully cracked
moment of inertia to
gross moment of inertia

$$\frac{I_{cr}}{I_g} = 0.131$$

Effective cracked moment of
inertia [ACI 318-71 Eqn 9-4]
(defined as a function of M_a)

$$I_e(M_{a_in}) := \min \left[\left(\frac{M_{cr}}{|M_{a_in}|} \right)^3 \cdot I_g + \left[1 - \left(\frac{M_{cr}}{|M_{a_in}|} \right)^3 \right] \cdot I_{cr}, I_g \right]$$



I_e / I_g Ratio for Bending about Horizontal Axis

I_e/I_g Ratio at Uncracked Section Temperature Moment Demand

Ratio of effective moment of inertia to gross moment of inertia at
moment demand for an un-cracked section due to operational
temperature.

$$\frac{I_e(M_{tgo})}{I_g} = 0.16$$

Ratio of effective moment of inertia to gross moment of inertia at
moment demand for an un-cracked section due to accidental
temperature.

$$\frac{I_e(M_{tga})}{I_g} = 0.15$$

6.2 Bending About Vertical Axis

Inputs

Section properties are obtained from Page I-03 of Calculation 160268-CA-09 Appendix I

depth to reinforcement $d := h - 3.5\text{in} - \frac{1.128\text{in}}{2} = 67.9\text{in}$

area of tension steel
(#9 @ 12in) $A_s := 1.00\text{in}^2$

ASR Loading Demands

The controlling combination load for the evaluation of the SFP North Wall is C03 (Section Cut 38 in Table 10, Calculation 160268-CA-09). Factored ASR axial compression demand and including the threshold factor of 1.2 applied in the horizontal direction of the SFP north wall are obtained from FSB_UC model of the FSB (Section 6.2, Calculation 160268-CA-09). Axial compression demand due to the thermal gradient is not considered. The restraint and inward pressure effects due to ASR expansion of the concrete backfill at the west side of the north wall leads to large axial compression demands. Including the axial compression demand due to temperature is considered to double-count the compressive effect and thus too conservative since its effect is only developed due to the restraint effect of the concrete backfill.

Unfactored ASR compression force. $P_u := 21098 \frac{\text{lbf}}{\text{in}} = 253.2 \frac{\text{kip}}{\text{ft}}$

ASR compressive stress due to combination load C03 $f_{\text{initial}} := \frac{\text{ASR_F} \cdot \text{TF} \cdot P_u}{h} = 563 \text{ psi}$

Temperature Loading Demands

The temperature moment demands for the un-cracked section of the wall are calculated based on thermal gradients defined in the original design calculation for the SFP mat and walls (FB-17) and considering fixed-fixed boundary conditions. Fixed boundary conditions for bending about vertical axis are judged adequate due to the restraint effects of the thick west wall of the SFP and north wall of the cask loading pool. Therefore, the same temperature moment demands considered in the evaluation for bending about the horizontal axis are used.

Determine M_{cr}

Cracking moment [ACI 318-71 Eqn 9-5] $M_{cr} := \frac{(f_r + f_{\text{initial}}) \cdot I_g}{0.5 \cdot h} = 841 \cdot \text{kip} \cdot \text{ft}$

Compute Cracked Moment of Inertia

Distance to neutral axis of cracked section $k_d := \left(\sqrt{1 + \frac{2b \cdot d}{n \cdot A_s}} - 1 \right) \cdot \frac{n \cdot A_s}{b} = 9.373 \cdot \text{in}$

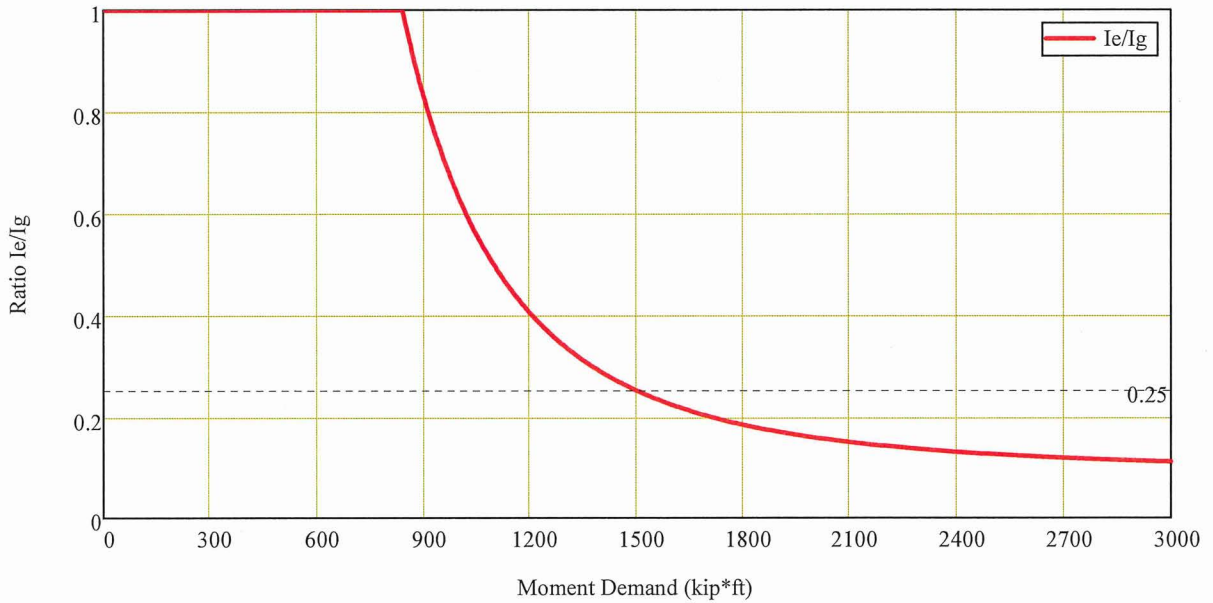
Fully cracked moment of inertia $I_{cr} := \frac{b \cdot k_d^3}{3} + n \cdot A_s \cdot (d - k_d)^2 = 3.416 \times 10^4 \cdot \text{in}^4$

Ratio of fully cracked moment of inertia to gross moment of inertia

$$\frac{I_{cr}}{I_g} = 0.092$$

Effective cracked moment of inertia [ACI 318-71 Eqn 9-4] (defined as a function of Ma)

$$I_{e(Ma_in)} := \min \left[\left(\frac{M_{cr}}{|Ma_in|} \right)^3 \cdot I_g + \left[1 - \left(\frac{M_{cr}}{|Ma_in|} \right)^3 \right] \cdot I_{cr}, I_g \right]$$



Ie / Ig Ratio for Bending about Vertical Axis

Ie/Ig Ratio at Uncracked Section Temperature Moment Demand

Ratio of effective moment of inertia to gross moment of inertia at moment demand for an un-cracked section due to operational temperature.

$$\frac{I_e(M_{tgo})}{I_g} = 0.3$$

Ratio of effective moment of inertia to gross moment of inertia at moment demand for an un-cracked section due to accidental temperature.

$$\frac{I_e(M_{tga})}{I_g} = 0.21$$

6.3 Evaluation of D/C Ratio for Bending about Vertical Axis in the SFP North Wall

Axial compression demands in the horizontal direction and bending demands about the vertical direction in the SFP north wall are obtained from FSB_FC model of the FSB. The demands correspond to Section Cut 38. (Section 6.2, Calculation 160268-CA-09).

Unfactored ASR axial compression demand $P_{ASR} := 17793 \frac{\text{lbf}}{\text{in}} = 213.5 \frac{\text{kip}}{\text{ft}}$

Unfactored ASR bending demand $M_{ASR} := 359990 \frac{\text{lbf} \cdot \text{in}}{\text{in}} = 360 \frac{\text{kip} \cdot \text{ft}}{\text{ft}}$

Factored ASR axial compression load due to combination load C03 $P_{ASR_C03} := ASR_F \cdot TF \cdot P_{ASR} = 410 \frac{\text{kip}}{\text{ft}}$

Factored ASR bending demand due to combination load C03 $M_{ASR_C03} := ASR_F \cdot TF \cdot M_{ASR} = 691 \frac{\text{kip} \cdot \text{ft}}{\text{ft}}$

Factored axial tension load due to combination load C03 w/o ASR loading $P_{C03} := -94.808 \frac{\text{lbf}}{\text{in}} = -1.1 \frac{\text{kip}}{\text{ft}}$

Factored bending demand due to combination load C03 w/o ASR loading (opposite to ASR moment) $M_{C03} := -13921 \frac{\text{lbf} \cdot \text{in}}{\text{in}} = -13.9 \frac{\text{kip} \cdot \text{ft}}{\text{ft}}$

Factored axial compression load due to combination load C03 $P_{uC03} := P_{ASR_C03} + P_{C03} = 408.8 \frac{\text{kip}}{\text{ft}}$

Factored bending demand due to combination load C03 $M_{uC03} := M_{ASR_C03} + M_{C03} = 677.3 \frac{\text{kip} \cdot \text{ft}}{\text{ft}}$

Amplification factor for M_{uC03} . The amplification factor to estimate the moment demand when accounting for the ASR loading compressive effect (f_{initial}) is conservatively calculated by the factor between the ratios of the effective moment of inertia I_e with and without f_{initial} .

$$I_{\text{amp}} := \frac{0.30}{0.25} = 1.2$$

Factored amplified bending demand due to combination load C03 $M_{uC03_amp} := I_{\text{amp}} \cdot (M_{uC03}) = 812.7 \frac{\text{kip} \cdot \text{ft}}{\text{ft}}$

PM capacity diagram file (From spColumn with adjusted capacity factors) $PMD := "0072_0083_0083_0406_0406.PMD"$

Load PM capacity diagram for section cut 38 $PM_File := \text{READFILE}(PMD, "delimited")$

Extract PM capacity curve

$$PM_CapM := \text{submatrix}(PM_File, 2, \text{rows}(PM_File), 1, 1) \cdot \frac{\text{kip}\cdot\text{ft}}{\text{ft}}$$

$$PM_CapP := \text{submatrix}(PM_File, 2, \text{rows}(PM_File), 2, 2) \cdot \frac{\text{kip}}{\text{ft}}$$

Compression capacity

$$P_n := 0.7 \cdot 0.80 \cdot \left[0.85 \cdot f_{pc} \cdot \left(h - 2 \frac{As}{b} \right) + 2 \frac{As}{b} \cdot f_y \right] = 1298.1 \cdot \frac{\text{kip}}{\text{ft}}$$

Cap axial compression to the design limit.

$$PM_CapP_capped := \begin{cases} \text{retval} & \text{rows}(PM_CapP) \leftarrow 0 \\ \text{for } row_i \in 1.. \text{rows}(PM_CapP) & \\ \text{retval}_{row_i} & \leftarrow \min(PM_CapP_{row_i}, P_n) \\ \text{retval} & \end{cases}$$

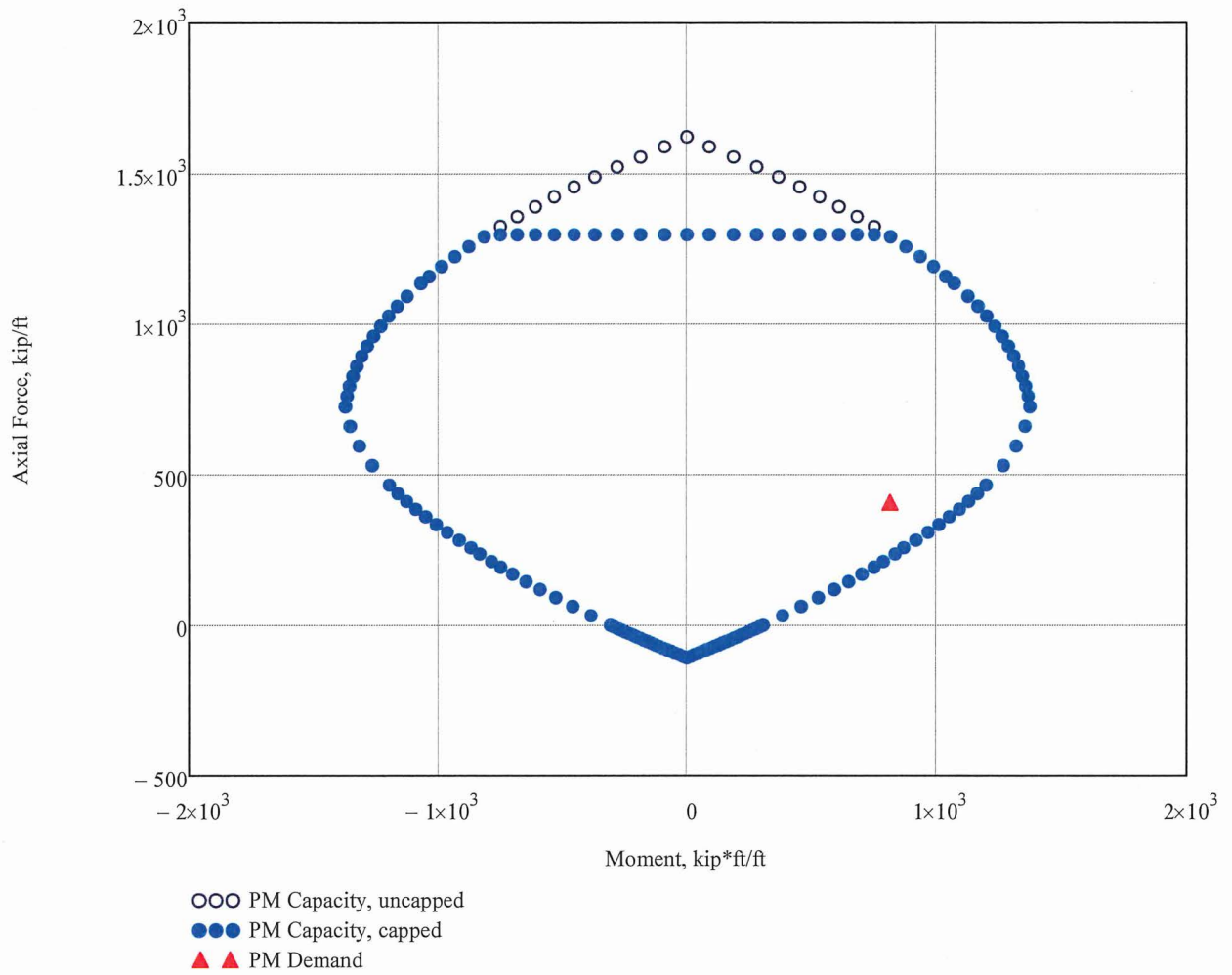
Demand point:

$$PM_DM := M_{uCO3_amp} = 812.712 \cdot \frac{\text{kip}\cdot\text{ft}}{\text{ft}}$$

$$PM_DP := P_{uCO3} = 408.813 \cdot \frac{\text{kip}}{\text{ft}}$$

Compute DCR for PM Interaction

$$DCR_{PM} := \begin{cases} \text{demandAngle} \leftarrow \text{angle} \left[\frac{PM_DM}{\left(\frac{\text{kip}\cdot\text{ft}}{\text{ft}} \right)}, \frac{PM_DP}{\left(\frac{\text{kip}}{\text{ft}} \right)} \right] & = 0.6 \\ \text{best_P} \leftarrow 0.0 \\ \text{best_M} \leftarrow 0.0 \\ \text{best_AngleDelta} \leftarrow 99999 \\ \text{for } ci \in 1.. \text{rows}(PM_CapP_capped) & \\ \text{thisAngle} \leftarrow \text{angle} \left[\frac{PM_CapM_{ci}}{\left(\frac{\text{kip}\cdot\text{ft}}{\text{ft}} \right)}, \frac{PM_CapP_capped_{ci}}{\left(\frac{\text{kip}}{\text{ft}} \right)} \right] & \\ \text{angleDelta} \leftarrow \text{thisAngle} - \text{demandAngle} & \\ \text{if } |\text{angleDelta}| < \text{best_AngleDelta} & \\ \text{best_AngleDelta} \leftarrow |\text{angleDelta}| & \\ \text{best_P} \leftarrow PM_CapP_capped_{ci} & \\ \text{best_M} \leftarrow PM_CapM_{ci} & \\ \text{demandLength} \leftarrow \sqrt{\left[\frac{PM_DM}{\left(\frac{\text{kip}\cdot\text{ft}}{\text{ft}} \right)} \right]^2 + \left[\frac{PM_DP}{\left(\frac{\text{kip}}{\text{ft}} \right)} \right]^2} & \\ \text{capacityLength} \leftarrow \sqrt{\left[\frac{\text{best_M}}{\left(\frac{\text{kip}\cdot\text{ft}}{\text{ft}} \right)} \right]^2 + \left[\frac{\text{best_P}}{\left(\frac{\text{kip}}{\text{ft}} \right)} \right]^2} & \\ \text{return } \frac{\text{demandLength}}{\text{capacityLength}} & \end{cases}$$



Axial Force Moment Interaction Diagram for Section 38